Development of Structurally Novel FMS (CSF-1R) Inhibitors for Cancer

A Thesis Submitted by:

Kanut Tangsangasaksri

In partial fulfilment of the requirements for the degree of:

Doctor of Philosophy

Supervisor: Professor Matthew J. Fuchter

Department of Chemistry

Imperial College London

February 2021

Declaration of Originality

I, Kanut Tangsangasaksri, hereby confirm that the work presented within this thesis is entirely my own, conducted at the Department of Chemistry, Imperial College London under the supervision of Professor Matthew J. Fuchter, unless otherwise stated. All work not performed by the author has been acknowledged within the text and has been appropriately and adequately cited.

Kanut Tangsangasaksri

February 2021

Copyright Declaration

The copyright of this thesis rests with the author and is made available under a Creative Commons Attribution Non-Commercial No Derivatives licence. Researchers are free to copy, distribute or transmit the thesis on the condition that they attribute it, that they do not use it for commercial purposes and that they do not alter, transform or build upon it. For any reuse or redistribution, researchers must make clear to others the licence terms of this work.

Abstract

Colony-stimulating factor-1 receptor (CSF-1R) or FMS is a hematopoietic growth factor responsible for cell differentiation, proliferation, and survival. Overexpression of FMS has been implicated in a large number of human pathologies, including inflammatory diseases and several cancers, due to its role in the activation of tumour-associated macrophages (TAMs) which can promote tumour progression and metastasis. Inhibition of FMS can therefore in principle provide therapeutic options for these diseases. In this thesis, we focus on the development of small molecule inhibitors against FMS kinase.

In Chapter 1, we report the design of a novel type of FMS inhibitor, based on promising compounds previously identified in the Fuchter group, and the synthesis of the desired inhibitor and its analogues. Despite significant challenges in the synthesis, the desired inhibitor was successfully synthesised and the routes developed were optimised to synthesise further analogues. Unfortunately, the target inhibitor was found only to be moderately potent against FMS.

In Chapter 2, we report the development of small molecule-based PROTACs (Proteolysis-Targeting Chimeras) which were specifically designed for target protein degradation of FMS. PROTACs have been recently introduced as a novel therapeutic approach since they possess some advantages over other small molecule modalities, including improved selectivity and a catalytic mechanism of action. Our FMS PROTACs were designed based on one of the lead structures presented in Chapter 1. The novel PROTACs were successfully synthesised, and initial biological properties of the synthesised PROTACs were assessed through an *in vitro* degradation assay. Although the initial biological assay showed that the synthesised PROTACs were not able to degrade FMS, further biological evaluation of the synthesised PROTACs is currently underway.

Acknowledgements

First and foremost, I would like to thank Professor Matthew Fuchter for giving me a great opportunity to join his group at Imperial College London. I am really grateful for his patience, guidance, and encouragement since I started in the group in 2015. Since then, I have improved myself to become a better chemist. This will always be my honour to be a part of Fuchter group.

I would like to thank Dr. Nick Dibb who helped me set up a biological assay and teach me many things that I have never known. Thanks also go to Dr. Caroline Low, Dr. Olan Dolezal, and Dr. Tom Peat. Without their help, this project would not have been fulfilled.

I would also like to thank Dr. Sandeep, Dr. Jochen, Dr. Ainoa, and other past and present members of Fuchter group who are always happy to help me whenever I encounter chemistry problems. It's a pleasure working with all of you. I would like to thank Davide for his help with the biological assays.

Thanks should also go to the analytical staff at Imperial College; Dr. Lisa Haigh and Pete Haycock who kindly give me help and support throughout my PhD study.

I would like to thank Prof. Matt, Dr. Jake, Ollie, Emily, Rosie, my sister, and Dr. Pumidech who proofread my thesis.

Years in my PhD life was so long and it was quite tough to get used to entirely new environments. It couldn't have been a delightful time without awesome friendships from Drs. Power: Emily, Amaia, Francesco, and Nadia. We shared lots of experiences in so many ways. Our friendships will last forever.

I would also like to express my gratitude to the Development and Promotion of Science and Technology Talents Project for providing me the opportunity to study abroad and for supporting my studentship. Thanks also go to all staffs in the Office of Educational Affairs, the Royal Thai Embassy.

Finally, my dream wouldn't be fulfilled without endless love and great support from Tangsangasaksri family. Thank you so much for everything you have done for me and thank you for always keeping me encouraged.

Abbreviations

Abl	Abelson kinase
Ac	Acetyl
ADP	Adenosine diphosphate
AGC	Protein kinase A, G, and C
aPK	Atypical protein kinase
Atm	Atmosphere (unit)
ATP	Adenosine triphosphate
Boc	*tert*-Butyloxycarbonyl
BRD4	Bromodomain-containing protein 4
BTK	Bruton's tyrosine kinase
CAMK	Ca^{2+}/calmodulin-dependent kinases
cIAP1	Cellular inhibitor of apoptosis protein 1
CK1	Casein kinase 1
CMGC	Cdk, MAPK, GSK, Cdk-like related
CML	Chronic myeloid leukemia
CRBN	Cereblon
CSF-1	Colony Stimulating Factor-1
CSF-1R or FMS	Colony-stimulating factor-1 receptor
CSIRO	Commonwealth Scientific and Industrial Research Organisation
DCM	Dichloromethane
DFG	Asp-Phe-Gly residues
DMEAD	Di-2-methoxyethyl azodicarboxylate
DMF	*N*,*N*-Dimethylformamide
DMSO	Dimethyl sulfoxide
EDC	1-Ethyl-3-(3-dimethylaminopropyl)carbodiimide
EGFR	Epidermal growth factor receptor
ePK	Eukaryotic protein kinase
Eq.	Equivalent

Et	Ethyl
FDA	Food and Drug Administration
FGFR	Fibroblast growth factor receptor
FLT-3	FMS-like tyrosine kinase-3
GIST	Gastrointestinal stromal tumour
HMTA	Hexamethylenetetramine
HOBt	1-Hydroxybenzotriazole hydrate
HRMS	High resolution mass spectrometry
Hz	Hertz
IC_{50}	Half maximal inhibitory concentration
Ig	Immunoglobulin
IMiD	Immunomodulatory drug
JAK	Janus kinase
JM	Juxtamembrane
KID	Kinase insert domain
LC-MS	Liquid chromatography-mass spectrometry
M	Molar (mol dm^{-3})
m/z	Mass-to-charge ratio
*m*CPBA	*meta*-Chloroperoxybenzoic acid
MDM2	Mouse double minute 2 homologue
Me	Methyl
MeOH	Methanol
MS	Mass spectrometry
NMR	Nuclear magnetic resonance
nRTK	Non-receptor tyrosine kinase
PDGFR	Platelet-derived growth factor receptors
POI	Protein of interest
ppm	Parts per million
PROTAC	Proteolysis-targeting chimeras
PTK	Protein tyrosine kinase
RGC	Receptor guanylyl cyclase

r.t.	Room temperature
RTK	Receptor tyrosine kinase
SPR	Surface plasmon resonance
Src	Sarcoma kinase
STE	Serine/threonine kinase
t	*tert*
TAM	Tumour-associated macrophage
TBAF	Tetrabutylammonium fluoride
TFA	Trifluoroacetic acid
THF	Tetrahydrofuran
TK	Tyrosine kinase
TKL	Tyrosine kinase-like
TLC	Thin layer chromatography
UPS	Ubiquitin-proteasome system
VEGFR	Vascular endothelial growth factor receptor
VHL	Von Hippel-Lindau
WHO	World Health Organization

Contents

Declaration of Originality 3

Copyright Declaration 4

Abstract 6

Acknowledgements 7

Abbreviations 8

Chapter 1 16

1. General introduction 17

1.1 Cancer 17

1.2 Kinase 18

1.2.1 Protein kinases 19

1.2.1.1 Tyrosine kinase (TK) 21

2. Introduction to colony-stimulating factor-1 receptor (CSF-1R) 23

2.1 Colony-stimulating factor-1 receptor (CSF-1R) or FMS 23

2.2 FMS Structure 23

2.3 Tumour-associated macrophages (TAMs) 25

2.4 FMS signaling pathway in cancer 26

2.5 FMS kinase as drug target 27

2.5.1 Active and inactive conformers 28

2.5.2 Types of kinase inhibitors 30

2.6 Small molecule kinase inhibitors 31

2.7 FMS kinase inhibitors 33

2.8 Project aim. 35

3. Results and Discussion. 37

3.1 Prior work. 37

3.2 Design of the target inhibitor. 40

3.3 Retrosynthetic strategies. 42

3.4 Synthesis of a model system. 43

3.5 Attempted synthesis of the proposed inhibitor **12**. 47

3.6 Reduced step synthesis of inhibitor **12**. 52

3.7 Synthesis of the second target inhibitor **36**. 54

3.8 Reduced step synthesis of inhibitor **36**. 57

3.9 Possible explanations for the failure of the cyclisation of the benzofuran-3(*2H*)-one core. 57

3.9.1 Addressing the solubility issue. 58

3.9.2 Addressing the substrate reactivity. 59

3.9.3 Addressing the choice of reagents for cyclisation. 61

3.10 New cyclisation approach based on a different disconnection. 64

3.10.1 Acylation of different substrates with chloroacetyl chloride. 67

3.10.2 New acylation conditions for **38**. 69

3.11 Synthesis of **74** from the rearrangement of **76**. 69

3.12 Cyclisation of intermediates at early stage. 71

3.13 Alternative designs of inhibitors. 73

3.14 Synthesis of the aurone core using the new strategy. 74

3.15 Attempted synthesis of flavone analogue. 77

3.16 Synthesis of flavone and aurone *via* the oxidation of ynol intermediate using Dess-Martin oxidation (DMP) 78
3.16.1 Optimisation of the oxidation of ynol intermediate. 80
3.17 Synthesis of aurone using $AgNO_3$. 83
3.18 Synthesis of the initial inhibitor **12** *via* ynol intermediate. 86
3.19 Biological Assays. 90
3.19.1 Cell-based assay. 90
3.19.2 Cell-free SPR assay. 91
3.19.3 Kinase assay. 96
3.20 Conclusions. 97
Chapter 2. 99
4. Introduction to PROTACs. 100
4.1 The Ubiquitin-Proteasome System (UPS) 100
4.2 Proteolysis-Targeting Chimeras or PROTACs. 101
4.3 PROTAC structure and mode of action. 102
4.4 Advantages and disadvantages of PROTACs. 104
4.5 Consideration of PROTAC components. 105
4.5.1 Ligand targeting the POI and site of attachment. 105
4.5.2 Type of E3 ligases. 107
4.5.3 Type of linkers. 107
4.6 Small molecule PROTACs and types of E3 ligase ligands. 109
4.6.1 MDM2-based PROTAC. 110
4.6.2 cIAP1-based PROTAC. 111

4.6.3 VHL-based PROTAC. 111

4.6.4 CRBN-based PROTAC. 113

4.7 Project aim. 114

5. Results and Discussion. 115

5.1 Designing the PROTACs. 115

5.2 Synthesis of FMS kinase ligand with an amine moiety for linker attachment. 116

5.3 Synthesis of the PROTAC with a 12- and 8-carbon linker chain. 118

5.4 Synthesis of inactive VHL ligand attached to a linker. 119

5.5 Biological assays. 121

5.6 Conclusions and future work. 123

6. Experimental. 126

6.1 General Experiment. 126

6.2 Synthetic procedures: Chapter 1. 127

6.3 Synthetic procedures: Chapter 2. 186

References. 201

——Chapter 1——

1. General introduction

1.1 Cancer

Cancer or malignant tumour, according to the World Health Organization (WHO), is the second leading cause of mortality worldwide and is responsible for an estimated 9.6 million deaths in 2018[1]. Cancer is a group of diseases in which cells in a specific part of the body grow and reproduce uncontrollably. These cells can damage or destroy surrounding healthy tissues. In addition, the cancerous cells can also invade or spread to adjoining parts of the body or other organs, a process termed metastasis. This process is attributed as a main cause of death from cancer. The examples of common cancer types are lung, breast, colorectal, and prostate cancer.[1]

Tumours are a group of abnormal cells that form lumps or growths and can be classified into two types: benign (non-cancerous) tumours and malignant (cancerous) tumours.[2] Benign tumours are made up of cells that resemble normal cells which cause no harm, while malignant tumours contain cancerous cells which can invade nearby tissue and metastasise.[2] Cancer cells typically arise from genetic mutations which transform a normal cell into a tumour cell in a multistage process. This results in development of a benign tumour to a malignant tumour. The mutation and transformation of cells occurs due to several reasons ranging from a genetic predisposition, to an exposure event from external factors such as chemicals, radiation, and infections from certain viruses.[3] In addition, when the primary tumour cells grow and become malignant, they can metastasise and invade adjoining tissues, resulting in a formation of secondary tumours at the respective tissues.[4]

Nowadays, several therapeutic methods have successfully been used in the clinic for cancer treatments, for example, classical cytotoxic chemotherapy, radiotherapy, hormone therapy, immunotherapy, gene therapy, and molecularly targeted cancer drugs. Even though classical cytotoxic chemotherapy is the most commonly used treatment method, a success rate for chemotherapy remains low due to several limitations such as toxicity of chemotherapy drugs, a limited localisation of drugs to the tumour sites, and an emerging of drug resistance.[5] To overcome those barriers in classical cytotoxic chemotherapy and to hopefully improve the chemotherapy success rate, molecularly targeted therapies have been introduced.

Molecularly targeted therapy is a type of cancer treatment that uses drugs to inhibit specific gene and protein functions concerning the growth and survival of cancer cells. In contrast to classical

cytotoxic chemotherapy that can damage or kill both normal and cancer cells, molecularly targeted therapy is designed to target specific targets associated with cancer and block the growth of tumour cells while it mostly does not affect normal cells.[6] Targeted therapies using small molecule inhibitors are currently the main focus in cancer treatments and have been developed over the last decade.[7,8] Many targeted cancer inhibitors have been approved by the Food and Drug Administration (FDA) to treat specific types of cancer. Examples of targeted cancer inhibitors will be discussed in section **2.6**. Since kinases, especially protein kinases, are involved in human cancer initiation and progression, they are one of the most popular targets for small molecule targeted therapies.[9]

1.2 Kinase

Kinases are enzymes that catalyse the transfer of phosphate groups from phosphate-donating molecules, an ATP, to specific substrates such as proteins, lipids, or carbohydrates (**Figure 1**). This process is called phosphorylation. Various functions of the substrates can be effected by phosphorylation such as their activity, reactivity, and ability to bind to other biological molecules.

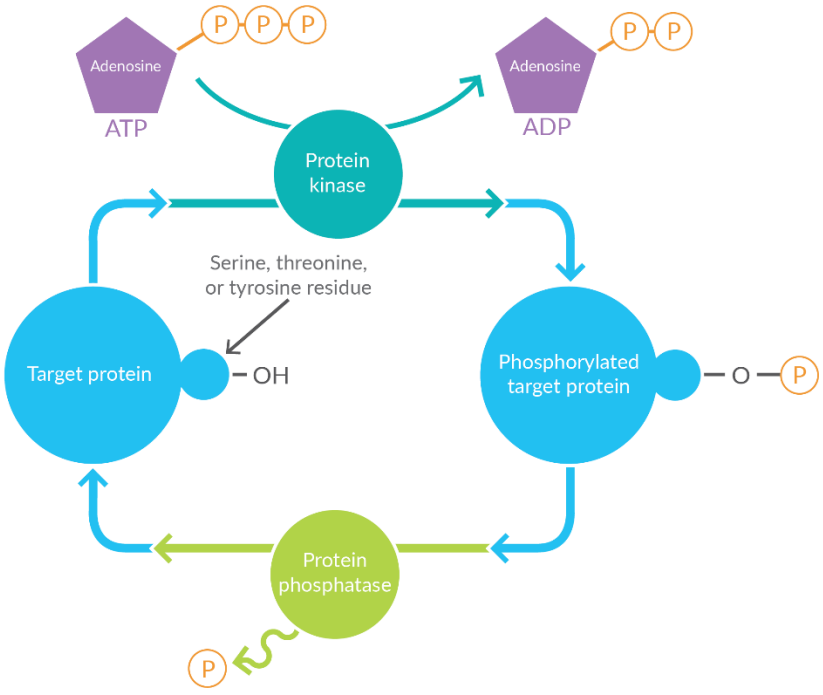


Figure 1: Phosphorylation pathway catalysed by a kinase. From Cayman chemical.[10]

This property makes kinases essential in various cellular pathways, i.e., cell signaling, protein regulation, and metabolism. Kinases can be classified into three sub-categories: protein kinases, lipid kinases, and carbohydrate kinases, according to the substrates they act upon. In this section, only protein kinases will be discussed and represent the largest group of targets for drug discovery efforts.

1.2.1 Protein kinases

The human kinome describes all the protein kinases included in the human genome. In humans, the kinome contains 518 protein kinases, which constitute 1.7% of human genes.[11] Out of the 518 protein kinases, 478 protein kinases have been identified to contain a eukaryotic protein kinase (ePK) catalytic domain. Although the other 40 protein kinases lack sequence similarity to the ePK domain, they possess biochemical kinase activity and are referred to as atypical protein kinases (aPKs).[11] aPKs are a set of protein kinases that have little sequence similarity to the ePK domain but they can involve in the phosphorylation-mediated regulation of several cellular processes.[12]

Protein kinases regulate most of the signal transduction in eukaryotic cells as well as cellular processes such as differentiation, transcription, cell cycle progression, and apoptosis *via* phosphorylation onto tyrosine, serine, threonine, or histidine residues. Different phosphorylation modifications of proteins lead to different protein functions which can effect various cellular processes such as intercellular communication, physiological responses, and homeostasis.[11] It should be noted that dysregulation and mutation of protein kinases are implicated in the causes of multiple diseases. This makes protein kinases an important biological target.[13,14,15]

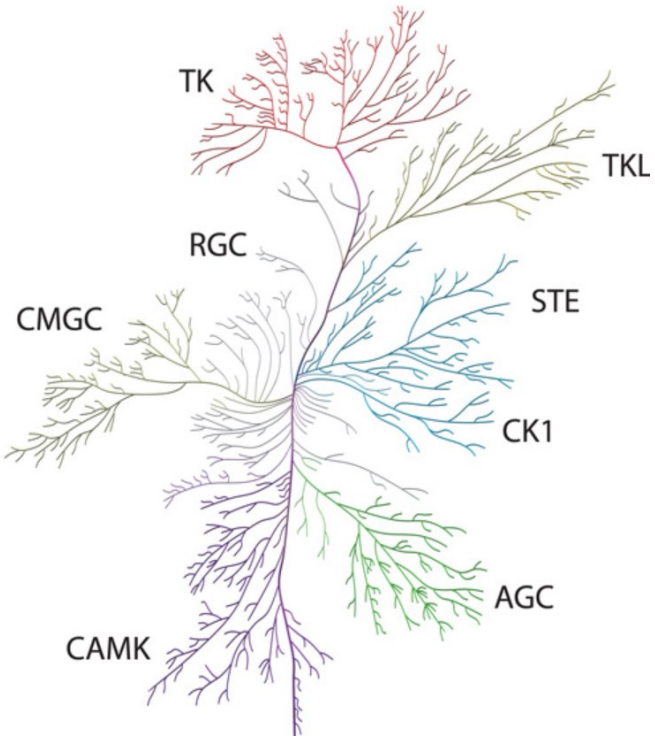


Figure 2: Human kinome and its sub-categories. TK: tyrosine kinase, TKL: tyrosine kinase-like, STE: serine/threonine kinase including three major sub-groups; STE20, STE11, and STE7 related, CK1: casein kinase 1, AGC: protein kinase A, protein kinase G, and protein kinase C related, CAMK: Ca^{2+}/calmodulin-dependent kinases, CMGC: Cdk, MAPK, GSK, Cdk-like related, RGC: receptor guanylyl cyclase. Adapted from Duong-Ly and Peterson.[16]

For humans, ePKs can be further classified into eight main groups based on the sequence similarity within the ePK domain: tyrosine kinase (TK), tyrosine kinase-like (TKL), serine/threonine kinase (STE), casein kinase 1 (CK1), protein kinase A, G, and C (AGC), Ca^{2+}/calmodulin-dependent kinases (CAMK), CMGC (named after the initials of Cdk, MAPK, GSK, Cdk-like related), and receptor guanylyl cyclase (RGC)[16] (**Figure 2**). Herein, only the TK group will be further discussed because it is the focus of this project.

1.2.1.1 Tyrosine kinase (TK)

Tyrosine kinases (TK) are enzymes that exclusively phosphorylate tyrosine residues. Tyrosine kinases play an important role in signal transduction within a cell and regulate cellular activity.[17] There are two different categories of tyrosine kinases: receptor tyrosine kinases (RTKs) and non-receptor tyrosine kinases (nRTKs).

Receptor tyrosine kinases (RTKs) are kinases that require a binding of a ligand to activate the downstream cascades. RTKs are transmembrane proteins that are involved in signaling at the cellular membrane. Transmission of signals across the cell membrane into the cytoplasm occurs as a result of ligand binding to the extracellular region of RTKs. This binding event triggers a series of structural rearrangements in the RTK, leading to its enzymatic activation on the intracellular face of the membrane[16] (**Figure 3**).

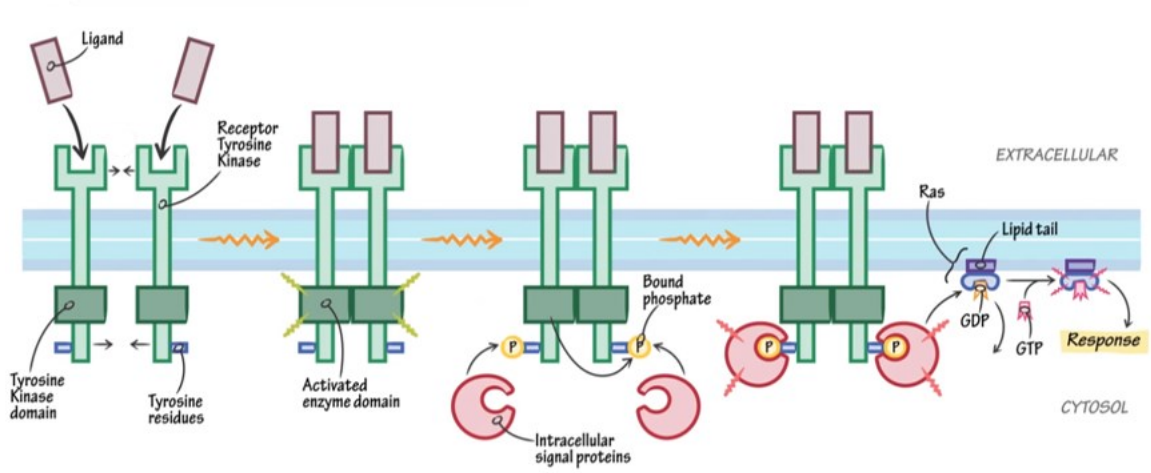


Figure 3: RTK signaling pathway. Upon binding of a ligand to the RTK, the RTK dimerises and is phosphorylated. The intracellular signal proteins then bind to the phosphorylated tyrosine residues which triggers several signaling cascades for a cellular response.[18] Adapted from Draw It to Know It.[19]

In humans, there are 58 RTKs that belong to 20 distinct families.[13,20] Examples of RTKs include the human epidermal growth factor receptor (EGFR) family (type I), platelet-derived growth factor receptors (PDGFR) family (type III) which includes colony-stimulating factor-1 receptor (CSF-1R), vascular endothelial growth factor receptor (VEGFR) family (type IV), and the fibroblast

growth factor receptor (FGFR) family (type V). All of the aforementioned RTK families have been found to be associated with cancer progression.[21-27]

Non-receptor tyrosine kinases (nRTKs) are the other group of tyrosine kinase which contain less members than the RTKs. These include sarcoma (Src), Abelson (Abl), and Janus (JAK) kinases, for example. Unlike RTKs, nRTKs lack receptor-like features such as an extracellular ligand-binding domain and a transmembrane region.[28] nRTKs regulate various cellular functions such as differentiation, proliferation, and apoptosis through transcriptional regulation of gene expression. Some members in nRTKs such as Abl and Src are also involved in various types of cancer.[29,30]

2. Introduction to colony-stimulating factor-1 receptor (CSF-1R)

2.1 Colony-stimulating factor-1 receptor (CSF-1R) or FMS

Colony-stimulating factor-1 receptor (CSF-1R) or FMS is encoded by *c-fms* proto-oncogene,[31] a cellular homologue of the retroviral oncogene *v-fms* of the Susan McDonough strain of feline sarcoma virus (SM-FeSV).[32] It is typically found in hematopoietic cells and cells in the female reproductive tract.[33,34] FMS is a member of type III RTK and is in the same family as PDGFR, c-KIT, and FLT-3 kinases.[35] FMS is a receptor for macrophage or monocyte colony-stimulating factor (M-CSF) or colony-stimulating factor-1 (CSF-1), which are hematopoietic growth factors that stimulate the survival, proliferation, and differentiation of cells of the mononuclear phagocyte lineage.[33]

Binding of FMS with its ligand, CSF-1, triggers a series of membrane-proximal tyrosine phosphorylation cascades, giving rise to rapid stimulation of cytoskeletal remodeling, gene transcription and protein translation.[36] It can also initiate a receptor dimerisation, *trans*-phosphorylation of seven conserved tyrosine residues located within the cytoplasmic domain, and an association of the intracellular domain of the receptor that activates multiple signal transduction pathways for controlling cell proliferation and differentiation.[37,38]

2.2 FMS Structure

The structure of FMS, similar to other kinases in the same family (PDGFR, c-KIT, and FLT-3), comprises an extracellular domain and an intracellular domain.[39] The extracellular domain contains five immunoglobulin (Ig) domains that bind to CSF-1. The extracellular and intracellular domains are connected by a single transmembrane domain. The intracellular domain consists of a juxtamembrane (JM) domain, which functions as an autoinhibitory domain,[40,41] and a protein tyrosine kinase domain which is divided into two domains by a kinase insert domain (KID): an ATP binding domain and a major kinase domain.[42,43] The structure of FMS is illustrated in **Figure 4**.

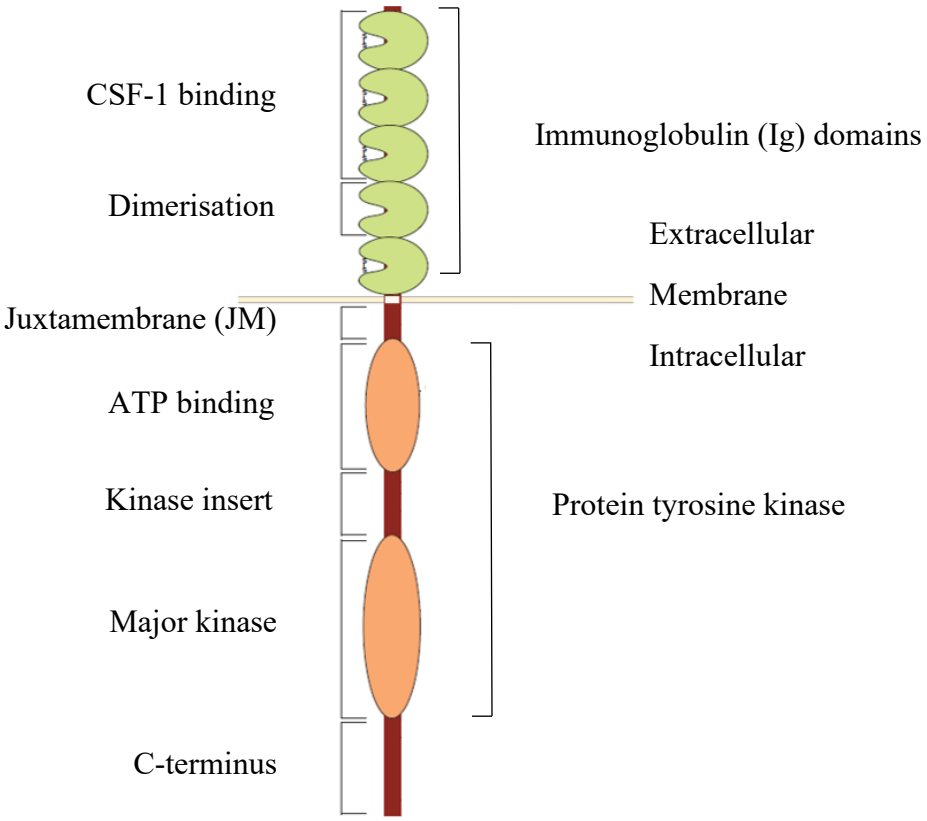


Figure 4: Representation of FMS structure domains. Adapted from Pixley *et al*.[31]

The overall structure of the protein tyrosine kinase (PTK) in FMS is composed of two lobes: N-terminal and C-terminal lobes.[39] The N-terminal lobe contains a five-stranded antiparallel β-sheet and a single α-helix called an αC-helix.[35] The C-terminal lobe comprises seven α-helices and two β-strands.[35] These two lobes are separated by a cleft for ATP binding and phosphate transfer[44] called a hinge region[39] (shown in salmon orange, **Figure 5**). The structure of FMS-PTK is depicted in **Figure 5**.

The N-lobe and hinge regions are in charge of nucleotide or inhibitor binding and provide some of the catalytic residues[39]. The C-lobe is responsible for substrate binding and catalysis.[39] Other essential structural motifs are in colour-coded shown in **Figure 5** which are the glycine-rich nucleotide-binding loop (P-loop) (shown in blue, **Figure 5**), the activation loop (A-loop) (shown in red, **Figure 5**), and the catalytic loop (C-loop) (shown in green, **Figure 5**).

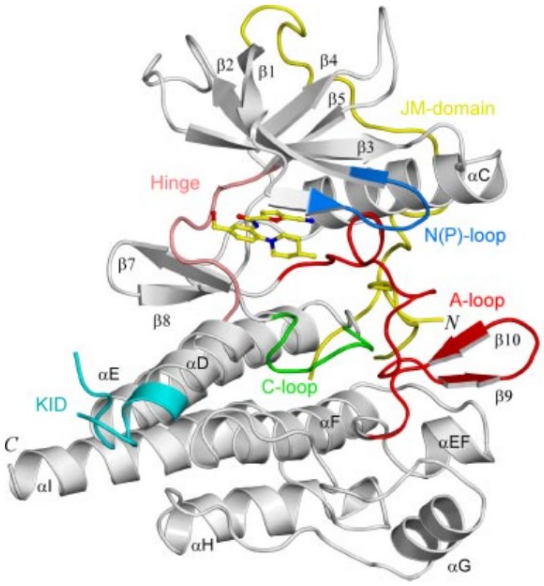


Figure 5: FMS-PTK structure bound with an inhibitor. Key binding regions are colour-coded: blue, nucleotide binding loop (P-loop); red, activation loop; green, catalytic loop; salmon, hinge region. From Schubert *et al*.[39]

2.3 Tumour-associated macrophages (TAMs)

Macrophages are an important component of the inflammatory micro-environment of tumours.[45] They can be classified into two classes of polarised macrophages which are 'classically activated' or M1 type macrophages and 'alternatively activated' or M2 type macrophages.[46,47]

M1 macrophages are potent effector cells that are responsible for killing microorganisms and tumour cells.[47] They are characterised by the release of inflammatory cytokines, reactive nitrogen intermediates, reactive oxygen intermediates, and microbicidal/tumouricidal activity.[48] In contrast, M2 macrophages are responsible for decreasing a production of pro-inflammatory cytokines and diminishing the microbial killing and phagocytosis activity.[49] They mediate resistance to parasites, immunoregulation, tissue repair, remodeling, and wound healing.[45,50] The properties involved in wound healing are supposed to influence M2 macrophages to stimulate tumour progression and metastasis which makes the M2 phenotype to be a polarisation of tumour-associated macrophages (TAMs).[48,51,52]

TAMs are the cells that create an immunosuppressive tumour microenvironment[53] and are the predominant leukocytes infiltrating solid tumours.[54] There are several lines of evidence which point out that TAMs can act as drivers for tumour progression.[45,55,56] TAMs are central to the tumour micro-environment[57,58] and can promote tumour progression and metastasis[51] which will result in a tumour growth.

Several clinical and experimental studies have demonstrated that TAMs enhance tumour progression to malignancy *via* supporting tumour-associated angiogenesis, promoting tumour cell invasion, migration and intravasation, and suppressing antitumour immune responses.[51,59,60] Since M2 macrophages, which are associated with TAMs,[48] are induced by CSF-1,[61,62] its receptor (FMS) presents a promising option for a development of drugs targeting TAMs.

2.4 FMS signaling pathway in cancer

TAMs not only play a crucial role promoting tumour progression and metastasis[51] but are also involved in the tumour micro-environment.[57,58] The growth of various tumour types is associated with an overexpression of FMS in cancer cells[63] which also correlates to poor prognosis.[64] Not only does FMS play a role in human cancer such as breast cancer, ovarian cancers, and endometrial carcinoma,[65] but it is also associated with a great number of human pathologies such as inflammatory diseases and osteoclast proliferation in bone osteolysis.[35,63]

Although FMS is important in mammary gland development during pregnancy and lactation, its role in breast cancer can eventually lead to tumour cell invasiveness and adverse clinical prognosis, if expressed abnormally.[34] The most invasive breast carcinoma cell line co-expressed with FMS promotes the concentration of disseminated CSF-1 which, in turn, stimulates osteoclastogenesis and prolongs osteoclast survival.[66,67] Apart from various kinds of cancer mentioned earlier, FMS can also play a role in leukemia if its regulator is irregularly changed.[68] In addition, TAMs activated by CSF-1 are also correlated to prostate cancer because they are a mediator for hormone resistance through a nuclear receptor depression pathway.[69]

When CSF-1 is overexpressed, the tumour densities and tumour infiltrating macrophages are strikingly increased causing the enhanced oncogenicity.[70,71] Therefore, the blockade of the FMS

kinase which will result in a reduction in the level of TAMs could be a promising treatment strategy in various types of cancers.[72,73]

2.5 FMS kinase as drug target

Kinases that constitute the human kinome are expressed ubiquitously throughout the body.[11] They account for almost all human protein phosphorylation events and mediate most cellular signal transduction and many other processes. Even though kinases are important enzymes for many cellular processes such as differentiation, proliferation, and survival of cells, de-regulation of kinases is implicated in various kind of diseases, especially cancer. Therefore, kinases have become widely targeted in oncology and have generated significant interest in the development of kinase inhibitors.[74]

The activity of FMS kinase, as well as other kinases, involves the binding of ATP and a protein substrate to the kinase. This process is followed by a phosphotransfer reaction which transfers a phosphate group from the ATP to the protein substrate, resulting in a phosphorylated product and an ADP which will finally detach from the kinase.[16] Therefore, the ATP binding site within the kinase has been the major target for a development of small molecule kinase inhibitors since the blockade of ATP binding will inhibit phosphorylation and hamper the downstream signalling.

As a result, ATP-mimic inhibitors have been developed to competitively bind to the ATP-binding site. These inhibitors tend to have similar structural features to ATP (**Figure 6**) which includes 1) Hydrogen-bond donor-acceptor-donor functionality to interact with the hinge region of the kinase, 2) largely hydrophobic in the adenine and sugar regions (light brown and purple regions, **Figure 6**), and 3) flat structure to be accommodated in the narrow cleft between N- and C-lobe.[75] The main challenge associated with the design and development of these inhibitors is the selectivity for the desired kinase while at the same time occupying novel intellectual property space.

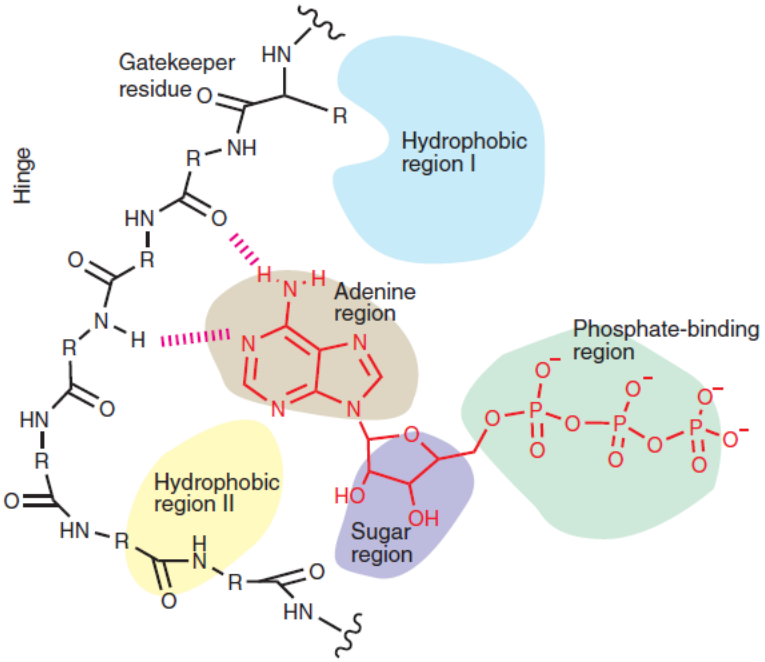


Figure 6: General binding mode of ATP to hinge binding residues. The highlighted regions signify important binding features. From Liu *et al*.[76]

2.5.1 Active and inactive conformers

In most kinases, the ATP binding site is well-conserved. ATP binds to the hinge region, the cleft between the N-lobe and C-lobe, which is lined by structural elements responsible for the activity of the kinase such as the activation loop (A-loop). Although a number of features in kinases are conserved, the A-loop is flexible which allows a degree of selectivity to be gained. The A-loop consisting of a conserved Asp-Phe-Gly (DFG) motif that can rearrange itself into two interchangeable conformations: DFG-in and DFG-out, which are referred to as the active and inactive conformation of the kinase, respectively[39] (**Figure 7**).

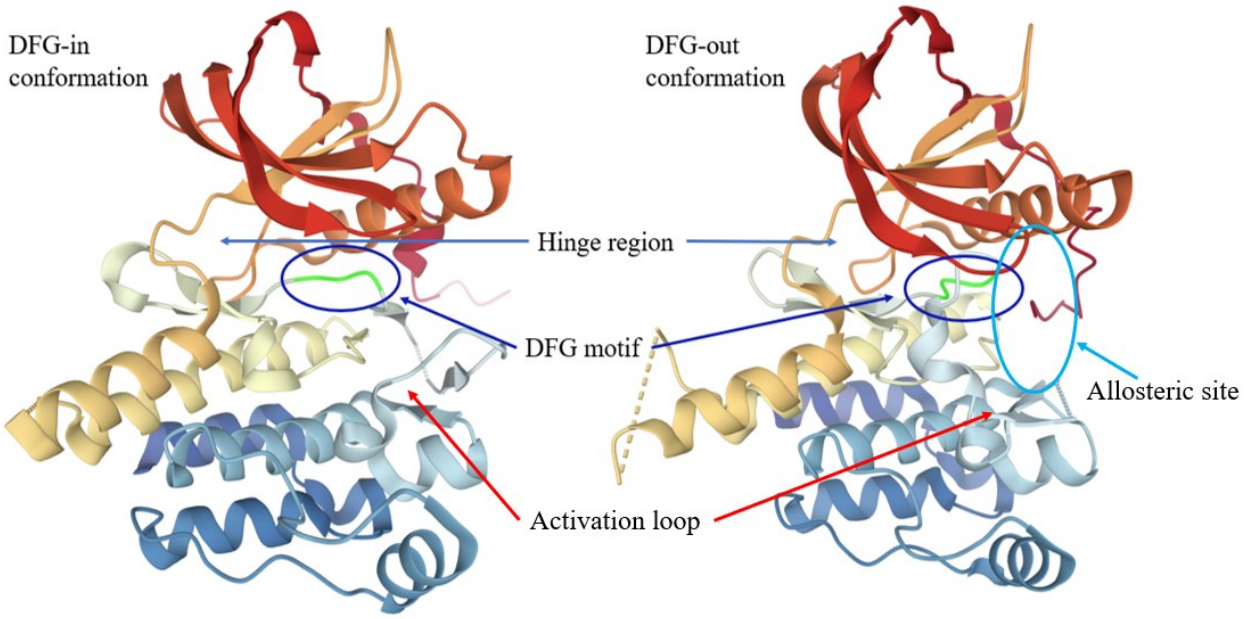


Figure 7: Left: DFG-in (active) (PDB: 3LCD) and Right: DFG-out (inactive) (PDB: 3LCO) conformers of FMS. The light green residues designate the DFG (Asp-Phe-Gly) motif.

In the active conformation (DFG-in), the A-loop is extended away from the ATP binding site and the DFG motif is buried within the hydrophobic pocket, leaving the ATP binding site open for binding to the substrate.[77] In the inactive state (DFG-out), the A-loop occupies the substrate binding region which prevents a binding of the ATP.[78] In addition, the morphology of the ATP binding site is changed in the DGF-out conformation. This not only prevents the binding of ATP but also opens up an additional hydrophobic site, called an allosteric site (shown in blue oval, **Figure 7**, right), which is unique to each kinase. This offers an additional opportunity to control the selectivity of inhibitors by exploiting hydrogen bonding and hydrophobic interactions within the allosteric site.[78]

As a member of type III RTKs, FMS also shares similar key binding features of ATP to the other kinases in the same group. ATP binds to an active form of FMS at the ATP binding site with different interactions as follows: 1) the interaction between the backbone of hinge region of FMS and the Hydrogen-bonding motif in the ATP from an adenine region which stays in a flat cavity, 2) the accommodation of the ribose moiety from adenosine in a largely hydrophobic sugar binding pocket in FMS that contains polar residues, and 3) the preoccupied hydrophobic back pocket by the DFG motif in the active conformation. In addition to the binding sites involve in the interaction

of the ATP with FMS, there is a solvent exposed area which is typically occupied by the phosphate region in the ATP.

2.5.2 Types of kinase inhibitors

Kinase inhibitors are typically categorised into type I and type II inhibitors depending on the binding function of the inhibitors to the kinase.[78] Type I inhibitors are ATP-competitive inhibitors which bind to the active (DFG-in) conformation of kinases while type II inhibitors (non ATP-competitive) bind to the inactive (DFG-out) conformation.[76] Since the ATP binding site across most kinases is well-conserved, achieving a selectivity of the type I inhibitors to the desired kinase is challenging. In comparison, while the type II inhibitors bind to the ATP-binding site using the same interactions as type I inhibitors, they also occupy an adjacent allosteric site of an inactive form of a kinase.[78] The occupation of the allosteric site can be exploited in order to design highly selective inhibitors because the allosteric site is less conserved among kinases. Nonetheless, type II inhibitors are susceptible to a resistance due to mutations in the kinase domain that can result in a loss of activity. While mutations that affect type I inhibitors may also prevent the binding of ATP substrate, which leads to dysfunctional kinases,[78] most of the FDA approved inhibitors and inhibitors that are currently in the clinical trials belong to these two classes.[74]

However, recently Wu *et al*. has reported additional classes of kinase inhibitors which are type III and type IV inhibitors[79] (**Figure 8**). Type III inhibitors exclusively bind to an allosteric site adjacent to ATP binding region without making any interaction with the ATP-binding site. For type IV inhibitors, they bind to an allosteric site far away from the ATP-binding site.[79]

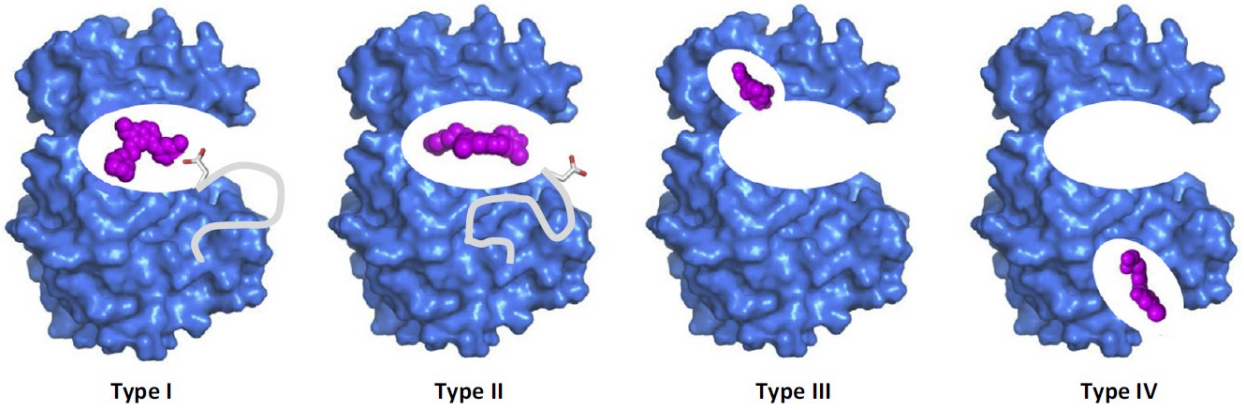


Figure 8: Types of kinase inhibitors and their mode of binding to protein kinase. From Wu *et al*.[79]

2.6 Small molecule kinase inhibitors

As of January 2020, there are a total of 52 small molecule kinase inhibitors which have been approved by the FDA.[80] Additionally, a number of potential inhibitors are either in development, in clinical trials, or waiting to be approved.

Imatinib is the first approved small molecule kinase inhibitor in 2001 that inhibits BCR-Abl (IC_{50} = 260 nM[81]), c-KIT (IC_{50} = 100 nM[82]), and PDGFR (IC_{50} = 250 nM[82]). It has been mainly used to treat chronic myeloid leukemia (CML) and other types of tumours such as gastrointestinal stromal tumours (GISTs) and malignant melanoma (MM).[83] Imatinib, a type II inhibitor, binds to the DFG-out conformation utilising three binding pockets, as shown in **Figure 9**. Nevertheless, the development of drug resistance has emerged due to point mutations in the kinase domain of BCR-Abl. This led to the development of the second-generation inhibitor, nilotinib, which possesses different allosteric binding moiety. This allows nilotinib to bind deeper and tighter within the allosteric pocket which makes it more potent against most mutations.[79] Nilotinib exhibits IC_{50} against BCR-Abl of 13 nM.[81]

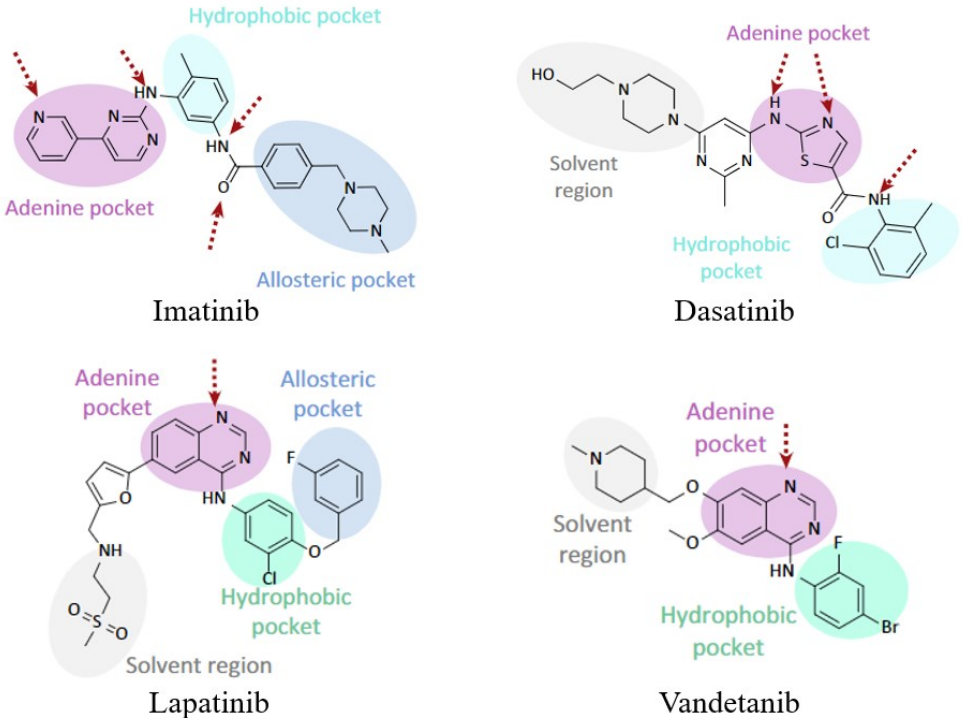


Figure 9: Examples of kinase inhibitors and their mode of binding. Red dotted arrows indicate the H-bond between the inhibitors and the residues in the hinge region within kinases. From Wu *et al.*[79]

Dasatinib, another CML treatment drug, binds to the DFG-in form of BCR-Abl (IC_{50} = 0.8 nM[81]) by occupying two binding pockets. However, the drug resistance due to point mutations in the gatekeeper residue can still occur with dasatinib.[79]

Another example of an RTK inhibitor is lapatinib (**Figure 9**). Lapatinib is a type II inhibitor for breast cancer that binds to the DFG-out form of EGFR (IC_{50} = 10.2 nM[84]). It contains the allosteric binding moiety, allowing a specific binding to an opened allosteric site of EGFR, leading to an increased selectivity of the molecule.[79] Vandetanib (**Figure 9**) is a type I, multiple RTK inhibitor against EGFR (IC_{50} = 500 nM[85]), VEGFR-2 (IC_{50} = 40 nM[85]), and RET (IC_{50} = 130 nM[85]). Vandetanib was designed to contain the solvent exposed region to increase the overall solubility of the molecule.[79]

As in the case of imatinib, drug resistance has emerged due to mutations in the kinase domain that commonly occurs in the gatekeeper residue, a single residue in the ATP binding pocket of protein kinases. These mutations can be typically found in most kinases, leading to a resistance to other

kinase inhibitors when used clinically. Moreover, in many cases, kinase inhibitors are found to be promiscuous for more than one target. They are often found to be off-target in the neighbouring kinase family owing to a high similarity in the ATP-binding site.[86] Thus, the development of the drugs to overcome drug resistance together with the increased potency towards a specific target is required.

2.7 FMS kinase inhibitors

Table 1: FMS inhibitors in current clinical development.

Compound	Target	Clinical Phase	Indication	Refer-ence
PLX7486	CSF-1R (and Trk)	1	Solid tumours	[26]
ARRY-382	CSF-1R	1	Solid tumours	[26]
JNJ-40346527	CSF-1R	1/2	Classic Hodgkin lymphoma (cHL)	[26]
BLZ945 (**6**)	CSF-1R	1/2	Solid tumours	[26]
ABT869	CSF-1R	2	Hepatocellular carcinoma	[87]

In 2019, the first FMS kinase inhibitor, pexidartinib, was approved by the FDA for the treatment of symptomatic tenosynovial giant cell tumour (TGCT) associated with severe morbidity or functional limitations and not amenable to improvement with surgery.[88] Several FMS inhibitors are currently under clinical development as shown in **Table 1**. Current FMS inhibitors are either type I or II designed to bind to the ATP-binding site.[86] The core chemotype of FMS inhibitors developed to date can be classified as follows: 1) anilides, 2) pyrimidines and pyrazines, 3) quinolines, 4) pyrrolo-pyridines, -pyrimidines and -pyrazines, 5) quinolinones and pyrido-pyrimidines, and 6) benzothiazoles.[86]

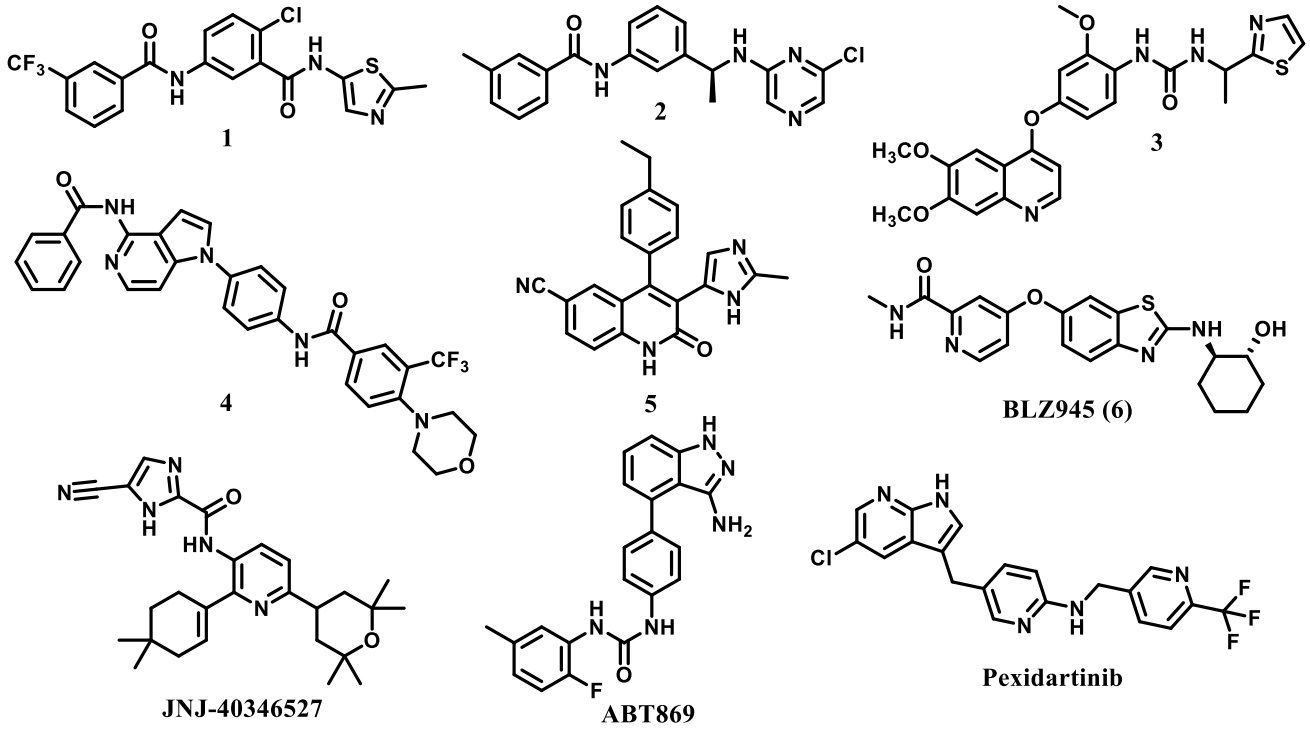


Figure 10: Examples of FMS kinase inhibitors for the different core chemotypes including 1) anilides (**1**), 2) pyrimidines and pyrazines (**2**), 3) quinolines (**3**), 4) pyrrolo-pyridines, -pyrimidines and -pyrazines (**4**), 5) quinolinones and pyrido-pyrimidines (**5**), and 6) benzothiazoles (**6**) and structures of **JNJ-40346527**, **ABT869**, and pexidartinib. The chemical structure of **PLX7496** and **ARRY-382** have not yet been disclosed.

An example of a compound in the anilide family is compound **1** (**Figure 10**). Even though there was limited selectivity against c-Raf, KDR and members of the Src family, compound **1** exhibited excellent potency in a biochemical FMS enzyme assay with an IC_{50} of 7 nM and a cellular assay with an IC_{50} of 50 nM.[89] Compound **1** also exhibited good selectivity against other type III RTKs and possessed good oral PK profiles as well as *in vivo* clearance.[89]

Compound **2** (**Figure 10**), which belongs to pyrimidine and pyrazine family, also exhibited magnificent enzymatic and cellular potency with IC_{50} of 2 and 211 nM, respectively.[90] Although the structure of **2** is similar to **1**, an amino substituted pyrazine replaces the thiazole amide moiety. Compound **2** shows similar biological properties to **1**. This includes good selectivity against other type III RTKs, comparable *in vivo* clearance and *in vivo* PK profiles. In addition, **2** does not exhibit cellular toxicity against human kidney and liver cell lines.[90]

Compound **3** (**Figure 10**) is a member in the quinoline family and has been demonstrated to possess high activity against FMS (IC_{50} = 2 nM) with reduced affinity for KDR, c-KIT, and PDGFR in response to CSF-1 in cell-based assays.[91] This compound showed extended selectivity to type IV RTK, KDR, with a higher IC_{50} of 12 nM. Compound **4** (**Figure 10**), a member of pyrrolo-pyridine, -pyrimidine and -pyrazine family, was also described as a potent FMS inhibitor.[92] Although **4** exhibited inhibitory activity against 47 different kinases, it was the most selective for FMS and KDR with IC_{50} values of 96 and 1058 nM, respectively.

Compound **5** (**Figure 10**), a member of quinolinone and pyrido-pyrimidine group, exhibited IC_{50} values of 2.5 nM in an *in vitro* assay and 5 nM in a cellular assay.[93] Compound **5** was also shown to exhibit good to excellent inhibitory activity against other type III RTKs. According to the PK profiles of **5**, this compound has good oral bioavailability even though the rate of clearance was high.[92] Compound **6** (**BLZ945**) (**Figure 10**) which is in the benzotriazole family was reported to be a potent and selective inhibitor of FMS showing IC_{50} values of 1 and 67 nM in enzyme and cellular assays, respectively.[94] Although **6** exhibited selectivity against more than 200 kinases including c-KIT and PDGFRβ, the selectivity of **6** against FMS is more than 1000-fold compared to other kinases.[94]

Despite the promise of these inhibitors, promiscuity and off-target activities are still apparent. In this project, we turn our attention to search for a novel type of FMS inhibitor that could target either the ATP binding site or the non-ATP pocket within the FMS kinase domain. We aimed to achieve improved selectivity of the inhibitors which will result in a reduced promiscuity and off-target effects.

2.8 Project aim

This project aims to design and synthesise a novel type of FMS-selective inhibitor that can be used as a drug for targeted cancer therapy. The design of novel inhibitors will be based on promising compounds previously identified in the Fuchter group. An X-ray co-crystal structure of the compounds bound to FMS kinase will be used to exploit structure-based design in order to improve the potency of the novel inhibitor. The successful synthetic route for the novel inhibitor will also be applied to synthesise analogues of the novel inhibitor in order to expand our compound library.

After obtaining a handful of the novel inhibitor and its analogues, biological assays will be used as a tool to assess the biological efficacy. Herein, cell growth assay will be used as a primary assessment to validate the potency of the synthesised inhibitors. Furthermore, the binding affinity of the inhibitors with FMS kinase will be determined using surface plasmon resonance assay. Finally, kinase assay will be conducted to evaluate the inhibitors' activity against FMS kinase catalytic domain.

3. Results and Discussion

3.1 Prior work

Previously in the Fuchter group, identification of a novel type of FMS kinase inhibitor scaffold was carried out by Dr. Robert Davidson using a virtual screening approach.[95] The virtual screening was performed using software from Cresset and Schrödinger and was based on a pharmacophore built from three different compounds: 1) **7**, a DFG-in inhibitor, which includes a hinge binding aminopyrazine moiety[96] (highlighted in red, **Figure 11**), 2) **8**, a DFG-out inhibitor, which incorporates methoxy and benzyloxy oxygen atoms for binding and accessing the DFG-out deep pocket[96] (highlighted in blue, **Figure 11**), and 3) a truncated version of **9**, from which the ethylene-linked pyrrolidine is removed, which contains a hinge binding anilino NH moiety, a pyrimidine nitrogen atom, as well as a carbonyl oxygen atom[97] (highlighted in green, **Figure 11).**

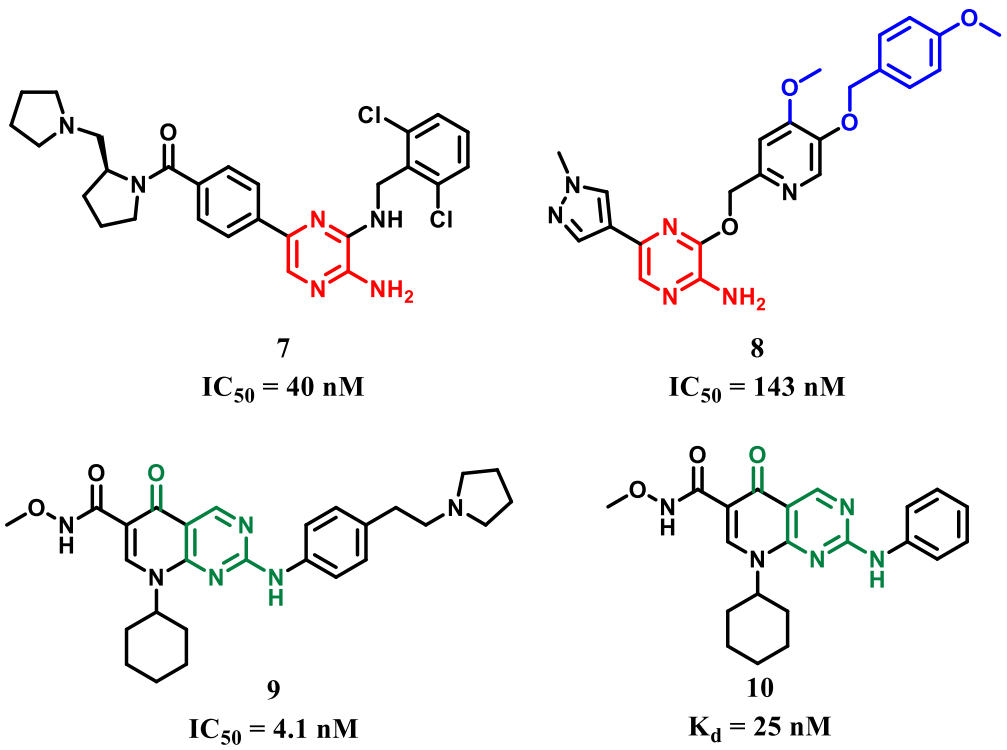
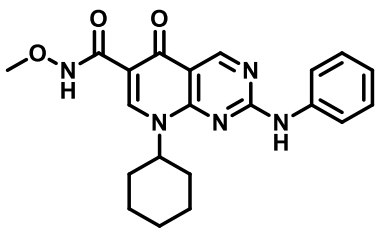
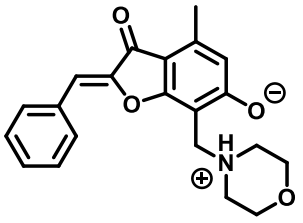


Figure 11: Pfizer compounds **7** (type I binder) and **8 (**type II binder), Johnson & Johnson compound **9** with their IC_{50} values against the FMS catalytic domain,[96,97] and a truncated version of compound **9**, compound **10**.

Compounds **7** and **8** were developed by Pfizer and are potent inhibitors of FMS with IC_{50} values of 40 nM and 143 nM,[96] respectively. The X-ray co-crystal structures of these compounds bound to FMS in both the DFG-in and DFG-out binding mode were disclosed.[96] The truncated version of **9**, compound **10** (**Figure 12**), was selected as a seed molecule for the virtual screening because the co-crystal structure of **9** had also already been solved and its K_d which was measured by our collaborators at CSIRO was 25 nM. The reason that the ethylene-linked pyrrolidine was removed from **9** was because this moiety was in a solvent exposed area and did not form significant bonding interaction with FMS.[95] It was therefore not considered essential to define a key pharmacophore.



10
K_d = 25 nM



11
K_d = 4.9 µM

Figure 12: A truncated version of compound **9**, compound **10**, and a commercially available compound, **11**.

Biological assessment of compounds from the virtual screening that were either synthesised in-house by Dr. Davidson or purchased from commercial sources was achieved by our collaborators at CSIRO. Specifically, a surface plasmon resonance (SPR) assay was performed by Dr. Olan Dolezal at CSIRO. From this assay, the compounds from the screening that exhibited the most promising FMS activity were **10** and **11** (**Figure 12**), with K_d of 25 nM and 4.9 µM, respectively. To gain further insight into these two compounds, **10** and **11**, their co-crystal structures with FMS were solved by Dr. Bin Ren at CSIRO. Alignment of the co-crystal structures of **10** and **11** with the original co-crystal structure conformation of compound **9** and the predicted overlay from Cresset software are shown in **Figure 13**.

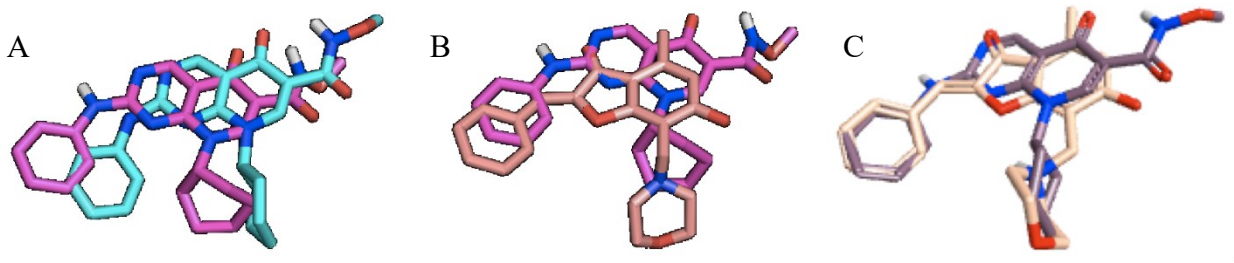
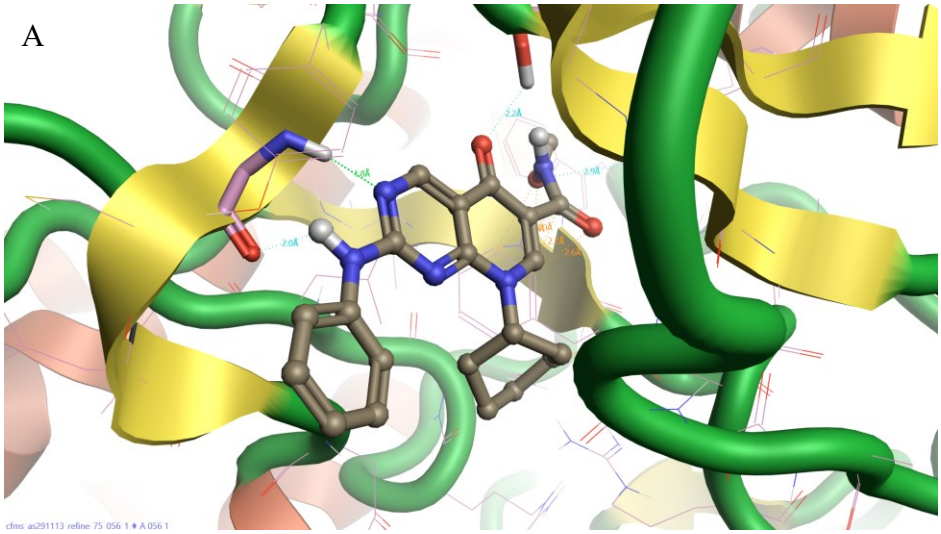


Figure 13: Co-crystal structure overlays of A) the truncated molecule of **9** from PDB:3DPK (blue) with **10** (magenta), B) **7** (magenta) and **11** (beige), and C) Conformational result of Cresset alignment of **10** and **11**. From Davidson's Ph.D. Thesis 2014.[95]

From the results obtained from Dr. Davidson's thesis, we selected two most potent novel FMS inhibitory hits, **10** and **11**, which exhibited promising biological properties and X-ray co-crystal structures (**Figure 14**). While the FMS potency of **11** is only modest, we note that it has an unusual structure for a kinase inhibitor which is the aurone derivative. Thus, it presents an interesting hit to develop, if we are able to improve its potency. Hence, the aim of this project is to exploit the structure-based design from the combined structure of the hits to improve the potency of a novel FMS inhibitor.



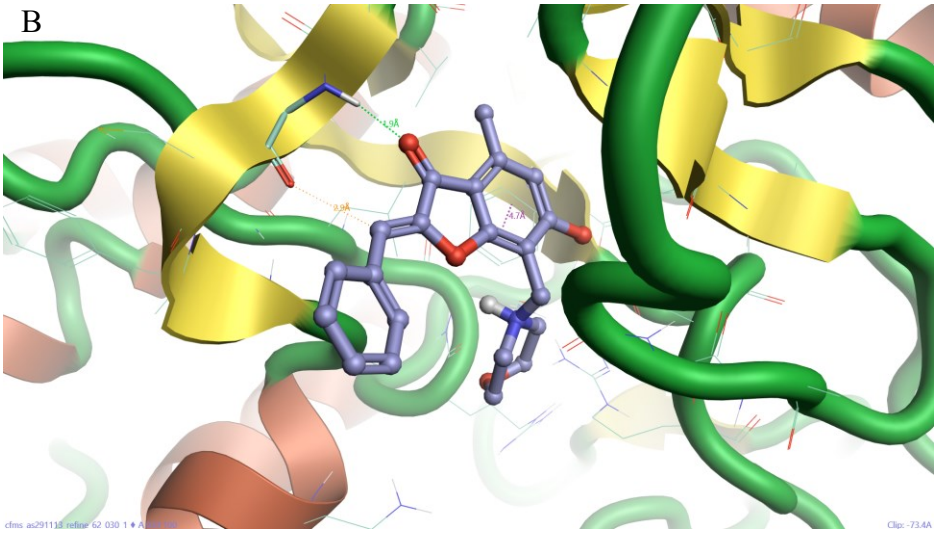


Figure 14: A) Co-crystal structure of **10** bound to the active site of FMS and B) Co-crystal structure of **11** bound to the active site of FMS.

3.2 Design of the target inhibitor

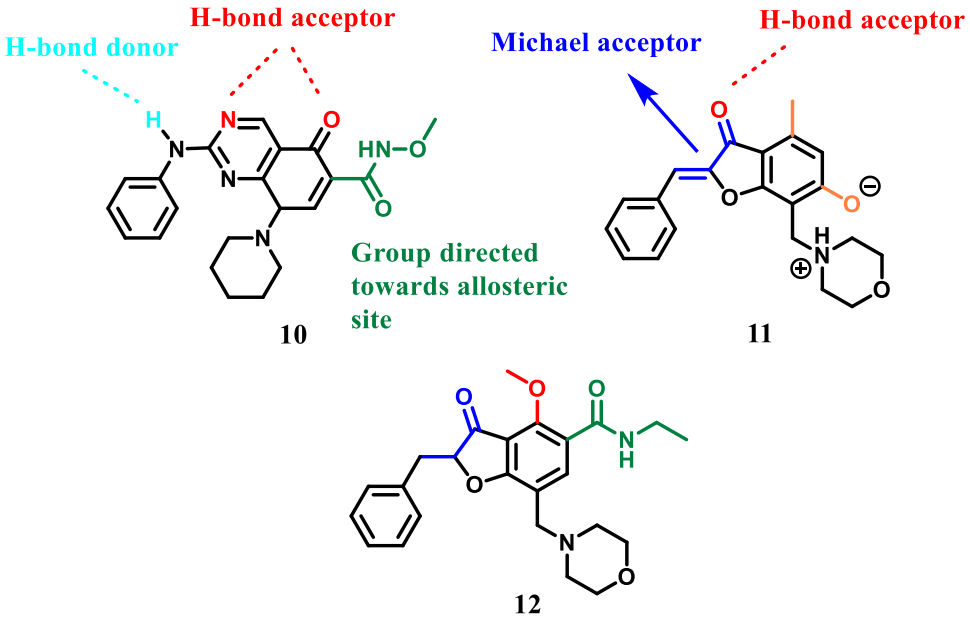


Figure 15: FMS inhibitors **10** and **11** and a desired inhibitor **12** with highlighted interactions in the FMS binding site and other key features.

Design of the novel FMS inhibitor in this project was focused on combination of the promising features from the hits, **10** and **11**. As can be seen in the co-crystal structure of **10** bound to the active site of FMS (**Figure 14**, **A**), there is an H-bonding interaction between the carbonyl oxygen in the 2,3-dihydropyridinone core (shown in red, **Figure 15**) and the backbone of the hinge residue Thr663 of FMS (shown in cyan, **Figure 14**, **A**). Additionally, there are the other two H-bonding interactions between the nitrogen atoms from the pyrimidine and aniline moieties (shown in red and cyan in **Figure 15**, respectively) and the hinge residue Cys666 of FMS (shown in green and cyan, **Figure 14**, **A**), which are classic hinge binding interactions. From compound **10**, there is also an *N*-methoxyamide side chain (shown in green, **Figure 15**) that projects towards the allosteric site in the pocket.

From the co-crystal structure of compound **11** with FMS depicted in **Figure 14**, **B**, there is a H-bonding interaction between the oxygen atom in the dihydrofuran-3(2*H*)-one core and the hinge residue Cys666 of FMS (shown in green, **Figure 14**, **B**). It should be noted that compound **11** forms fewer H-bond contacts in the ATP binding site than compound **10** which likely contributes to its lower potency compared to **10**. In addition, **11** also contains a potentially reactive Michael acceptor (highlighted in blue, **Figure 15**). Although there is no evidence for a covalent reaction between the Michael acceptor and FMS in the crystal structure, it would be best to remove this promiscuous group due to potential reactive and/or off target effects in the target inhibitor. Moreover, the methyl and phenol groups in compound **11** (highlighted in orange, **Figure 15**) appear not to be needed for binding to the FMS binding site. Hence, these two groups could be removed and/or replaced with a group that could make a H-bonding interaction in the active site of FMS.

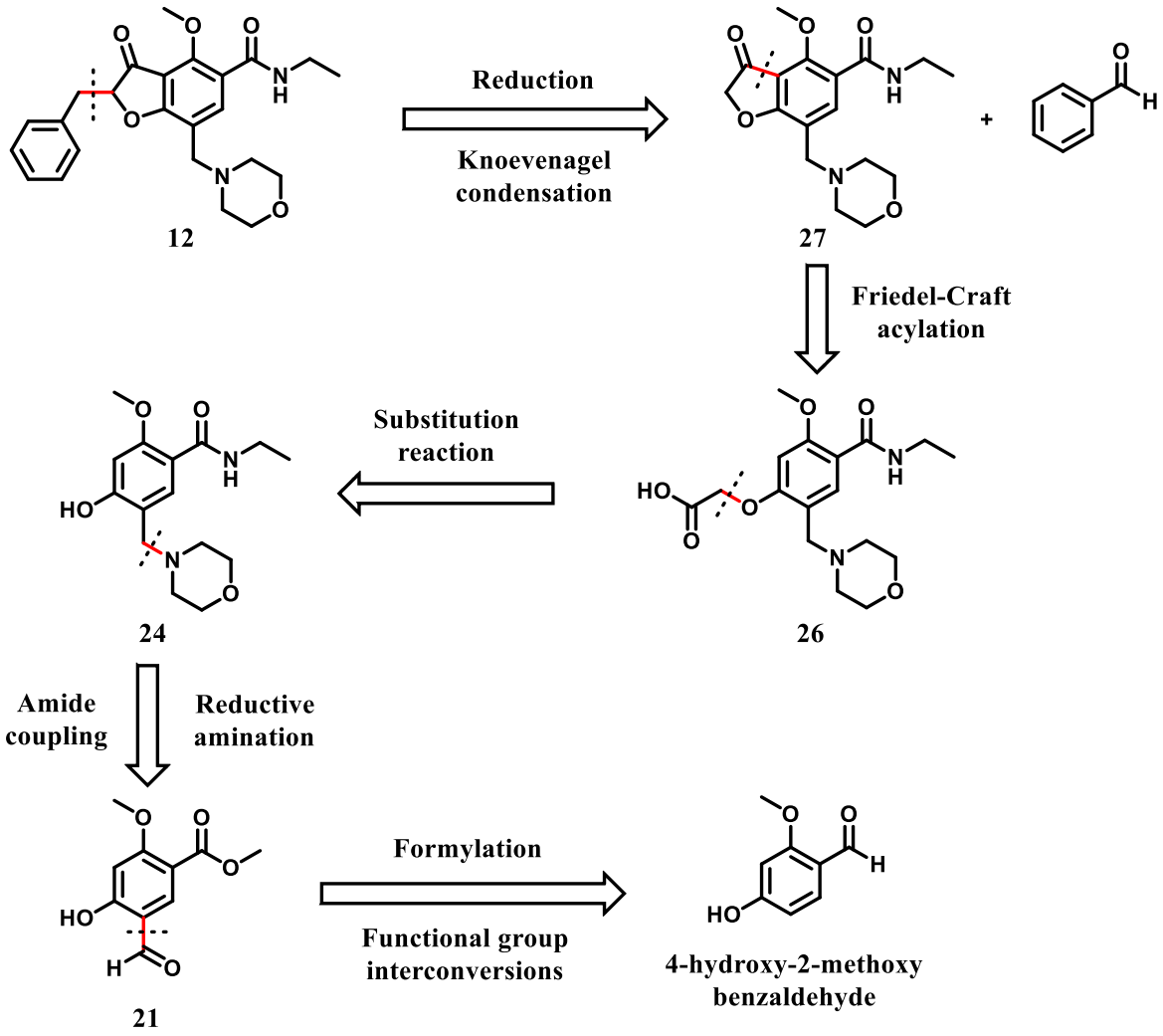
From all of the promising features from both **10** and **11**, the novel inhibitor **12** as a hinge binder was designed. The core scaffold of **12** was designed based on an aurone scaffold (2-benzylidene-1-benzofuran-3(2*H*)-one) which is present in **11**. The final structure of our novel inhibitor, **12**, is shown in **Figure 15**.

It should be noted that our target structure is an aurone. Aurones are members of the flavonoid family, which consists of flavone, isoflavone, and chalcone, for example. Although other members in the flavonoid family have been studied extensively for their pharmacological and therapeutical activities, the pharmacological study of aurones are still less explored.[98] However, recently,

aurones have gained more attention in medicinal chemistry.[99,100] Several reports have shown that derivatives of aurone exhibited a therapeutic effect. For example, aurone derivatives reported by Schoepfer *et al*. could inhibit cyclin-dependent kinases 1 (CDK1),[101] another aurone reported by French *et al*. could inhibit sphingosine kinase (SK) *in vivo* in an animal model without overt toxicity,[102] and other aurones reported by Huang *et al*. exhibited *in vitro* antitumour activities against four cancer cell lines including HCCLM-7 (hepatoma carcinoma cell), Hep-2 (laryngocarcinoma cell), MDA-MB-435S (mammary adenocarcinoma cell), and SW-480 (colon carcinoma cell).[103]

3.3 Retrosynthetic strategies

Initially, the retrosynthesis of the target inhibitor, **12**, was designed based on the work conducted by Wallez *et al*.[104] for a formation of a hydrogenated species, **12**, and Sim *et al*.[105] for a formation of an aurone scaffold. From **Scheme 1**, the retrosynthesis of the proposed final compound **12** started with the reduction of the α,β-unsaturated carbonyl moiety, according to Wallez *et al*.[104] This was followed by the disconnection of the resulted intermediate *via* a Knoevenagel-type condensation to yield intermediate **27** and benzaldehyde, according to Sim *et al*.[105] Then, **27** was disconnected using an intramolecular Friedel-Crafts acylation to give **26**. The acid side chain in **26** was detached based on a substitution reaction to give a hydroxyl group in compound **24**. The morpholine incorporated in **24** was disconnected based on the reductive amination pathway, according to Sato *et al*.,[106] resulting in **21**, which consisted of an aldehyde functional group. The intermediate **21** was then disconnected using a formylation reaction from Agarwal *et al*.[107] to give a core structure followed by functional group interconversion from a methyl ester to an aldehyde to give a commercially available starting material 4-hydroxy-2-methoxybenzaldehyde.



Scheme 1: Retrosynthetic analysis of target inhibitor **12**.

3.4 Synthesis of a model system

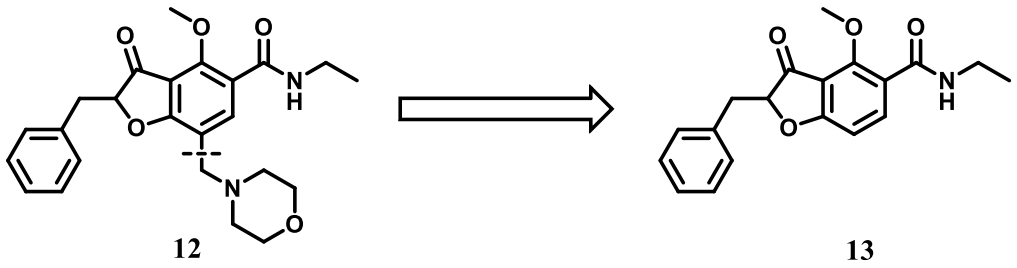
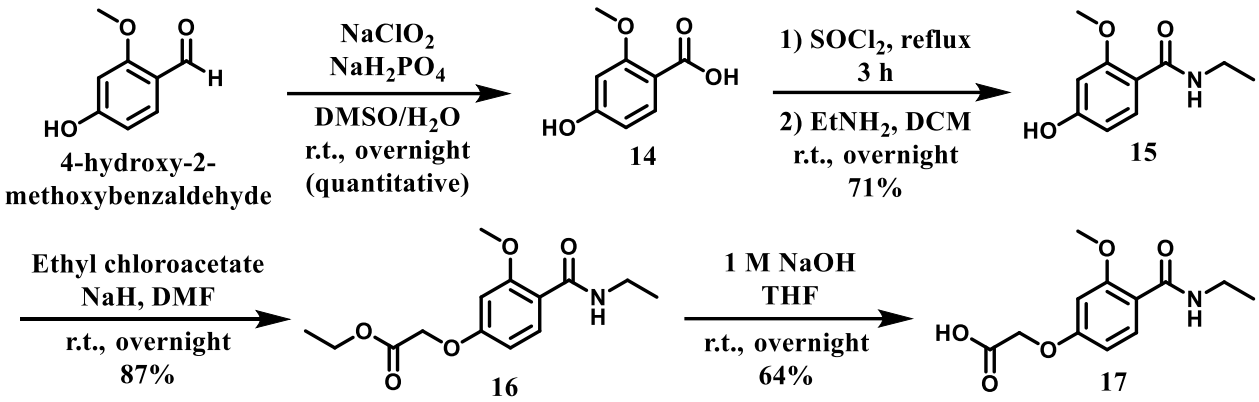


Figure 16: Structure of a model inhibitor **13**.

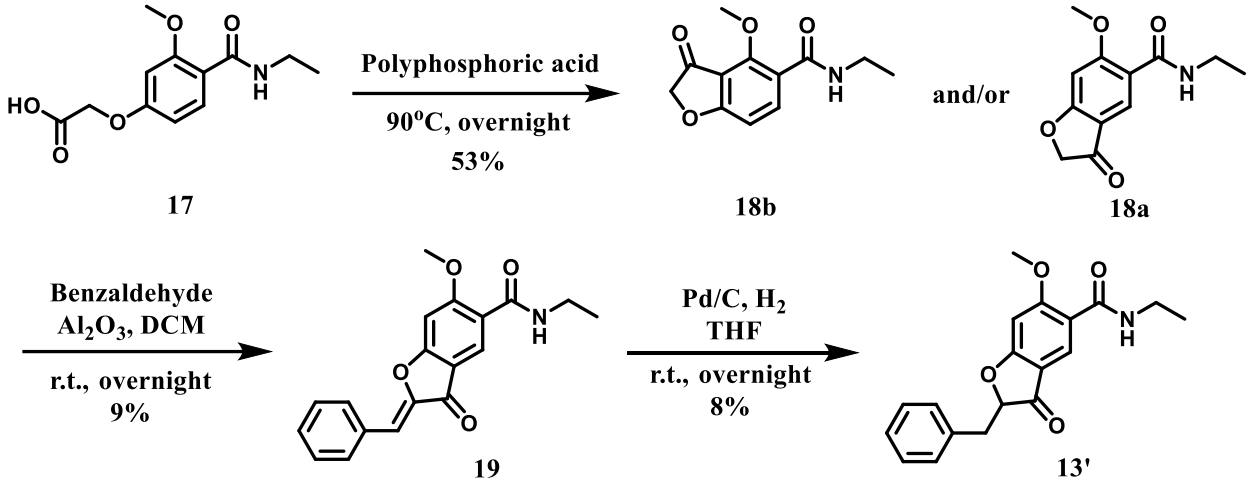
In order to rapidly validate our synthetic strategy, using an acid-catalysed Friedel-Crafts acylation to form the aurone core, compound **12** could be simpified to the model, compound **13** shown in **Figure 16**. This would allow the optimisation of the synthetic conditions and would act as a proof of concept for this approach before the more elaborated compound **9** was being synthesised.



Scheme 2: The first four steps of the synthesis of a model inhibitor **13**.

The initial inhibitor **13** was synthesised from a commercially available starting material 4-hydroxy-2-methoxybenzaldehyde (shown in **Scheme 2**). Pinnick oxidation methodology[108] was used to oxidise 4-hydroxy-2-methoxybenzaldehyde affording **14** in a quantitative yield. Amidation of **14** through a 2-step process, acyl chloride formation and the substitution with ethylamine,[109] afforded **15** in a good yield (71%). Initially, we attempted to use chloroacetic acid with NaH in DMF[110] to install the carboxylic acid side chain. However, with the use of NaH, no reaction occurred. This might be due to the fact that chloroacetic acid was deprotonated leading to a competitive self reaction. Thus, an alternative route was used which consisted of two steps: the generation of ester **16** *via* a substitution reaction of **15** with ethyl chloroacetate, followed by hydrolysis of the ethyl ester to give the acid **17**.

Having prepared **17** in 64% yield, intramolecular Friedel-Crafts acylation was carried out using polyphosphoric acid[105] to activate the carboxylic acid. While the reaction was successful, the cyclisation could have two regiochemical outcomes; either (1) the position *para* to the methoxy group or (2) the position *ortho* to the methoxy group, giving **18a** and/or **18b**, respectively (**Scheme 3**).



Scheme 3: Synthesis of **13′** starting from **17**.

To confirm the regioselectivity of the formation of either **18a** and/or **18b**, ^{1}H-NMR analysis was used. As indicated in **Figure 17**, characteristic signals that were used to identify the formation of **18a** over **18b** were the singlet at 6.87 ppm and the other singlet at 8.10 ppm. These two signals corresponded to the H atoms in the aromatic ring *para* to each other in **18a**. In contrast, for **18b**, the aromatic protons would couple to each other and appear as a pair of doublets.

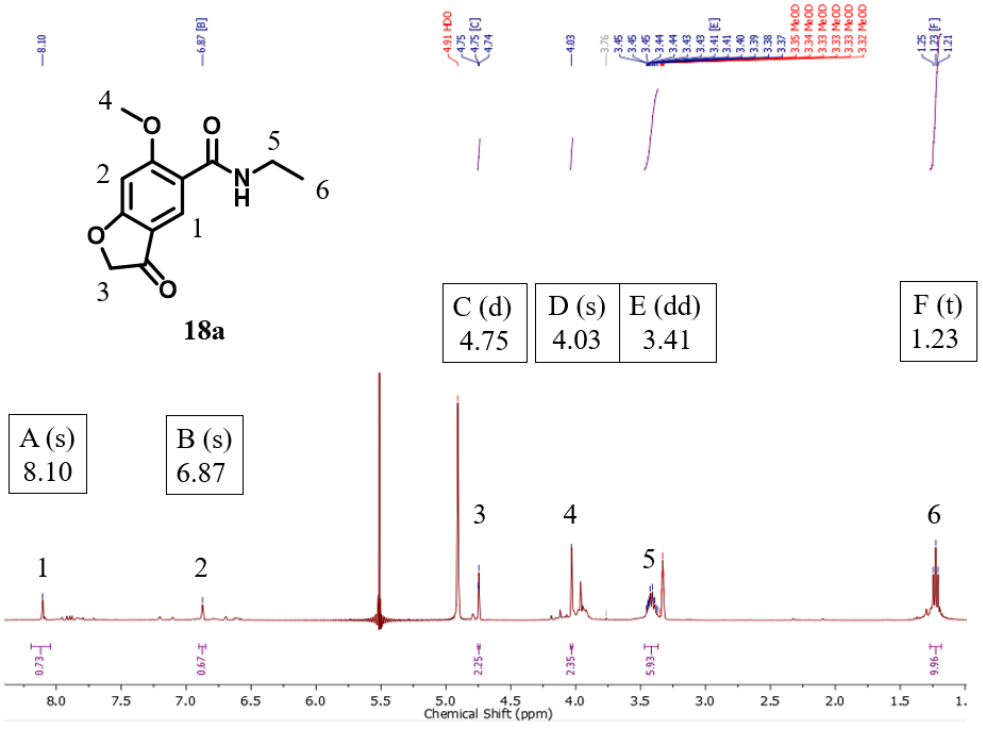


Figure 17: ^{1}H-NMR signals of compound **18a**.

We proposed that **18a** was the only product formed from the cyclisation reaction because of the steric hindrance from the methoxy group. Although the product obtained from the cyclisation reaction was not the one we targeted, we continued with the reaction sequence to test out the final steps. Knoevenagel-type condensation between **18a** and benzaldehyde using aluminium(III) oxide as a catalyst[104] successfully provided **19** in 9%. The relatively low yield of this condensation might be attributed to the use of activated, neutral aluminium(III) oxide, which was not basic enough to catalyse the condensation.

To further confirm the successful synthesis and structure of compound **19**, a single crystal of this compound was grown and studied by X-ray crystallography. The crystal structure of **19** was determined as shown in **Figure 18**. According to the crystal structure of **19**, it was confirmed that compound **19** was in *Z* configuration. The results confirmed that the Knoevenagel-type condensation could furnish the aurone core scaffold with *Z* configuration.

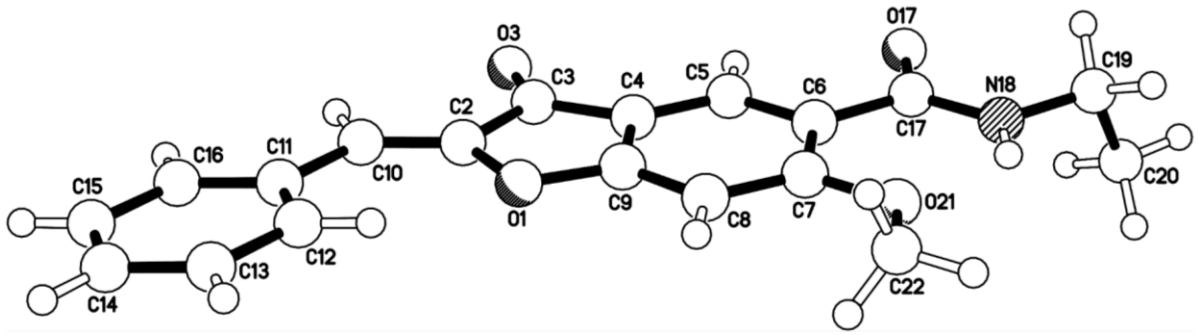


Figure 18: Crystal structure of **19**.

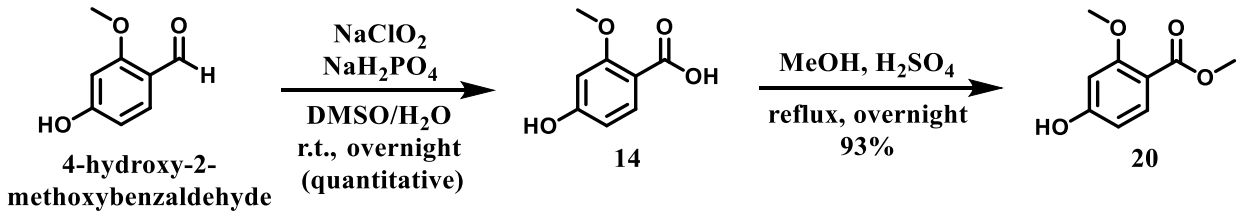
The formation of **19** was followed by a hydrogenation reaction at the double bond, utilising Pd/C as a catalyst, giving **13′** in 8% yield. The issue regarding the low yield of hydrogenation of **19** was due to side reactions giving a number of unidentified by-products. The overall yield of the synthesis of the model compound, **13′**, was 0.15% in 7 steps. The relatively low yield from the whole synthesis was ascribed to the last two steps which gave the product at only 9% and 8%, respectively.

The synthesis of **13′** certified that the synthetic strategies for making the aurone target were valid and could be applied directly to the synthesis of the desired inhibitor **12** with additional steps for the morpholino moiety attachment. Although the cyclisation of **17** did not provide **18a** with the right regiochemistry, the cyclisation conditions used in this section could still be used since the 5-

position would be blocked with the morpholino moiety in the actual target. Therefore, the only possibility for the cyclisation reaction would be the cyclisation to the 3-position giving the correct regioselectivity for the desired inhibitor **12**.

3.5 Attempted synthesis of the proposed inhibitor 12

After successfully synthesising the model compound, attention was turned to the synthesis of the proposed inhibitor **12**. The synthesis, as before, began with a Pinnick oxidation of 4-hydroxy-2-methoxybenzaldehyde to yield intermediate **14** in a quantitative yield (**Scheme 4**). The next step was to protect the carboxylic acid as an ester. As such, the formation of methyl ester **20** by a simple esterification using methanol and a few drops of sulfuric acid as a catalyst was undertaken.



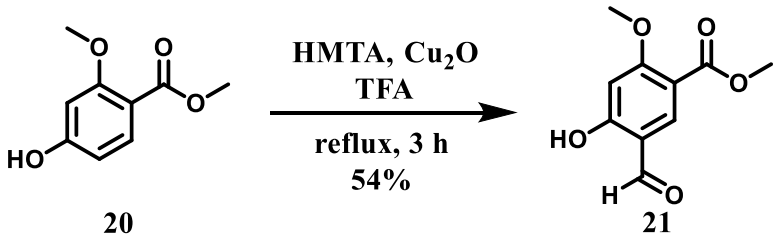
Scheme 4: The first two steps of the synthesis of the proposed product **12**.

After obtaining ester **20** (93% yield), many methods were screened to attach the aldehyde moiety in the next step. Firstly, a Vilsmeier-Haack reaction using DMF and phosphoryl chloride was attempted. Unfortunately, this reaction was unsuccessful likely due to the low reactivity of **20**. Therefore, the alternative pathways were tested in order to allow *ortho*-formylation as listed in **Table 2**. In entry 2, *ortho*-formylation of **20** using α,α-dichloromethyl methyl ether and $TiCl_4$, according to Ramos-Tomillero *et al*.,[111] was attempted. However, no reaction occurred. Another trial for *ortho*-formylation of **20** using paraformaldehyde in the presence of a $MgCl_2$–Et_3N base system (entry 3, **Table 2**) was attempted according to Akselsen *et al*.[112] Unfortunately, this reaction was still unsuccessful. The failures from the last two attempts were likely due to the low reactivity of **20**.

Table 2: Screening reaction conditions for formylation of **20**.

Entry	Reagents and conditions	Results	References
1	1) DMF, $POCl_3$ (2.5 eq.), 100°C, 22 h 2) H_2O work-up	No reaction	[113]
2	α,α-dichloromethyl methylether (6.3 eq.), $TiCl_4$ (11.2 eq.), DCM, r.t., 18 h	No reaction	[111]
3	$MgCl_2$ (2 eq.), Et_3N (2 eq.), $(CH_2O)_n$ (3 eq.), THF, reflux, 48 h	No reaction	[112]
4	1) HMTA (2 eq.), Cu_2O (1 eq.), TFA, reflux 4.5 h 2) 3 M HCl solution, r.t., 1 h	Obtained the desired product **21**, 54%	[114]

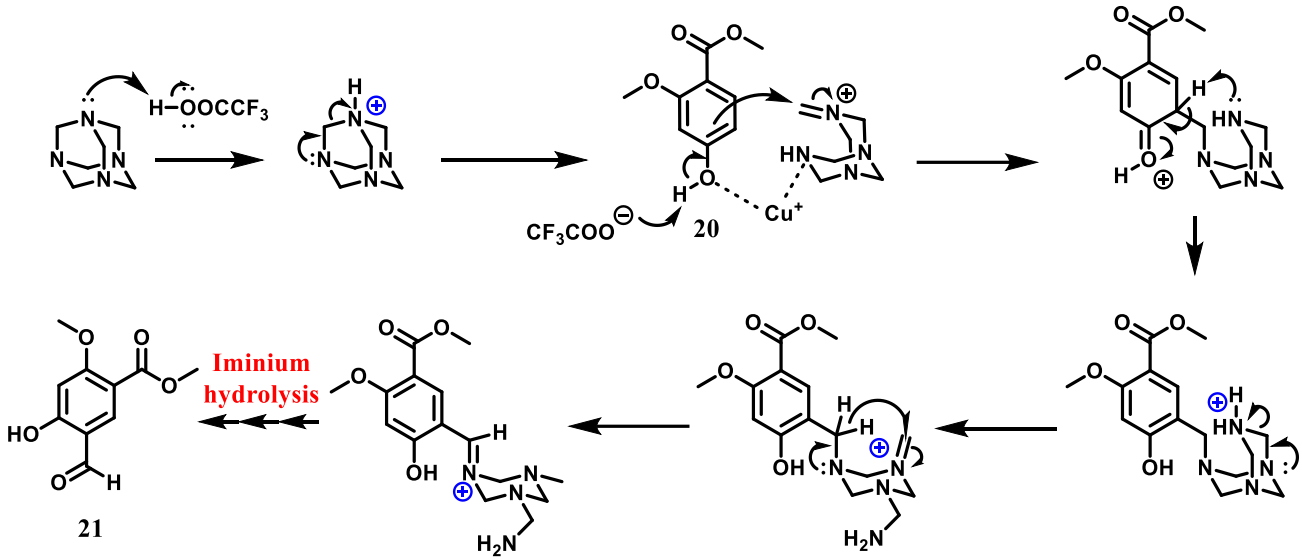
According to Fu *et al*., the formylation of phenol substrates bearing carbonyl substituents could be achieved by using copper(II) oxide as a catalyst.[114] Therefore, a copper-mediated Duff reaction was performed (entry 4, **Table 2**) as shown in **Scheme 5**.



Scheme 5: Copper-mediated Duff reaction of **20**.

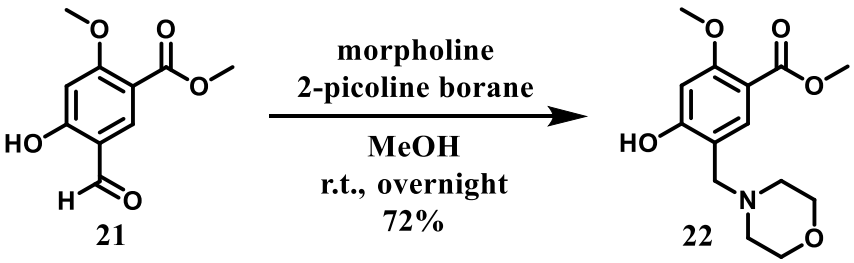
Although the mechanism of the Duff reaction (**Scheme 6**) is somewhat similar to the Vilsmeier-Haack reaction, a different reagent (hexamethylenetetramine or HMTA) was used. According to Fu *et al*.,[114] the successful synthesis of **21** could perhaps be attributed to the use of the Cu(I) species which could coordinate to the hydroxyl oxygen and induced the deprotonation of the phenol by trifluoroacetate. The Cu(I) species also coordinated to the amine of HMTA, bringing the HMTA

close to the *ortho* position of the substrate and promoting the *ortho* formylation (**Scheme 6**). Given the outcome of the reaction, the desired product **21** was obtained in 54% yield.



Scheme 6: Proposed mechanism for the copper-mediated Duff reaction with the intermediate **20** to give **21**, reproduced from Fu *et al.*[114] and Wang *et al.*[115]

As mentioned in the synthesis of **18a** (**Scheme 3**), there could be two possible products of the reaction of **18**, the 5-substituted or 3-substituted products. The product that was recovered in this case showed only singlets in the aromatic region of the ^{1}H-NMR which indicated that the product was 5-substituted. Therefore, this confirmed that we could successfully synthesise the intermediate **21**.



Scheme 7: Reductive amination of **21**.

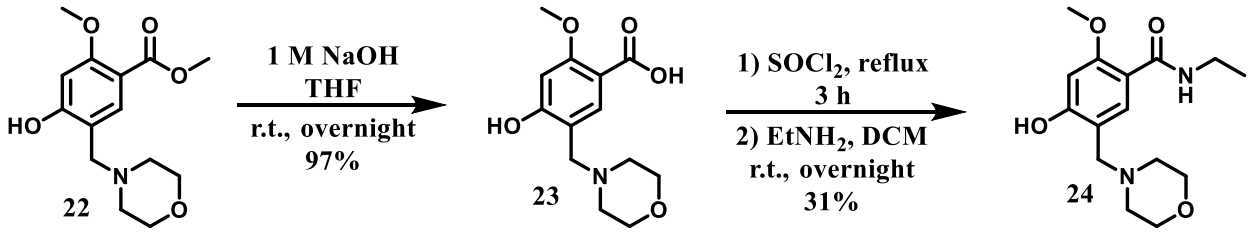
Having isolated **21**, a reductive amination using 2-picoline borane with morpholine at room temperature was performed to give the intermediate **22** in high yield (72%) as shown in **Scheme 7**. Next, we attempted to install the amide side chain. There are a number of reports in the literature

whereby an ester is converted to an amide in one step, which could reduce the number of steps taken in the synthesis. These include the use of either lanthanum(III) trifluoromethanesulfonate ($La(OTf)_3$) or 1,5,7-triazabicyclo[4.4.0]dec-5-ene (TBD) as a catalyst.

Table 3: Screening reaction conditions for direct aminolysis of **22**.

Entry	Reagents and conditions	Results	References
1	$La(OTf)_3$ (0.05 eq.), $EtNH_2$ (1.2 eq.), toluene, 50°C, 72 h	No reaction	[116]
2	TBD (0.3 eq.), $EtNH_2$ (1.2 eq.), THF, reflux, 22 h	No reaction	[117]

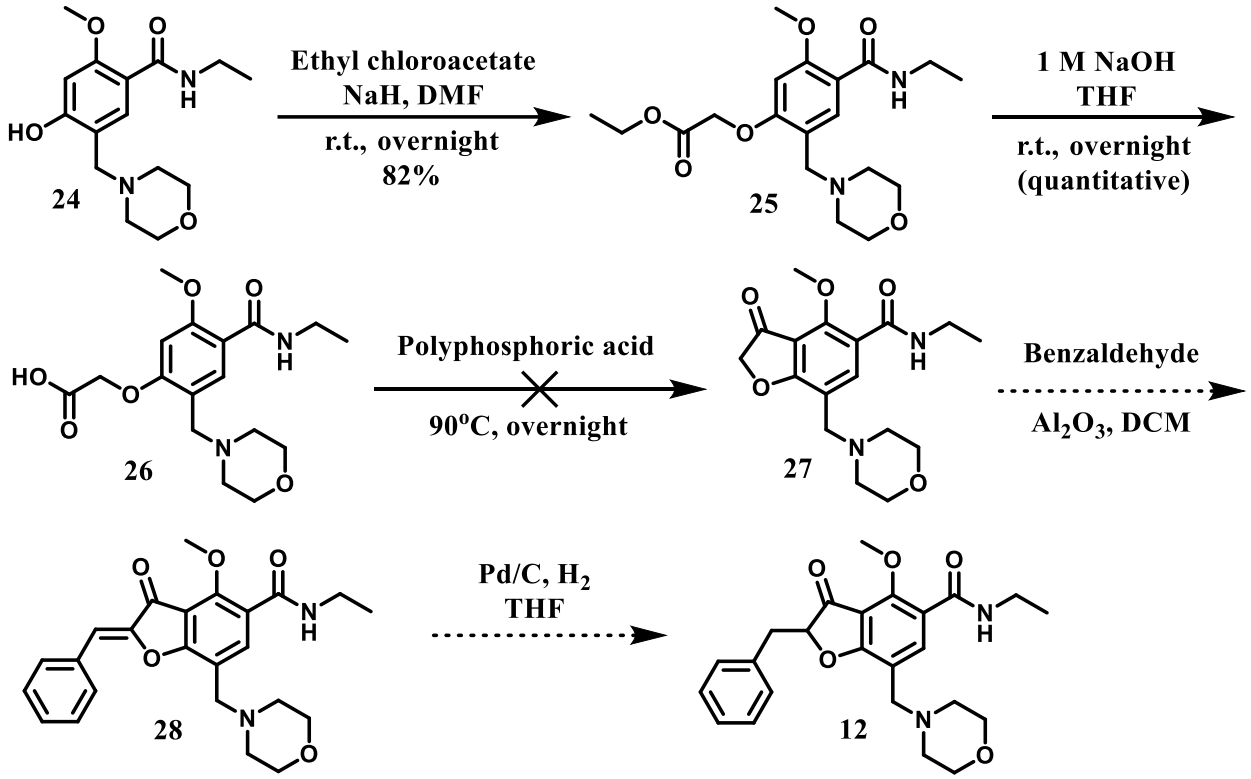
As indicated in **Table 3**, two different conditions for direct aminolysis reaction were attempted. For the first entry, direct amidation of **22** catalysed by $La(OTf)_3$ was attempted. The reaction was stirred at room temperature for 72 hours. Unfortunately, no reaction occurred, noting only the recovery of starting material **22**. The rationale behind this failure might be attributed to the coordination of $La(OTf)_3$ to the *ortho* hydroxyl and carbonyl oxygens forming a 6-membered ring chelate complex. The other direct transformation of the ester to the amide using TBD as a catalyst was attempted by refluxing the mixture in THF for 22 hours. This reaction condition was also unsuccessful.



Scheme 8: 2-step amidation of **22** to give **24**.

Since the direct amidation conditions that were attempted failed, indirect methods including a 2-step synthesis could be performed instead (**Scheme 8**). The first reaction in this sequence was the hydrolysis of **22** to give a carboxylic acid **23** using 1 M NaOH solution in THF. This reaction gave the intermediate **23** in a high yield (97%). Subsequently, **23** was heated under a reflux condition

with thionyl chloride to make an acid chloride as an active intermediate. After the acid chloride was formed, it was treated with ethylamine in DCM under inert atmosphere to give the amide **24** (31%).



Scheme 9: Proposed synthetic pathway of **12** starting from **24**.

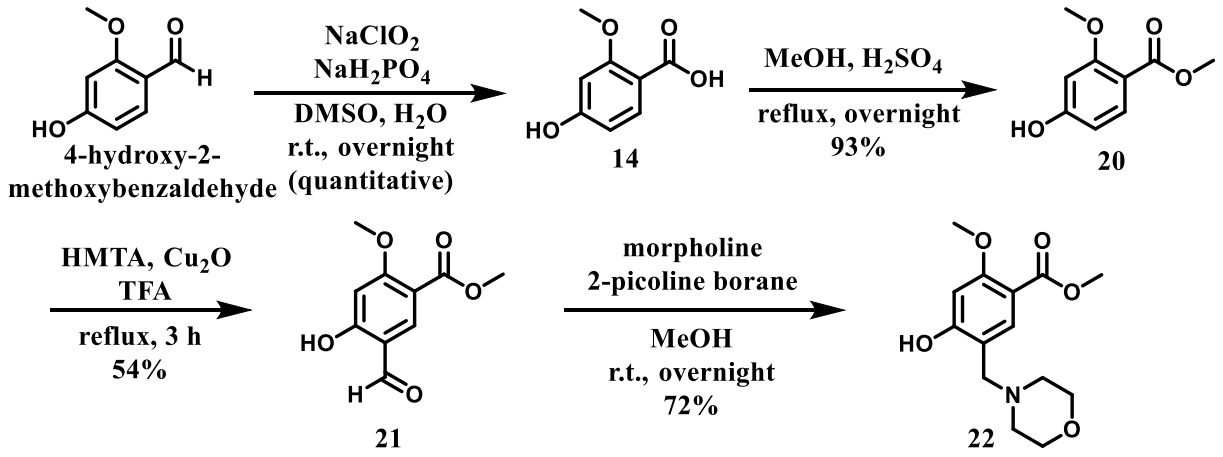
The next two steps were performed using the same reaction conditions as in the synthesis of the model compound as shown in **Scheme 2**, which involved the substitution of the hydroxyl group with ethyl chloroacetate to give intermediate **25** followed by the ester hydrolysis to give **26** (**Scheme 9**). However, when **26** was treated with polyphosphoric acid, as was use for the model compound, the results were different. There was only little conversion as indicated by TLC.

The ^{1}H-NMR signals obtained from the crude product in this step did not contain the expected signal which corresponds to the CH_2 group of the tetrahydrofuran-3-one moiety. Additionally, there were two peaks in the aromatic region which were still present, indicating that no cyclisation occurred. Analysis of the ^{1}H-NMR spectrum indicated that the product obtained from this reaction was the cleavage of the phenoxy alkyl bond in the intermediate **26** to give compound **24**, which matched with the MS result obtained from mass spectrometry. The phenoxy alkyl bond cleavage

could be achieved instead of the cyclisation due to the adjusted reaction condition to higher temperature and longer reaction time. Although we tried to adjust the reaction conditions in terms of the amount of the polyphosphoric acid, reaction time, and temperature in order to minimise the phenoxy alkyl bond cleavage, all the efforts gave out the same outcome; i.e., no cyclisation, but the production of the phenoxy alkyl bond cleavage varied.

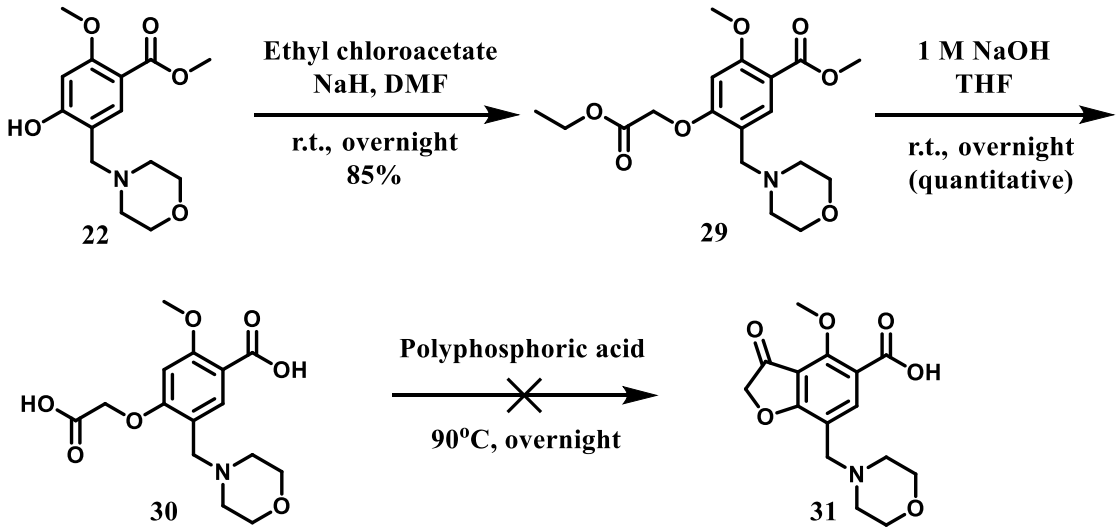
3.6 Reduced step synthesis of inhibitor 12

While we made good progress towards the target, the route so far was relatively long. We therefore wanted to reduce the number of steps involved. Building on our strategy so far, we proposed an alternative synthetic pathway shown in **Scheme 10**.



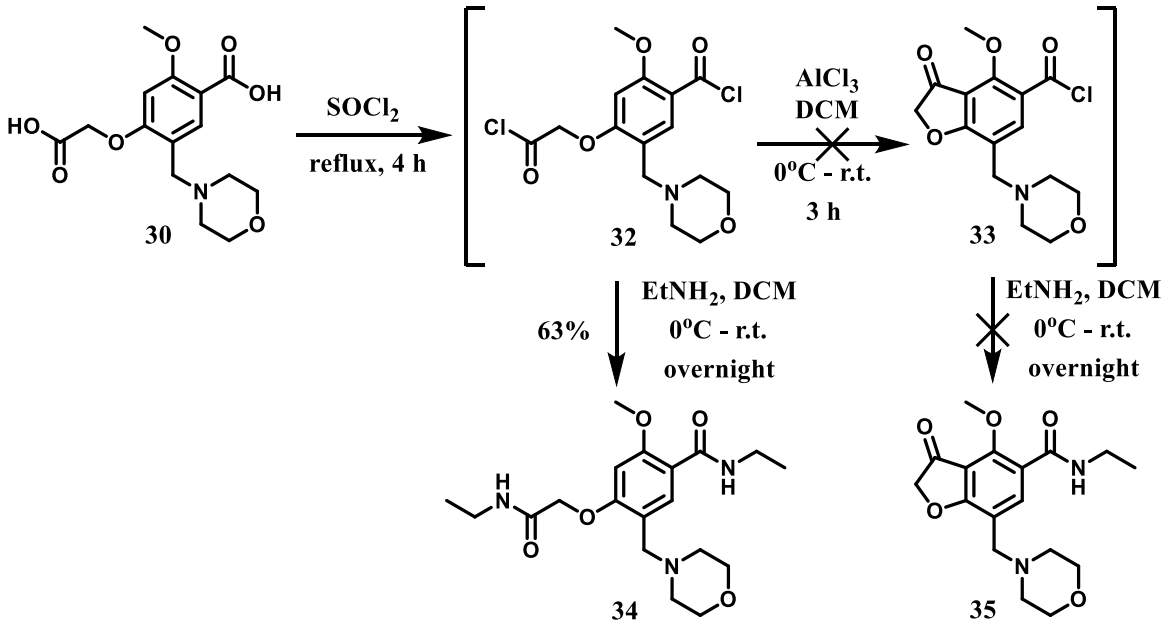
Scheme 10: The first four steps of the reduced step synthetic pathway for inhibitor **12**.

The first four steps are the same as the synthesis of **12** (**Scheme 4**, **5**, and **7**). However, instead of performing the ester hydrolysis followed by amidation, we decided to do the substitution reaction first in order to install the side chain required for cyclisation (**Scheme 11**). This successfully yielded **29** which only required one hydrolysis step using 1 M NaOH to hydrolyse both esters in **29** to give the two free acid side chains. After that, the cyclisation using polyphosphoric acid was attempted. Unfortunately, no cyclised product was observed.



Scheme 11: Attempted synthesis of **31** from **22**.

We also tried a one-pot synthesis of **35**, starting from **30**, which is depicted in **Scheme 12**.



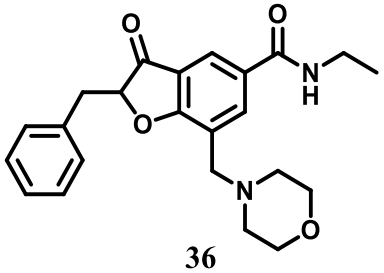
Scheme 12: Attempted one-pot synthesis of **35**.

We attempted to firstly convert both carboxylic acids to their corresponding acid chlorides by reacting **30** with neat thionyl chloride. After four hours, the reaction was assumed to be complete and intermediate **32** was assumed to be formed. After removing the remaining thionyl chloride, compound **32** was re-dissolved in anhydrous DCM at 0°C and aluminium chloride was added to

catalyse the cyclisation. The reaction was left to stir at room temperature for 3 hours as the reaction was monitored by TLC periodically. Once all the starting material seemed to be consumed, the aluminium chloride was filtered off and the intermediate was treated with ethylamine. The product obtained following work-up and purification still contained some impurities, but ^{1}H-NMR had clearly indicated that no cyclisation occurred. Instead, the amide coupling took place at both ends of the acid chloride in **32,** giving the double amide product, **34**.

3.7 Synthesis of the second target inhibitor 36

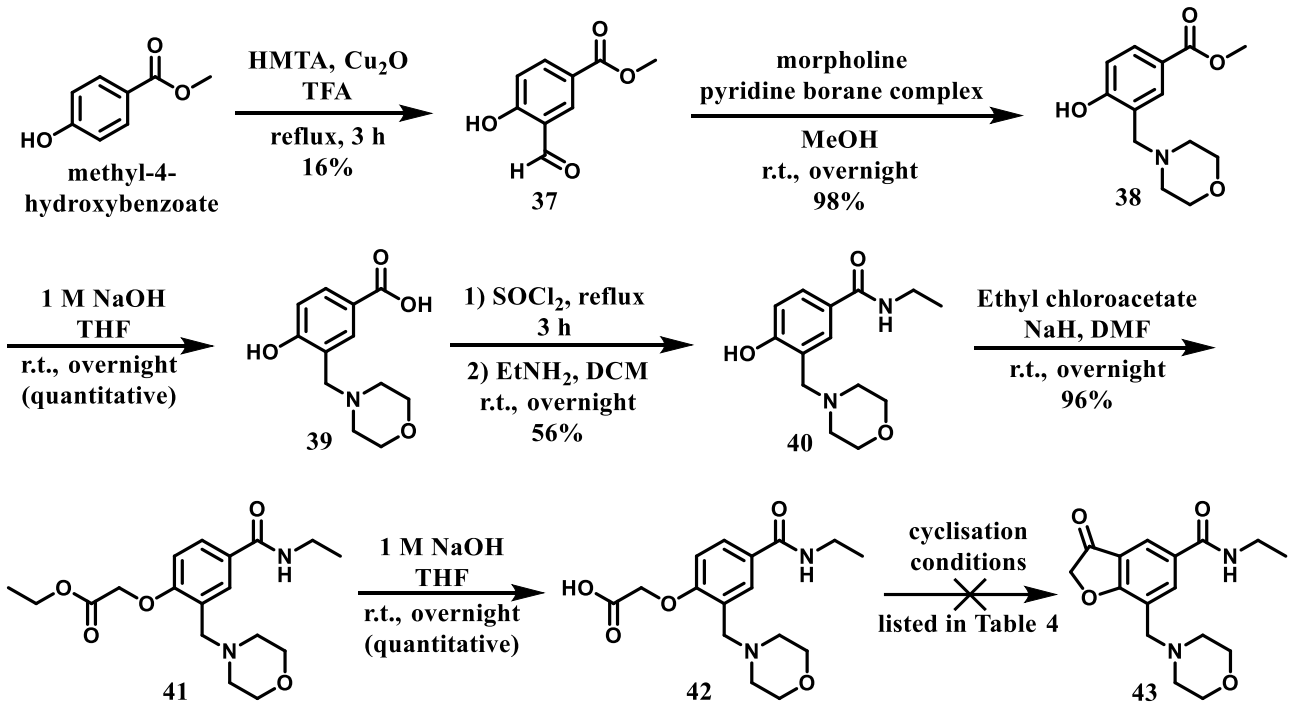
To investigate the cyclisation reaction using polyphosphoric acid with a substrate bearing morpholino moiety, another substrate, **36** (**Figure 19**), which closely resembles compound **12** would be synthesised. This analogue does not contain the aromatic methoxy group, which was present in compound **12**, and hence has one less H-bond acceptor as shown in **Figure 19**.



36

Figure 19: Structure of the second target inhibitor, **36**.

The synthetic route of **36** was based on the synthesis of **12**. This is summarised in **Scheme 13** and starts from the commercially available methyl-4-hydroxybenzoate. Duff reaction conditions (HMTA, Cu_2O) under a reflux condition for 3 hours were applied to formylate the starting material. This gave **37** in a low yield (16%). After that, **37** was subjected to reductive amination by reacting with a pyridine borane complex and morpholine at room temperature to give **38**, followed by hydrolysis of the methyl ester moiety using 1 M NaOH to give **39**. The free carboxylic acid was transformed to the ethyl amide in **40** and the hydroxyl side chain was substituted with ethyl chloroacetate to give **41** (96%). The ethyl ester was subsequently hydrolysed to give compound **42** which was the key intermediate for the cyclisation reaction.



Scheme 13: Synthesis of the second target inhibitor **36**.

Cyclisation of **42** was initially attempted using polyphosphoric acid in various reaction conditions (different reaction temperatures and durations, **Table 4**). In all cases, the production of the cyclised product was still unsuccessful. Following a literature search, we decided to utilise other conditions which were previously reported for the synthesis of the required benzofuran-3(*2H*)-one core scaffold. Those conditions are summarised in **Table 4**.

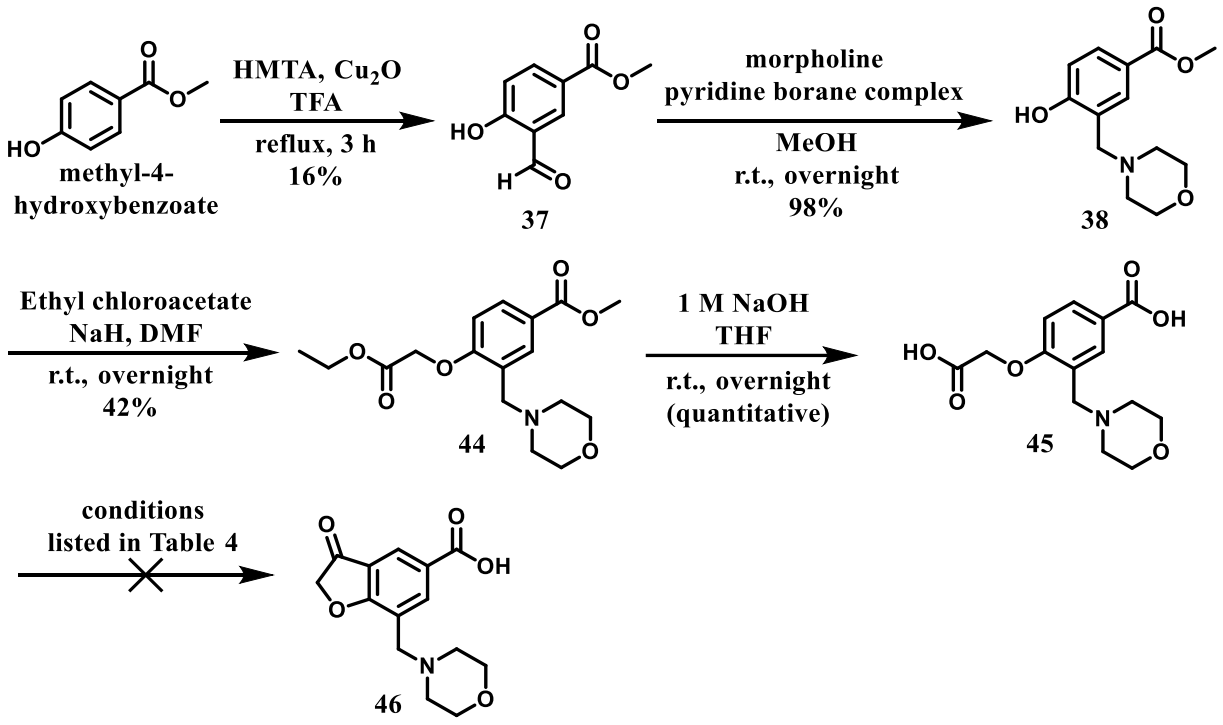
Table 4: Screening reaction conditions for cyclisation of benzofuran-3(*2H*)-one core scaffold of **42**.

Entry	Reagents and conditions	Results	References
1	Polyphosphoric acid (excess), 90°C, overnight	No reaction	[105]
2	Polyphosphoric acid (excess), 90°C, 48 h	No reaction	
3	Polyphosphoric acid (excess), 90°C, 72 h	No reaction	
4	Polyphosphoric acid (excess), 80°C, 5 days	No reaction	
5	TfOH (30 eq.), DCM, 0°C – r.t., overnight	No reaction	[118]
6	1) $SOCl_2$ (excess), reflux, 4 h 2) $AlCl_3$ (2 eq.), DCM, 0°C – r.t., overnight	No reaction	[119]

The first attempt was to use trifluoromethanesulfonic acid (TfOH) at room temperature. These milder reaction conditions from Wang *et al.*[118] were only explored for the cyclisation of cores containing electron donating groups. This might explain why no cyclisation of **42** was observed, since our molecule contains one electron withdrawing group attached to the benzene ring. We also tried to increase the temperature to 50°C and leave the reaction for longer, but no improvement in the conversion was observed. We then decided to convert the acid side chain in **42** to the more reactive acid chloride derivative. This was subsequently treated with a Lewis acid catalyst for a Friedel-Crafts acylation according to a reported procedure.[119] In all cases, the reactions were unsuccessful and no reaction was observed.

3.8 Reduced step synthesis of inhibitor 36

The optimised, shorter synthesis previously described in section **3.6** was also employed in order to accelerate the synthesis of **36**. The modified pathway is shown in **Scheme 14**. Intermediate **45** was successfully synthesised in four steps and was then subjected to a series of different cyclisation reaction conditions listed in **Table 4**. However, once again, none of them gave the desired product.



Scheme 14: Reduced step synthetic pathway for the second inhibitor **36**.

3.9 Possible explanations for the failure of the cyclisation of the benzofuran-3(*2H*)-one core

Despite the many attempts at the cyclisation of our intermediates into the desired benzofuran-3(*2H*)-one core, this reaction was proved to be unsuccessful. This could be due to a variety of reasons, most of which are discussed below.

1) **The low solubility of the intermediate**: The presence of both the morpholino moiety and the free carboxylic acid in all intermediates causes them to exist in a zwitterionic form at neutral pH. This makes the intermediates less soluble in organic solvent. The evidence could be deduced from the work up process of the cyclisation reaction; most of the

unreacted starting material was completely soluble in the aqueous layer regardless of its pH. This also made it very difficult to recover the starting material.

2) **The substrate reactivity**: The electron withdrawing amide substituent on the benzene ring decreases the electron density of the aromatic ring and thus reduces its reactivity towards electrophilic substitution reactions.

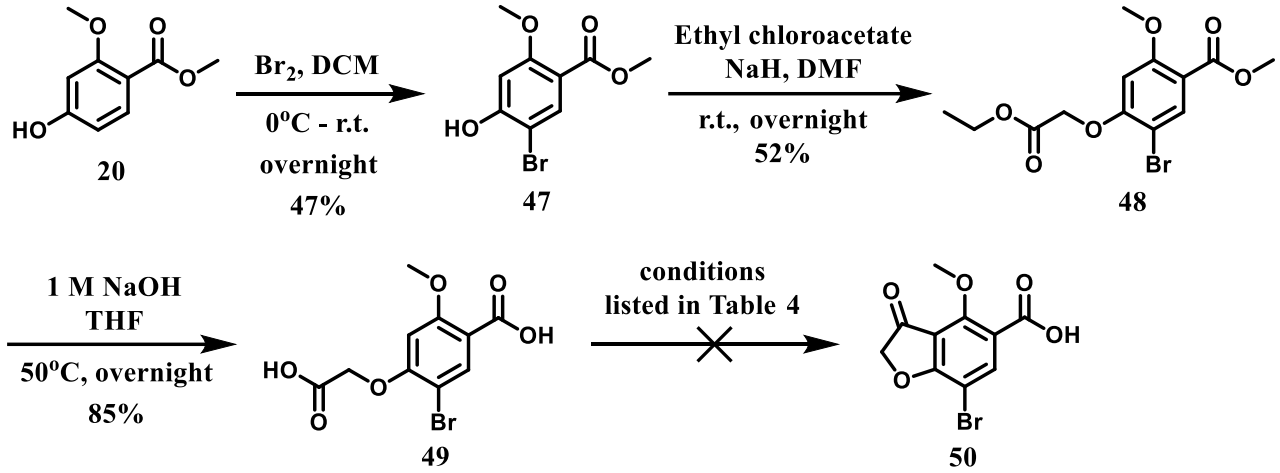
Apart from the potential issues which impeded the cyclisation of the benzofuran-3(*2H*)-one core discussed above, we would also explore the choice of reagents aside from the ones listed in **Table 4**.

We decided to address each issue, one by one, in order to successfully form the cyclised benzofuran-3(*2H*)-one core. All modifications undertaken are summarised below.

3.9.1 Addressing the solubility issue

Based on the results we acquired throughout the syntheses stated earlier, it was evident that the morpholino moiety was a critical feature in the solubility of the molecule. Therefore, we decided to change the morpholino moiety into another functional group which could later be transformed into this required moiety. Following a literature search, we found a procedure which employed a Mannich-type three-component reaction between an aromatic halide, a paraformaldehyde, and an amine to synthesise a functionalised tertiary benzylamine.[120] The best halide substituent of aromatic halide from the literature precedent was bromine.[120] For this reason, we decided to incorporate a bromine substituent into our intermediates and attempt the cyclisation.

To do this (**Scheme 15**), compound **20** was brominated using elemental bromine dissolved in DCM starting from 0°C to room temperature overnight, affording **47** (47%), where the bromine was found to be present at the expected 5-position of the aromatic ring. Reaction of **47** with ethyl chloroacetate added the side chain ready for the cyclisation reaction. Both esters in the molecule were hydrolysed using 1 M NaOH at 50°C overnight to give **49** (85%). Not only did **49** prove to be more soluble in various organic solvents compared to **30** (**Scheme 12**), but the purification process of this molecule was also less troublesome due to its improved solubility.



Scheme 15: Synthetic scheme used to change the morpholine substituent to bromide in order to improve the solubility of the compound.

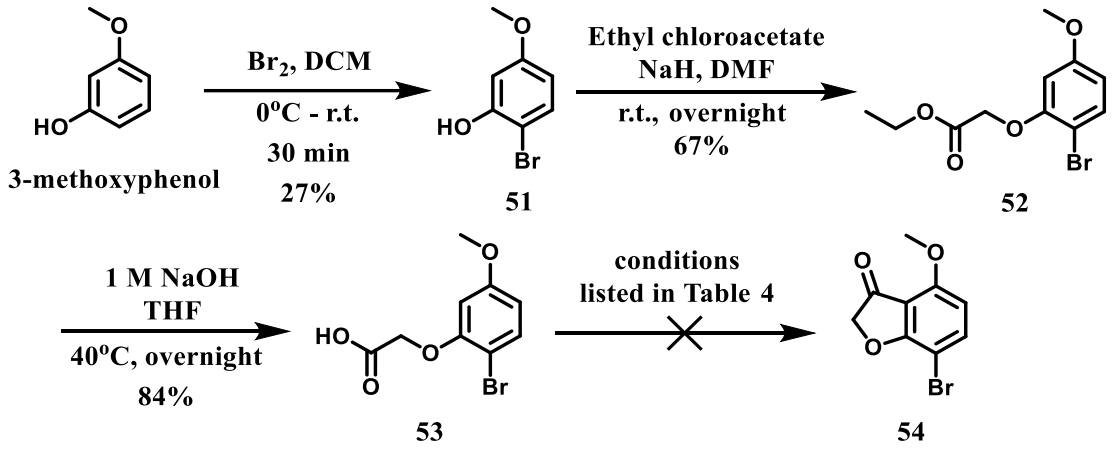
Once the cyclisation intermediate was generated, it was subjected to cyclisation with the reaction conditions listed in **Table 4**. Although the solubility of intermediate **49** was improved, the cyclisation was still not accomplished, which implied that solubility alone was not the determining factor in the unsuccessful chemistry.

3.9.2 Addressing the substrate reactivity

We then investigated the electronic effect of the benzene ring substituents, primarily the carbonyl functionality from either the carboxylic acid, or the ester, or the amide group. Even though these electron withdrawing substituents are meta directing and thus directing the cyclisation to the required position, they also decrease the electron density of the aromatic ring thus making it less activated.

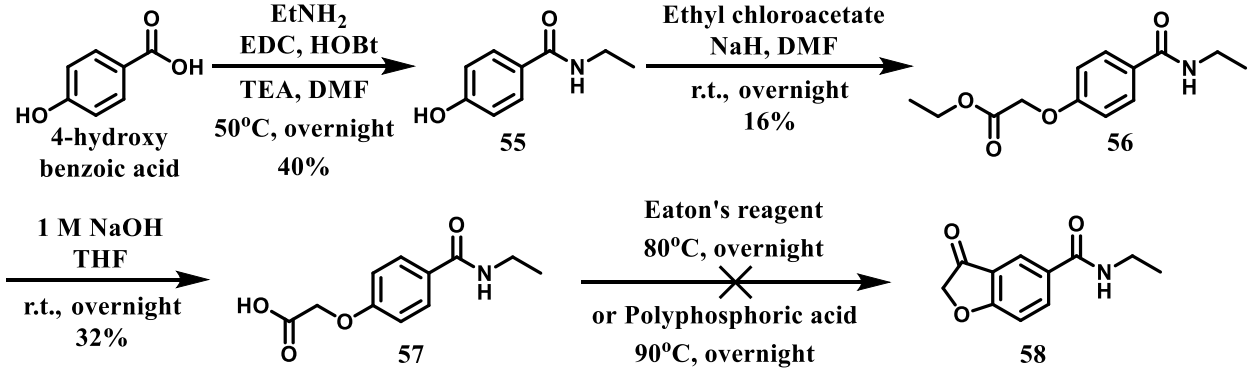
We performed a model synthesis of the core aromatic system as shown in **Scheme 16**. The synthesis began with the bromination of the commercially available starting material 3-methoxyphenol using elemental bromine dissolved in DCM, giving **51**. This bromination was achieved in poor yield (27%). The low yield of the bromination came from the side reactions which generated di- and tri-substituted bromine.

Reaction of **51** with ethyl chloroacetate followed by hydrolysis of the resulting intermediate **52** was performed, yielding **53** (84%). Then, **53** was treated with polyphosphoric acid at various temperatures and for different durations, as well as using other conditions listed in **Table 4**. Unfortunately, none of these conditions were successful, indicating that an electronic effect alone cannot be used to explain the failure of the cyclisation reaction with polyphosphoric acid.



Scheme 16: Modified synthesis to investigate the effect of electron withdrawing substituents on cyclisation.

Then, we examined the possibility that a steric effect might play in preventing cyclisation of the core scaffold. This steric effect was thought to arise predominantly from the neighbouring methoxy group. In this case, we carried out the investigation by using 4-hydroxy benzoic acid as the starting material. The modified synthetic scheme is shown in **Scheme 17**.



Scheme 17: Modified synthesis to investigate the effect of sterics on cyclisation.

We started by carrying out an amide coupling reaction of 4-hydroxybenzoic acid with new conditions, using EDC, HOBt, triethylamine, and the amine of interest at 50°C overnight.[121] The formed amide derivative **55** was then reacted with ethyl chloroacetate and hydrolysed to give **57** (32%). The cyclisation reaction was then attempted again, using polyphosphoric acid. This reaction was still unsuccessful.

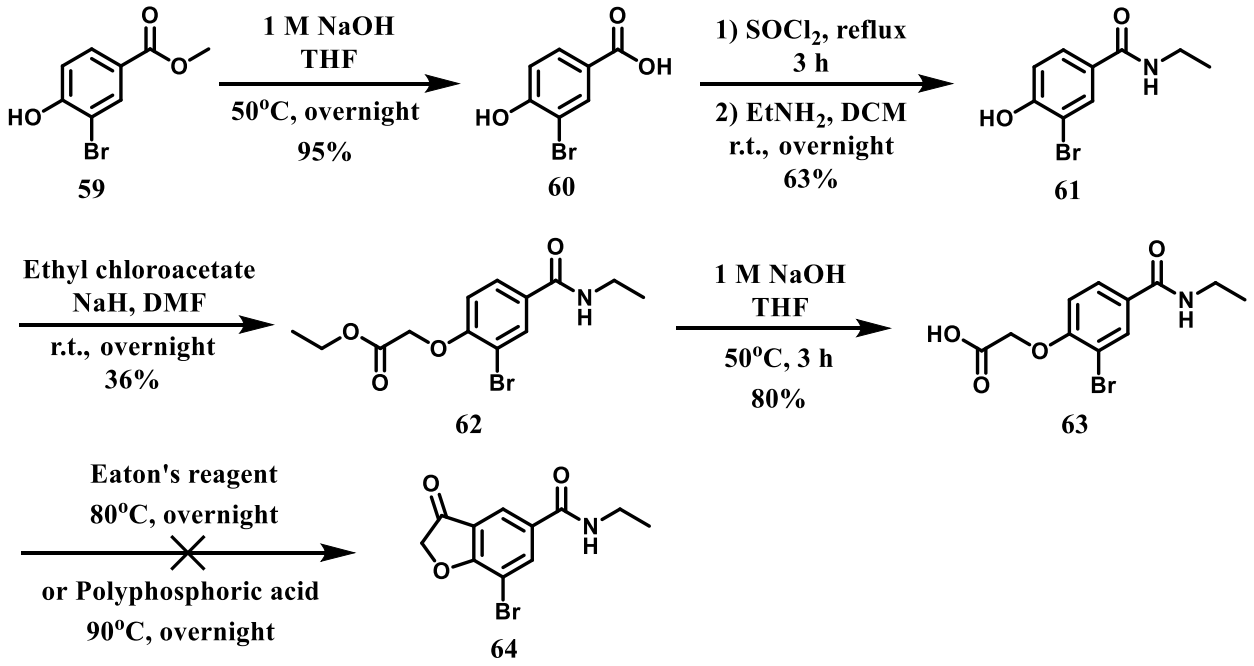
As was seen for the synthesis of the model compound **13′** (**Scheme 3**), the cyclisation reaction took place with a similar core scaffold, but when the structure of the precursor **17** (**Scheme 3**) had the additional methoxy group, it was able to increase the electron density in the aromatic ring. Therefore, taking into consideration both the steric effect and electron density in the aromatic system, we propose that the problem with the cyclisation reaction of our intermediates could be from both effects acting together.

3.9.3 Addressing the choice of reagents for cyclisation

Since the cyclisation conditions listed in **Table 4** and the one used in the one-pot synthesis in **Scheme 12** did not lead to the cyclised product, we considered other reagents. Although polyphosphoric acid is widely used across a range of reactions including alkylation and acylation reactions on aromatic and olefinic systems, it has challenging physical properties; for example, its exceptionally high viscosity, which makes it extremely difficult to stir or utilise at a temperature below 80°C. Not only was it inconvenient to handle, but certain organic compounds were not able to fully dissolve in it even at higher temperatures. This also led to challenging work-ups which required a great deal of base to neutralise all the acid since it was usually used as a solvent. All these problems led us to seek alternative cyclisation reagents with better properties.

Eaton *et al*.[122] have developed a more user friendly reagent, Eaton's reagent, that can be used in place of polyphosphoric acid. Eaton's reagent is prepared by mixing phosphorus pentoxide and methanesulfonic acid in 1:10 proportion by weight. This new reagent has better physical properties; it can be transferred easily and stirred effortlessly, it is safe to handle, and work-up is simple to carry out, giving a clean product. We therefore decided to use Eaton's reagent in our synthesis.

As shown in **Scheme 18**, we prepared the intermediate **63** for the first trial with Eaton's reagent beginning from **59**. The methyl ester side chain in **59** was hydrolysed to the carboxylic acid using 1 M NaOH at 50°C overnight to give **60** in 95% yield. The acid side chain was then converted to an ethyl amide functionality by refluxing with thionyl chloride for 3 hours, followed by treatment with ethylamine at room temperature overnight. This resulted in the formation of **61** (63%). The side chain at the other position was installed by treating **61** with ethyl chloroacetate and sodium hydride overnight to give **62** (36%). The ester side chain in **62** was then hydrolysed by treatment with 1 M NaOH to give **63** which was ready for the attempted cyclisation using Eaton's reagent.



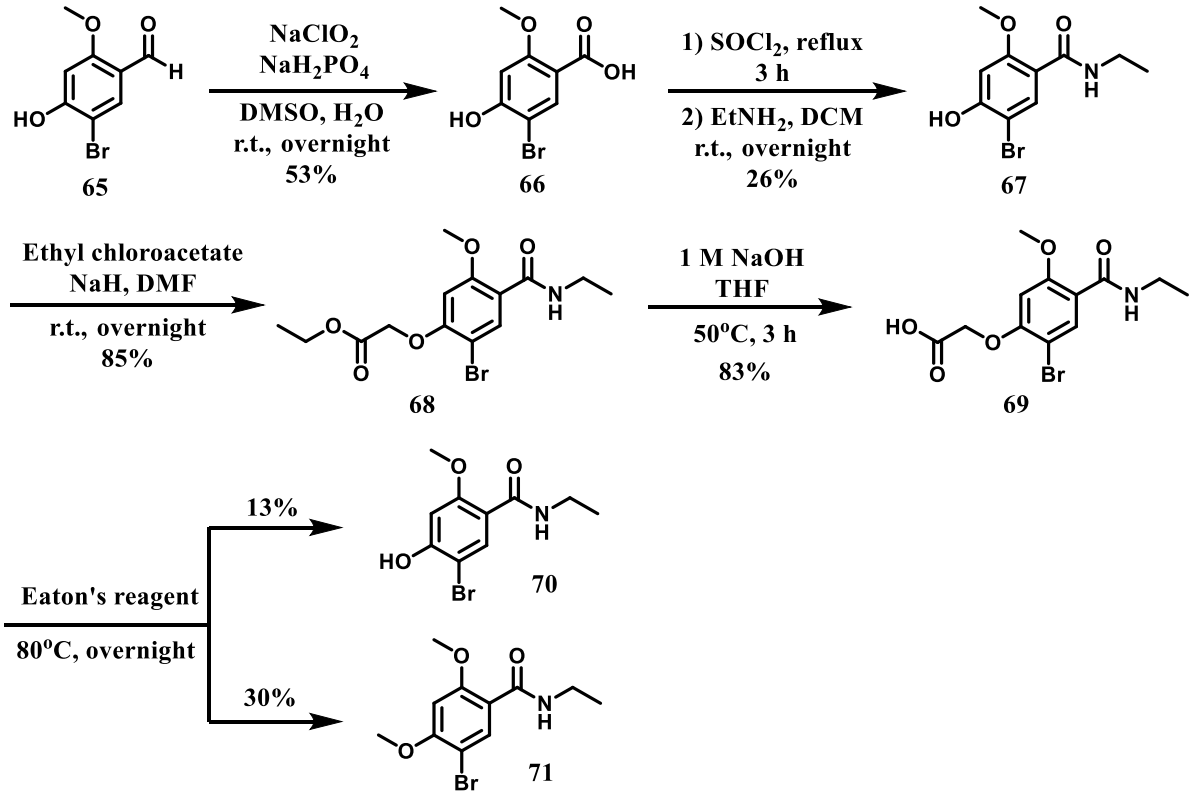
Scheme 18: Modified synthesis to investigate the use of Eaton's reagent.

Before using Eaton's reagent, we attempted the cyclisation of **63** with polyphosphoric acid. Consistent with previous results, the cyclisation of **63** using polyphosphoric acid did not give a positive result. We then attempted to use Eaton's reagent to cyclise **63**. In this reaction, **63** was dissolved in Eaton's reagent and the reaction solution was heated to 80°C.

After leaving the reaction overnight, work-up was performed and the crude product was analysed by ^{1}H-NMR. The signals obtained showed the characteristic three signals in the aromatic region which perfectly matches the proton signals of the starting material. Moreover, no signals

corresponding to the protons of the product were observed. Despite this disappointing result, we continued to explore the use of Eaton's reagent for the cyclisation of other intermediates.

The first compound in our series, other than **63**, that we would try to cyclise with Eaton's reagent was **69**. This molecule was made starting from **65** which was brominated from 4-hydroxy-2-methoxybenzaldehyde. In **Scheme 19**, compound **65** was oxidised *via* Pinnick oxidation to give **66** in 53% yield. Compound **66** was then subjected to amidation by refluxing with $SOCl_2$ for 3 hours, followed by treatment with ethylamine at room temperature overnight to afford **67** (26%). Compound **67** was then substituted with ethyl chloroacetate, followed by hydrolysis using 1 M NaOH to give **69**. We then attempted to cyclise **69** using Eaton's reagent and, with this attempt, we got different results to those obtained before.



Scheme 19: Investigation of the effect of Eaton's reagent with **69**.

Compound **69** was treated with Eaton's reagent which was used as the solvent at 80°C overnight. After work-up, two new spots on the TLC were purified by flash column chromatography and each product was identified by ^{1}H-NMR. From the ^{1}H-NMR, the first product retained two proton signals in the aromatic region while most of the other signals remained the same as in its starting

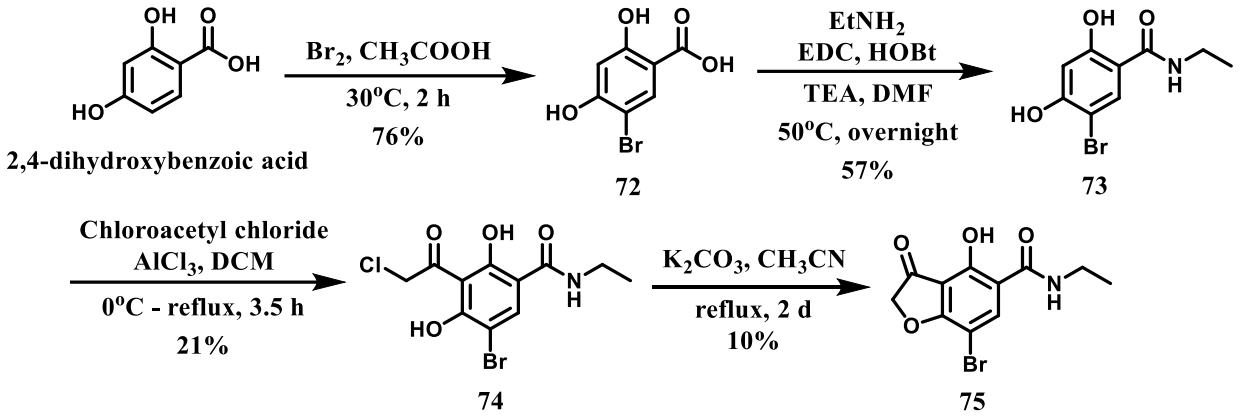
material. However, there was an additional signal at 3.48 ppm which, from the integration, consisted of three protons. This was consistent to a new CH_3 group that was adjacent to a high electronegativity atom. Thus, it was assigned to structure **71** which was further confirmed by ^{13}C-NMR.

The ^{1}H-NMR spectrum of the second product also possessed two signals of protons in the aromatic region with the integration equal to one for each signal. In addition to those signals, there was an additional signal of one proton at 9.36 ppm which corresponded to a proton from a phenol. Moreover, in ^{13}C-NMR, there were only 10 signals which suggested that the whole side chain was removed to give phenol **70**. This was further confirmed by MS.

Since, at high temperature, the cleavage of the phenoxy alkyl bond tended to occur, we decided to try the same cyclisation with Eaton's reagent at different temperatures. The first trial started with the cyclisation reaction of **69** using Eaton's reagent at room temperature. This reaction was allowed to stir for 24 hours before monitoring by TLC. The first TLC showed that there was no product developed in the reaction. Therefore, the reaction was stirred for up to four days. Despite the long time for this cyclisation, there was still no observable reaction taking place and the starting material was recovered. The reaction was then heated to 40°C and was stirred for two days, however no change was observed over this interval. Therefore, the reaction temperature was increased to 60°C and it was stirred for additional six days. It was shown that at 60°C the cleavage of the phenoxy alkyl bond took place without any signs of cyclisation. This was confirmed by the TLC which was compared to the products obtained from the same reaction at 80°C.

3.10 New cyclisation approach based on a different disconnection

Since we could not make any cyclised product by either improving the solubility of the intermediate or changing and modifying the reagents and the reaction conditions, it was clear that a completely new approach was required. Firstly, we wanted to use a simpler molecule which, at the same time, was more electronically activated and may assist the acylation reaction. For this reason, 2,4-dihydroxybenzoic acid was selected as a starting material for a new method for the cyclisation reaction as shown in **Scheme 20**.



Scheme 20: Synthetic scheme of the substitution-based cyclisation.

The synthesis began with bromination of 2,4-dihydroxybenzoic acid by reacting with elemental bromine dissolved in acetic acid at 30°C for 2 hours. As expected, a bromine atom was added to the 5-position to give **72** in a high yield (76%). Then, **72** underwent an amide coupling with EDC and HOBt at 50°C overnight to give **73** (57%). The next step was to perform the acylation reaction of **73** with chloroacetyl chloride using aluminium chloride as a catalyst. This reaction would make the chloroacetyl group attach to the aromatic ring at the 3-position which would give an opportunity for **74** to perform a new method of cyclisation *via* a nucleophilic substitution reaction.

In the first attempt, the acylation of **73** was achieved with a low yield of 21%. Following this, we attempted the cyclisation reaction of **74** with K_2CO_3 in acetonitrile at 30°C for 3 hours. The crude product obtained was firstly analysed by ^{1}H-NMR. Although the structure of the product was uncertain, the signals in the ^{1}H-NMR were consistent with the formation of the cyclised product **75**. The crude product was then subjected to purification by flash column chromatography. However, the product obtained after the purification still contained some impurities. As we only recovered a small amount of the contaminated product, we decided not to do further purification and instead synthesise more material.

According to **Table 5**, in the second attempt, we increased the reaction time to 12 hours. The product obtained after the purification was still not 100% clean and the yield was lower than 10%. Then, we increased the reaction time to 24 hours. After a series of purifications, the amount of the pure product obtained was extremely low and was not enough to proceed to the next step.

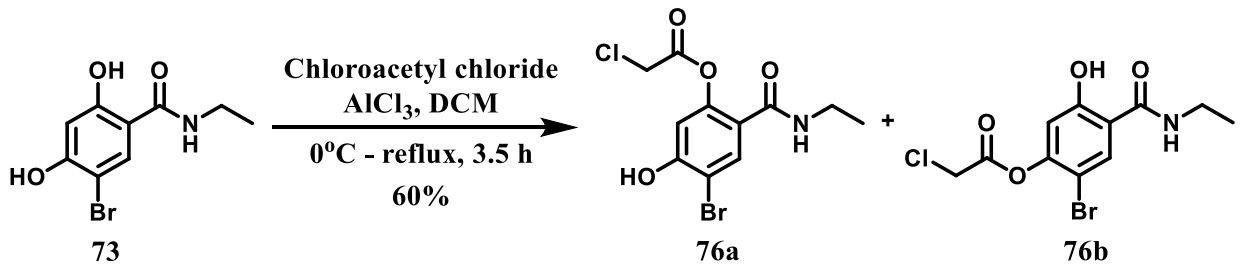
Table 5: Screening reaction conditions for the substitution-based cyclisation of **74**.

Entry	Reagents	Conc.	Temp.	Time	Yield	Results
1	K_2CO_3 (3 eq.), CH_3CN	0.8 M	30°C	3 h	5%<	Product contained some impurities
2	K_2CO_3 (3 eq.), CH_3CN	0.8 M	30°C	12 h	10%<	Product contained some impurities
3	K_2CO_3 (3 eq.), CH_3CN	0.8 M	30°C	24 h	10%<	Obtained pure product
4	K_2CO_3 (3 eq.), CH_3CN	0.2 M	82°C	48 h	10%	Obtained pure product
5	Cs_2CO_3 (3 eq.), CH_3CN	0.2 M	82°C	24 h	13%	Obtained pure product

One of the reasons that could lead to the poor yield of the cyclised product **75** was the competitive reaction between intramolecular and intermolecular reaction of **74** as was evident from an additional spot seen in the TLC of this reaction.

In the next attempt (entry 4, **Table 5**), we kept the concentration of the reactant in the range of 0.2-0.5 M to favour the intramolecular reaction. We also increased the temperature from 30°C to the reflux temperature of acetonitrile at 82°C for 48 hours. After several purification methods used to purify the crude products in entry 4, we could confirm that the desired cyclised product **75** was obtained in 10% yield.

To optimise the reaction conditions and potentially produce more product, we changed the base used in the reaction to Cs_2CO_3 which had higher solubility compared to K_2CO_3 (entry 5, **Table 5**). Nevertheless, the results obtained were not different from the use of K_2CO_3. When we then attempted to re-synthesise **75**, compound **76** (both **76a** and **76b**) was obtained as a major product, despite the same reaction environment and conditions shown in **Scheme 21**.



73 **76a** **76b**

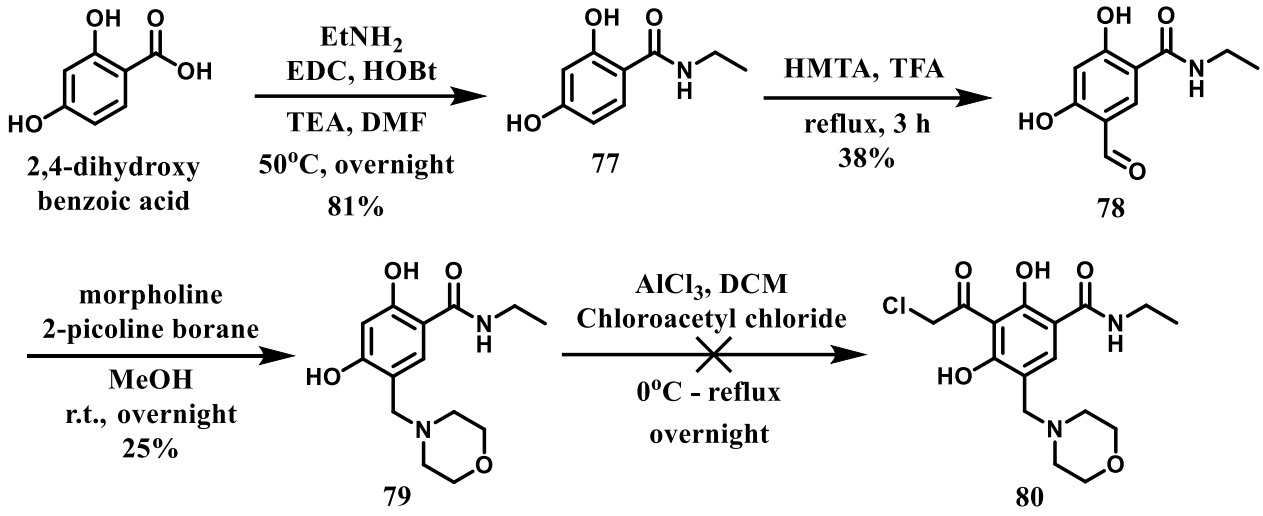
Scheme 21: Side reaction of **73** leading to the O-alkylated product (**76a** and **76b**).

This outcome could arise from the quality of the aluminium chloride catalyst. After several attempts to make the desired product by adjusting the amount of the catalyst used and reaction time, we could not obtain **74**. Regardless of our attempts to make **74**, we only recovered **76** (both **76a** and **76b**) as a major product. Although this synthesis also provided **74** as a minor product, the combined amount of **74** from several syntheses was still not enough for preparation of **75** considering that the yield of **75** was extremely low and there were several other steps until the final compound would be made. We later attempted O to C rearrangement of **76** (see section **3.11**)

3.10.1 Acylation of different substrates with chloroacetyl chloride

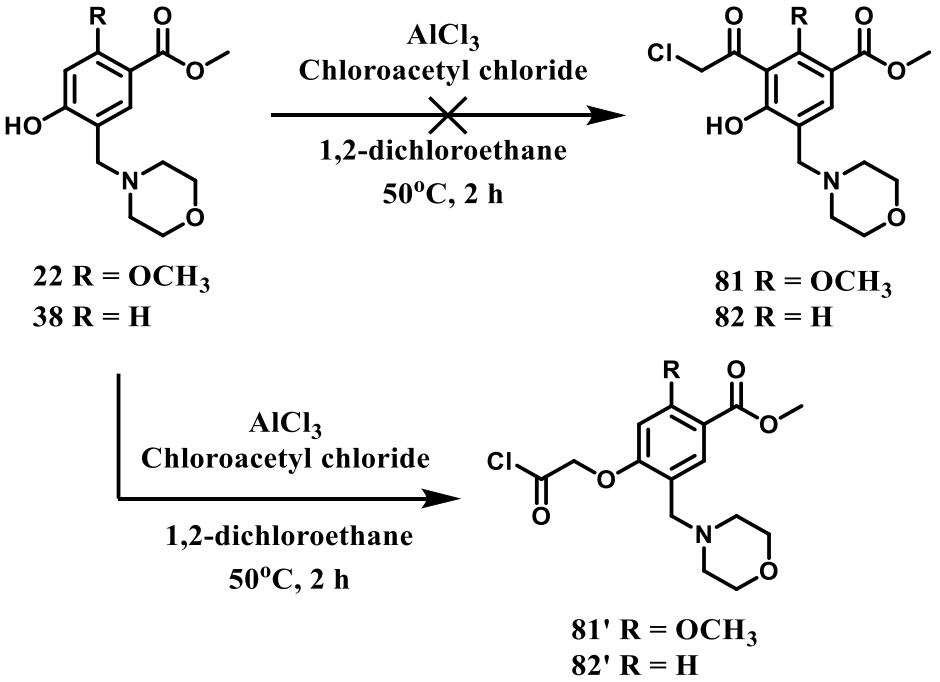
We also tried this new strategy on an intermediate with the morpholino moiety (**Scheme 22**). For the preparation of intermediate **79**, we started with the same reactant 2,4-dihydroxybenzoic acid. It was subjected to an amide coupling using EDC, HOBt, triethylamine, and ethylamine in DMF at 50°C overnight to afford **77** in 81% yield. Compound **77** was subjected to Duff reaction using HMTA and Cu_2O under a reflux condition for 3 hours to incorporate the formyl group to the aromatic ring giving **78** (38%). After that, **78** underwent reductive amination with morpholine to give **79** (25%). However, the acylation of **79** with chloroacetyl chloride was not successful giving

only O-alkylated product. We also tried the acylation with **78**. Unfortunately, the acylation of **78** yielded O-alkylated product as well.



Scheme 22: Synthetic scheme of the acylation of a substrate with morpholino moiety.

Since the molecule bearing two hydroxyl groups was prone to undergo O-alkylation instead of the desired acylation reaction, we used the intermediates synthesised earlier which possess only one hydroxyl group, **22** and **38**, applying the same acylation reaction conditions (**Scheme 23**).

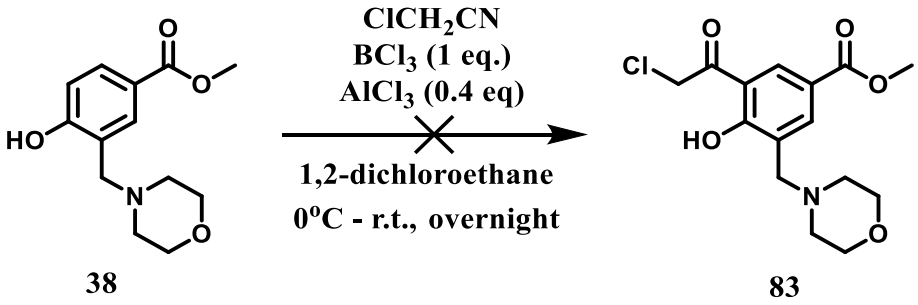


Scheme 23: Synthetic scheme of the acylation of **22** and **38**.

The sole product found in the reaction of **38** with chloroacetyl chloride was the O-alkylated product. However, in the reaction involving **22**, we could see the presence of the desired acylated product in the mixture of its O-alkylated product and the expected product, although the proportion of the desired product was too low to carry on the synthesis.

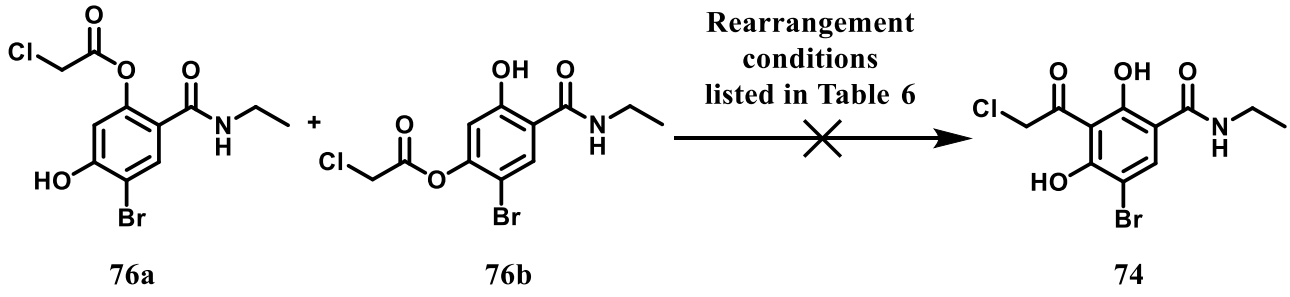
3.10.2 New acylation conditions for 38

We then tried to find alternative conditions for the acylation reaction. Toyoda *et al*. successfully performed the ortho *α*-chloroacetylation of phenols to give *α*-chloroacetophenone products by utilising chloroacetonitrile and boron trichloride and aluminium trichloride as catalysts in 1,2-dichloroethane.[123] We used **38** as a test system and followed this procedure (**Scheme 24**). However, in our case, after leaving the reaction for 3 days, no conversion was observed.



Scheme 24: Alternative condition of acylation reaction of **38**.

3.11 Synthesis of 74 from the rearrangement of 76



Scheme 25: Rearrangement of **76** with different conditions listed in **Table 6**.

As we had large amount of **76** from the selective O-alkylation, we tried to find conditions that could transform **76** into **74**; i.e., the rearrangement reaction as shown in **Scheme 25**.

Table 6: Screening reaction conditions for the rearrangement of **76**.

Entry	Reagents and conditions	Results	References
1	$AlCl_3$ (3.2 eq), neat, 170°C, 2 h	- Starting material seemed to be a major product by ^{1}H-NMR - Contained lots of impurities which were hard to separate	[124]
2	$TiCl_4$ (1.1 eq.), 1,2-dichloroethane, r.t., 20 h	- No reaction	[125]
3	$ZrCl_4$ (4 eq.), DCM, r.t., overnight	- No reaction	[126]
4	$Bi(OTf)_3$ (10% mol), toluene, 110°C, 4 days	- The expected product (**74**) was obtained with starting material also recovered - The yield was extremely low (5%)	[127]

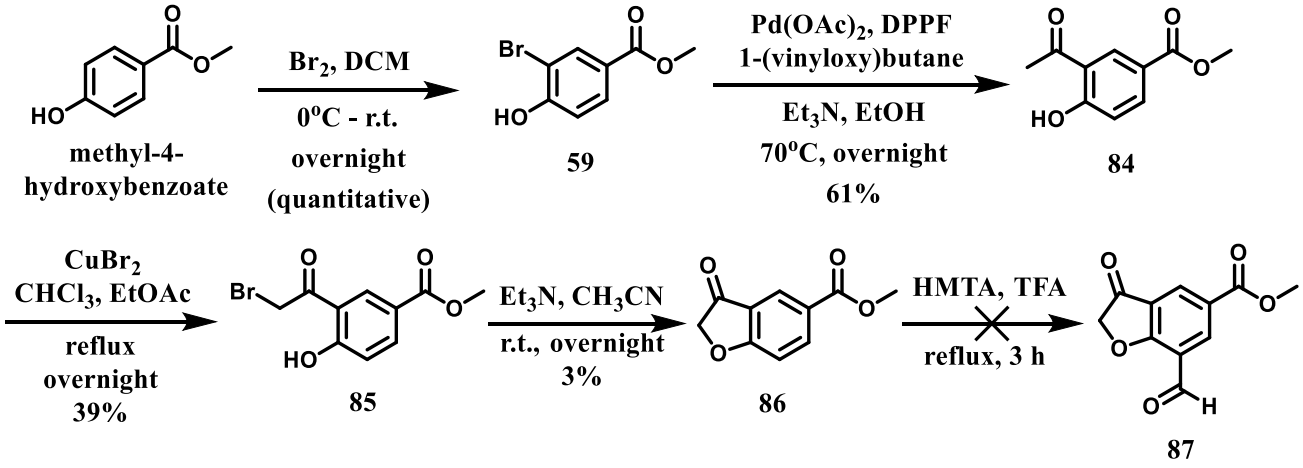
First, in **Table 6**, we tried a Fries rearrangement, which converted a phenolic ester to the hydroxy aryl ketone using a Lewis acid catalyst. This reaction was performed without solvent and aluminium chloride was used as the catalyst.[124] The reaction was heated to 170°C for 2 hours and then subjected to work-up. Analysis of the crude product by ^{1}H-NMR showed that there were two major signals in aromatic region which corresponded to the starting material **76**. Nevertheless, the crude product was potentially a mixture of more than two compounds which appeared difficult to

separate. Therefore, we did not put an effort to purify the crude product from the first Fries rearrangement attempt.

In the second entry, we followed the reaction conditions from Donnelly *et al*. using $TiCl_4$ as a catalyst.[125] However, no reaction occurred. We then tried to use $ZrCl_4$ as a catalyst according to Brigmann *et al*.[126]. Unfortunately, still no reaction was observed. Finally, we tried $Bi(OTf)_3$ as a catalyst. The reaction was performed in toluene at 110°C for four days. However, when purifying the crude product by using preparative TLC, we could acquire the rearrangement product **74** together with the recovered reactant although the yield was extremely low (5%). Therefore, we did not continue the rearrangement of **76** and tried to find another way to perform the cyclisation.

3.12 Cyclisation of intermediates at early stage

Since earlier efforts towards the cyclisation reaction at a late stage of the syntheses were unsuccessful, we attempted to change the route such that the cyclisation was performed at an earlier stage (**Scheme 26**).



Scheme 26: Early stage cyclisation of benzofuran-3(2*H*)-one core scaffold.

Starting from methyl-4-hydroxybenzoate, compound **59** was obtained by following the literature procedure from Barlaam *et al.*[128] Selective bromination resulted in quantitative yields of **59**. This product was in turn reacted with an electron-rich olefin *via* a Heck reaction. The use of an electron rich olefin, together with a bidentate phosphine, led to the exclusive formation of the regioselective

α-arylation product which upon treating with an acid was hydrolysed to give aryl methyl ketone, **84** (61%). Compound **84** was reacted with copper(II) bromide to give the α-brominated ketone, **85** (39%). Cyclisation of **85** with triethylamine in acetonitrile at room temperature successfully afforded the product, **86**, despite a very low yield (3%). This low yield was due to poor conversion from starting material.

Given the success of obtaining **86**, we had to find a way to incorporate a functional group that could be converted to the needed morpholino moiety. As before, we decided to use the Duff reaction. The Duff reaction of **86** using HMTA in TFA under a reflux condition for 3 hours showed a mixture of three spots by TLC that stained with 2,4-DNP, indicating possible formylation. However, after the purification by flash column chromatography, no product was obtained. This could be due to instability of the product on silica or that the amount of the product was too small to be observed. Accordingly, the reaction was repeated with the reaction time extended to overnight in order to allow the reaction to go to completion. Unfortunately, starting material was still present and no product was obtained.

In the original literature for the Duff reaction procedure,[114] the author utilised copper(I) oxide as a catalyst for the *ortho*-selective formylation reaction (as shown in **Scheme 5**). Although we found that the use of copper salt made the purification of the intermediates more difficult, the reaction was repeated with the same conditions from entry 2 (**Table 7**). No product was observed. Although the new cyclisation strategy was achieved in principle, we still faced the difficulty in incorporating the desired morpholino moiety into the target molecules.

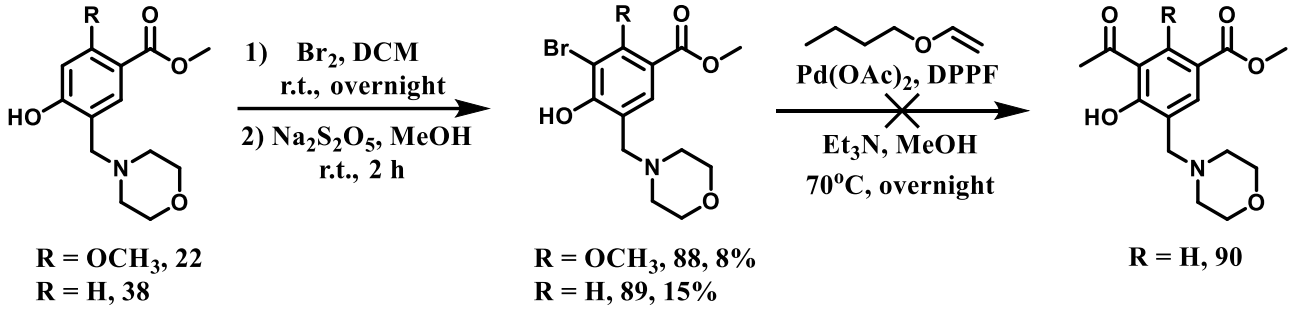
Table 7: Screening reaction conditions for formylation of **86**.

Entry	Reagents	Temp.	Time	Results
1*	HMTA, TFA	73°C	3 h	- No product observed after purification
2*	HMTA, TFA	73°C	Overnight	- No product observed after purification
3*	HMTA, Cu_2O, TFA	73°C	Overnight	- No product observed after purification

*All entries underwent work-up process with 3 M HCl after the reaction was stopped

We attempted to apply this strategy to the more heavily functionalised compounds made earlier (**22** and **38**, **Scheme 27**). Firstly, bromination of **22** and **38** produced **88** and **89** with the poor yields of 8% and 14%, respectively, which was attributed to a poor conversion of the starting material and possibly the decomposition of the products during purification. Since the amount of **89** obtained by bromination was more than **88**, we used **89** as a model to study the Heck reaction with 1-(vinyloxy)butane using the previously employed reaction procedure (**Scheme 26**).

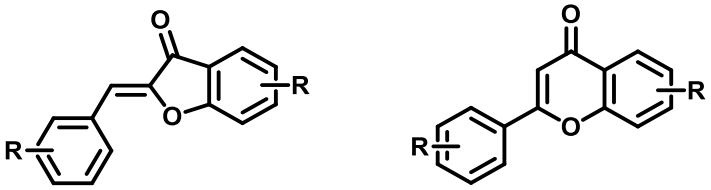
For the first attempt, the reaction was stirred overnight at 70°C. The crude mixture was analysed by ^{1}H-NMR, which revealed that the starting material had been recovered. The reaction time was extended to 3 days to no avail. This route was therefore also abandoned.



Scheme 27: Cyclisation of **22** and **38** at early stage.

3.13 Alternative designs of inhibitors

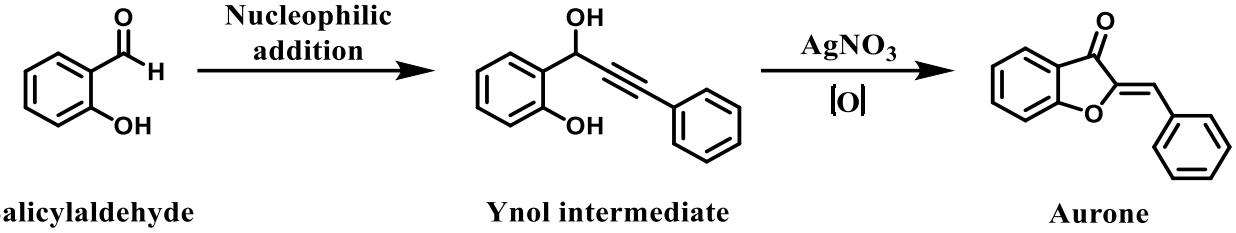
Although numerous attempts to synthesise the desired aurone-based compounds using different strategies were made, we still did not achieve a successful synthesis of the target compound. Therefore, new ways for cyclisation and/or a new design of the final products were required. The aurone-based final product without the morpholino moiety was selected for the ease of the next synthetic plans. Moreover, the core scaffold of the final products was expanded to include the flavone scaffold inspired by the new synthetic plan (**Figure 20**).



Aurone **Flavone**

Figure 20: Chemical structures of aurone and flavone units.

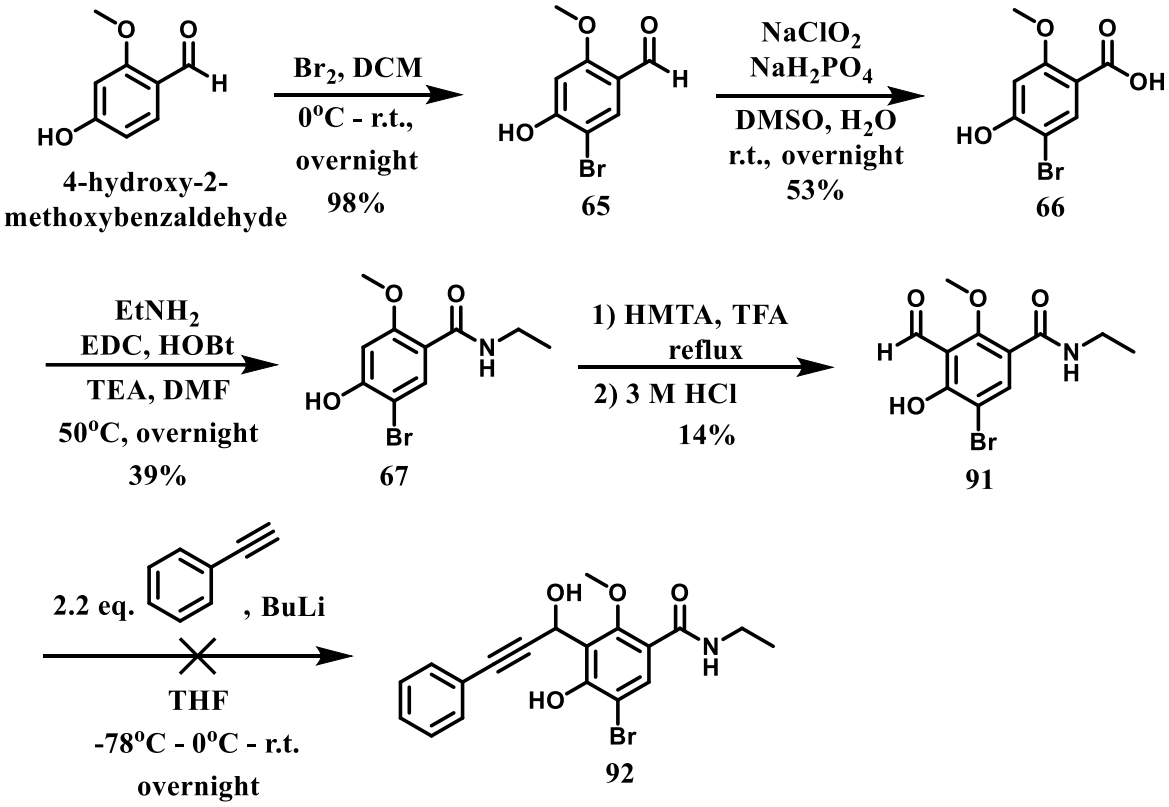
Specifically, we investigated a strategy to make the aurone core *via* 2-step cyclisation and oxidation of a corresponding salicylaldehyde[129] (**Scheme 28**). In the literature, $AgNO_3$ was employed during the cyclisation of ynol intermediate both as a catalyst as well as an oxidising agent. This method required the salicylaldehyde or its derivatives as a starting material. Nucleophilic addition using phenylacetylene or its derivatives is used to give the substrate ready for a cascade reaction with $AgNO_3$.



Scheme 28: A 2-step synthesis of aurone from a salicylaldehyde.

3.14 Synthesis of the aurone core using the new strategy

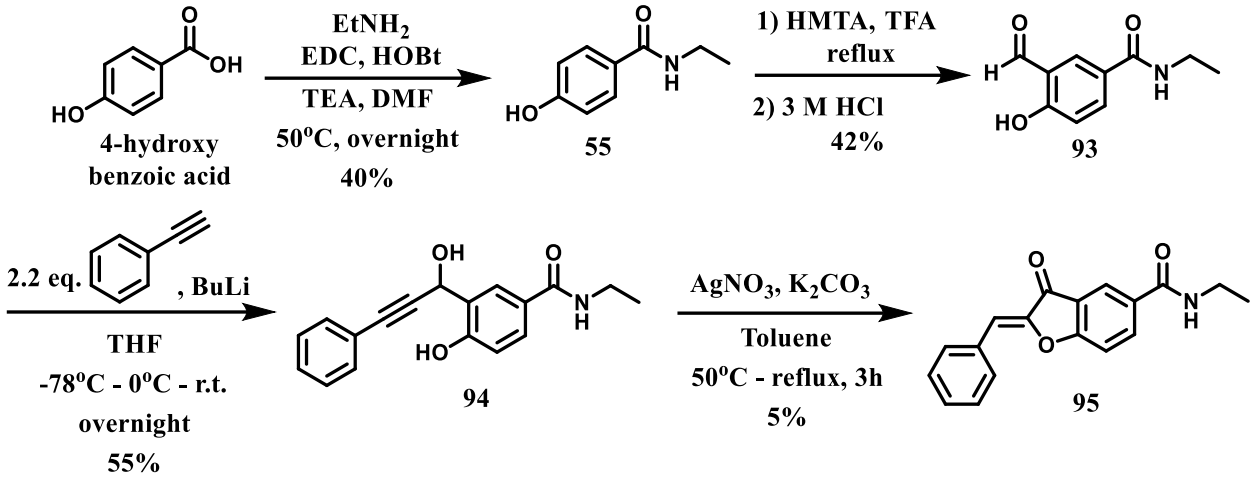
Since we have already explored the reaction to make an *ortho*-hydroxy benzaldehyde using the Duff reaction as seen in **Scheme 22**, we applied the same synthetic method to make the new target. According to **Scheme 29**, 4-hydroxy-2-methoxybenzaldehyde underwent bromination reaction using elemental bromine dissolved in DCM at room temperature overnight to give **65** (98%). This was followed by the oxidation of the aldehyde *via* Pinnick oxidation to give the corresponding benzoic acid **66** (53%). Compound **66** was subjected to an amide coupling using EDC, HOBt, triethylamine, and ethylamine in DMF at 50°C overnight to afford **67** (39%). Duff reaction using HMTA in TFA was performed on **67** to give **91**, although the yield was comparatively low (14%).



Scheme 29: Synthetic scheme for making the aurone core *via* the salicylaldehyde derivative **91**.

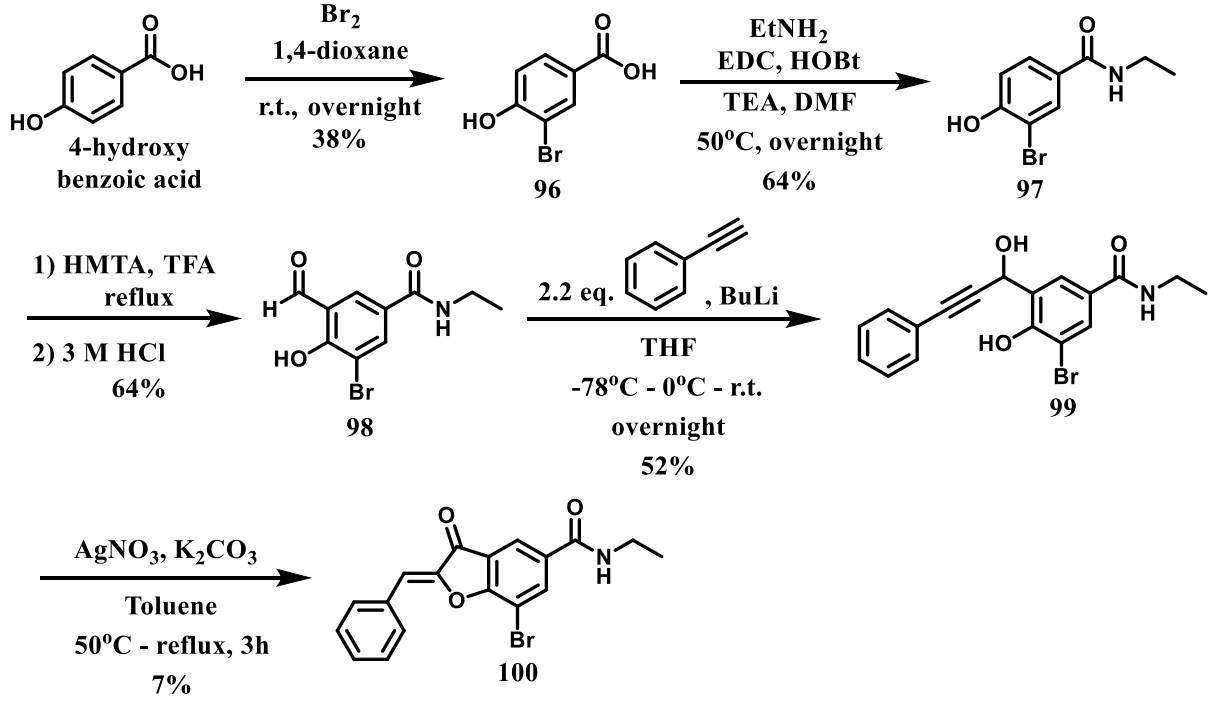
Then, we attempted the new cyclisation/oxidation strategy using **91**. Firstly, the phenylacetylide nucleophile was prepared *in situ* from phenylacetylene and BuLi at -78°C. After the nucleophile was generated, it was added to **91**. The reaction was monitored by TLC after stirring overnight at room temperature. A new spot on the TLC was observed. However, the expected product was not obtained following purification which was possibly due to the decomposition of the product during purification.

After the first attempt failed, we decided to try a simpler starting material, 4-hydroxybenzoic acid. As in **Scheme 30**, we followed the same reaction pathway in **Scheme 29** to make **93** which is an amide derivative of salicylaldehyde. From here, the nucleophilic addition of phenylacetylide to **93** was successful, giving **94** as the product with moderate yield (55%) following purification. Then, **94** was reacted with $AgNO_3$ and K_2CO_3 for a cascade reaction of cyclisation followed by oxidation reaction to give **95**, although the yield was relatively low (5%). This was the first time we successfully made the cyclised product, especially that it had already contained the styrene moiety.



Scheme 30: Synthesis of **95** *via* cyclisation and oxidation using $AgNO_3$.

We then applied the reaction conditions that we used in **Scheme 30** to make the brominated species of **95** in **Scheme 31**.



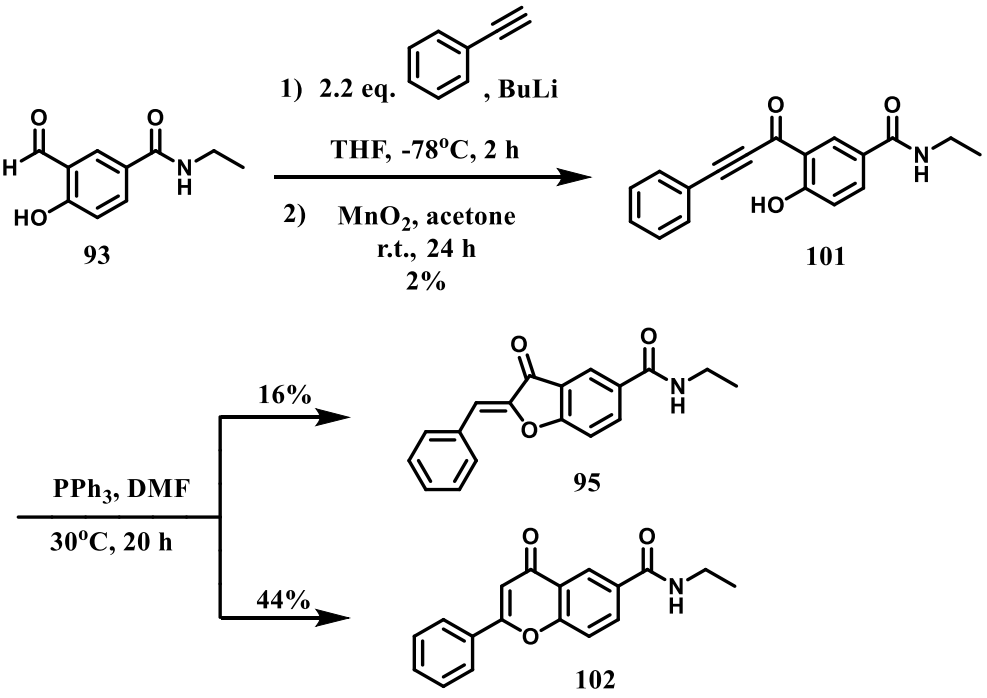
Scheme 31: Synthesis of **100** *via* cyclisation and oxidation using $AgNO_3$.

We started from the bromination of 4-hydroxybenzoic acid using elemental bromine dissolved in 1,4-dioxane at room temperature overnight to give **96** (38%). Compound **96** was then subjected to an amide coupling using EDC, HOBt, triethylamine, and ethylamine to give **97** (64%) followed

by a formylation reaction using Duff reaction affording **98** in 64% yield. Compound **97** was reacted with phenylacetylide nucleophile generated *in situ* to give the ynol intermediate **99**. Compound **99** was then subjected to the new cyclisation/oxidation strategy using $AgNO_3$ and K_2CO_3 in toluene under a reflux condition for 3 hours to afford the final product, **100** which was obtained with the overall yield of 1% in 5 steps.

3.15 Attempted synthesis of flavone analogue

It is reported that O-alkynoylphenol can undergo both 6-*endo*-digonal cyclisation and 5-*exo*-digonal cyclisation in competition to give flavone and aurone, respectively.[130] As both scaffolds were targeted, we could exploit the conditions that produced both products in good yield. The easiest way to prepare the O-alkynoylphenol was from the oxidation of the ynol with a mild oxidant such as MnO_2.



Scheme 32: Synthesis of **95** and **102** *via* the oxidation of ynol intermediate using MnO_2.

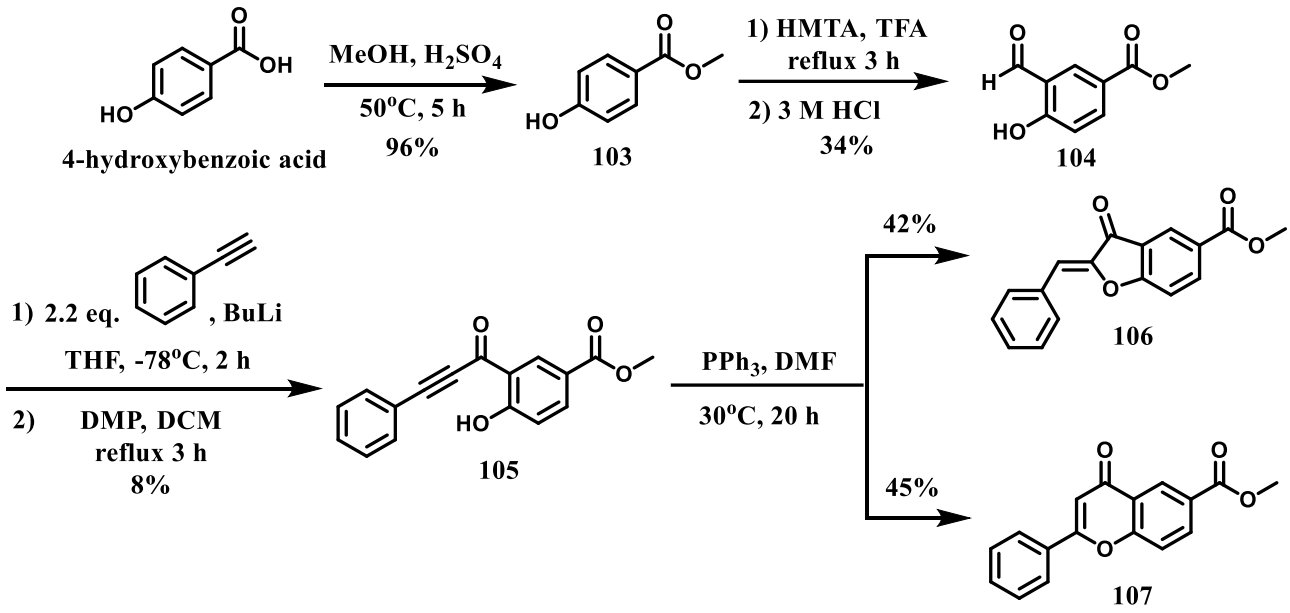
We firstly used **93** as our model for this reaction as shown in **Scheme 32**. In the first step, compound **93** underwent the 1,2-addition of phenylacetylene to give the corresponding ynol product which was used without further purification. The ynol was then oxidised using MnO_2 to

afford **101** in low yield (2%) potentially due to the low quality of the MnO_2. Despite the optimised conditions in the literature for the regioselective cyclisation to exclusively give the flavone,[130] other conditions were selected to generate both flavone and aurone in comparable yield. Compound **101** was cyclised using triphenylphosphine (PPh_3) in DMF at 30°C for 20 hours to give **95** and **102** in 16% and 44%, respectively.

In order to ensure that MnO_2 was activated this time, it was washed with 10% HNO_3 followed by washing with water until the wash was neutral. Then MnO_2 was dried in an oven at 105°C for 2 days. After that, we did the oxidation reaction again with different ynol substrates. However, even after MnO_2 was activated, the yield of the product did not improve. In addition, the product formation from the oxidation reaction using MnO_2 was not consistent. Thus, we had to find other conditions to oxidise the ynol substrates.

3.16 Synthesis of flavone and aurone *via* the oxidation of ynol intermediate using Dess-Martin oxidation (DMP)

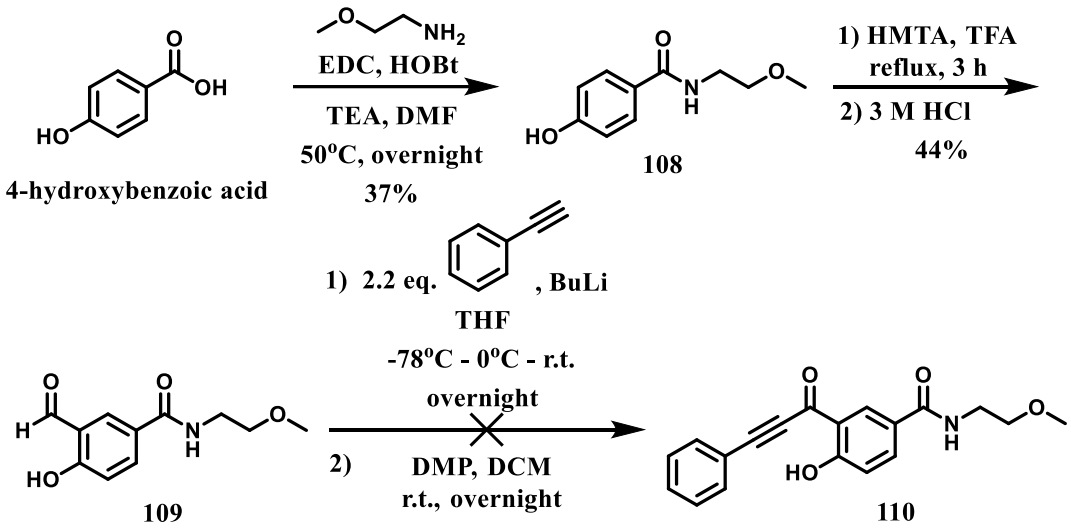
Since only mild oxidation conditions were required, an alternative oxidation that was selected was the Dess-Martin protocol (**Scheme 33**). We changed the amide to methyl ester side chain in order to generate different target compounds. Esterification of 4-hydroxybenzoic acid was performed using methanol and sulfuric acid as a catalyst to give **103** (96%). Formylation using Duff reaction conditions (HMTA in TFA under a reflux condition for 3 hours) was then performed to give **104**, followed by a 1,2-addition of phenylacetylene to give the ynol intermediate. The ynol intermediate was subsequently oxidised by DMP in DCM under a reflux condition to give **105** in low yield (8%). After that, **105** was cyclised using PPh_3 in DMF at 30°C for 20 hours to give two products, **106** and **107**.



Scheme 33: Synthesis of **106** and **107** via the oxidation of ynol intermediate using DMP.

As we successfully synthesised both the desired products with the flavone and aurone core scaffolds, this pathway was used to synthesise other final products bearing different side chains. In compound **10**, there is an *N*-methoxyamide side chain (shown in green, **Figure 15**) that projects towards the allosteric site of FMS. Based on the co-crystal structure of compound **10** bound to the active site of FMS (**Figure 14**, **A**), there is also an additional space in the allosteric site of FMS that can accommodate a larger and/or longer side chain which may form more interactions within the pocket. Therefore, we started to synthesise other potential compounds by varying the amide side chain.

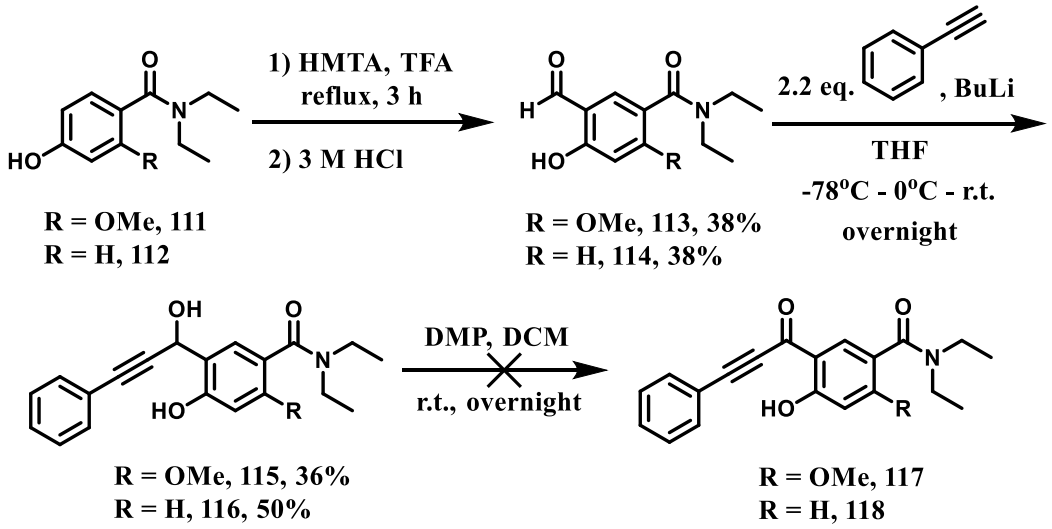
In **Scheme 34**, we attempted to synthesise a new final product with a different amide side chain. We started from an amide coupling of 4-hydroxybenzoic acid using EDC, HOBt, triethylamine, and 2-methoxyethan-1-amine at 50°C overnight to generate **108** in 37% yield. Compound **108** was then subjected to a formylation reaction using HMTA in TFA under a reflux condition for 3 hours to give **109** (44%). Nevertheless, a 1,2-addition of phenylacetylene to **109** followed by oxidation of the resulting intermediate was unsuccessful.



Scheme 34: Synthetic scheme used to make the O-alkynoylphenol intermediates **110**.

For the oxidation of the ynol intermediates, it proved to be not consistent as most of the attempts ended in failure to make the O-alkynoylphenol intermediate. This might be due to the use of the ynol intermediates without further purification.

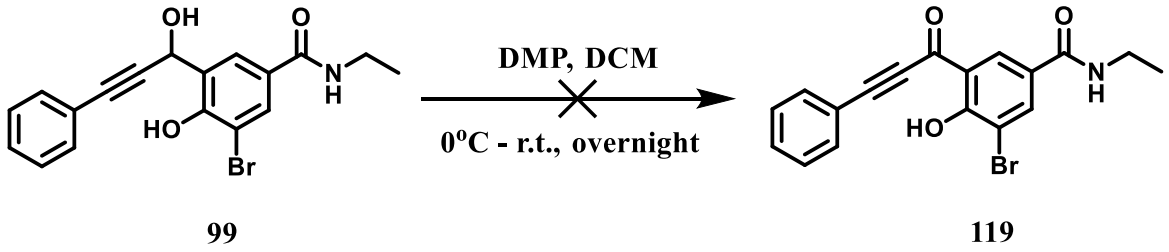
3.16.1 Optimisation of the oxidation of ynol intermediate



Scheme 35: Synthesis of O-alkynoylphenol after purification of the ynol.

Since the DMP oxidation did not give consistent results, we investigated whether impurities interfered with the oxidation. Purification of the O-alkynoylphenol intermediates was carried out prior to oxidation. Dess-Martin oxidation using the purified intermediates **115** and **116** failed to provide the expected products in both cases (**Scheme 35**).

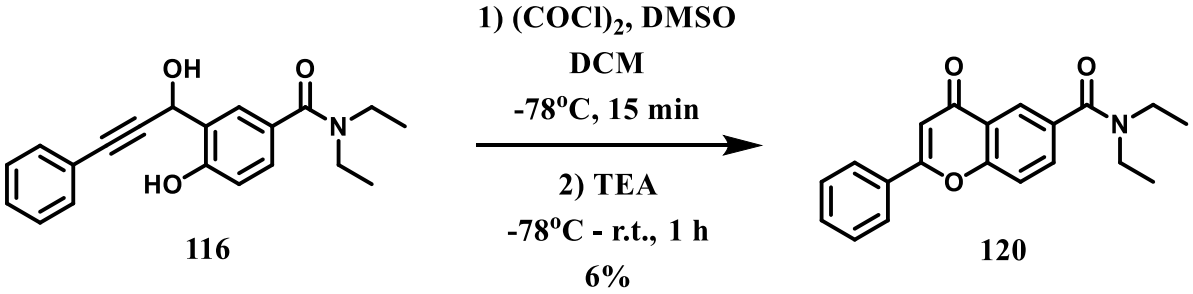
We re-attempted Dess-Martin oxidation with **99** (**Scheme 36**). For this synthesis, the Dess-Martin oxidation conditions were modified from the previous attempt in **Scheme 35** as follows: the solution containing the starting material was cooled to 0°C and DMP was added. The reaction was stirred at 0°C for 30 minutes. The mixture was warmed to room temperature and stirred for additional 1.5 hours. Characterisation of the different reaction species by ^{1}H-NMR did not show the expected product. The reaction was repeated with the addition of $NaHCO_3$ in order to neutralise the acetic acid that was generated from the DMP oxidation, which might interfere with the intermediate or the reaction. However, despite addition of $NaHCO_3$, the same results were obtained.



99 **119**

Scheme 36: Optimisation of the oxidation of ynol intermediate **99** using DMP.

Since the Dess-Martin oxidation of the ynol intermediate did not give consistent results, we wanted to find another mild oxidation condition. The Swern oxidation was attempted using **116** (**Scheme 37**).



116 **120**

Scheme 37: Swern oxidation of **116**.

We used the conventional conditions for the Swern oxidation which was to treat **116** with a mixture of oxalyl chloride and DMSO in anhydrous DCM at -78°C. TLC analysis showed two separated spots. These spots gave an orange colour when stained with 2,4-DNP indicating the presence of the carbonyl functional group that was expected from the desired product. Unfortunately, ^{1}H-NMR analysis of the purified two products showed that they contained significant impurities. Since the normal column chromatography was not be able to purify the products, we used preparative TLC to further purify each product. After the second purification, ^{1}H-NMR analysis showed only one highly pure product, **120**.

The ^{1}H-NMR signals of the high pure product looked very promising as the desired product (**120**), although there was an additional proton signal in aromatic region which had the integration of one proton that we did not expect to observe in the desired oxidised product. We propose this product with one additional proton is the cyclised form of the starting material (**120**). MS confirmed that the product obtained from this reaction was the cyclised product with its mass of 322.14 m/z.

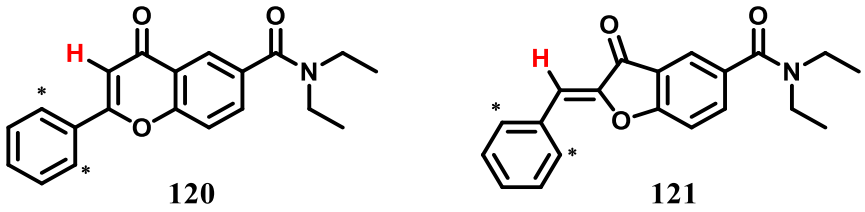
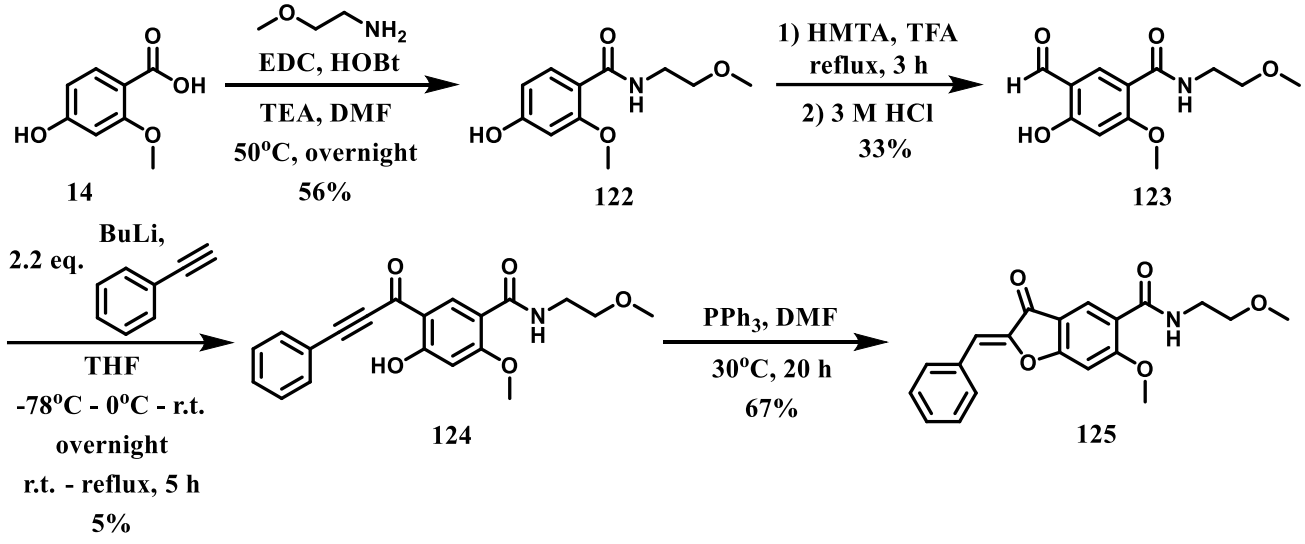


Figure 21: Flavone (**120**) and aurone (**121**) products of **116**.

From the ^{1}H-NMR, it was difficult to distinguish between the aurone (**121**) and flavone (**120**) as in both cases the additional proton would appear in the aromatic region. Moreover, the ^{13}C-NMR signals of the aurone (**121**) and flavone (**120**) were also difficult to distinguish. Therefore, 2-D NMR including HMBC was used. From the HMBC spectrum, the was no correlation between the proton (shown in red in **Figure 21**) and the carbons (with asterisks in **Figure 21**) from a free aromatic ring which exactly matched with the flavone (**120**). In contrast to the aurone (**121**), there would be the aforementioned correlation. Therefore, we concluded that the product obtained from the Swern oxidation was the flavone **120** which underwent spontaneous cyclisation following oxidation. This was potentially from the addition of the excess triethylamine which further assisted the cyclisation.

3.17 Synthesis of aurone using $AgNO_3$

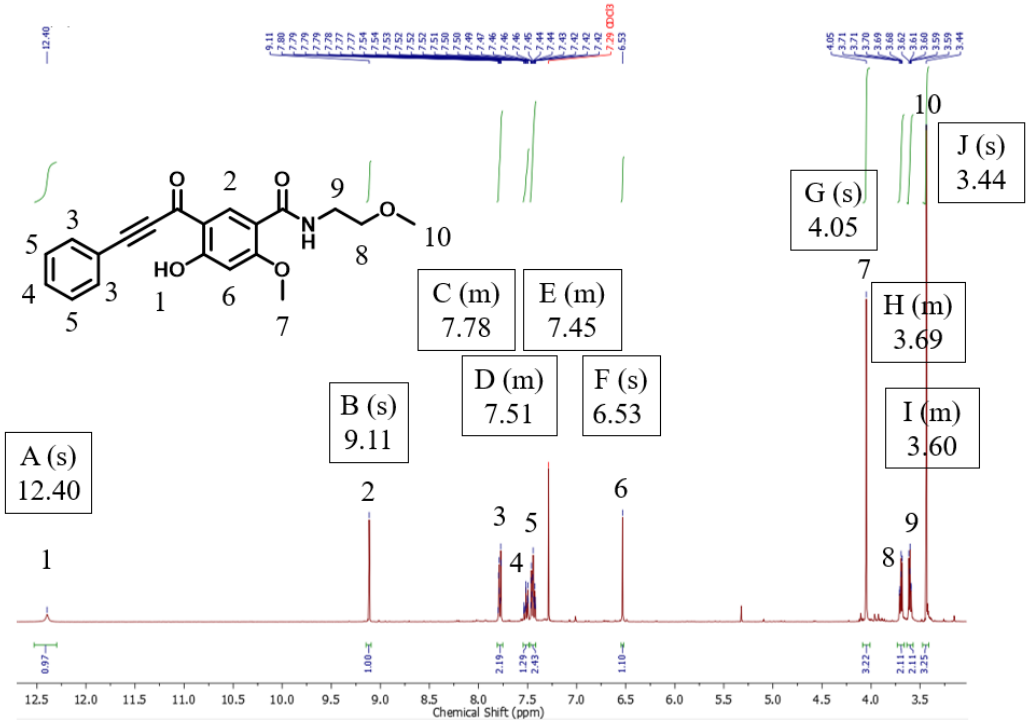
Since the synthetic pathway from the ynol intermediate to give both aurone and flavone products was not consistent due to the oxidation reaction of the ynol, cyclisation of the ynol to give only aurone product as performed previously in **Scheme 30** was selected for this new target. The synthesis of the new target started from an amide coupling of **14** and 2-methoxyethan-1-amine to give **122** (56%). Duff reaction (HMTA in TFA under a reflux condition for 3 hours) was performed on **122** followed by a 1,2-addition of phenylacetylene to the resulting intermediate **123** (**Scheme 38**).



Scheme 38: Synthetic scheme used to make **125**.

However, at the third step to generate the ynol intermediate, we did not get the expected product. A full characterisation of the unknown product was performed to identify its structure. From the ^{1}H-NMR, there was a lack of the characteristic proton signal that usually appeared at around 6 ppm which corresponded to the proton adjacent to the hydroxyl group of the ynol. Moreover, there was an additional signal around 180 ppm which belonged to a carbonyl group (blue asterisk in **Figure 22**, **B**). This suggested that the unknown product could be the oxidised form of the ynol, compound **124**.

A



B

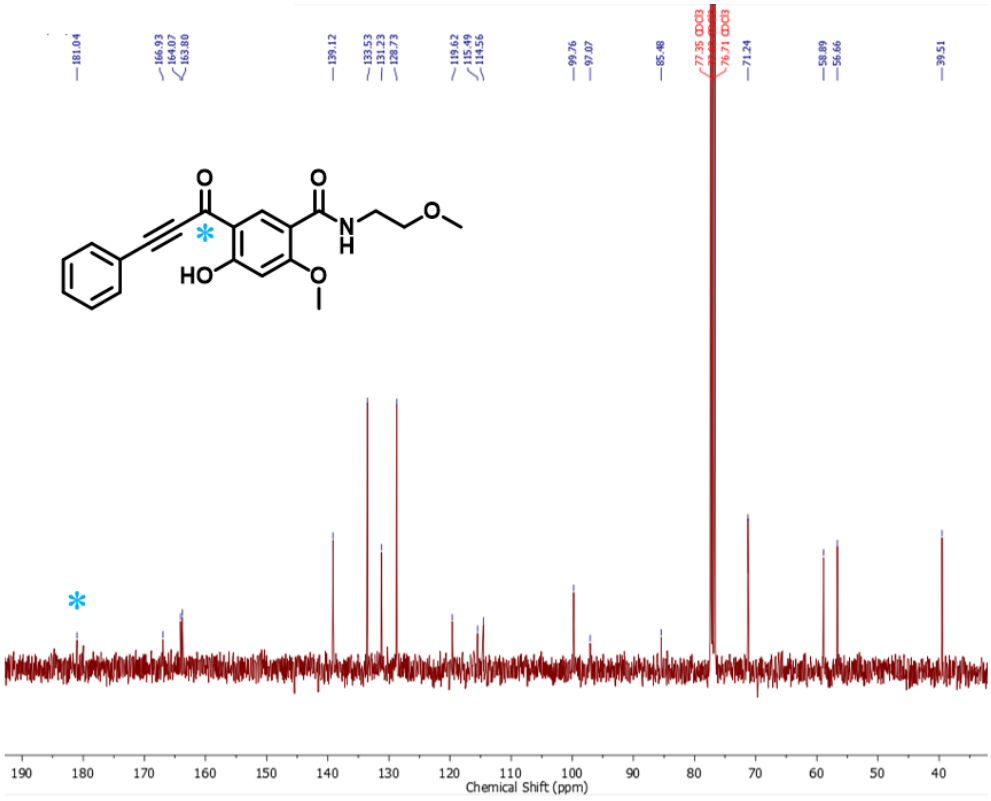


Figure 22: A) ^{1}H-NMR of **124**, B) ^{13}C-NMR of **124**.

This assignment was confirmed using MS as the mass of this product exactly matched with the mass of the O-alkynoylphenol intermediate, **124**. This outcome could be the result of heating under a reflux condition for 5 hours without ensuring that the reaction was under inert atmosphere (i.e. aerobic oxidation). The O-alkynoylphenol intermediate **124** was treated with PPh_3 in DMF in order to generate both the aurone and flavone. Unfortunately, from this reaction, the only product that we acquired was the aurone **125**.

The same synthetic strategy from **Scheme 30** was used to generate the other two final compounds, **126** and **127** (**Figure 23),** in 14% and 7%, respectively.

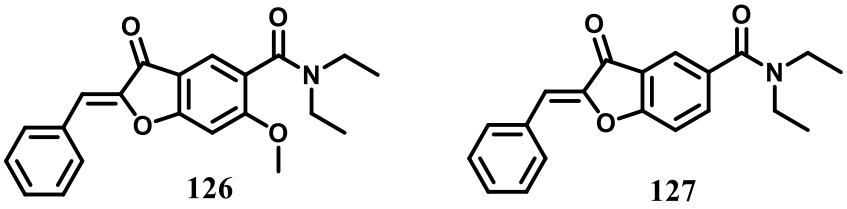
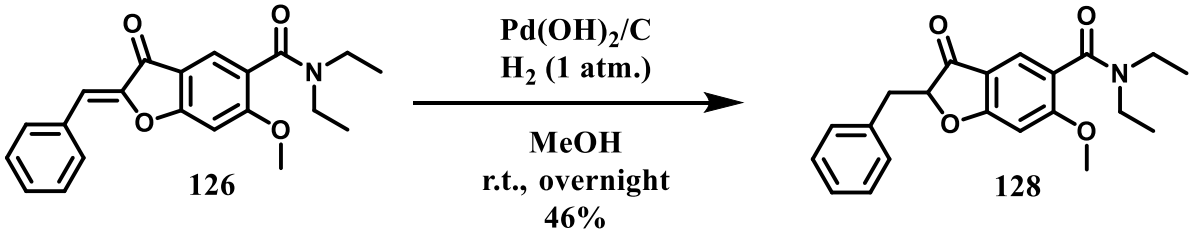


Figure 23: Chemical structure of **126** and **127**.

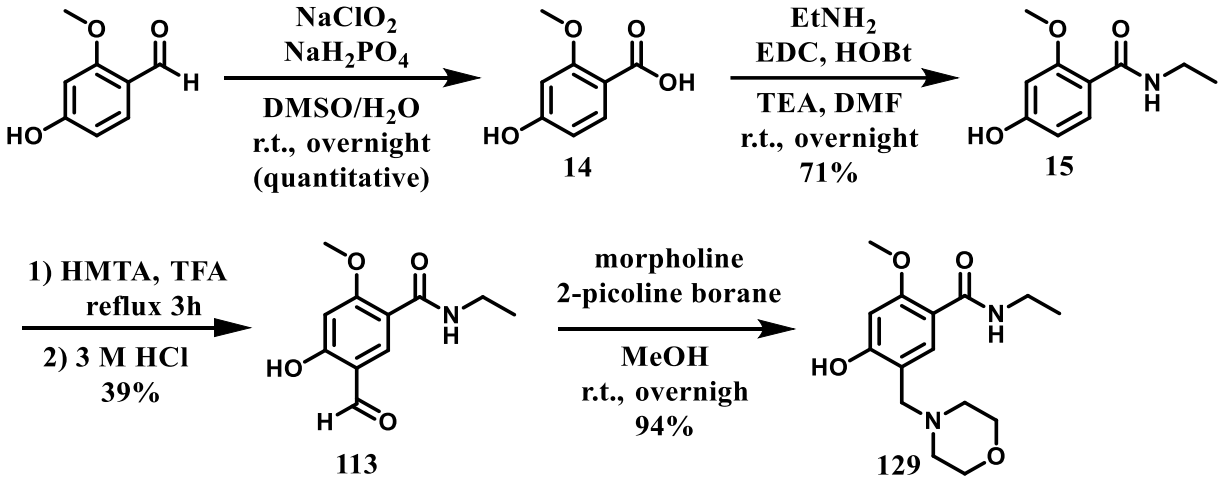
To generate follow on analogues that did not contain a Michael acceptor, **126** was subjected to hydrogenation to reduce the double bond (**Scheme 39**). This hydrogenation went smoothly under 1 atm of hydrogen gas using Pearlman's catalyst ($Pd(OH)_2/C$) in methanol to give **128** as the final product in 46% yield.



Scheme 39: Hydrogenation of **126** to give **128**.

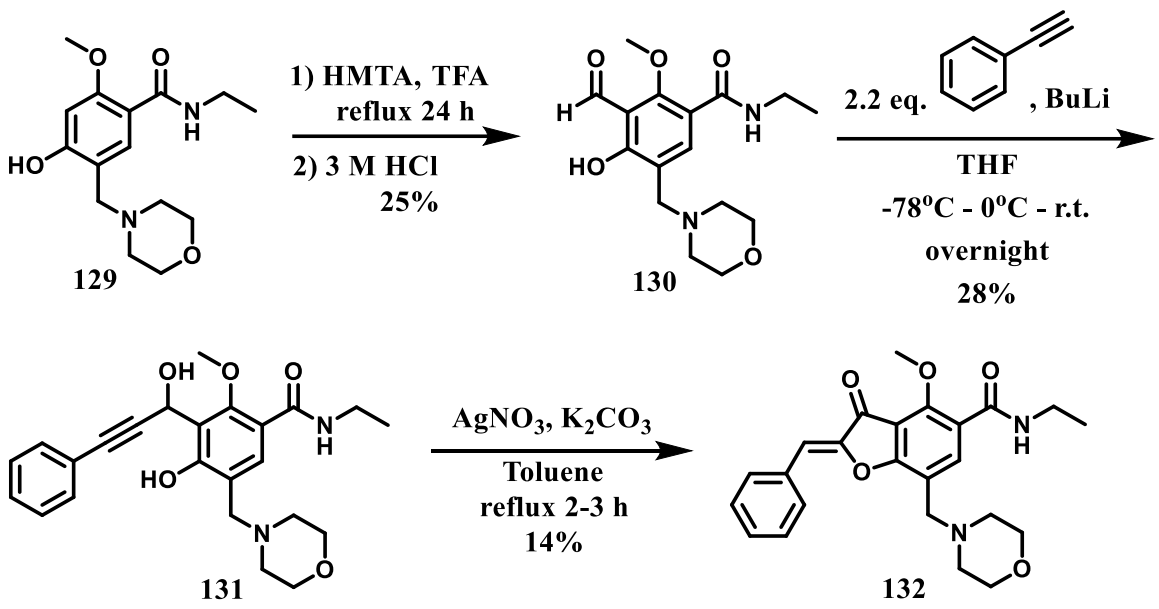
3.18 Synthesis of the initial inhibitor 12 *via* ynol intermediate

Since the developed synthesis that we used to generate the aurone products worked relatively well, we revisited our initial designed inhibitor **12** and applied the developed synthetic strategy as shown in **Scheme 40**, **41**, and **42**.



Scheme 40: The first four steps of the synthesis of the firstly designed inhibitor **12**.

The synthesis started from 4-hydroxy-2-methoxybenzaldehyde which underwent Pinnick oxidation using $NaClO_2$ and NaH_2PO_4 in a mixture of DMSO/H_2O at room temperature overnight to give **14** in quantitative yield. Compound **14** was then subjected to an amide coupling with ethylamine using EDC, HOBt, and triethylamine to afford **15** (71%). Duff reaction (HMTA in TFA under a reflux condition for 3 hours) was performed on **15** followed by reductive amination of the resulted intermediate using morpholine and 2-picoline borane to give **129** in 94% yield (**Scheme 40**).



Scheme 41: Synthesis of **132** from **129** *via* ynol intermediate.

Then, compound **129** was subjected to the other formylation using Duff reaction conditions to give **130** followed by the 1,2-addition of phenylacetylene to give the corresponding ynol **131** (28%). Compound **131** was subjected to a cyclisation/oxidation reaction using $AgNO_3$ and K_2CO_3 in toluene under a reflux condition for 3 hours to give **132** (14%) as shown in **Scheme 41**.

Comparing this synthetic strategy to the other one used to synthesise **12** in section **3.5**, it was obvious that the aurone synthesis *via* a 2-step reaction utilising $AgNO_3$ as a catalyst was more reliable. With this strategy, other analogues of the aurone could also be synthesised in the future.

To further confirm that the 2-step aurone synthesis gave the same configuration of the aurone product as the cyclisation in section **3.4**, a single crystal of **132** was grown and studied using X-ray crystallography. This was done by applying the same technique used to grow the crystal of **18a** (in section **3.4**). Then, the crystal structure of **132** was determined as shown in **Figure 24**. According to the crystal structure of **132**, it was confirmed that compound **132** was in the *Z* configuration as in compound **18a**.

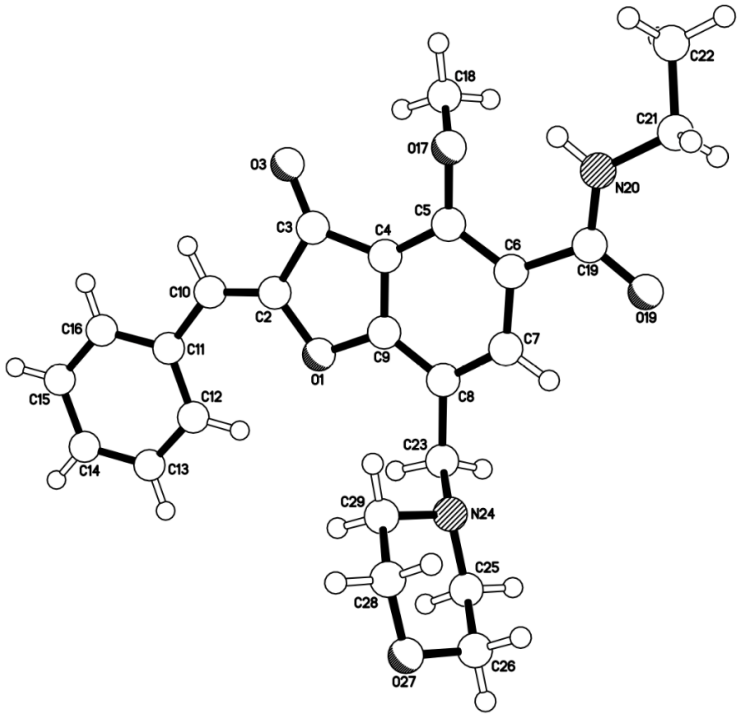
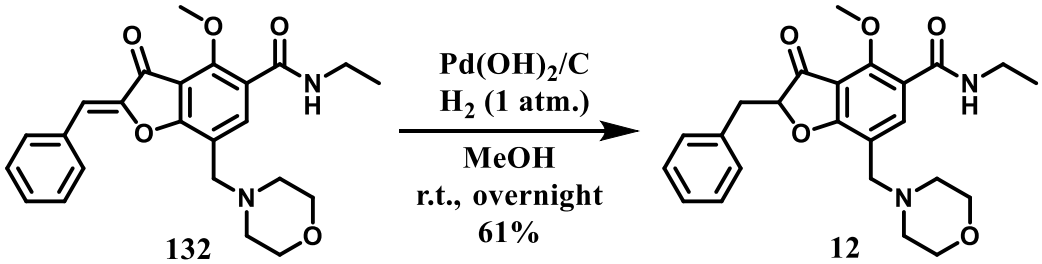


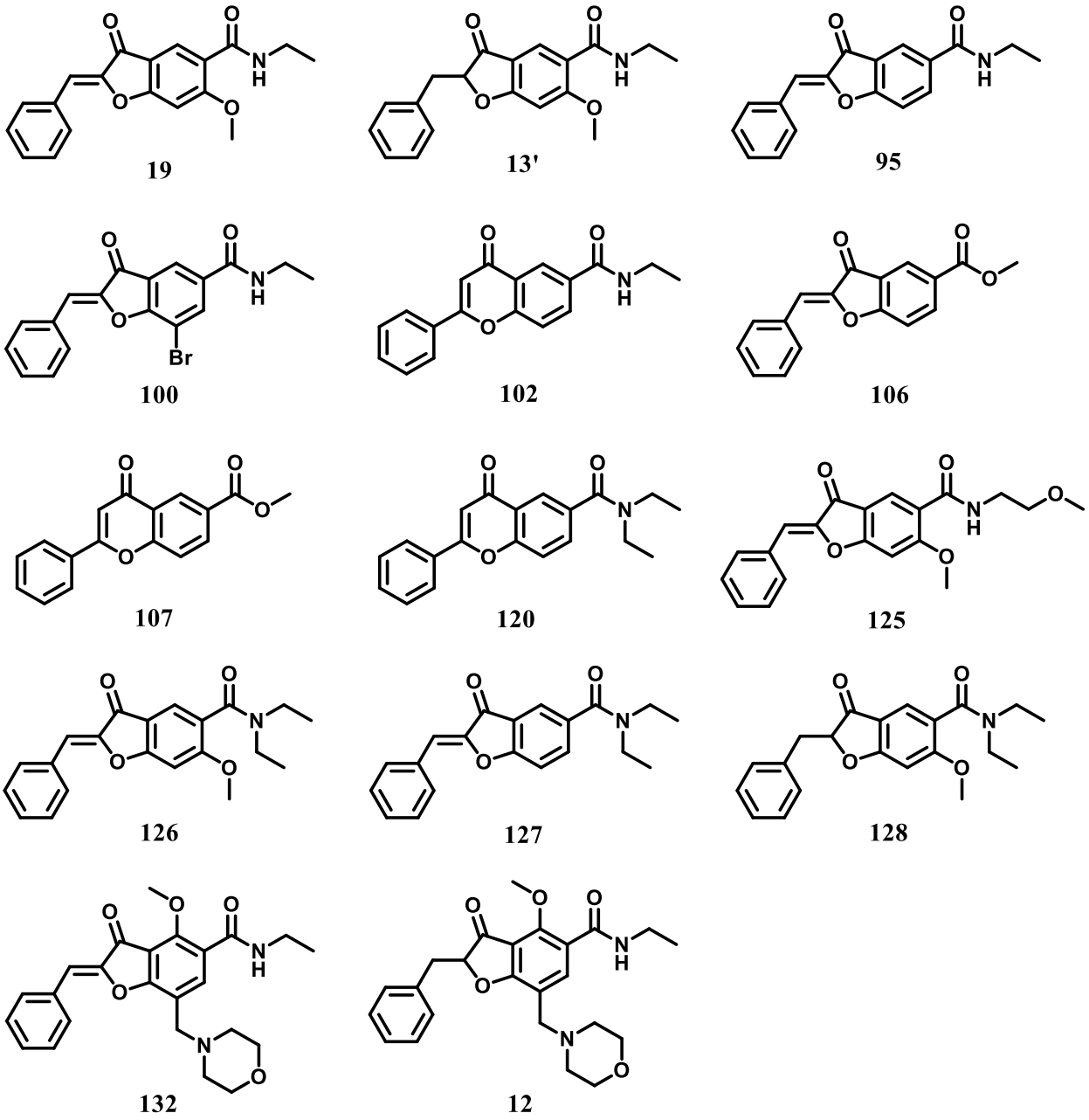
Figure 24: Crystal structure of **132**.

Finally, **132** was hydrogenated in order to eliminate the double bond to give **12** as the desired final product with the overall yield of 1.5% in 8 steps (**Scheme 42**).



Scheme 42: Synthesis of the firstly designed inhibitor **12** from **132**.

In summary, we successfully synthesised 14 target compounds as shown in **Scheme 43**.



Scheme 43: Summary of successfully prepared target compounds.

3.19 Biological Assays

3.19.1 Cell-based assay

A cell-based assay was used to test the synthesised compounds. In this assay, we used a Rat-2 *v-fms* cell line which expresses the *v-fms* oncogene. The line was provided by Dr. Nick Dibb.[131] The *v-fms* oncogene can express a mutant CSF-1 receptor that is active even in the absence of CSF-1.

The reason that the Rat-2 *v-fms* assay was chosen was because of two properties: 1) when this cell line grows in plastic, it shows contact inhibition which means that it stops growing when it forms a confluent monolayer of cells and 2) when it expresses the *v-fms* oncogene, it doesn't show contact inhibition and carries on growing so the cells pile up on top of each other. This effect is very easy to see and so it is a useful phenotypic assay. Normally, if a compound inhibits *v-fms*, it will stop the cell line from being transformed and the morphology of Rat-2 *v-fms* will revert to a Rat-2 morphology which has a much rounder appearance as shown in **Figure 25**.

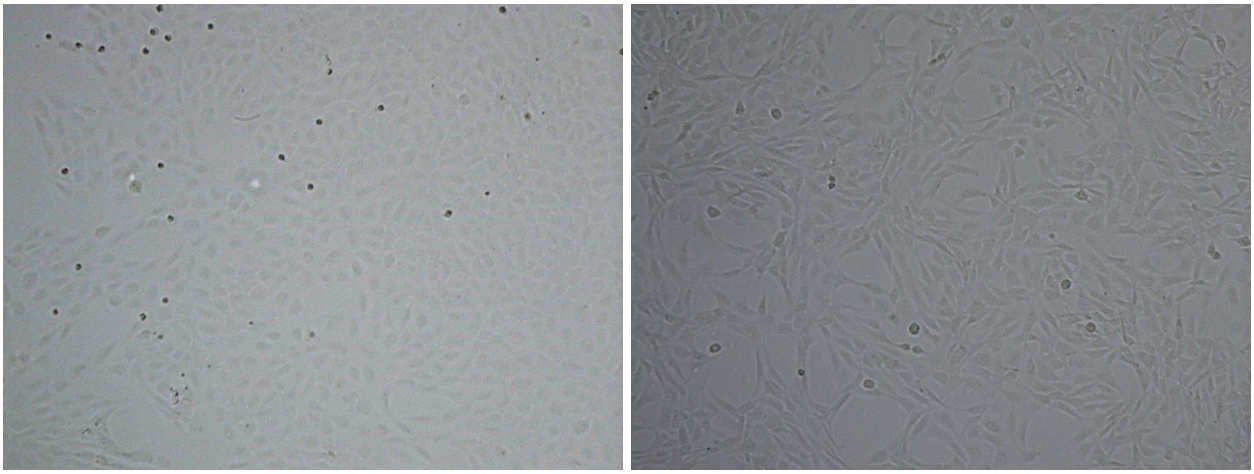


Figure 25: Rat-2 *v-fms* cells with FMS inhibitor dasatinib (left) and without dasatinib (right).

With help from Dr. Nick Dibb, the Rat-2 *v-fms* cell line was cultured in a 24-well plate for 7 days. After that, the final compounds that were synthesised including **12**, **13′**, **19**, **95**, **106**, **125**, **126**, **127**, **128**, and **132** were administered into each well in a serial dilution from 100 μM to 1 μM. We also tested compound **11** and dasatinib as a positive control which were administered to the cells using the same serial dilution along with a negative control (only DMSO). The cells which were treated with the compounds were incubated for 24 hours. The results were collected after the incubation period as shown in **Figure 26**.

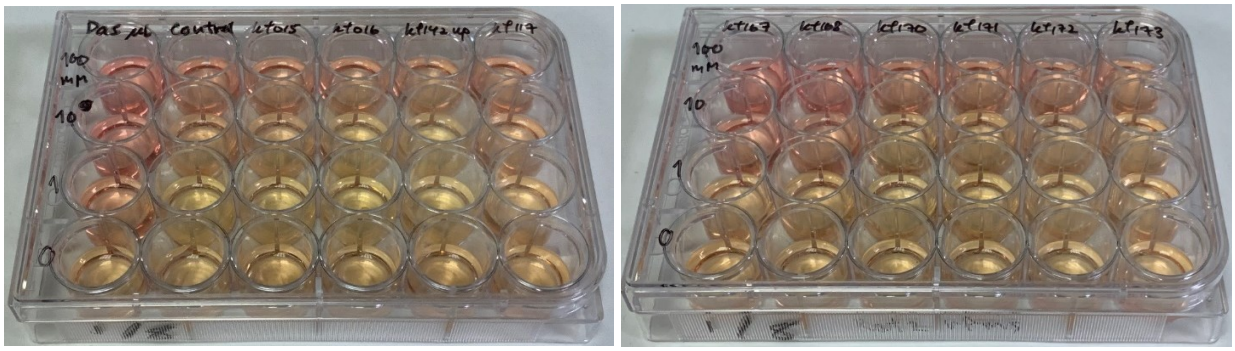


Figure 26: Left: Rat-2 *v-fms* cells treated with dasatinib, **11**, **19**, **13′**, **106**, and **95** (from left to right). The concentrations of the compounds were in a serial dilution from 100 µM, 10 µM, 1 µM, and 0 µM (only DMSO) as a negative control (from top to bottom). Right: Rat-2 *v-fms* cells treated with **126**, **127**, **132**, **125**, **128**, and **12** (from left to right) with the same sequence of concentrations from Left. The red media such as that shown in the top left in **Figure 26** indicated inhibition of cell proliferation while the yellow media such as that shown in the bottom row indicated cell growth (RPMI media used: indicator – phenol red).

From the results obtained, there was no evidence that the inhibitors were having any effect in this assay. At 100 µM, all inhibitors inhibited cell growth. This could be due to non-specific cytotoxicity of all inhibitors at 100 µM. At 10 µM, there was much less cell growth inhibition, but importantly there was no change in cell morphology from transformed to non-transformed morphology that could be seen with the dasatinib control (**Figure 25**, left).

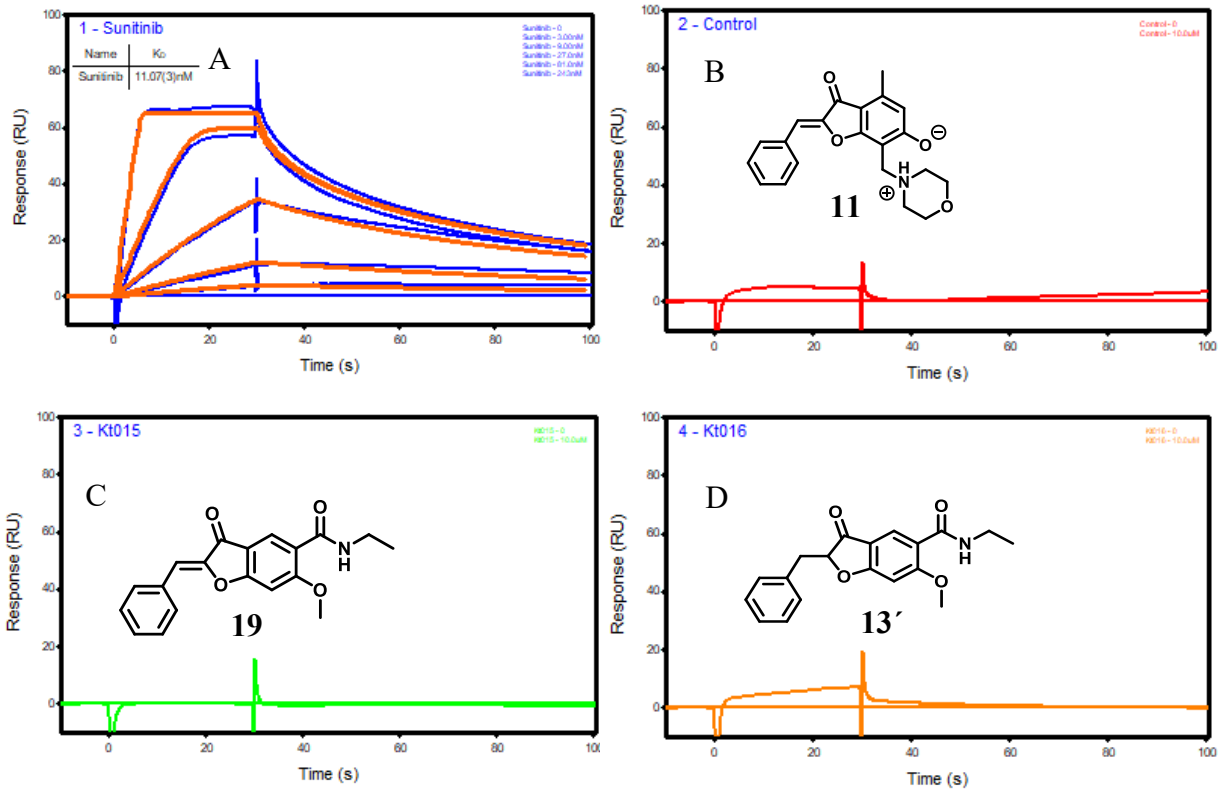
While further replication would be preferable, we concluded that the inhibitors developed were not potent compounds for FMS kinase.

3.19.2 Cell-free SPR assay

The next assay that was used was the cell-free surface plasmon resonance (SPR) assay. SPR is a technique used to assess the binding interaction between a protein and a ligand from which the dissociation constant (K_d) can be derived. It starts with immobilisation of a protein to a sensor chip surface. Then, a ligand is added to a buffer that flows over the protein surface. The interaction of the ligand and protein is measured and the kinetic profile is recorded as a sensorgram (**Figure 27**) which is a plot of response against time, showing the progress of the interaction. From the

sensorgram, the dissociation constant can be calculated. The SPR assay in this project was performed by Dr. Olan Dolezal at CSIRO.

The first batch of the inhibitors that were tested included **11**, **13′**, **19**, **106**, and **107**. In this assay, the FMS kinase was used as immobilised protein surface and sunitinib was used as a positive control. All inhibitors were preliminary tested at 10 μM concentration. From the results provided (**Figure 27**), sunitinib (**Figure 27, A**) bound well to FMS kinase giving a K_d of 11 nM. However, the other inhibitors did not bind to FMS kinase in a measurable way since no measurable curve is observed in the sensorgram (**Figure 27, B-F**).



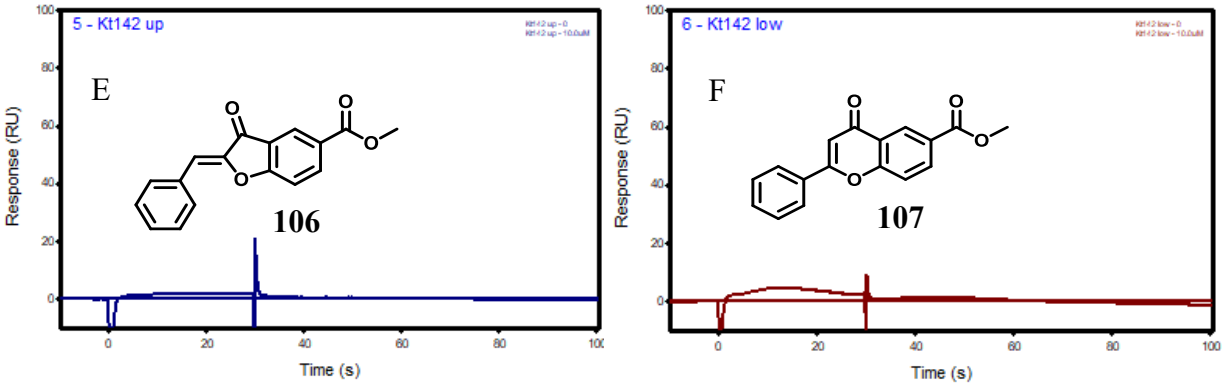
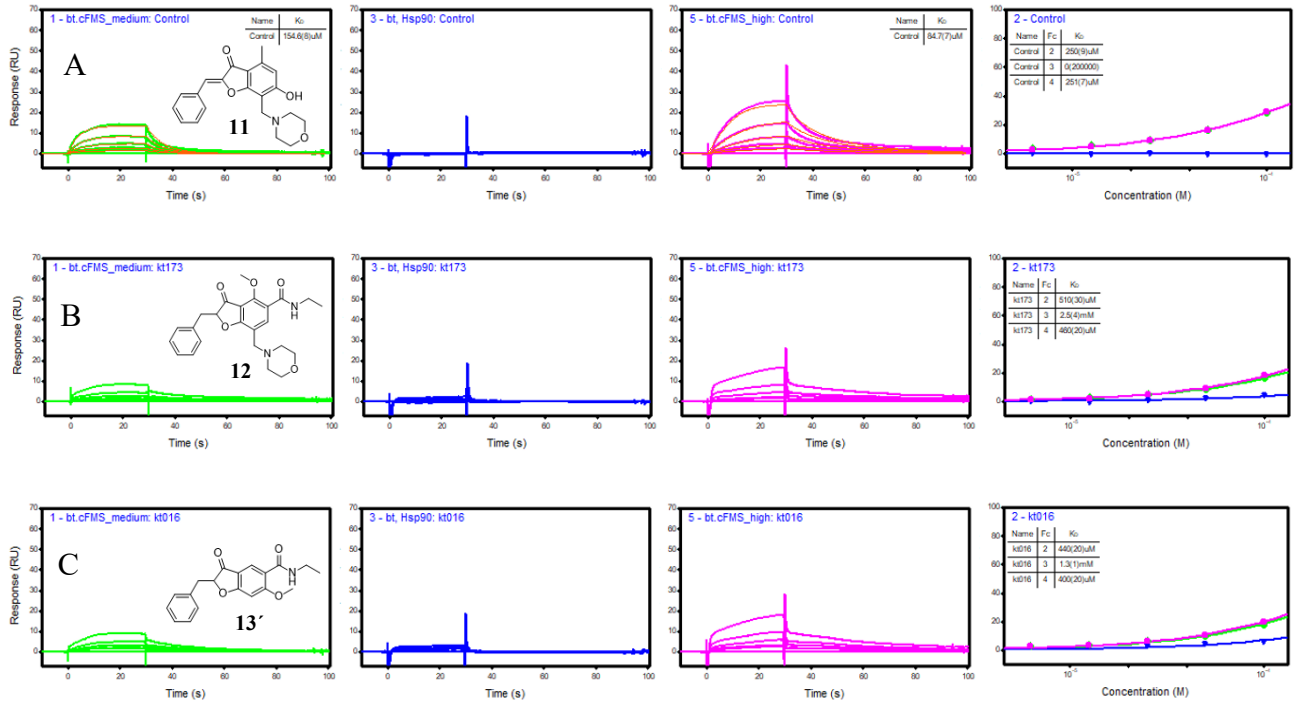
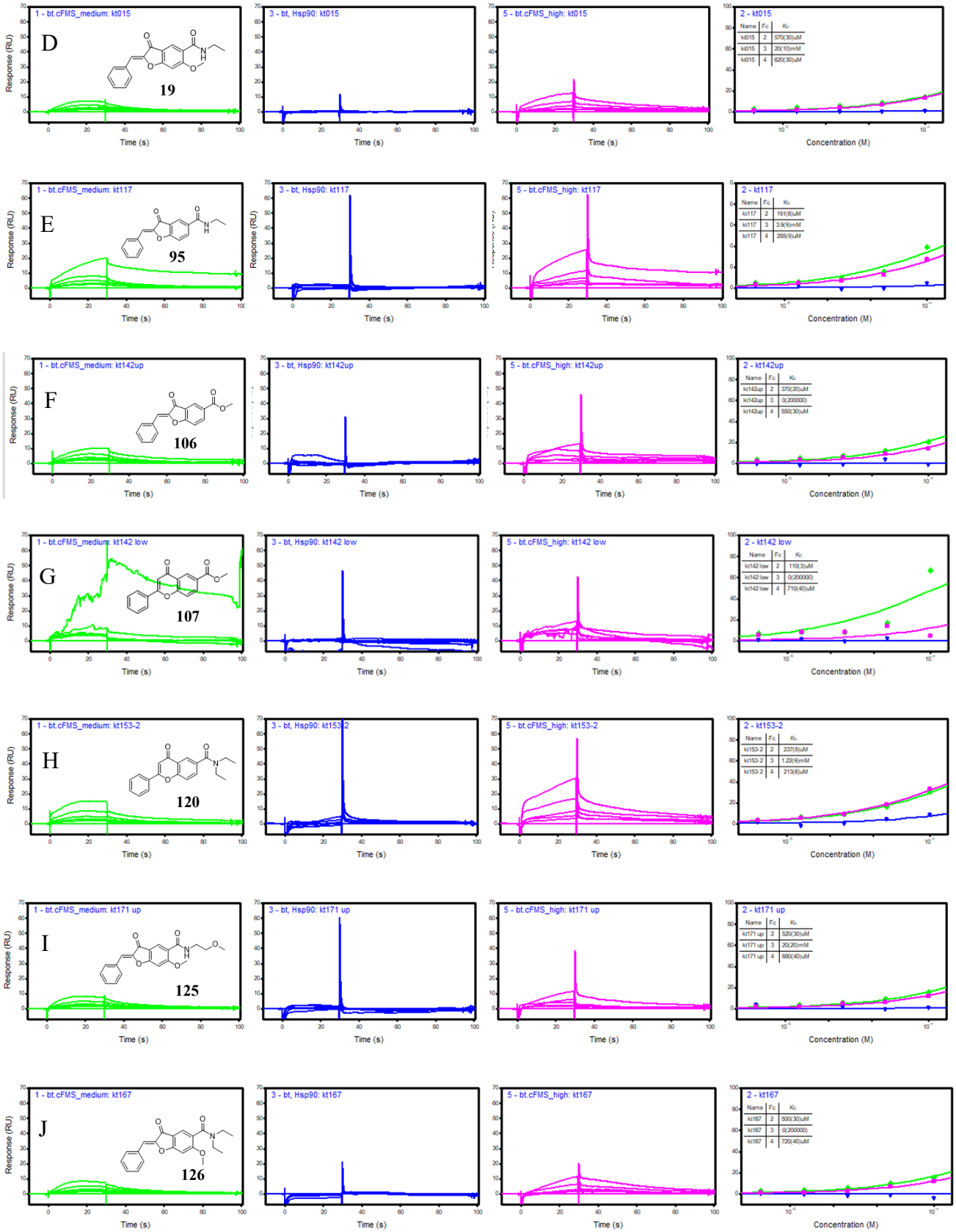


Figure 27: SPR assay sensorgrams of sunitinib (A), **11** (B), **19** (C), **13′** (D), **106** (E), and **107** (F).

A second batch of the inhibitors including **12**, **95**, **120**, **125**, **126**, **127**, **128**, and **132** was tested in the SPR assay along with the first batch of the inhibitors. Three different surfaces in three separate flow cells were prepared including FMS kinase (higher and lower density) and Hsp90 as a negative control (shown in magenta, green, and blue sensorgram in **Figure 28**, respectively). The inhibitors were run in a serial dilution from 100 µM, 50 µM, 25 µM, 12.5 µM and 6.25 µM.




D
19
1 - bt.cFMS_medium: kt015
3 - bt, Hsp90: kt015
5 - bt.cFMS_high: kt015
2 - kt015
E
95
1 - bt.cFMS_medium: kt117
3 - bt, Hsp90: kt117
5 - bt.cFMS_high: kt117
2 - kt117
F
106
1 - bt.cFMS_medium: kt142up
3 - bt, Hsp90: kt142up
5 - bt.cFMS_high: kt142up
2 - kt142up
G
107
1 - bt.cFMS_medium: kt142 low
3 - bt, Hsp90: kt142 low
5 - bt.cFMS_high: kt142 low
2 - kt142 low
H
120
1 - bt.cFMS_medium: kt153-2
3 - bt, Hsp90: kt153-2
5 - bt.cFMS_high: kt153-2
2 - kt153-2
I
125
1 - bt.cFMS_medium: kt171 up
3 - bt, Hsp90: kt171 up
5 - bt.cFMS_high: kt171 up
2 - kt171 up
J
126
1 - bt.cFMS_medium: kt167
3 - bt, Hsp90: kt167
5 - bt.cFMS_high: kt167
2 - kt167
Response (RU)
Time (s)
Concentration (M)

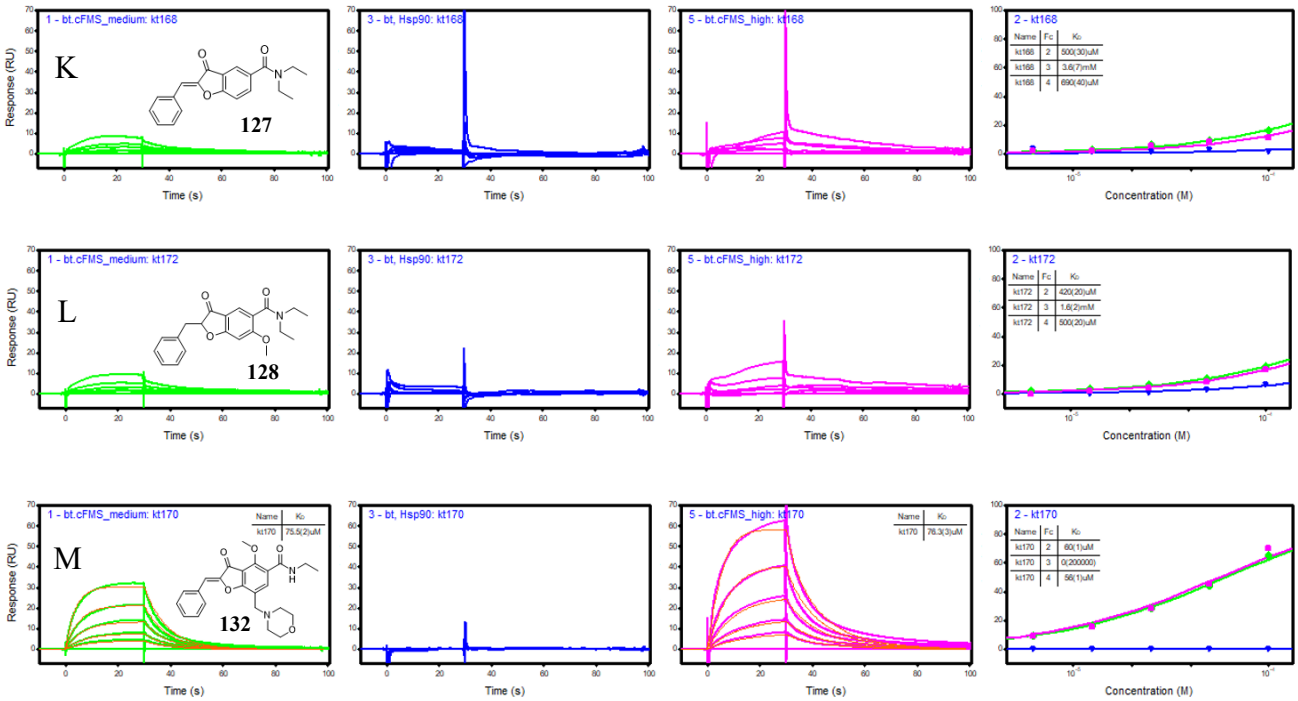


Figure 28: SPR Assay Sensorgrams of **11** (A), **12** (B), **13′** (C), **19** (D), **95** (E), **106** (F), **107** (G), **120** (H), **125** (I), **126** (J), **127** (K), **128** (L), and **132** (M). Green sensorgram represented low density biotinylated FMS surface. Blue sensorgram represented biotinylated Hsp90 N terminal domain (control protein) surface. Magenta sensorgram represented high density biotinylated FMS surface. The far right sensorgram showed the plot of response against concentration.

Disappointingly, a few of the compounds showed poor solubility and/or bad SPR behaviour at concentrations ≥10 μM. Therefore, any estimated K_d might not be accurate. From the results shown in **Figure 28**, compound **11** and **132** were the inhibitors that exhibited robust binding interactions with K_d at 250.5 μM and 58 μM, respectively. Nevertheless, compound **11** was precipitated out of the solution which clearly affected the estimated K_d that might be higher than usual.

From the SPR assay, most of the inhibitors synthesised in this project did not exhibit good binding interactions with FMS kinase apart from the two inhibitors which were **11** and **132**, although the estimated K_d of the inhibitors might have been incorrect because of the solubility issues of the inhibitors. This could be seen from the difference in the K_d of **11** from the prior work[95] which was 4.9 μM, whereas the measurement of the K_d of **11** in this project was 250.5 μM.

3.19.3 Kinase assay

The final assay used to screen the inhibitors against FMS kinase catalytic domain was an activity assay. The inhibitors were sent to Reaction Biology to perform the HotSpot™ kinase assay. The HotSpot™ kinase assay is a radioactive assay in which ^{33}P-labelled phosphate from ATP is transferred to the kinase substrate measuring enzyme activity and the results are provided as IC_{50} value. The inhibitors were tested against FMS kinase in a 10-dose IC_{50} measurement with 3-fold serial dilution starting at 100 μM. Reactions were carried out at 10 μM ATP.

Table 8: Summary of IC_{50} of the active inhibitors.

Compound	Compound IC_{50}
11	0.081 ± 0.012 μM
19	>100 μM
95	34.4 ± 4.5 μM
127	>100 μM
132	1.33 ± 0.23 μM
Staurosporine	1.25 ± 0.15 nM

*An IC_{50} value higher than 100 μM was estimated based on the best curve fitting available.
**The other inhibitors had no inhibition or compound activity that could be fit to an IC_{50} curve.
***Values are reported as mean ± standard deviation.

The kinase assay for our inhibitors was performed in triplicate in order to test the reproducibility. However, there were only five inhibitors which were listed in **Table 8** that exhibited measurable FMS activities. Compound **11**, which was the template compound that initiated the project

exhibited the best IC_{50} of 0.081 ± 0.012 μM. Compound **95** and **132** showed modest IC_{50} values of 34.4 ± 4.5 μM and 1.33 ± 0.23 μM, respectively.

3.20 Conclusions

In this chapter, we designed new molecules that were expected to act as FMS kinase inhibitors. The design of the new inhibitors was based on two novel molecules from the former Fuchter group member, Dr. Robert Davidson. By combining potential features from the aforementioned molecules, **10** and **11**, (see section **3.2**) we finally designed a novel molecule **12** (**Figure 15**), an aurone-based compound, which incorporated two hydrogen bond acceptors and a group projected towards the allosteric site in FMS.

Apart from the successful synthesis of **12** and its unsaturated form, compound **132**, we also successfully synthesised analogues of compound **12** and their unsaturated form by varying a side chain in the core aromatic ring or changing an amide side chain. These included **13′**, **19**, **95**, **100**, **106**, **125**, **126**, **127**, and **128**. Other target compounds with a flavone core that were successfully synthesised were **102**, **107**, and **120**.

For the biological aspect, the final products were tested in three different assays: a cell-based assay, a cell-free SPR assay, and a kinase assay. Disappointingly, the biological data obtained from all assays suggested that no compounds were sufficiently potent against FMS to warrant further investigation.

While we did not obtain satisfactory results from the compounds successfully synthesised, we believe that the potency of aurone-based compounds as FMS inhibitors can still be improved. In future work, it may be worth to consider changing side chains in the core aromatic ring in order to acquire better binding interactions with the hinge and allosteric regions in FMS. A substituted aromatic ring can be used instead of the free aromatic ring in the molecule in order to improve solubility and/or permeability of the inhibitors. It is also interesting to expand the compound library further than aurone scaffold which includes the compounds in the flavonoid family such as flavones, isoflavones, flavanones, and isoflavanones.

——Chapter 2——

4. Introduction to PROTACs

The levels of intracellular proteins are regulated through two major mechanisms: the rate of protein synthesis and the rate of protein degradation. Protein degradation removes undesirable, damaged, or excess proteins from cells. In eukaryotic cells, the ubiquitin-proteasome pathway and the lysosomal proteolysis mediated pathway are two main pathways for protein degradation, with the former being the most commonly employed one.[132]

4.1 The Ubiquitin-Proteasome System (UPS)

The Ubiquitin-Proteasome System (UPS) is the primary intracellular mechanism for the destruction of damaged or misfolded proteins. Ubiquitin is a polypeptide that comprises 76 amino acid residues and is used as a marker.[133] Attachment of one or more ubiquitin molecules (referred to as mono- or poly-ubiquitination) to a lysine residue of a protein is used to determine different cellular responses such as protein degradation, gene regulation, and DNA repair.[134] However, protein degradation by the 26S proteasome, a multi-subunit protease complex, usually occurs when a poly-ubiquitin chain is formed through Lys48 in the ubiquitin.[135]

The mechanism of adding ubiquitin to a lysine residue in a target protein is achieved using three enzyme species and is illustrated in **Figure 29**. These are an E1 activating enzyme, an E2 conjugating enzyme, and an E3 ligase. An E1 activating enzyme activates the free ubiquitin and forms the complex between the ubiquitin and the E1 activating enzyme. The activated ubiquitin is subsequently transferred to an E2 enzyme, forming a ubiquitin-E2-complex. With the help of an E3 ligase, the ubiquitin-E2 complex is brought into proximity with a protein of interest (POI) and the ubiquitin is then transferred to a lysine residue in the POI.[136] Polyubiquitination can occur at one or more of the other surface lysine residues in the ubiquitin, mostly *via* internal Lys48 of the ubiquitin. As part of the UPS, the recognition of polyubiquitin by 26S proteasome leads to the degradation of the protein into short peptide fragments followed by a removal of the ubiquitin units which can be recycled within the cells.[137,138]

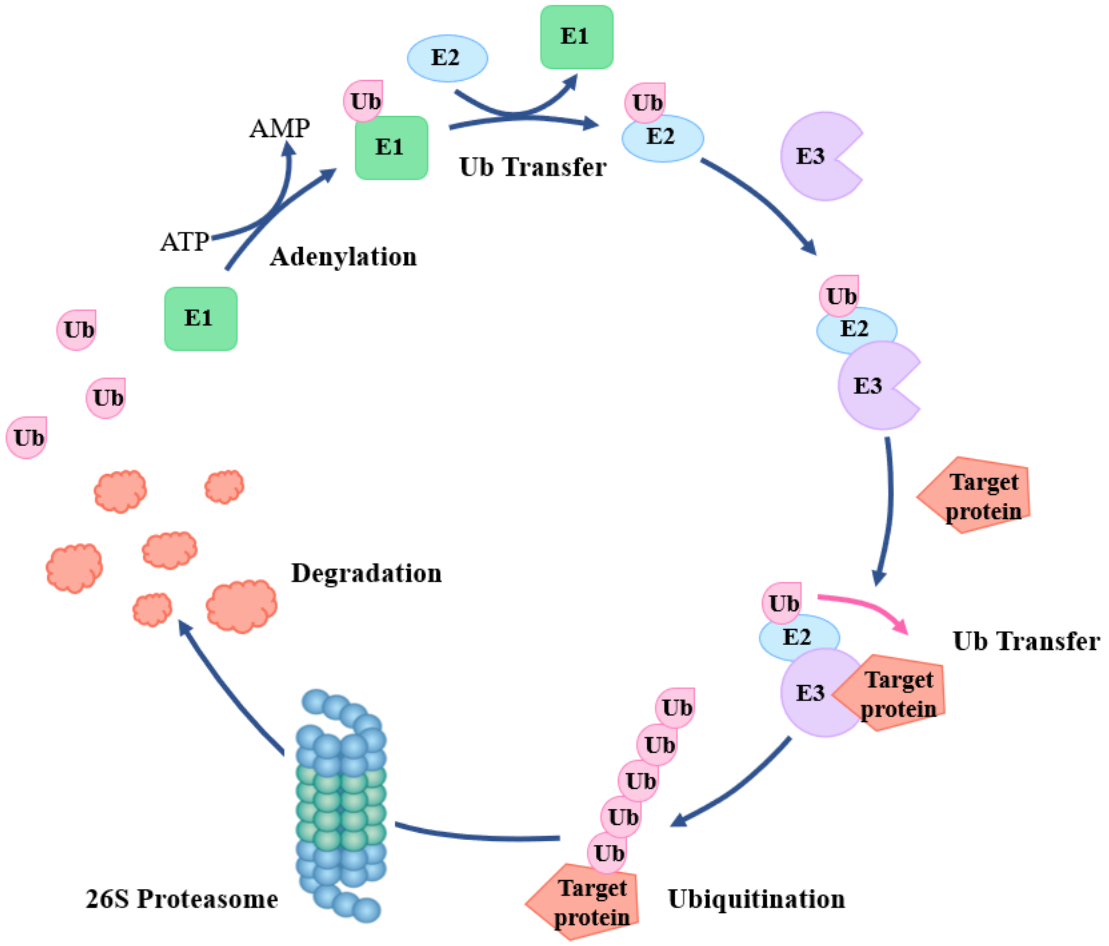


Figure 29: Mechanism of protein degradation mediated by the ubiquitin-proteasome pathway.

4.2 Proteolysis-Targeting Chimeras or PROTACs

Proteolysis-targeting chimeras or PROTACs were first reported in 2001 by Sakamoto *et al*. as a new class of compounds developed to hijack the UPS for target protein degradation.[139] PROTACs have gained lots of interest in the last two decades due to their novel therapeutic action.[140-142] PROTACs have the potential to expand the druggable proteome since they operate *via* an "event-driven pharmacology model". This is in comparison to conventional small molecule inhibitors, where the binding of a small molecule within an active pocket of the protein is an "occupancy-driven pharmacology model".[143] An occupancy-driven mode of action requires high target occupancy where a high concentration of the drug is needed, leading to potential off-target activities and undesired side effects.[141,144] On the other hand, the operation of PROTACs through

an “event-driven pharmacology model” does not require direct inhibition of the functional activities but only needs a transient or weak binding with the target proteins. As a result, the off-target side effects can be reduced and a higher selectivity can be achieved.

Several proteins associated with different types of cancers have been successfully degraded using PROTACs.[145-147] This showcases that PROTAC technology possesses potential to be a novel therapeutic for cancer therapy. Examples of proteins degraded by PROTACs include the androgen and estrogen receptors,[148] the bromodomain-containing protein 4 (BRD4),[145] Bruton’s tyrosine kinase (BTK),[149] BRC-Abl,[150] FMS-like tyrosine kinase 3 (FLT-3),[149] and many others.[142]

4.3 PROTAC structure and mode of action

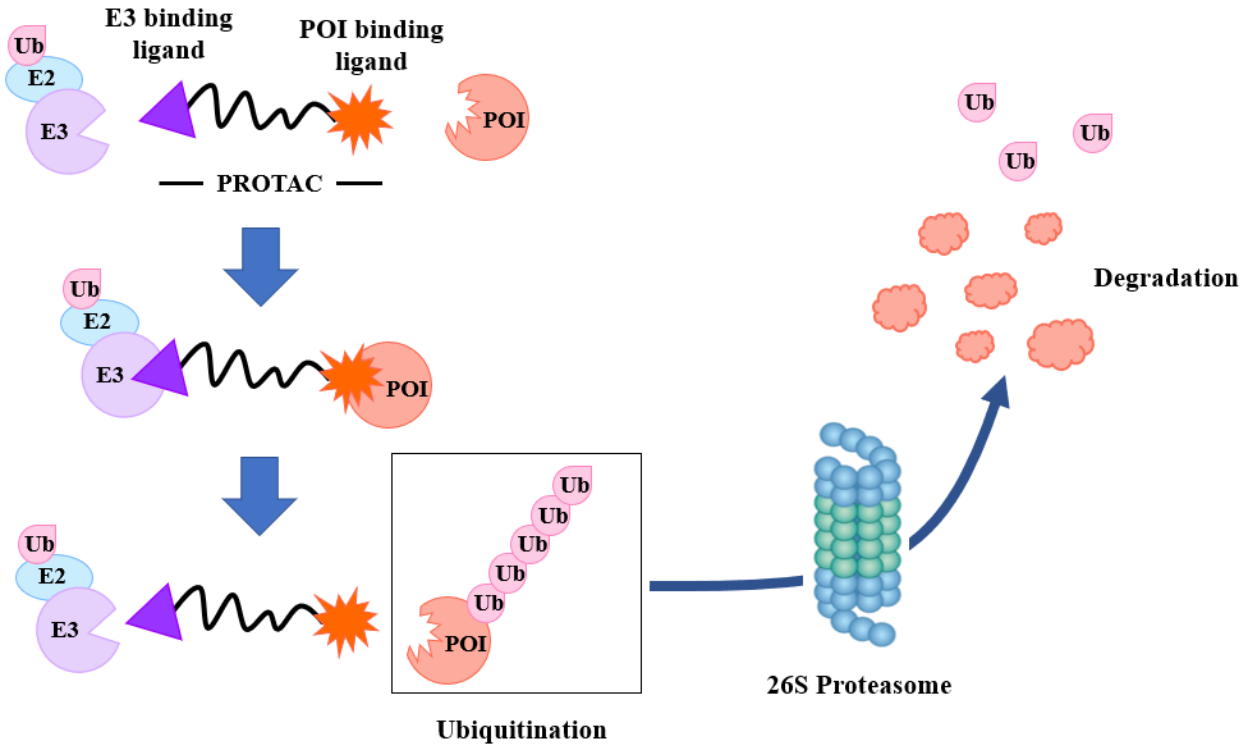


Figure 30: Schematic structure and mechanism of a PROTAC.

PROTACs are hetero-bifunctional molecules consisting of 1) a ligand (or a warhead) which targets a POI, 2) a ligand that recruits an E3 ubiquitin ligase (E3), and 3) a linker that connects these two. PROTACs function by forming a ternary complex between the POI and the E3 ligase (POI–PROTAC–E3 ligase), bringing the POI into close proximity with the E3 ligase. Subsequently, this

POI is subjected to polyubiquitination, resulting in degradation of the target protein by the 26S proteasome[151-153] (**Figure 30**). This leads to a complete removal of the POI from cells, thus terminating downstream signaling.

In humans, there are more than 600 E3 ligases.[154] However, only a handful of E3 ligases with small molecule ligands are currently available. Examples of these E3 ligases are the mouse double minute 2 homologue (MDM2), cellular inhibitor of apoptosis protein 1 (cIAP1), Von Hippel-Lindau (VHL), and cereblon (CRBN).[155] The first generation of PROTACs utilised peptide fragments as a ligand to recruit both the E3 ligases and the POI[139,148,156] (shown in **Figure 31**).

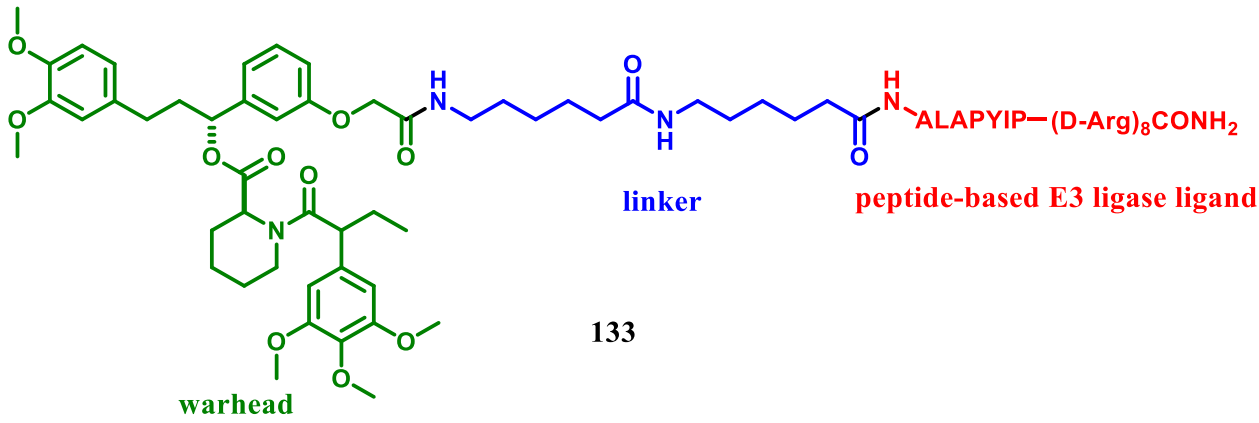


Figure 31: An example of a peptide-based PROTAC.[156] The coloured segments indicate each component in a PROTAC.

These peptide-based PROTACs have been shown to successfully degrade the target proteins in a low-micromolar range concentration. The required high concentration of this first generation is possibly due to a poor cellular activity of the peptide-based PROTACs.[143]

Because of the poor cellular activity of the first generation PROTACs which limited further advancement of the PROTAC technology, the development of small molecule PROTACs has emerged. The first all small molecule-based PROTAC which induced the degradation of the androgen receptor was reported in 2008.[157] This modification enabled PROTACs to have improved drug-like properties like better stability, cellular biodistribution, and permeability.[157] Although there are several E3 ligases that are being targeted, the two most commonly targeted E3 ligases are VHL and CRBN.[158,159]

4.4 Advantages and disadvantages of PROTACs

PROTACs have several advantages over classical small molecule inhibitors. Since PROTACs operate *via* an event-driven mechanism, they possess the ability to function catalytically and can be involved in multiple rounds of target protein degradation.[160] In addition, owing to PROTACs' catalytic functions, the induced degradation is also sub-stoichiometric.[161] Since PROTACs possess the capacity to mediate multiple rounds of target protein ubiquitination and degradation, only a low concentration of the drug is required. Additionally, PROTACs can potentially target any POI including those which are considered undruggable since they do not require to bind to a specific active site of a protein,[162] thus providing another advantage of PROTACs. Due to the involvement of PROTACs in rapid and sustained depletion of the POIs, inhibition of the downstream signaling cascades of the POIs is observed.[161]

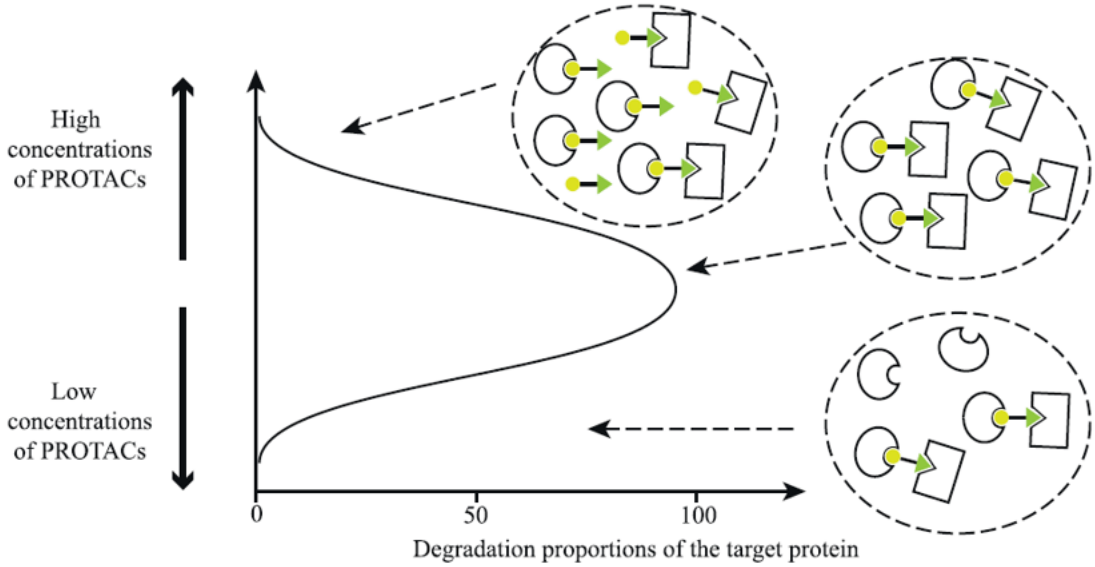


Figure 32: Schematic representation of the hook effect. The hook effect usually occurs when the PROTAC concentration is too high with regards to the concentrations of the POI and E3 ligase. This results in the formation of two unwanted dimeric complexes, PROTAC–E3 ligase and PROTAC–POI, instead of the desired ternary complex, POI–PROTAC–E3 ligase. From An *et al.*[161]

However, PROTACs also pose several challenges for the researcher to overcome. Firstly, at high concentration of PROTACs, the hook effect is frequently observed.[163,164] The hook effect (**Figure 32**), a common phenomenon associated with three-component systems, is described as a formation

of an unproductive binary complex instead of the required ternary complex. The binary complexes form *via* the binding of two separate PROTACs to the POI and the E3 ligase, thus, preventing the formation of the desired ternary complex and subsequent proteasomal degradation. Secondly, the design and synthesis of PROTACs can be a time-consuming process since the modification, optimisation, and development of ligands targeting both the POI and the E3 ligases as well as linkers are needed. Lastly, small-molecule PROTACs usually possess high molecular weight which results in a poor cell permeability.

4.5 Consideration of PROTAC components

As PROTAC molecule consists of three different parts including a POI targeted ligand (or warhead), a linker, and an E3 ligase ligand (shown in **Figure 30** and **31**), it is crucial to carefully select the PROTAC components in order to properly design and optimise the molecule for POI degradation. The selection of these components is important since the formation of the ternary complex between POI–PROTAC–E3 ligase determines the effect of PROTACs. A warhead and an E3 ligase ligand are usually developed and optimised separately for distinct interactions with the proteins involved. Thereafter, the warhead and the E3 ligase ligand are joined by a linker; length and composition was shown to provide an effect on the extent of protein degradation and isoform specificity.[165,166] Therefore, in the PROTAC design and development, the following features need to be considered.

4.5.1 Ligand targeting the POI and site of linker attachment

Currently, most of the PROTAC warhead designs are based on small molecule inhibitors,[141] for example, **ARV-825** (**135**) which incorporates the potent BRD4-targeting drug candidate, **OTX-105** (**134**),[167] and **MZ1** (**137**) which utilises **JQ1** (**136**), a BRD4 inhibitor[168] (**Figure 33**).

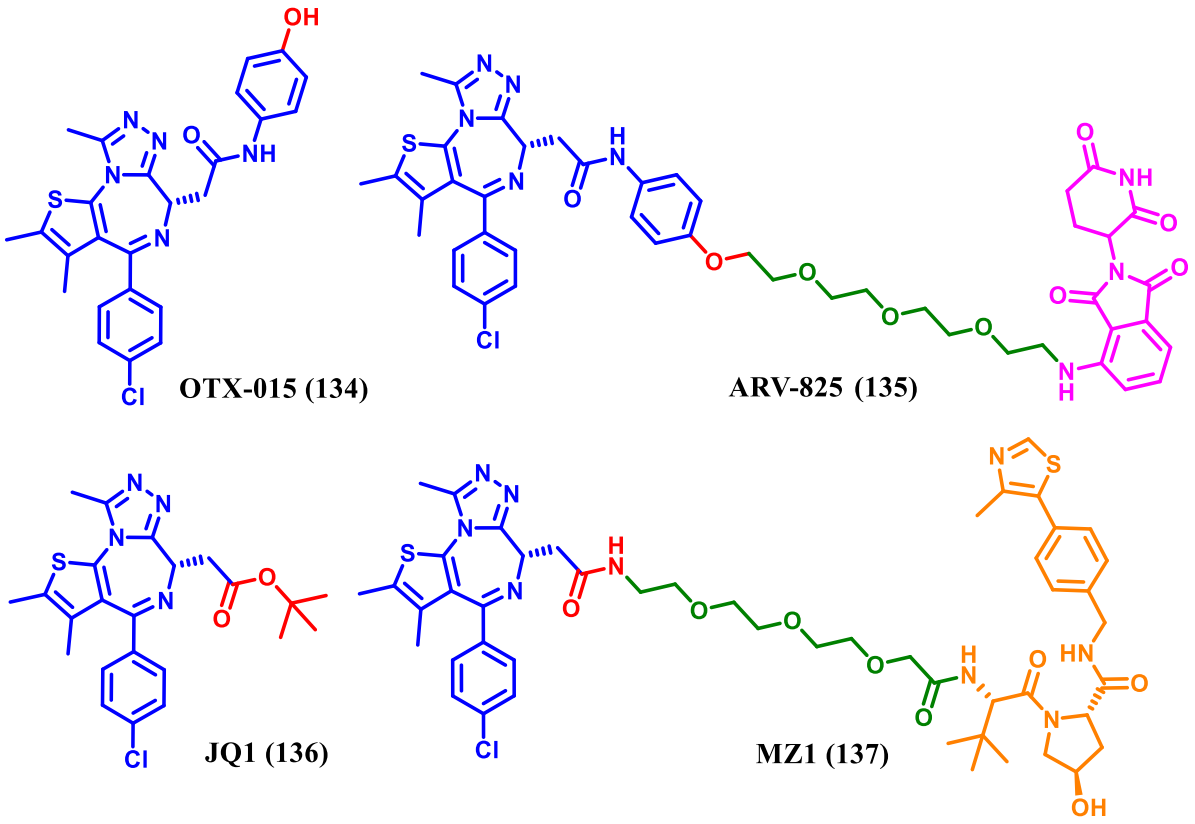


Figure 33: Examples of Examples of small-molecule inhibitors (highlighted in blue) and their site of linker attachment (highlighted in red) and PROTACs from corresponding inhibitors (**ARV-825** (**135**) from **OTX-015** (**134**)[167] and **MZ1** (**137**) from **JQ1** (**136**)[168]) with different E3 ligase ligand (magenta: CRBN and orange: VHL).

The site of linker attachment is usually determined from the solvent exposed area of the ligand-protein binding structures.[169] An example of the selection of the site of linker attachment is shown in **Figure 34**. Although potent affinity of the warhead is needed, increasing the affinity does not necessarily increase the rate of protein degradation.[144] Since the PROTACs also promote the interaction between the POI and the E3 ligase, it is important to note that, in order to achieve the best degradation profile, a stable ternary complex between POI–PROTAC–E3 ligase is needed.

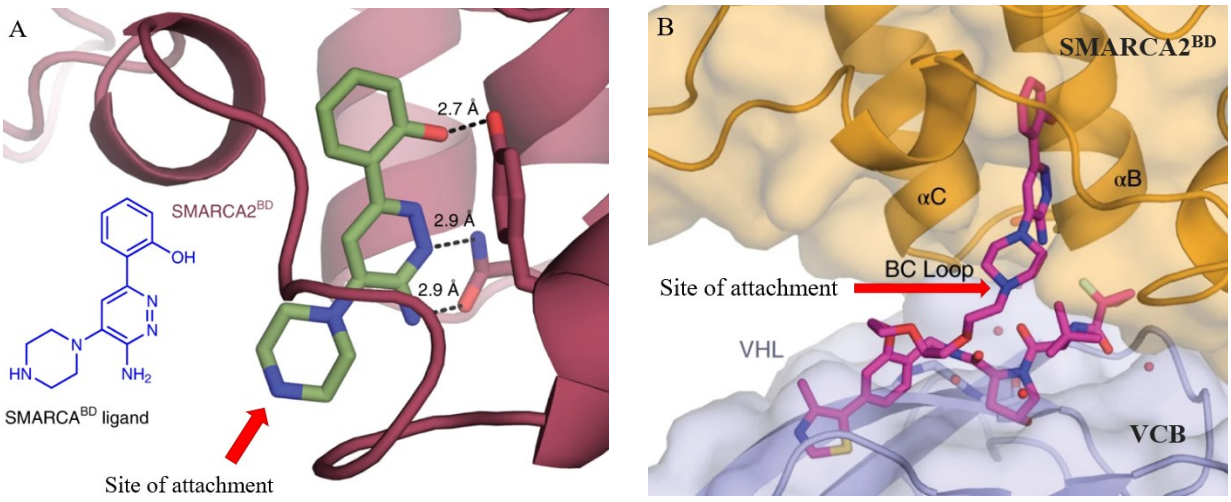


Figure 34: A) Chemical structure of a SMARCA^{BD} ligand and a co-crystal structure of it bound to SMARCA2^{BD}. B) Co-crystal structure of VCB:PROTAC1:SMARCA2^{BD}. The PROTAC1 is shown in stick with magenta carbon. Red arrows indicate the site of linker attachment which is in solvent exposed area of SMARCA^{BD}. From Farnaby *et al*.[170]

4.5.2 Type of E3 ligases

Since the first generation of PROTACs showed some drawbacks, small molecule E3 ligase ligands have been developed for small molecule-based PROTACs.[143] In recent studies, most of the PROTACs reported are small molecule-based PROTACs that utilise MDM2, cIAP1, VHL, and CRBN E3 ligases. However, these E3 ligases show restricted substrate specificity.[149,171] In addition, the efficiency of protein degradation depends on the types of E3 ligase. For example, CRBN-based PROTACs can degrade the fusion protein BCR-Abl while VHL-based PROTACs can only degrade Abl.[150] This might be due to the fact that the target proteins can only be recognised by a specific type of E3 ligases.[144] Therefore, the selection of E3 ligase is also crucial in the PROTAC design. Further information of E3 ligases will be discussed in section **4.6**.

4.5.3 Type of linkers

So far, hydrocarbon chains, polyethylene glycol (PEG) chains, and polyamides have been used as linkers in PROTACs.[171,172] The linkers play a crucial role in determining the biological activity as

well as pharmacokinetics and physicochemical properties of the PROTACs. The permeability and solubility of the PROTACs can be adjusted depending on the types of the linker.[159] Additionally, the linker length also plays a role in determining a successful degradation of the POI by the PROTAC[171] as well as its selectivity and affinity.[173] An example of different types of a linker that may have an effect on the degradation profiles is shown in **Figure 35**. Two BRD4 PROTACs that were constructed using similar warheads but different linkers, **ARV-825** (**135**) and **dBET1** (**138**), exhibited different DC_{50} (the concentration at which 50% of the target protein has been degraded) at 1 < nM[167] and 460 nM,[174] respectively (**Figure 35)**. Therefore, to improve the activity of PROTACs, the choice of the linker requires careful consideration.

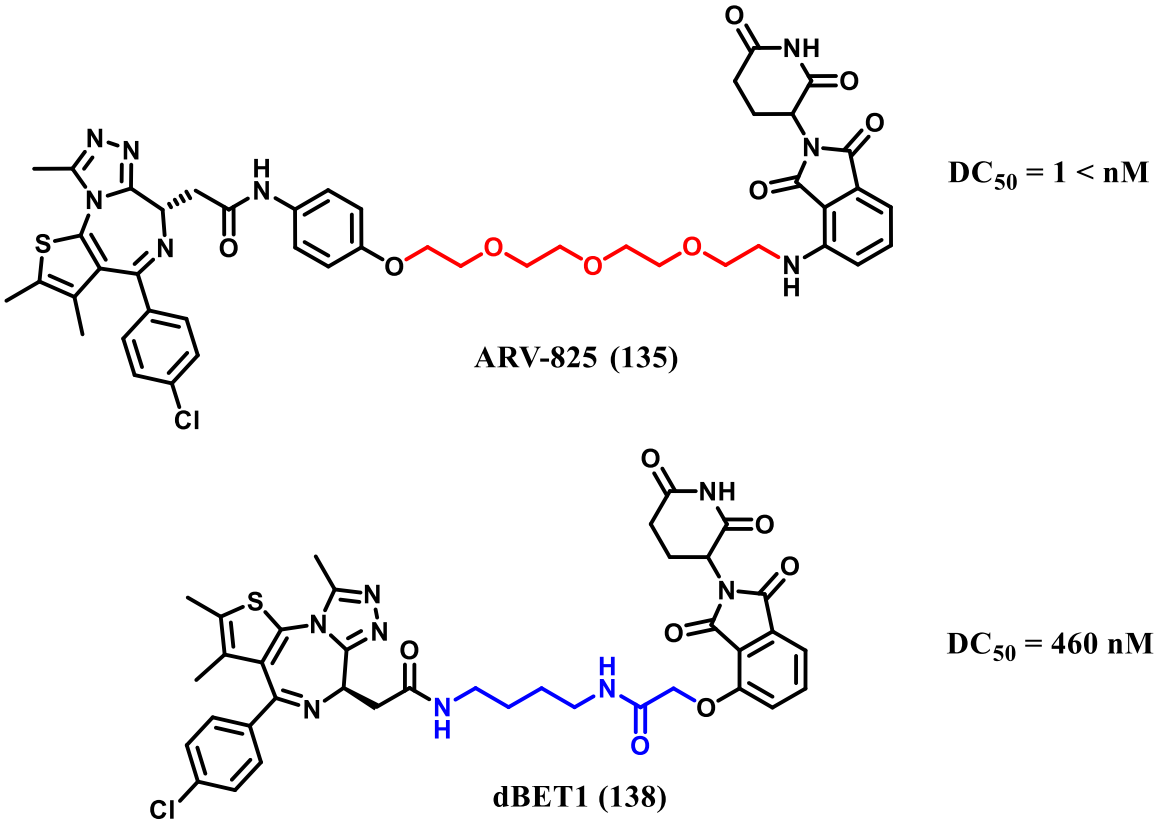


Figure 35: Examples of two BRD4 PROTACs having the same E3 ligase ligand and similar warhead, but a different linker (highlighted in red and blue).

Not only does the type of the linker have an effect on the degradation of the POI but the length of the linker also plays a major role in the degradation profile. Mainly, the optimisation of the PROTACs focuses on varying the length of the linker in order to achieve a better protein degradation profile.[144] For example, when the linker length of a lapatinib-based PROTAC was

increased by one ethylene glycol unit, the degradation profile was changed from degrading both the epidermal growth factor (EGFR) and human epidermal growth factor 2 (HER2) to degrading only the EGFR.[175]

4.6 Small molecule PROTACs and types of E3 ligase ligands

As mentioned in section **4.3**, there are many drawbacks posed by the first-generation (short peptide chain based) PROTACs. These are a lack of traditional drug-like properties and a requirement for a high concentration of the PROTACs to attain the desired effects. Moreover, due to the high molecular weight of these molecules, the cell permeability was limited, thus leading to a low cellular activity.[143] Therefore, the direction of PROTAC development turned to small molecule-based PROTACs in order to overcome these drawbacks.

Although there are more than 600 E3 ligases in humans, only a small number of E3 ligases have been utilised in PROTACs, namely MDM2, cIAP1, VHL, and CRBN E3 ligases. Examples of ligands of the most commonly used E3 ligases are shown in **Figure 36**. Various PROTACs incorporating these E3 ligase ligands are discussed below.

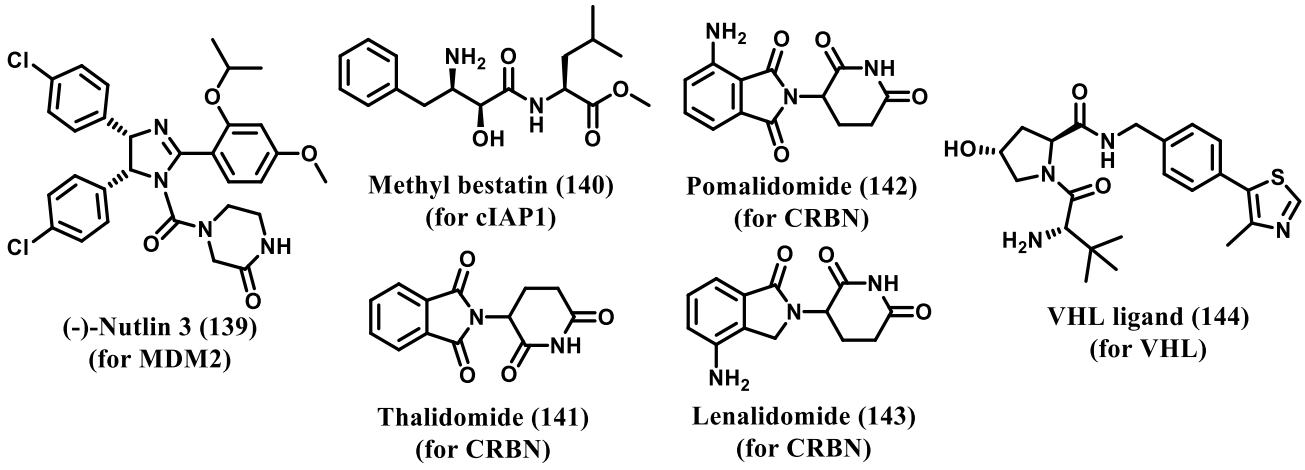
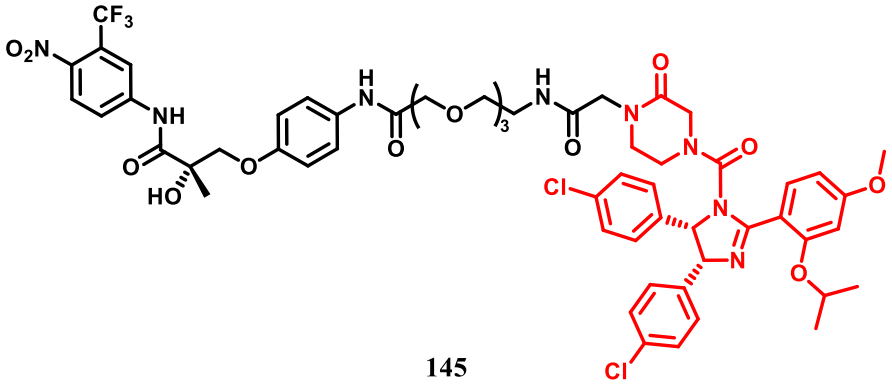


Figure 36: Examples of E3 ligase ligands.

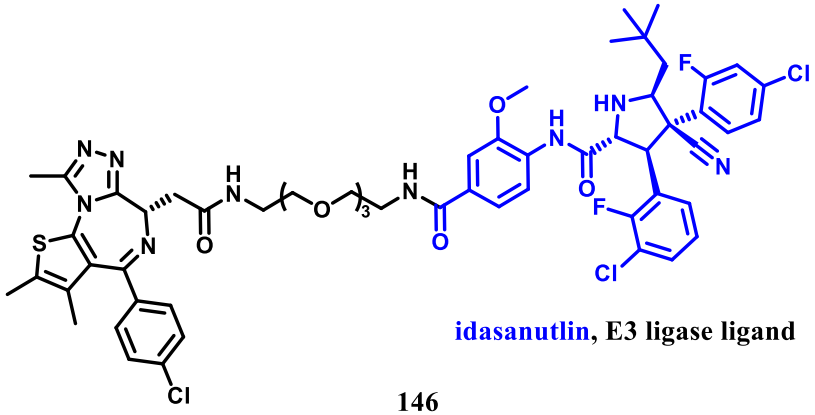
4.6.1 MDM2-based PROTAC

MDM2 is an important negative regulator of the p53 tumour suppressor. It functions as an E3 ligase and an inhibitor of p53 transcriptional activation. The PROTACs utilising the MDM2-based ligand incorporate nutlin and its analogues which is a ligand that binds to the p53-binding pocket of MDM2. Two MDM2-based PROTACs, **145** and **146** (**Figure 37**), which have shown to degrade the androgen receptor (AR)[157] and BRD4[176] were successfully synthesised by Schneekloth *et al*. and Hines *et al*., respectively. Although compound **145** was capable of degrading AR, its effective concentration is in low-micromolar range.[157] In contrast, compound **146** was capable of degrading BRD4 with nanomolar potency.[176] This indicates a potential of all small-molecule PROTACs based on MDM2 as novel cancer therapeutics. However, the majority of MDM2-based PROTACs were usually effective only in a low-micromolar range[177] thus decreasing the potential of this strategy.



145

(-)-nutlin 3, E3 ligase ligand



idasanutlin, E3 ligase ligand

146

Figure 37: Example of small-molecule MDM2-based PROTACs, **145** and **146**, utilising (-)-nutlin 3 and idasanutlin as E3 ligase ligands (highlighted in red and blue), respectively.[157,176]

4.6.2 cIAP1-based PROTAC

cIAP1, a member of the IAP family, is a multi-functional protein which can be found in the nucleus of tumour cells. It is overexpressed in various tumour cells, rendering it a promising target for cancer therapy. Bestatin, a dipeptidomimetic compound, was found to activate E3 ligase activity of cIAP1[178] and was later used as a cIAP1 ligand in designing PROTACs. The cIAP-based PROTAC utilising methyl bestatin, **147** (**Figure 38**), was successfully synthesised by the Hashimoto group.[179] Compound **147** has been shown to degrade the target protein CRABP-1 and CRABP-2[179]. Additionally, in 2013, the Naito group successfully prepared SNIPER-3 (**148**, **Figure 38**), another cIAP1-based PROTAC, that is capable of degrading the ERα protein.[180] Even though successful protein degradation was achieved through the cIAP1-based PROTACs, there are some limitations involving the use of these ligands. First, the cIAP1 ligands often lead to an auto-ubiquitination which can result in a degradation of the E3 ligase itself instead of the POI. Second, the effective degradation of target protein is achieved only at high concentration of PROTACs.[178,181]

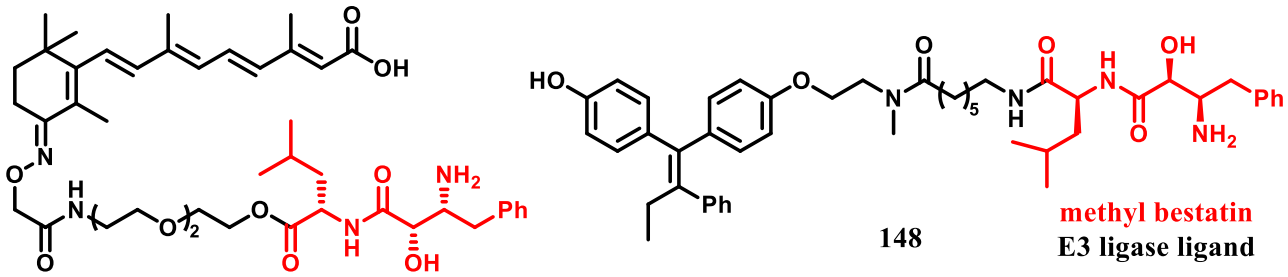


Figure 38: Examples of small-molecule cIAP1-based PROTACs, **147** and **148**, utilising methyl bestatin as an E3 ligase ligand (highlighted in red).[179,180]

4.6.3 VHL-based PROTAC

VHL is an important tumour suppressor protein which can also function as an E3 ligase. The first generation of VHL-based PROTACs was built from peptide fragments.[156] Later, the peptide fragments in the PROTACs were replaced with small molecules containing the hydroxyproline

moiety, allowing an improved binding affinity for VHL.[160] The small molecule VHL-based PROTACs (**149** and **150**, **Figure 39**) were shown to degrade various kinds of proteins including ERRα, RIPK2 kinase,[160] and several transmembrane tyrosine kinases such as EGFR, HER2, and c-Met.[175]

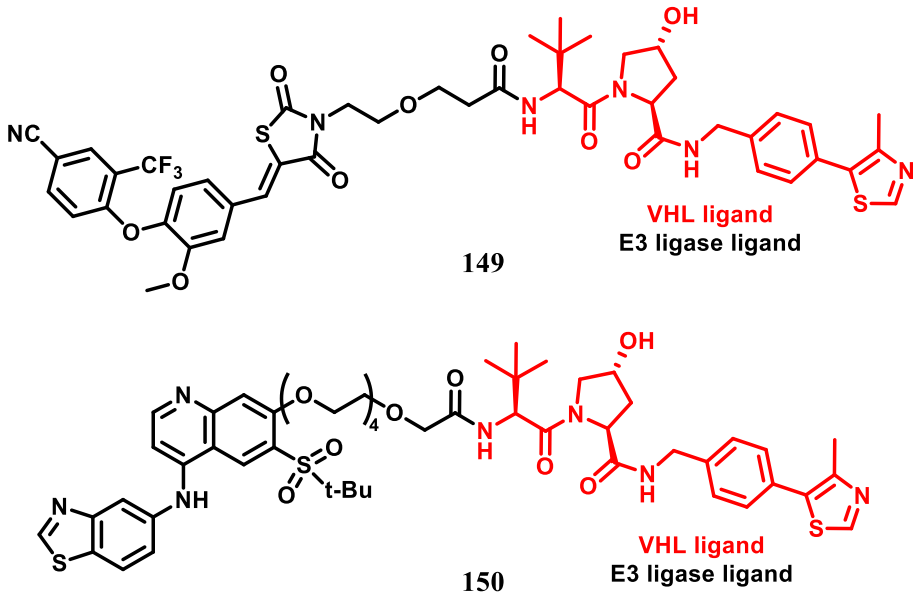


Figure 39: Examples of small-molecule VHL-based PROTACs, **149** and **150**, utilising VHL ligand as an E3 ligase ligand (highlighted in red).[160]

According to Zoppi *et al.*,[182] the *trans* epimer of the hydroxyproline moiety of VHL ligand (*R* configuration of the hydroxyl group) is required for the binding to VHL (active VHL ligand). Changing the stereochemistry of the hydroxyproline moiety of VHL ligand from *trans* to *cis* (*S* configuration) will result in the loss of binding affinity to VHL (inactive VHL ligand). The structures and stereochemistry of active and inactive VHL ligands are shown in **Figure 40**.

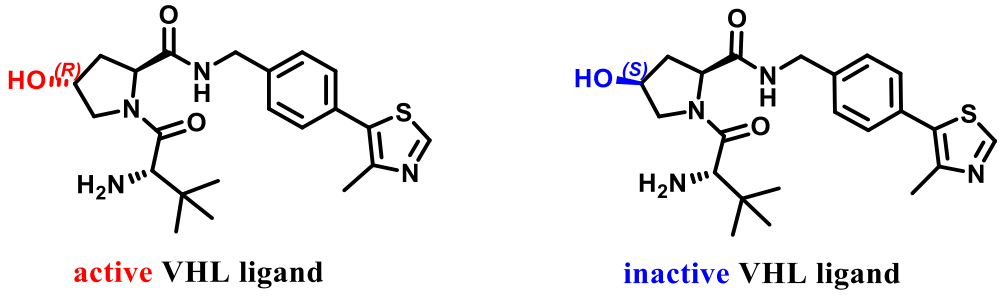


Figure 40: Active versus inactive VHL ligand.

4.6.4 CRBN-based PROTAC

CRBN is a component of a cullin–RING ubiquitin ligase (CRL) complex. It is involved in many biological processes such as the regulation of ion transport and metabolism in cells.[183] Thalidomide and its analogues including pomalidomide and lenalidomide are immunomodulatory drugs (IMiDs) that are also used as ligands for targeting CRBN. Targeting CRBN results in the degradation of transcription factors IKZF1 and IKZF3 in multiple myeloma.[184,185]

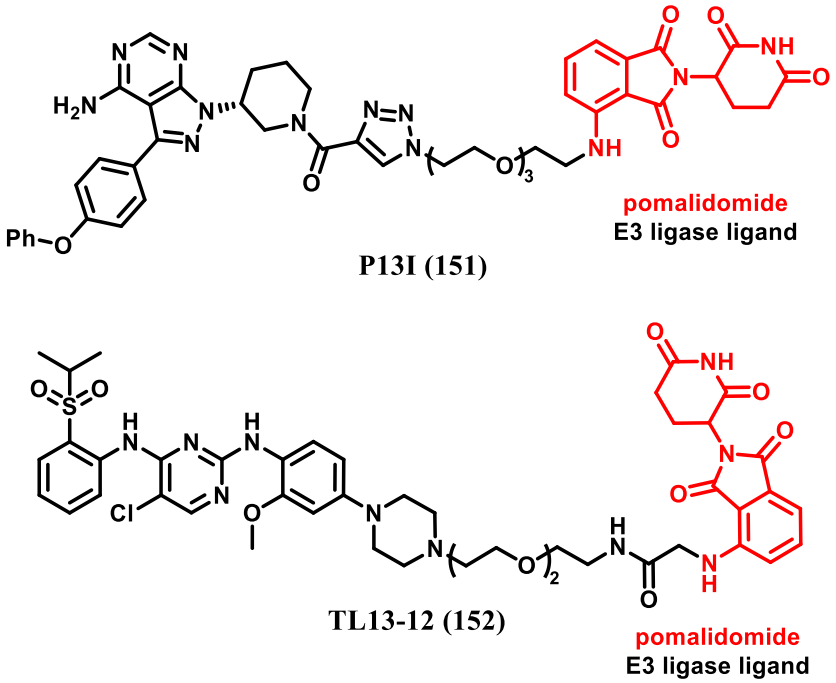


Figure 41: Examples of small-molecule CRBN-based PROTACs, **151** and **152**, utilising pomalidomide as an E3 ligase ligand (highlighted in red).[186,187]

Several PROTACs that utilise IMiDs to target CRBN were also reported to degrade various kinds of proteins such as Sirt2,[188] FLT3,[149] BTK,[149,189] and ALK.[190] For example, **P13I** (**151**) (**Figure 41**) which was constructed from ibrutinib and pomalidomide could degrade BTK[186] and **TL13-12** (**152**) (**Figure 41**) which was constructed from an ALK inhibitor and pomalidomide could degrade ALK.[187]

4.7 Project aim

There are several disadvantages associated with the use of small molecule inhibitors as therapeutic agents. For example, a high concentration of small molecule inhibitors is often required for treatment of several diseases which can lead to potential off-target activities and undesired side effects[141,144]. In order to overcome these barriers, PROTACs have been recently introduced as a novel therapeutic agent due to their improved selectivity and sub-stoichiometric properties.[191] This project aims to develop novel PROTACs that specifically target the FMS kinase.

FMS kinase has been implicated in a great number of human pathologies such as inflammatory diseases, osteoclast proliferation in bone osteolysis, and several kinds of cancer.[35,63] Inhibiting FMS can, therefore, provide therapeutic benefits for these diseases.

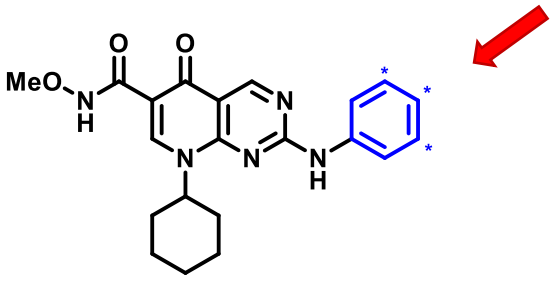
Herein, we aim to incorporate the promising inhibitor(s) that were successfully synthesised in Chapter 1 as PROTAC warheads. The site of linker attachment will be examined based on the X-ray crystal structure of the inhibitor(s) bound to FMS catalytic site. The novel PROTACs will be synthesised and the biological activity of the synthesised PROTACs will be further assessed through an *in vitro* degradation assay.

5. Results and Discussion

A previous study by Dr. Robert Davidson identified a potent compound that efficiently binds to FMS. We therefore decided to use this molecule for the development of our PROTAC reagents. Compound **10** is a truncated version of a Johnson & Johnson ligand that exhibits a potent FMS activity in cell free SPR assay with a K_d of 25 nM.[95] In addition, from the kinase activity assay run by Reaction Biology, it was shown that **10** exhibited an IC_{50} against the FMS catalytic domain of less than 5 nM.

5.1 Designing the PROTACs

From the crystal structure of **10** bound to FMS kinase, it is clearly observed that the best position to attach a linker is the aromatic ring on the right-hand side of compound **10** (shown in blue, **Figure 42**, top). It should be noted that, on the aromatic ring, it is possible that the linker could be attached to either the *meta* or *para* position (**Figure 42**, top, denoted with asterisks). However, the best option for a linker attachment is most likely at the *para* position since this position is exposed to a free space outside the FMS kinase (solvent exposed area) which will maximise the chance for the PROTAC to bind to the E3 ligase. In addition, the *para* position is also suitable for an attachment of large chemical structures, specifically the linker and the E3 ligase ligand, as shown in **Figure 42**, bottom.



10

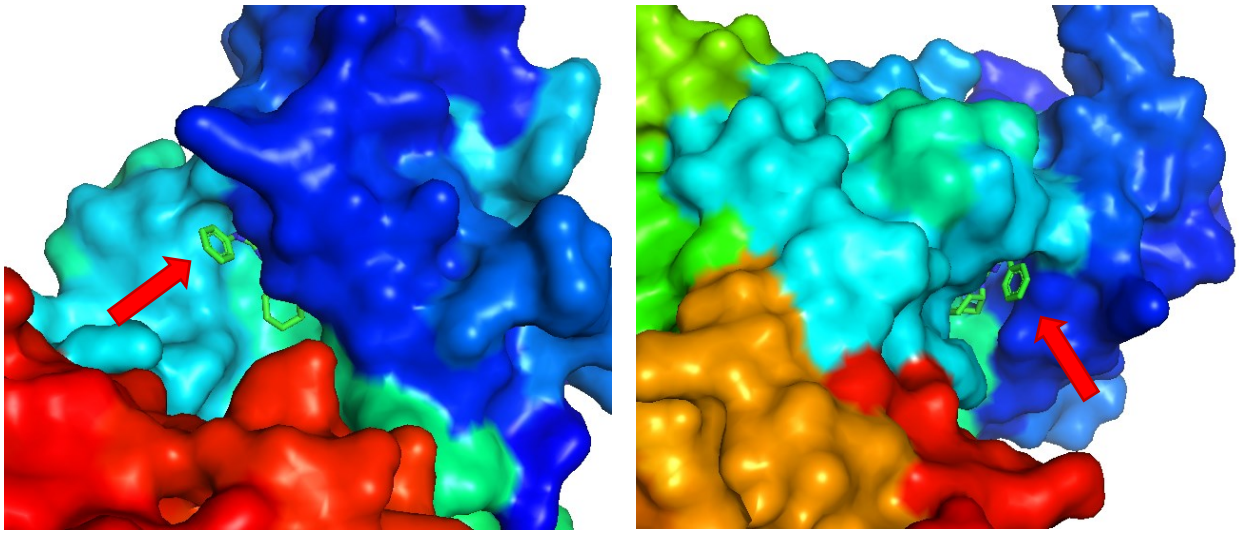
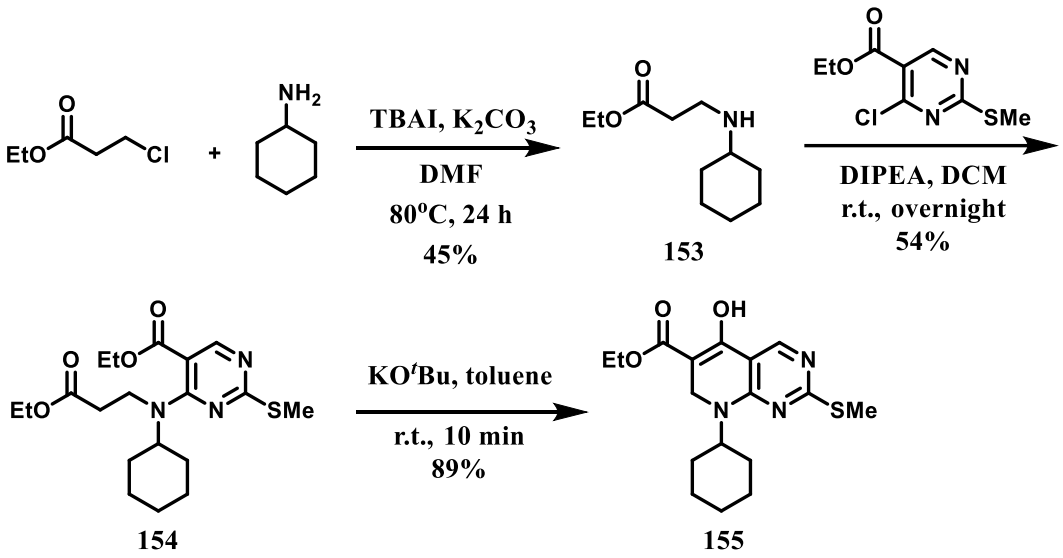


Figure 42: Top: chemical structure of compound **10** with potential positions for attaching to a linker (shown with asterisks). Bottom: crystal structure of **10** bound to FMS kinase in different viewing angles. Red arrow indicates the solvent exposed aromatic ring.

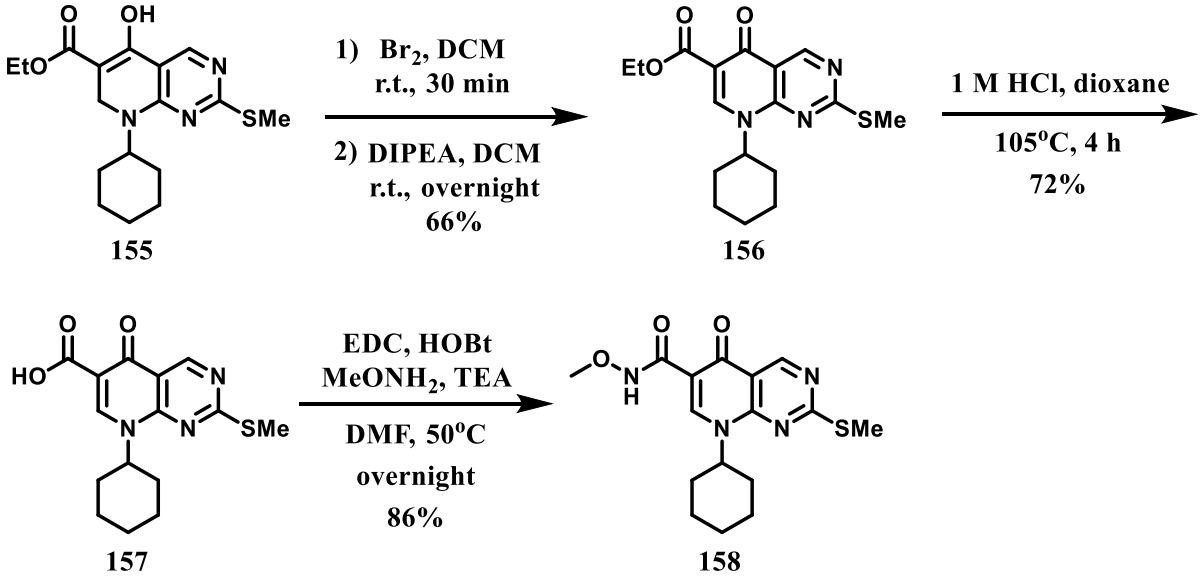
5.2 Synthesis of FMS kinase ligand with an amine moiety for linker attachment

The synthesis of **10** was adapted from the approach previously reported by Dr. Robert Davidson[95] in order to install a different side chain. The modified synthesis (as shown in **Scheme 44**) began with the substitution reaction of ethyl 3-chloropropanoate and cyclohexanamine in DMF at 80°C for 24 hours to give **153** as a product. Although it was difficult to monitor this reaction and to purify the crude product because the reactants and the product were UV-inactive, this reaction worked well and resulted in a moderate yield (45%). Then, **153** was subjected to a S_NAr reaction with the commercially available ethyl 4-chloro-2-(methylthio)pyrimidine-5-carboxylate at room temperature overnight to give **154** (54%). Next, **154** underwent a Dieckmann cyclisation reaction with KO^{t}Bu in toluene at room temperature for 10 minutes in order to form the 6-membered ring product, **155**. A ^{1}H-NMR of the crude product obtained from the Dieckmann cyclisation showed that the sample contained both the enol and keto forms of compound **155**, in the ratio 2.5:1. Despite this, it was decided to carry this mixture to the next step without further purification.



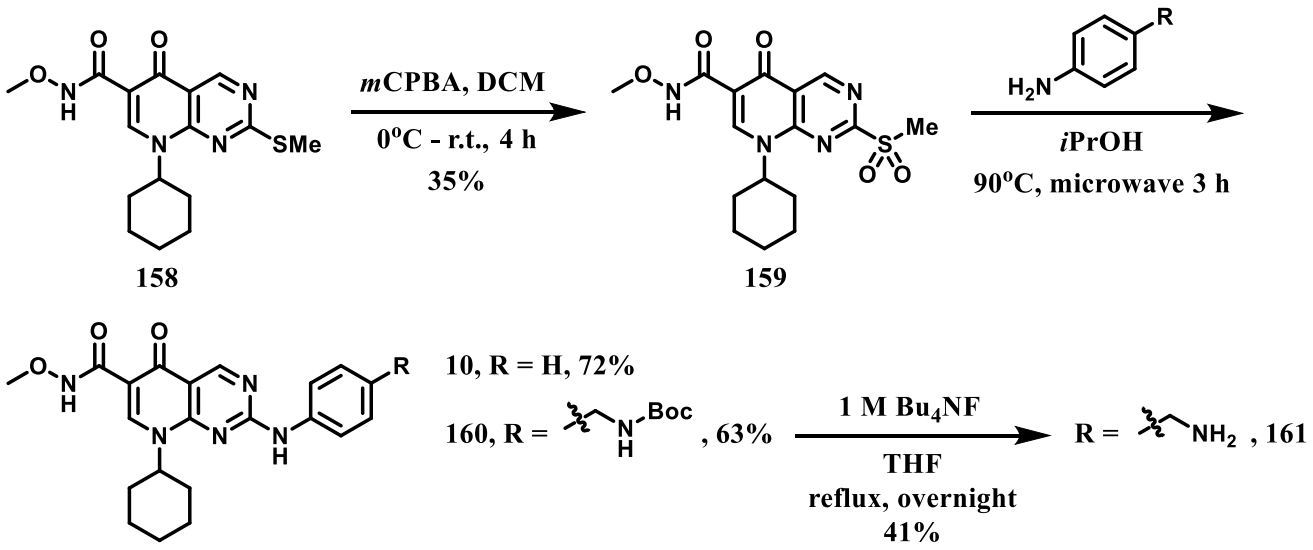
Scheme 44: Synthesis of **155** from ethyl 3-chloropropanoate and cyclohexanamine.

The mixture of **155** was transformed to **156** by reacting with bromine, dissolved in DCM at room temperature for 30 minutes followed by DIPEA overnight. The ethyl ester side chain in **156** was then hydrolysed with 1 M HCl in dioxane at 105°C for 4 hours to give **157** (72%). Compound **157** was then subjected to an amide coupling using EDC, HOBt, triethylamine, and O-methylhydroxylamine to give **158** in 86% yield (**Scheme 45**).



Scheme 45: Synthesis of **158** from **155**.

The sulfide moiety in **158** was then oxidised with an excess amount of *m*CPBA to give the corresponding sulfone product, **159** (35%). To make **10**, compound **159** was partly dissolved in isopropanol. Then, aniline was added to the suspension and the reaction was heated in a microwave reactor at 90°C for 3 hours (**Scheme 46**). The obtained crude product was purified by column chromatography to give compound **10** with the overall yield of 2.2% in 8 steps.



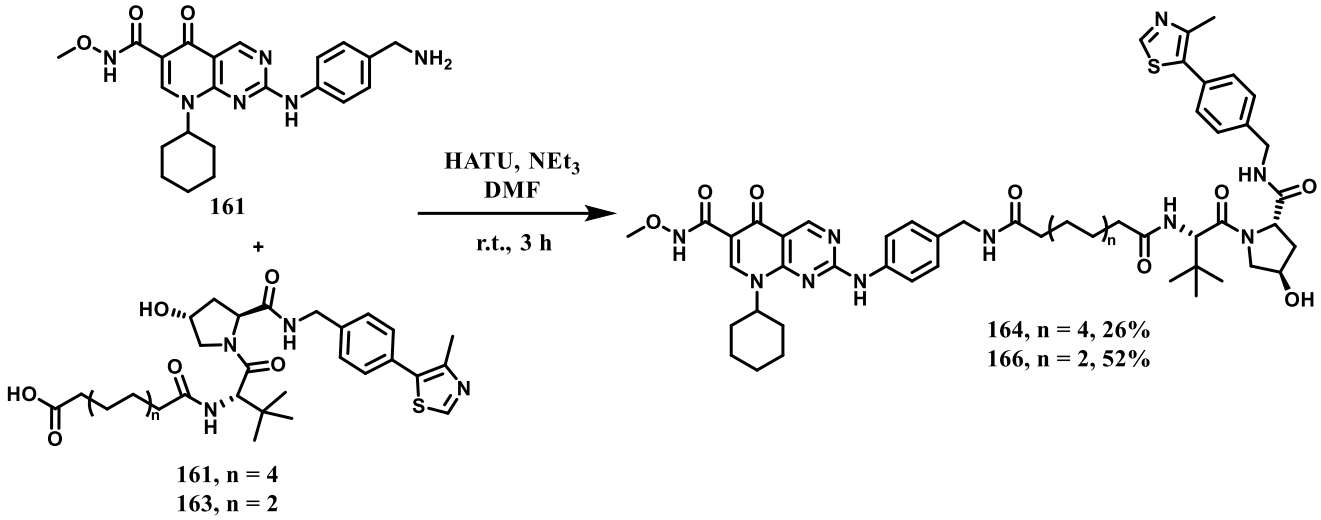
Scheme 46: Synthesis of FMS kinase ligand (from **158**) with a part for linker attachment.

An analogue of this compound was also made, using *tert*-butyl (4-aminobenzyl)carbamate as the reagent instead of aniline and the same reaction conditions as before. The addition of the extra amine arm was done in order to allow subsequent linker attachment. After purification, compound **160** was obtained. This was deprotected using 1 M Bu_4NF in THF to give the free amine, **161**, with the overall yield of 0.8% in 9 steps (**Scheme 46**).

5.3 Synthesis of FMS-VHL PROTACs

Following the successful synthesis of the FMS warhead (**161**), it was time to synthesise the full PROTAC molecules. To do this, an amide coupling reaction was employed between the amine warhead and the acid of choice, using HATU and triethylamine in DMF (**Scheme 47**). Two different acid molecules with different linker lengths, namely an 8- and a 12-carbon long chain, were used, both incorporating the VHL ligand which was pre-attached onto a linker molecule.

Both reactions worked as expected, giving the two PROTAC products, **164** and **166**, after PTLC purification in 26% and 52% yield, respectively.

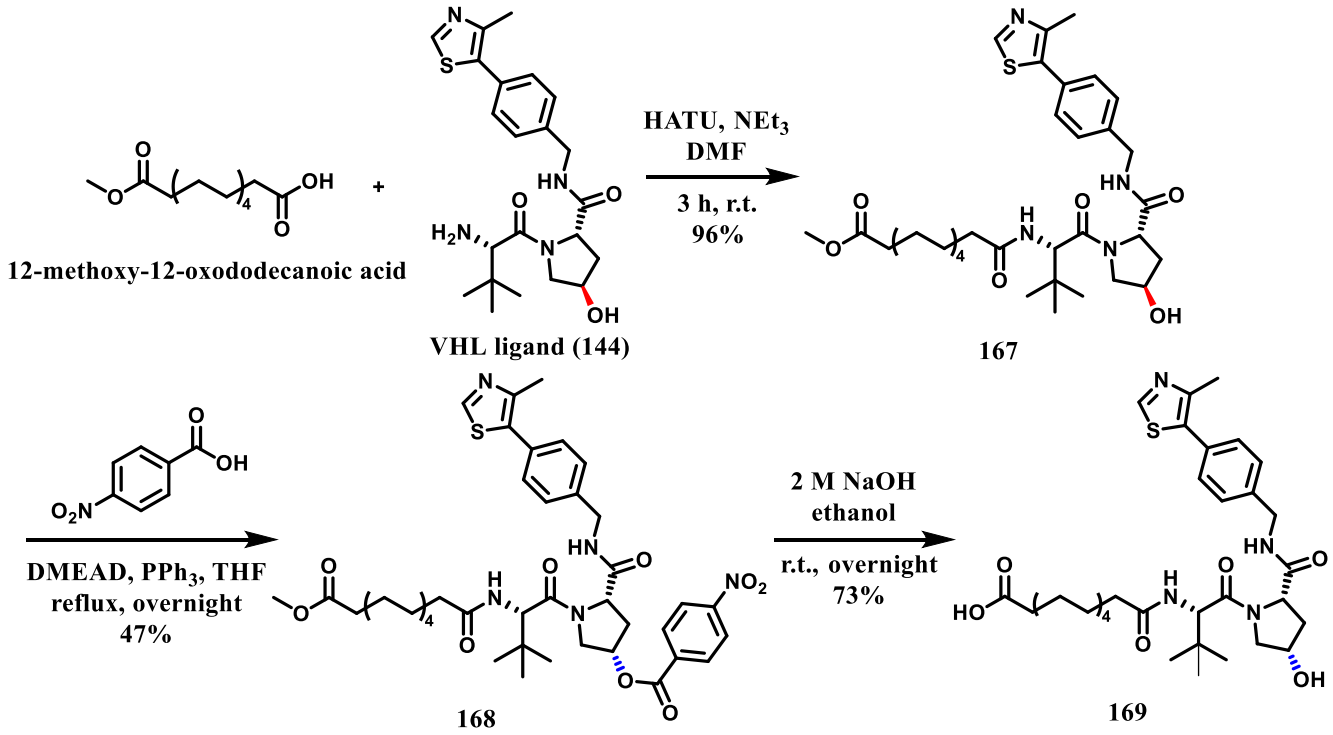


Scheme 47: Synthesis of FMS-VHL PROTACs with an 8- and a 12-carbon long linker chain.

5.4 Synthesis of inactive VHL ligand attached to a linker

Since we incorporated a highly potent FMS ligand, **10**, into the design and synthesis of our PROTACs, there are two possible pathways that the molecule can exert its function. First, the FMS ligand, **10**, acts as a part of the PROTAC that induces FMS kinase degradation. Second, compound **10** can also function as an inhibitor and binds to the FMS kinase, inhibiting the kinase functions. In order to determine the correct mode of action of these novel molecules, a negative control compound containing the inactive VHL ligand was needed to be synthesised and used in the biological assessment.

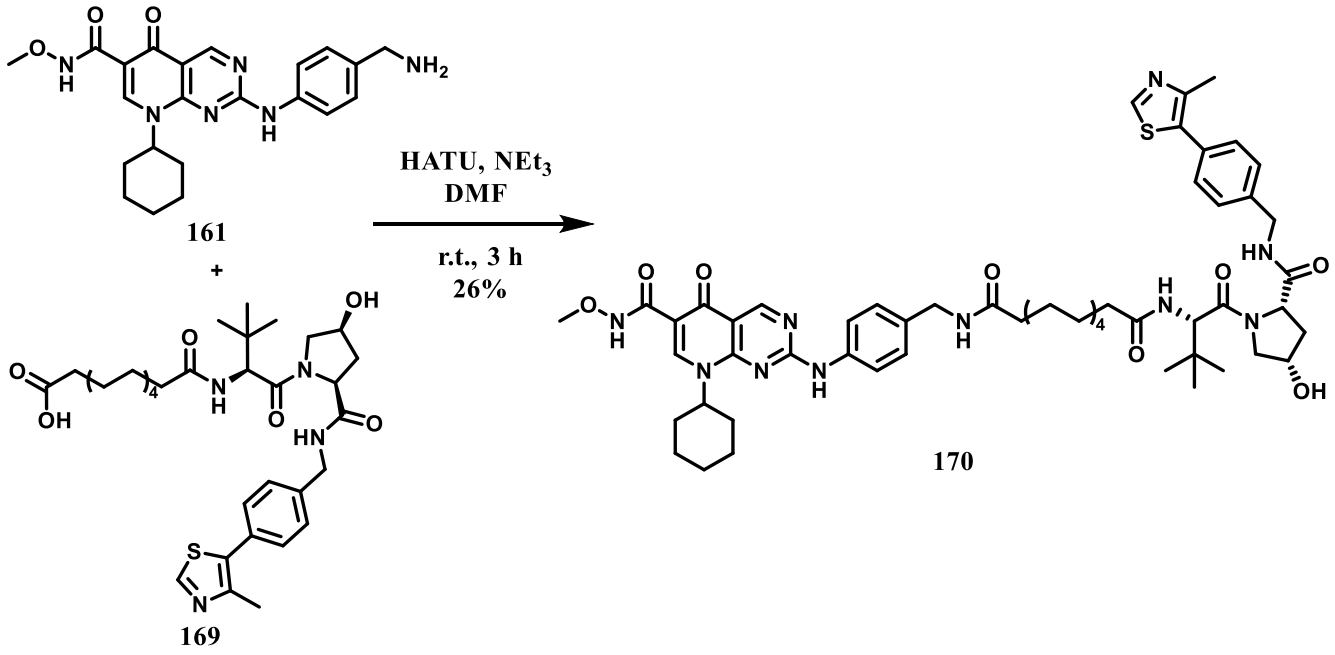
The conversion of the active VHL ligand to the inactive form could be achieved through a Mitsunobu reaction as shown in **Scheme 48**.



Scheme 48: Synthesis of the inactive VHL ligand attached to a 12-carbon linker chain.

The active ligand was initially coupled to 12-methoxy-12-oxododecanoic acid using HATU and triethylamine in DMF at room temperature for 3 hours to give **167** (96%). Then, **167** was subjected to the Mitsunobu reaction by heating the compound under a reflux condition (66°C) with DMEAD, PPh_3, and 4-nitrobenzoic acid in THF in order to change the stereocenter of the hydroxyproline VHL binding element in **167** from *R* to *S*. After the reaction was complete, the crude product was purified by flash column chromatography. Although some impurities were still observed in the product, it was used in the next reaction without further purification with an anticipation that the impurities could be separated in the next step. Next, the hydrolysis of both esters in **168** was performed under basic conditions using 2 M NaOH in ethanol at room temperature overnight to give **169** (73%). It should be noted that, the impurities carried over from the former step were removed with the purification of **169**. Ultimately, the inactive ligand attached to the linker was acquired in 73% yield.

After obtaining the inactive VHL ligand attached to the 12-carbon linker, **169**, the inactive PROTAC was synthesised as shown in **Scheme 49**, using compound **161** and the reaction conditions previously mentioned for the synthesis of the active molecules (**Scheme 47**). The final product, **170**, was obtained in 26% yield.



Scheme 49: Synthesis of the inactive PROTAC with a 12-carbon linker chain.

5.5 Biological assay

In vitro activity of the synthesised PROTACs were evaluated against THP-1, a human monocytic, cell line in a degradation assay. This *in vitro* assay was conducted by Davide Croci, Department of Oncology, EPFL. THP-1 cells, expressing fluorescently labeled FMS, were treated with the active PROTACs, including **164** and **166**, and the inactive PROTAC, **170** (a negative control) at a concentration ranging from 0.01 nM to 1000 nM.

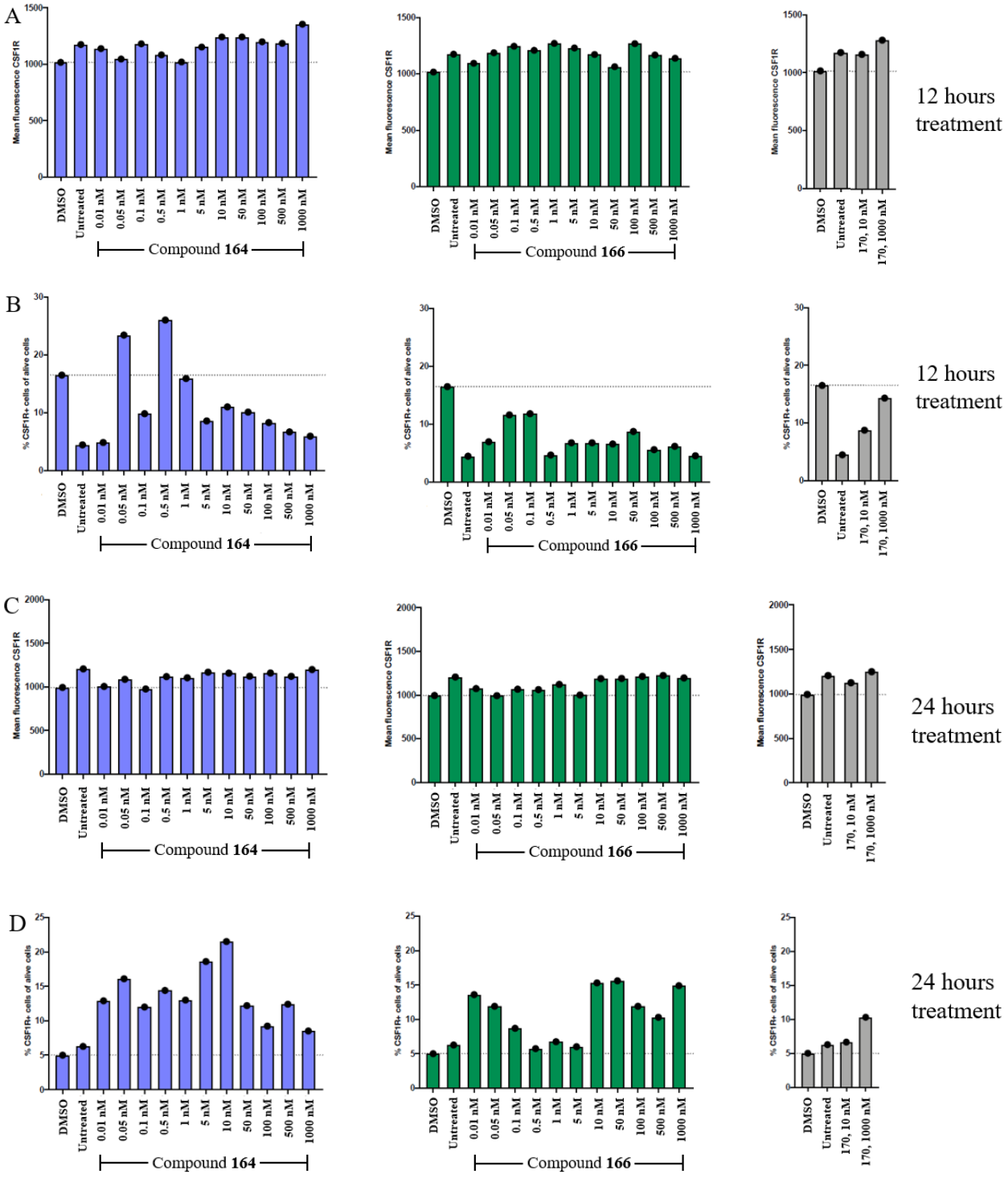


Figure 43: THP-1 cells treated with the active PROTACs, **164** and **166**, or the inactive PROTAC, **170**, for 12 and 24 hours. **A** and **C** show the mean fluorescence intensity of CSF-1R (FMS) after 12- and 24-hours incubation, respectively. **B** and **D** show % CSF-1R (FMS) + cells of alive cells after 12- and 24-hours incubation, respectively.

As shown in **Figure 43**, **A** and **C**, no reduction of the mean fluorescence intensity of FMS was observed for the cells treated with the active PROTACs even after 24 hours incubation. Increasing the concentration of the PROTACs up to 1000 nM did not lead to the degradation of FMS in THP-1 cells. Similar FMS expression was observed in the cells treated with the inactive PROTAC (negative control) and the active PROTACs. It should be noted that the THP-1 cell line used in this experiment has only a small population of FMS expressing cells (even after propidium monoazide, PMA, treatment). In addition, in each sample there was a variability of FMS expressing cells which is most likely due to the biological heterogeneity of THP-1 cells and their low FMS expression (**B** and **D**, **Figure 43**). Therefore, although it seems the PROTACs designed in this project are not able to degrade FMS, it may be that the cellular model selected is not the most appropriate. Further evaluation of the synthesised PROTACs is ongoing using different cellular models and experimental conditions. For example, immediate future studies plan to use freshly isolated human monocytes from buffy coat or a cell line that over-expresses FMS.

5.6 Conclusions and future work

In this chapter, the idea of extending small molecule inhibitors into PROTACs was pursued based on the promising inhibitor **10**. From the co-crystal structure of **10** bound to the active site of FMS (**Figure 42**), the free aromatic ring of **10** was identified as the point for linker attachment based on the solvent exposed moiety (highlighted in blue in **Figure 42**).

The FMS ligand with an extra side chain used to attach to a linker, **161**, was successfully synthesised with the overall yield of 0.8% in 9 steps. Compound **161** was coupled with **163** and **165** to yield two active PROTACs: **164** and **166**, respectively. However, due to the potent activity of **161**, a high cellular activity could arise from either the activity of **161** as an FMS kinase inhibitor or as part of the PROTAC. Therefore, the inactive form of the PROTAC that utilised the inactive VHL ligand, **170**, was synthesised as a negative control in biological assays.

For the biological aspect, the synthesised PROTACs were tested in a degradation assay using THP-1 cell line expressing fluorescently labeled FMS. The data suggested that the synthesised PROTACs were unable to degrade FMS in THP-1 cells. However, further evaluation of the synthesised PROTACs is ongoing using different cellular models and experimental conditions.

In future work, a study of different types and lengths of a linker can be an option to optimise the PROTAC molecules. Furthermore, changing a type of the E3 ligase ligand, i.e., from VHL to CRBN, can also be considered as another option for PROTAC development.

6. Experimental

6.1 General Experiment

All reagents were obtained from commercial sources and were used as purchased from the manufacturers unless stated otherwise. All reactions involving moisture-sensitive reagents were conducted under nitrogen or argon atmosphere using standard Schlenk line techniques and with oven-dried glassware. Anhydrous solvents were dispensed using Pure SolvTM solvent drying towers (Innovative Technology Inc., China) or were obtained commercially.

Organic phases were dried over anhydrous $MgSO_4$ or Na_2SO_4. Brine refers to a saturated aqueous solution of sodium chloride. *In vacuo* refers to the use of a rotary evaporator attached to a diaphragm pump to remove bulk solutions.

Thin layer chromatography (TLC) was conducted on pre-coated aluminium backed plates with Merck Kiesegel 60 F254 (230–400 mesh). The plates were visualised under UV light (254 nm) and were stained with either $KMnO_4$ (aq. potassium permanganate), ninhydrin solution, vanillin solution, 2,4-dinitrophenylhydrazine (DNP) solution, or PMA (phosphomolybdic acid solution).

Flash column chromatography was carried out on Merck Kiesegel 60 silica gel (230–400 mesh, 0.040 0.063 mm) or Fluorochem 60 silica gel (230–400 mesh, 40-63 μm), eluting with solvents as supplied, under positive air pressure. Microwave reactions were performed in a Biotage® Initiator+ microwave reactor. Hydrogenation reactions at higher pressures than atmospheric were carried out in a 3911 Parr shaker hydrogenator at room temperature.

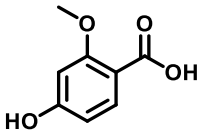
^{1}H- and ^{13}C-NMR spectra were obtained using a Bruker Advance 400 spectrometer at 400 MHz and 101 MHz, respectively. For some compounds, ^{13}C-NMR spectra were obtained using a Bruker Advance 500 spectrophotometer at 126 MHz. Chemical shifts are referenced to the stated residual solvent peak. Chemical shift (δ) are reported in parts per million (ppm) to the nearest 0.01 ppm. Coupling constant (J) are quoted in Hertz (Hz) and recorded to the nearest 0.1 Hz. The coupling constants are determined by analysis using calculated MestreNova© NMR software. ^{1}H-NMR spectra are reported as follows: chemical shift, signal splitting (singlet (s), doublet (d), t (triplet), q (quartet), m (multiplet) or as a combination of these), coupling constant, integration,

assignment). ^{13}C-NMR spectra were recorded with broadband proton spin decoupling and chemical shifts are quoted to the nearest 0.1 ppm.

High- and low-resolution mass spectra (HRMS, EI, ES) were recorded by the Imperial College London Department of Chemistry Mass Spectroscopy Service on a Micromass Platform II and Micromass AutoSpeq-Q spectrometers.

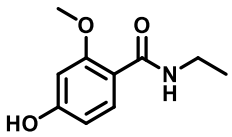
6.2 Synthetic procedures: Chapter 1

4-Hydroxy-2-methoxybenzoic acid (14)



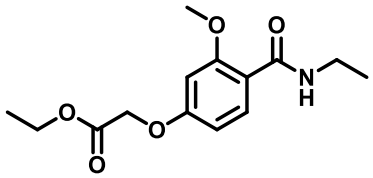
Based on a procedure by Boyle *et al*.[192] To a stirred solution of 4-hydroxy-2-methoxybenzaldehyde (2.84 g, 18.70 mmol) in a mixture of DMSO (60 mL) and water (45 mL) at 0°C was added sodium dihydrogen phosphate (8.97 g, 74.80 mmol) and sodium chlorite (4.87 g, 65.50 mmol). The mixture was allowed to warm up to room temperature and stirring was continued overnight. After this time, the mixture was diluted with water (150 mL) and the pH of the solution was adjusted to 8 by using solid $NaHCO_3$. The solution was washed with EtOAc (150 mL), the pH of the aqueous layer was adjusted to 4 by the addition of 1 M HCl aqueous solution, and the solution was extracted with EtOAc (6 x 50 mL). The organic extracts were combined and washed with brine (50 mL), dried over anhydrous Na_2SO_4, filtered and evaporated *in vacuo* to afford **14** (3.14 g, quatitative yield) as a brown solid which was used without further purification. R_f= 0.32 (EtOAc:hexane = 4:1, v/v); ^{1}H-NMR (400 MHz, Methanol-d4) δ 3.91 (s, 3H), 6.46 (dd, J = 8.5, 2.0 Hz, 1H), 6.54 (d, J = 2.0 Hz, 1H), 7.82 (d, J = 8.5 Hz, 1H); ^{13}C-NMR (101 MHz, Methanol-d4) δ 55.0, 98.8, 107.5, 109.4, 134.2, 161.5, 163.6, 167.7. The spectroscopic data corresponded to previously reported data.[192]

***N*-Ethyl-4-hydroxy-2-methoxybenzamide (15)**



A solution of **14** (1.20 g, 7.15 mmol) in thionyl chloride (20 mL) was heated under a reflux condition (75°C) for 2.5 hours. After this time, the remaining solvent was removed *in vacuo*. The residue was azeotroped with benzene (3 x 1 mL) to ensure the complete removal of thionyl chloride. The resulting crude acid chloride was dissolved in anhydrous DCM (30 mL), cooled to 0°C in an ice bath, placed under a nitrogen atmosphere, and stirred. Then a solution of ethylamine (2 M in THF, 7.15 mL, 14.30 mmol) was added dropwise. The mixture was allowed to warm to room temperature and stirring continued overnight. After this time, the reaction mixture was diluted with DCM (30 mL), washed with 10% w/v aqueous $NaHCO_3$ (3 x 20 mL), brine (3 x 20 mL), and the organic phase was dried over anhydrous $MgSO_4$ and filtered. The solution was concentrated *in vacuo* followed by flash column chromatography using EtOAc:hexane = 4:1 as the eluent to afford **15** (0.71 g, 71% yield) as pale yellow solid R_f= 0.35 (EtOAc:hexane = 4:1, v/v); ^{1}H-NMR (400 MHz, Methanol-d4) δ 1.20 (t, J = 7.0 Hz, 3H), 3.40 (q, J = 7.0 Hz, 2H), 3.88 (s, 3H), 6.49 (d, J = 8.0 Hz, 1H), 6.50 (s, 1H), 7.85 (d, J = 8.0 Hz, 1H); ^{13}C-NMR (101 MHz, Methanol-d4) δ = 13.9, 34.2, 55.0, 98.6, 107.7, 112.4, 132.6, 159.5, 162.3, 166.5; HRMS (ESI) *m/z* calculated for $C_{10}H_{14}NO_3$ (MH^+) 196.0974, found 196.0981.

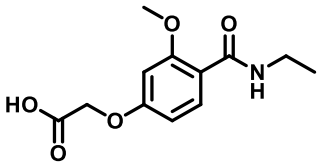
Ethyl-2-(4-(ethylcarbamoyl)-3-methoxyphenoxy)acetate (16)



To a solution of **15** (0.27 g, 1.38 mmol) in anhydrous DMF (20 mL) was added sodium hydride (60% dispersion in mineral oil, 0.08 g, 3.46 mmol). The mixture was allowed to stir for 10 minutes then added ethyl chloroacetate (0.16 mL, 1.52 mmol) dropwise. The mixture was stirred at room temperature under nitrogen atmosphere overnight. After this time, the solvent was evaporated *in vacuo* and washed with 5% LiCl aqueous solution (2 x 10 mL). The organic phase was dried over anhydrous $MgSO_4$, filtered, and concentrated *in vacuo* to afford **16** (0.34 g, 87% yield) as white

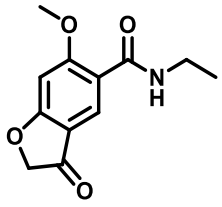
solid which was used without further purification. R_f= 0.48 (EtOAc:hexane = 4:1, v/v); ^{1}H-NMR (400 MHz, Methanol-d4) δ 1.21 (t, J = 7.0 Hz, 3H), 1.26 (t, J = 7.0 Hz, 3H), 3.38 – 3.46 (m, 2H), 3.91 (s, 3H), 4.23 (q, J = 7.0 Hz, 2H), 4.74 (s, 2H), 6.56 (dd, J = 8.5, 2.5 Hz, 1H), 6.62 (d, J = 2.5 Hz, 1H), 7.92 (d, J = 8.5 Hz, 1H); ^{13}C-NMR (101 MHz, Methanol-d4) δ = 13.2, 13.9, 34.2, 55.3, 61.7, 64.8, 99.0, 105.6, 114.9, 132.6, 159.1, 161.8, 165.8, 168.8; LC-MS (ESI) *m/z* $C_{14}H_{20}NO_5$ (MH^+) found 282.1.

2-(4-(Ethylcarbamoyl)-3-methoxyphenoxy)acetic acid (17)



To a solution of **16** (0.96 g, 3.43 mmol) in THF (10 mL) was added 1 M NaOH aqueous solution (10 mL). The mixture was stirred at room temperature overnight. After this time, the mixture was diluted with water (20 mL) and the pH of the mixture was adjusted to 1 by the addition of 2 M HCl aqueous solution. The mixture was extracted with EtOAc (3 x 30 mL) and the organic extracts were combined. This was then washed with brine (2 x 20 mL), dried over anhydrous Na_2SO_4, filtered and evaporated *in vacuo*. The resulting solid was subsequently triturated with DCM to afford **17** (0.56 g, 64% yield) as white solid. ^{1}H-NMR (400 MHz, Methanol-d4) δ 1.24 (t, J = 7.0 Hz, 3H), 3.43 (q, J = 7.0 Hz, 2H), 3.98 (s, 3H), 4.77 (s, 2H), 6.64 (dd, J = 8.5, 2.5 Hz, 1H), 6.72 (d, J = 2.5 Hz, 1H), 7.93 (d, J = 8.5 Hz, 1H); HRMS (ESI) *m/z* calculated for $C_{12}H_{16}NO_5$ (MH^+) 254.1028, found 254.1032.

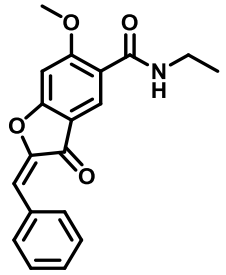
***N*-Ethyl-6-methoxy-3-oxo-2,3-dihydrobenzofuran-5-carboxamide (18a)**



Polyphosphoric acid (4.00 g, excess) was heated to 80°C in a heating mantle, after which was added **17** (0.53 g, 2.10 mmol) in one portion. The reaction mixture was allowed to stir at 90°C overnight and then poured into ice-water (100 mL) and subsequently extracted with DCM (4 x 50

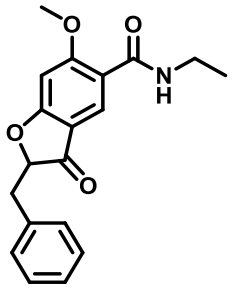
mL). The organic extracts were combined and washed with brine (2 x 30 mL), dried over anhydrous Na_2SO_4, filtered and concentrated *in vacuo* to afford **18a** (0.26 g, 53% yield). R_f= 0.30 (EtOAc:hexane = 4:1, v/v); ^{1}H-NMR (400 MHz, Methanol-d4) δ 1.27 (t, J = 7.0 Hz, 3H), 3.41 (q, J = 7.0 Hz, 2H), 3.96 (s, 3H), 4.75 (s, 2H), 6.87 (s, 1H), 8.10 (s, 1H); HRMS (ESI) *m/z* calculated for $C_{12}H_{14}NO_4$ (MH^+) 236.0923, found 236.0929.

(*E*)-2-Benzylidene-*N*-ethyl-6-methoxy-3-oxo-2,3-dihydrobenzofuran-5-carboxamide (19)



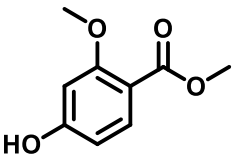
To a solution of **18a** (0.26 g, 1.12 mmol) and benzaldehyde (0.24 g, 2.24 mmol) in anhydrous DCM (5 mL) was added aluminium oxide (activated, basic, *Brockmann Grade I*, 3.43 g, 33.64 mmol). The reaction mixture was stirred vigorously overnight at room temperature under nitrogen atmosphere with exclusion of light. The suspension was then filtered off and the solid residue was washed with DCM (3 x 50 mL). The filtrate was evaporated *in vacuo* and the resulting residue was purified by flash column chromatography using EtOAc:hexane = 4:1 as the eluent to afford **19** (33 mg, 9% yield). R_f= 0.43 (EtOAc:hexane = 4:1, v/v); ^{1}H-NMR (400 MHz, Chloroform-d) δ 1.26 (t, J = 7.5 Hz, 3H), 3.51 (qd, J = 7.5, 5.5 Hz, 2H), 4.10 (s, 3H), 6.84 (s, 1H), 6.86 (s, J = 6.0 Hz, 1H), 7.38 – 7.48 (m, 3H), 7.86 (d, J = 1.5 Hz, 1H), 7.88 (d, J = 1.5 Hz, 1H), 8.64 (s, 1H); ^{13}C-NMR (101 MHz, Chloroform-d) δ = 14.9, 34.8, 56.9, 95.4, 112.8, 115.0, 119.4, 128.9, 129.7, 129.9, 131.4, 132.0, 147.5, 163.7, 164.5, 169.0, 182.5; HRMS (ESI) *m/z* calculated for $C_{19}H_{18}NO_4$ (MH^+) 324.1236, found 324.1230.

2-Benzyl-*N*-ethyl-6-methoxy-3-oxo-2,3-dihydrobenzofuran-5-carboxamide (13′)



To a Schlenk flask evacuated and flushed with argon was added 10% Pd/C (11 mg, 0.01 mmol). To the flask was added a solution of **19** (33 mg, 0.10 mmol) in anhydrous THF (5 mL). The atmosphere was evacuated and then back filled with hydrogen gas. The reaction mixture was stirred at room temperature for 4 hours. After this time, the reaction was filtered, and the remaining solid was extracted with THF (3 x 20 mL). The extracts were combined with the filtrate and concentrated *in vacuo.* The resulting residue was purified by flash column chromatography using the gradient eluent of EtOAc:hexane = 3:7 to 4:1 to afford **13′** (3 mg, 8% yield). R_f= 0.33 (EtOAc:hexane = 4:1, v/v); ^{1}H-NMR (400 MHz, Chloroform-d) δ 1.23 (t, J = 7.5 Hz, 3H), 3.01 (dd, J = 14.5, 8.5 Hz, 1H), 3.37 (dd, J = 14.5, 3.5 Hz, 1H), 3.48 (qd, J = 7.5, 5.5 Hz, 2H), 4.01 (s, 3H), 4.85 (dd, J = 8.5, 3.5 Hz, 1H), 6.58 (s, 1H), 7.27 – 7.29 (m, 5H), 8.51 (s, 1H); ^{13}C-NMR (101 MHz, Chloroform-d) δ = 14.9, 34.7, 37.4, 56.6, 87.1, 95.2, 114.5, 118.1, 127.0, 128.5, 129.3, 129.8, 135.7, 163.8, 165.4, 175.5, 198.0; HRMS (ESI) *m/z* calculated for $C_{19}H_{20}NO_4$ (MH^+) 326.1392, found 326.1392.

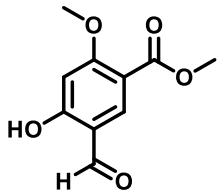
Methyl-4-hydroxy-2-methoxybenzoate (20)



Based on a procedure by Boyle *et al.*[192] To a stirred solution of **14** (2.37 g, 14 mmol) in methanol (40 mL) was added 98% (w/v) sulfuric acid (1 mL). The reaction mixture was refluxed at 65°C overnight. After this time, the mixture was concentrated by evaporation of the solvent *in vacuo*. The crude solid was subsequently extracted with EtOAc (3 x 50 mL). The organic extracts were combined and washed with saturated $NaHCO_3$ aqueous solution (2 x 20 mL), dried over anhydrous

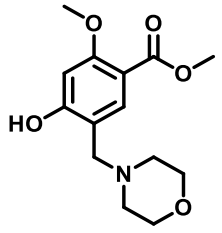
Na_2SO_4, filtered, and evaporated *in vacuo*. This afforded **20** (2.30 g, 93% yield) as a brown solid which was used without further purification. R_f= 0.55 (EtOAc:hexane = 4:1, v/v); ^{1}H-NMR (400 MHz, Methanol-d4) δ 3.82 (s, 3H), 3.84 (s, 3H), 6.40 (dd, J = 8.5, 2.0 Hz, 1H), 6.50 (d, J = 2.0 Hz, 1H), 7.74 (d, J = 8.5 Hz, 1H); ^{13}C-NMR (101 MHz, Methanol-d4) δ 50.5, 54.7, 99.0, 106.9, 109.8, 133.5, 161.9, 163.3, 166.7; HRMS (ESI) *m/z* calculated for $C_9H_{11}O_4$ (MH^+) 183.0657, found 183.0662. These spectroscopic data corresponded to previously reported data.[192]

Methyl-5-formyl-4-hydroxy-2-methoxybenzoate (21)[193]



To a solution of **20** (0.51 g, 2.79 mmol) in trifluoroacetic acid (5 mL) was added hexamethylenetetramine (0.78 g, 5.59 mmol) and copper(I) oxide (0.40 g, 2.79 mmol). The reaction mixture was refluxed at 75°C for 4.5 hours. After this time, the mixture was cooled to room temperature followed by the addition of 3 M HCl (5 mL). After stirring for further 1 hour, the mixture was concentrated *in vacuo* to give a crude brown solid. The resulting solid was then purified by flash column chromatography using the gradient eluent of EtOAc:hexane = 1:1 to 4:1 to afford **21** (0.32 g, 54% yield) as a yellow solid. R_f= 0.61 (EtOAc:hexane = 4:1, v/v); ^{1}H-NMR (400 MHz, Methanol-d4) δ 3.84 (s, 3H), 3.86 (s, 3H), 5.57 (s, 1H), 6.52 (s, 1H),7.93 (s, 1H); HRMS (ESI) *m/z* calculated for $C_{10}H_{11}O_5$ (MH^+) 211.0606, found 211.0600.

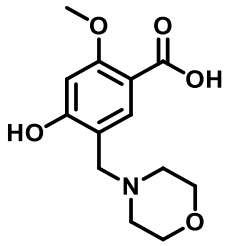
Methyl-4-hydroxy-2-methoxy-5-(morpholinomethyl)benzoate (22)



To a stirred solution of **21** (0.37 g, 1.75 mmol) in methanol (15 mL) was added morpholine (153 µL, 1.75 mmol) followed by 2-picoline borane complex (0.24 g, 2.28 mmol). The reaction mixture was allowed to stir overnight at room temperature under argon atmosphere. After this time, the

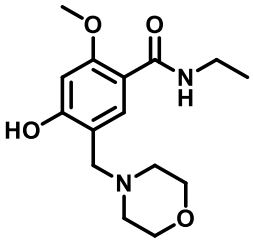
mixture was concentrated *in vacuo* and purified by flash column chromatography using the gradient eluent of EtOAc:hexane = 1:1 to 4:1 to afford **22** (0.35 g, 72% yield) as a colourless oil. R_f= 0.30 (EtOAc:hexane = 4:1, v/v); ^{1}H-NMR (400 MHz, Methanol-d4) δ 2.53 (t, J = 6.5 Hz, 4H), 3.64 (s, 2H), 3.71 (t, J= 4.5 Hz, 4H), 3.81 (s, 3H), 3.82 (s, 3H), 6.47 (s, 1H), 7.60 (s, 1H); ^{13}C-NMR (101 MHz, Methanol-d4) δ 50.7, 52.5, 54.9, 59.2, 66.4, 99.4, 109.5, 113.1, 133.2, 161.4, 163.0, 166.4; HRMS (ESI) *m/z* calculated for $C_{14}H_{20}NO_5$ (MH^+) 282.1341, found 282.1355.

4-Hydroxy-2-methoxy-5-(morpholinomethyl)benzoic acid (23)



To a solution of **22** (0.24 g, 0.85 mmol) in THF (5 mL) was added 1 M NaOH aqueous solution (1.70 mL, 1.70 mmol). The reaction mixture was allowed to stir at 50°C for 4 hours. The mixture was concentrated *in vacuo*. The crude residue was suspended in methanol (5 mL) and filtered to remove the solids. The filtrate was evaporated *in vacuo* to afford **23** (0.22 g, 97% yield) as a yellow solid which was used without further purification. R_f= 0.32 (DCM:MeOH = 9.7:0.3, v/v); ^{1}H-NMR (400 MHz, Methanol-d4) δ 2.57 (t, J = 4.5 Hz, 4H), 3.37 (s, 3H), 3.60 (s, 2H), 3.71 (t, J = 4.5 Hz, 4H), 6.34 (s, 1H), 7.46 (s, 1H); HRMS (ESI) *m/z* calculated for $C_{13}H_{18}NO_5$ (MH^+) 268.1185, found 268.1191.

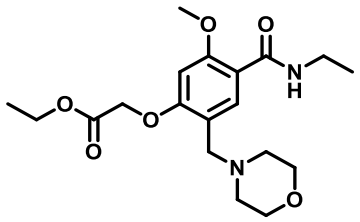
***N*-Ethyl-4-hydroxy-2-methoxy-5-(morpholinomethyl)benzamide (24)**



A solution of **23** (0.20 g, 0.75 mmol) in thionyl chloride (3 mL) was heated under a reflux condition (75°C) for 2.5 hours. After this time, the remaining solvent was removed *in vacuo*. The residue was azeotroped with benzene (2 x 1 mL) to insure the complete removal of thionyl chloride. The

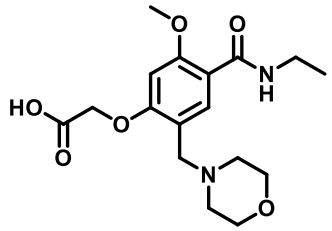
resulting crude acid chloride was dissolved in anhydrous DCM (5 mL), then a solution of ethylamine (2 M in THF, 0.75 mL, 15.00 mmol) was added dropwise to the stirred solution under nitrogen atmosphere. The reaction was stirred overnight. After this time, the reaction mixture was diluted with DCM (5 mL), washed with 10% w/v $NaHCO_3$ aqueous solution (3 x 5 mL) and brine (3 x 5 mL). The organic phase was dried over anhydrous Na_2SO_4, filtered, and concentrated *in vacuo*. The resulting residue was purified by flash column chromatography using DCM:MeOH = 9.7:0.3 as the eluent to afford **24** (69 mg, 31% yield) as a brown oil. R_f= 0.12 (DCM:MeOH = 9.7:0.3, v/v); ^{1}H-NMR (400 MHz, Chloroform-d) δ1.22 (t, *J* = 7.0 Hz, 3H), 2.44 – 2.69 (m, 4H), 3.38 – 3.53 (m, 2H), 3.67 – 3.82 (m, 6H), 3.91 (s, 3H), 6.42 (s, 1H), 7.88 (s, 1H); ^{13}C-NMR (101 MHz, Chloroform-d) *δ* 15.0, 34.5, 52.8, 56.0, 60.9, 66.7, 99.5, 112.8, 113.3, 132.8, 158.7, 161.7, 165.1; HRMS (ESI) *m/z* calculated for $C_{15}H_{23}N_2O_4$ (MH^+) 295.1658, found 295.1669.

Ethyl-2-(4-(ethylcarbamoyl)-5-methoxy-2-(morpholinomethyl)phenoxy)acetate (25)



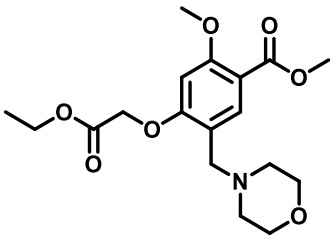
To a solution of **24** (0.20 g, 0.70 mmol) in DMF (5 mL) was added sodium hydride (60% dispersion in mineral oil, 70 mg, 1.75 mmol). The solution was allowed to stir for 10 minutes followed by a dropwise addition of ethyl chloroacetate (80 µL, 0.77 mmol). The mixture was stirred at room temperature under nitrogen atmosphere overnight. After this time, the mixture was partitioned between water (10 mL) and EtOAc (20 mL). The layers were separated and the organic phase was washed with water (2 x 10 mL), 5% LiCl aqueous solution (2 x 10 mL), dried over anhydrous $MgSO_4$, filtered, and concentrated *in vacuo*. The crude material was then purified by flash column chromatography using DCM:MeOH = 9.5:0.5 as the eluent to afford **25** (0.22 g, 82% yield). R_f= 0.36 (DCM:MeOH = 9:1, v/v); ^{1}H-NMR (400 MHz, Chloroform-d) *δ* 1.22 (t, *J* = 7.0 Hz, 3H), 1.29 (t, *J* = 7.0 Hz, 3H), 2.46 – 2.53 (m, 4H), 3.47 (qd, *J* = 7.0, 5.5 Hz, 2H), 3.58 (s, 2H), 3.64 – 3.71 (m, 4H), 3.93 (s, 3H), 4.26 (q, *J* = 7.0 Hz, 2H), 4.69 (s, 2H), 6.37 (s, 1H), 8.15 (s, 1H); HRMS (ESI) m/z calculated for $C_{19}H_{29}N_2O_6$ (MH^+) 380.1947, found 381.2040.

2-(4-(Ethylcarbamoyl)-5-methoxy-2-(morpholinomethyl)phenoxy)acetic acid (26)



To a stirred solution of **25** (0.22 g, 0.59 mmol) in THF (5 mL) was added 1 M NaOH aqueous solution (1.20 mL, 1.20 mmol). The reaction mixture was allowed to stir at 30°C overnight. After this time, the mixture was then concentrated *in vacuo*. The resulting residue was triturated with DCM:MeOH (9.5:0.5, 10 mL). The suspension was filtered and the filtrate was concentrated *in vacuo* to afford **26** (quantitative conversion) which was used without further purification. R_f= 0.11 (DCM:MeOH = 9:1, v/v); ^{1}H-NMR (400 MHz, Methanol-d4) δ 1.23 (t, J = 7.0 Hz, 3H), 2.57 (d, J = 5.0 Hz, 4H), 3.43 (q, J = 7.0 Hz, 2H), 3.67 (s, 2H), 3.68 – 3.73 (m, 4H), 3.99 (s, 3H), 4.54 (s, 2H), 6.59 (s, 1H), 7.95 (s, 1H); HRMS (ESI) calculated mass for $C_{17}H_{25}N_2O_6$ (MH^+) 352.1634, found 353.1725.

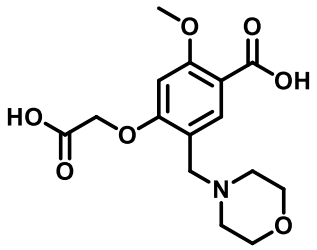
Methyl-4-(2-ethoxy-2-oxoethoxy)-2-methoxy-5-(morpholinomethyl)benzoate (29)



To a solution of **22** (0.29 g, 1.04 mmol) in DMF (10 mL) was added sodium hydride (60% dispersion in mineral oil, 0.11 g, 2.60 mmol). The solution was allowed to stir for 10 minutes followed by a dropwise addition of ethyl chloroacetate (0.12 mL, 1.15 mmol). The mixture was stirred at room temperature under nitrogen atmosphere overnight. After this time, the mixture was partitioned between water (10 mL) and EtOAc (20 mL). The layers were separated and the organic phase was washed with water (2 x 10 mL), 5% LiCl aqueous solution (2 x 10 mL), and brine (2 x 10 mL), dried over anhydrous $MgSO_4$, filtered, and concentrated *in vacuo* to afford **29** (0.32 g, 85% yield). R_f= 0.17 (DCM:MeOH = 9.5:0.5, v/v); ^{1}H-NMR (400 MHz, Methanol-d4) δ 1.31 (t, J = 7.0 Hz, 3H), 2.47 – 2.58 (m, 4H), 3.61 (s, 2H), 3.58 – 3.73 (m, 4H), 3.85 (s, 3H), 3.89 (s, 3H),

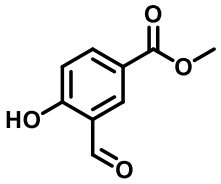
4.28 (q, J = 7.0 Hz, 2H), 4.88 (s, 2H), 6.61 (s, 1H), 7.86 (s, 1H); HRMS (ESI) m/z calculated for $C_{18}H_{26}NO_7$ (MH^+) 367.1631, found 368.1709.

4-(Carboxymethoxy)-2-methoxy-5-(morpholinomethyl)benzoic acid (30)



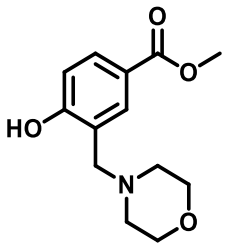
To a solution of **29** (0.32 g, 0.89 mmol) in THF (10 mL) was added 1 M NaOH aqueous solution (3.54 mL, 3.54 mmol). The reaction mixture was allowed to stir at room temperature overnight. After this time, the mixture was concentrated *in vacuo* to afford **30** (quatitative conversion) which was used without further purification. ^{1}H-NMR (400 MHz, Methanol-d4) δ 3.22 (m, 4H), 3.88 (s, 3H), 3.95 (m, 4H), 4.22 (s, 2H), 4.71 (s, 2H), 6.81 (s, 1H), 7.52 (s, 1H); HRMS (ESI) calculated mass for $C_{15}H_{20}NO_7$ (MH^+) 325.1162, found 326.1255.

Methyl-3-formyl-4-hydroxybenzoate (37)[194]



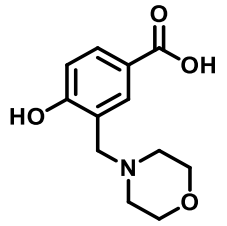
To a solution of methyl-4-hydroxybenzoate (5.0 g, 32.9 mmol) in trifluoroacetic acid (15 mL) was added hexamethylenetetramine (9.2 g, 65.8 mmol) and copper(I) oxide (4.7 g, 32.9 mmol). The mixture was refluxed at 75°C for 5 hours. After this time, the mixture was cooled to room temperature followed by the addition of 3 M HCL aqueous solution (20 mL). After stirring for 1 hour, the mixture was concentrated *in vacuo* to give a crude green oil. The resulting crude oil was purified by flash column chromatography using the gradient eluent of 100% DCM to DCM:MeOH = 9.5:0.5 to afford **37** (0.95 g, 16% yield) as a white solid. R_f= 0.73 (DCM:MeOH = 9.5:0.5, v/v); ^{1}H-NMR (400 MHz, Methanol-d4) δ 3.92 (s,3H), 7.05 (d, J = 8.5 Hz, 1H), 8.17 (dd, J = 8.5, 2.3 Hz, 1H), 8.42 (d, J = 2.0 Hz, 1H), 10.14 (s, 1H).

Methyl-4-hydroxy-3-(morpholinomethyl)benzoate (38)



To a stirred solution of **37** (0.95 g, 5.27 mmol) in methanol (15 mL) was added morpholine (0.46 mL, 5.27 mmol) followed by pyridine borane complex (0.70 mL, 6.85 mmol). The reaction mixture was allowed to stir at room temperature under nitrogen atmosphere overnight. After this time, the mixture was partition between water (10 mL) and EtOAc (20 mL). The layers were separated and the organic phase was washed with water (2 x 10 mL), saturated $NaHCO_3$ aqueous solution (2 x 10 mL), and concentrated *in vacuo*. The resulting solid was purified by flash column chromatography using the gradient eluent of 100% DCM to DCM:MeOH = 9.5:0.5 to afford **38** (1.30 g, 98% yield). R_f= 0.40 (DCM:MeOH = 9.5:0.5, v/v); ^{1}H-NMR (400 MHz, Methanol-d4) δ 2.52 – 2.74 (m, 4H), 3.70 – 3.77 (m, 6H), 3.86 (s, 3H), 6.82 (d, J = 8.5 Hz, 1H), 7.79 (d, J = 2.0 Hz, 1H), 7.83 (dd, J = 8.5, 2.0 Hz, 1H); ^{13}C-NMR (101 MHz, Chloroform-d) δ = 51.8, 52.8, 61.5, 66.7, 116.1, 120.3, 121.3, 130.8, 131.1, 162.2, 166.9; HRMS (ESI) calculated mass for $C_{13}H_{18}NO_4$ (MH^+) 252.1236, found 252.1239.

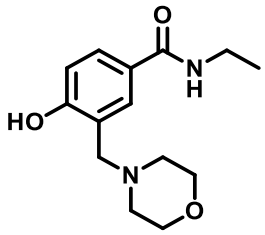
4-Hydroxy-3-(morpholinomethyl)benzoic acid (39)



To a stirred solution of **38** (1.41 g, 5.60 mmol) in THF (15 mL) was added 1 M NaOH aqueous solution (11.2 mL, 11.2 mmol). The reaction mixture was allowed to stir at 30°C overnight. After this time, the mixture was then concentrated *in vacuo*. The resulting residue was triturated with DCM:MeOH (9.5:0.5, 25 mL). The suspension was filtered and the filtrate was concentrated *in vacuo* to afford **39** (quantitative conversion) which was used without further purification. R_f= 0.36 (DCM:MeOH = 9:1, v/v); ^{1}H-NMR (400 MHz, Methanol-d4) δ 2.60 (d, J = 4.5 Hz, 4H), 3.63 (s,

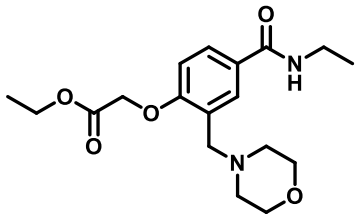
2H), 3.72 (t, J = 4.5 Hz, 4H), 6.61 (d, J = 8.5 Hz, 1H), 7.68 (dd, J = 8.5, 2.5 Hz, 1H), 7.81 (d, J = 2.5 Hz, 1H); ^{13}C-NMR (101 MHz, Methanol-d4) δ 53.0, 57.9, 66.5, 117.6, 122.4, 122.6, 130.0, 132.3, 168.1, 176.0; HRMS (ESI) calculated mass for $C_{12}H_{16}NO_4$ (MH^+) 238.1079, found 238.1084.

_N_-Ethyl-4-hydroxy-3-(morpholinomethyl)benzamide (40)



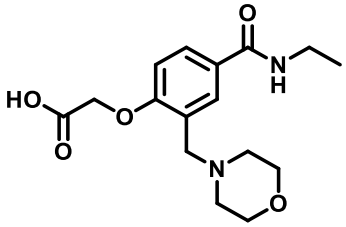
A solution of **39** (1.33 g, 5.60 mmol) in thionyl chloride (10 mL) was heated under a reflux condition (75°C) for 3 hours. After this time, the remaining solvent was removed *in vacuo*. The resulting crude acid chloride was dissolved in anhydrous DCM (10 mL) and cooled down to 0°C in an ice bath. Then a solution of ethylamine (2 M in THF, 5.60 mL, 11.20 mmol) was added dropwise to the stirred solution under a nitrogen atmosphere. The mixture was allowed to warm up to room temperature and the reaction was stirred overnight. After this time, the reaction mixture was diluted with DCM (10 mL) and washed with 10% w/v aqueous $NaHCO_3$ (3 x 5 mL) and brine (3 x 5 mL). The organic phase was dried over anhydrous $MgSO_4$, filtered, and concentrated *in vacuo* followed by a purification using flash column chromatography with EtOAc:hexane = 8.5:1.5 as the eluent to afford **40** (0.33 g, 22% yield) as a brown solid. R_f= 0.5 (DCM:MeOH = 9:1, v/v); ^{1}H-NMR (400 MHz, Chloroform-d) δ1.27 (t, J = 7.0 Hz, 3H), 2.62 (s, 4H), 3.50 (qd, J = 7.0, 5.5 Hz, 2H), 3.79 (s, 6H), 6.86 (d, J = 8.5 Hz, 1H), 7.56 (dd, J = 8.5, 2.0 Hz, 1H), 7.59 (s, 1H); HRMS (ESI) *m/z* calculated for $C_{14}H_{21}N_2O_3$ (MH^+) 265.1552, found 265.1558.

Ethyl 2-(4-(ethylcarbamoyl)-2-(morpholinomethyl)phenoxy)acetate (41)



To a solution of **40** (0.33 g, 1.25 mmol) in DMF (15 mL) was added sodium hydride (60% dispersion in mineral oil, 0.12 g, 3.12 mmol). The solution was allowed to stir for 20 minutes followed by a dropwise addition of ethyl chloroacetate (0.15 mL, 1.38 mmol). The solution mixture was stirred at room temperature under nitrogen atmosphere overnight. After this time, the mixture was partitioned between water (15 mL) and EtOAc (30 mL). The layers were separated and the organic phase was washed with water (2 x 15 mL) and 5% LiCl aqueous solution (2 x 10 mL), dried over anhydrous $MgSO_4$, filtered, and concentrated *in vacuo* to afford **41** (0.41 g, 94% yield). R_f= 0.12 (DCM:MeOH = 9.5:0.5, v/v); ^{1}H-NMR (400 MHz, Chloroform-d) δ 1.21 (t, J = 7.0 Hz, 3H), 1.27 (t, J = 7.0 Hz, 3H), 2.46 – 2.54 (m, 4H), 3.45 (qd, J = 7.0, 5.0 Hz, 2H), 3.62 (s, 2H), 3.69 (t, J = 5.0 Hz, 4H), 4.23 (q, J = 7.0 Hz, 2H) 4.66 (s, 2H), 6.74 (d, J = 8.5 Hz, 1H), 7.67 (dd, J = 8.5, 2.5 Hz, 1H) 7.81 (d, J = 2.5 Hz, 1H); ^{13}C-NMR (101 MHz, Chloroform-d) δ 14.1, 14.9, 34.8, 53.5, 56.2, 61.4, 65.6, 66.9, 111.2, 126.4, 127.6, 128.0, 129.6, 158.4, 166.9, 168.4; HRMS (ESI) calculated mass for $C_{18}H_{27}N_2O_5$ (MH^+) 351.1920, found 351.1930.

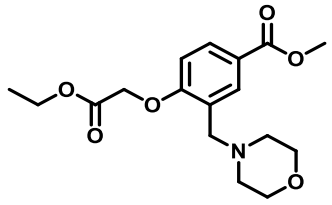
2-(4-(Ethylcarbamoyl)-2-(morpholinomethyl)phenoxy)acetic acid (42)



To a stirred solution of **41** (0.36 g, 1.04 mmol) in THF (10 mL) was added 1 M NaOH aqueous solution (2.10 mL, 2.08 mmol). The reaction mixture was allowed to stir at 40°C overnight. After this time, the mixture was concentrated *in vacuo*. The resulting residue was triturated with DCM:MeOH (9.5:0.5, 20 mL). The suspension was filtered and the filtrate was concentrated *in vacuo* to afford **42** (0.33 g, quantitative yield) which was used without further purification. ^{1}H-

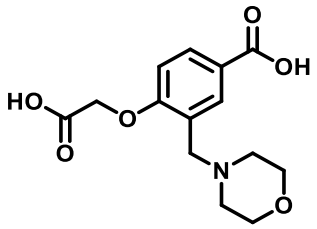
NMR (400 MHz, Methanol-d4) δ 1.23 (t, J = 7.0 Hz, 3H), 2.53 – 2.60 (m, 4H), 3.41 (q, J = 7.0 Hz, 2H), 3.68 – 3.75 (m, 6H), 4.51 (s, 2H), 6.92 (d, J = 8.5 Hz, 1H), 7.75 (dd, J = 8.5, 2.5 Hz, 1H), 7.86 (d, J = 2.5 Hz, 1H); ^{13}C-NMR (101 MHz, Chloroform-d) δ 13.7, 34.4, 53.2, 56.2, 66.4, 67.6, 111.2, 125.2, 126.2, 127.6, 130.2, 160.0, 168.2, 174.73 HRMS (ESI) calculated mass for $C_{16}H_{23}N_2O_5$ (MH^+) 323.1607, found 323.1623.

Methyl-4-(2-ethoxy-2-oxoethoxy)-3-(morpholinomethyl)benzoate (44)



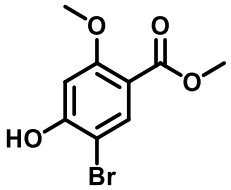
To a solution of **38** (1.33 g, 5.27 mmol) in DMF (15 mL) was added sodium hydride (60% dispersion in mineral oil, 0.53 g, 13.20 mmol). The solution was allowed to stir for 10 minutes followed by a dropwise addition of ethyl chloroacetate (0.62 mL, 5.80 mmol). The solution mixture was stirred at room temperature under nitrogen atmosphere overnight. After this time, the mixture was partitioned between water (20 mL) and EtOAc (40 mL). The layers were separated and the organic phase was washed with water (2 x 20 mL) and 5% LiCl aqueous solution (2 x 10 mL), dried over anhydrous $MgSO_4$, filtered, and concentrated *in vacuo*. The crude material was then purified by flash column chromatography using the gradient eluent of hexane:EtOAc = 1:1 to 1:4 to afford **44** (0.74 g, 42% yield) as a white solid. R_f= 0.47 (DCM:MeOH = 9.5:0.5, v/v); ^{1}H-NMR (400 MHz, Chloroform-d) δ 1.27 (t, J = 7.0 Hz, 3H), 2.48 – 2.60 (m, 4H), 3.63 (s, 2H), 3.67 – 3.77 (m, 4H), 3.87 (s, 3H), 4.24 (q, J = 7.0 Hz, 2H), 4.69 (s, 2H) 6.75 (d, J = 8.5 Hz, 1H), 7.90 (dd, J = 8.5, 2.0 Hz, 1H), 8.05 (d, J = 2.0 Hz, 1H); ^{13}C-NMR (101 MHz, Chloroform-d) δ 14.1, 51.9, 53.5, 56.2, 61.4, 65.5, 67.0, 110.9, 123.3, 126.6, 130.3, 132.5, 159.8, 166.8, 168.2; HRMS (ESI) calculated mass for $C_{17}H_{24}NO_6$ (MH^+) 337.1525, found 338.1620.

4-(Carboxymethoxy)-3-(morpholinomethyl)benzoic acid (45)



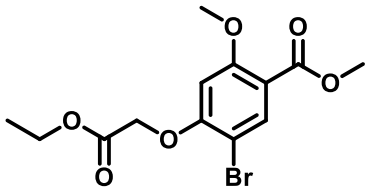
To a solution of **44** (0.36 g, 1.07 mmol) in THF (10 mL) was added 1 M NaOH aqueous solution (4.28 mL, 4.28 mmol). The reaction mixture was allowed to stir at room temperature overnight. The mixture was then concentrated *in vacuo* to afford **45** (quantitative conversion) which was used without further purification; ^{1}H-NMR (400 MHz, D_2O) δ 2.52 (t, J = 4.5 Hz, 4H), 3.56 (s, 2H), 3.62 (t, J = 4.5 Hz, 4H), 4.46 (s, 2H) 6.74 (d, J = 8.5 Hz, 1H), 7.66 (d, J = 2.0 Hz, 1H), 7.72 (dd, J = 8.5, 2.0 Hz, 1H); ^{13}C-NMR (101 MHz, D2O) δ 52.5, 56.3, 66.1, 67.3, 111.2, 123.2, 128.2, 130.6, 133.5, 159.2, 175.1, 176.9; HRMS (ESI) calculated mass for $C_{14}H_{18}NO_6$ (MH^+) 295.1056, found 296.1131.

Methyl 5-bromo-4-hydroxy-2-methoxybenzoate (47)



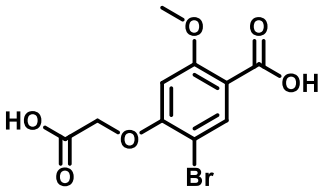
To a solution of **20** (1.02 g, 5.60 mmol) in DCM (15 mL) was added Br_2 (0.32 mL, 6.16 mmol) dropwise at 0°C under inert atmosphere. The solution was allowed to warm to room temperature and stirred overnight. After this time, the organic phase was washed with water (2 x 20 mL) followed by brine (2 x 20 mL) and dried over anhydrous $MgSO_4$ and filtered. The solution was then concentrated *in vacuo* followed by a purification using flash column chromatography using DCM:MeOH = 10:0.1 as the eluent to afford **47** (0.69 g, 47% yield). ^{1}H-NMR (400 MHz, Methanol-d4) δ 3.83 (s, 3H), 3.85 (s, 3H), 6.62 (s, 1H), 7.96 (s, 1H); ^{13}C-NMR (101 MHz, Chloroform-d) δ 22.8, 29.3, 50.8, 55.0, 99.7, 111.4, 136.0, 159.3, 160.8; HRMS (ESI) calculated mass for $C_9H_8O_4Br$ (MH^-) 258.9606, found 258.9618.

Methyl 5-bromo-4-(2-ethoxy-2-oxoethoxy)-2-methoxybenzoate (48)



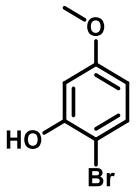
To a solution of **47** (89 mg, 0.34 mmol) in DMF (2 mL) was added sodium hydride (60% dispersion in mineral oil, 34 mg, 0.85 mmol). The solution was allowed to stir for 20 minutes followed by a dropwise addition of ethyl chloroacetate (40 µL, 0.38 mmol). The solution mixture was stirred at room temperature under nitrogen atmosphere overnight. After this time, the mixture was partitioned between water (5 mL) and EtOAc (10 mL). The layers were separated and the organic phase was washed with water (2 x 5 mL) and 5% LiCl aqueous solution (2 x 10 mL), dried over anhydrous $MgSO_4$, filtered, and concentrated *in vacuo*. The crude material was then purified by flash column chromatography using hexane:EtOAc = 2.5:1 as the eluent to afford **48** (61 mg, 52% yield). R_f= 0.24 (hexane:EtOAc = 2.5:1, v/v); ^{1}H-NMR (400 MHz, Chloroform-d) δ 1.31 (t, J = 7.0 Hz, 3H), 3.87 (s, 3H), 3.89 (s, 3H), 4.29 (q, J = 7.0 Hz, 2H), 4.76 (s, 2H), 6.41 (s, 1H), 8.09 (s, 1H); HRMS (ESI) calculated mass for $C_{13}H_{16}O_6Br$ (MH^+) 347.0130, found 347.0137.

5-Bromo-4-(carboxymethoxy)-2-methoxybenzoic acid (49)



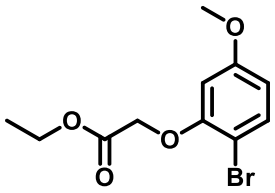
To a stirred solution of **48** (40 mg, 0.12 mmol) in THF (2 mL) was added 1 M NaOH aqueous solution (0.29 mL, 0.29 mmol). The reaction mixture was allowed to stir at 50°C overnight. After this time, 3 M HCl aqueous solution was added to the mixture to adjust the pH of the mixture to 3 followed by the extraction with EtOAc (3 x 20 mL). The collected organic phase was dried over anhydrous $MgSO_4$, filtered, and concentrated *in vacuo* to afford **49** (31 mg, 85% yield) which was used without further purification. ^{1}H-NMR (400 MHz, Methanol-d4) δ 3.92 (s, 3H), 4.92 (s, 2H), 6.68 (s, 1H), 8.06 (s, 1H); ^{13}C-NMR (101 MHz, Chloroform-d) δ 55.4, 65.3, 98.0, 101.4, 113.1, 136.2, 158.9, 160.6, 166.3, 169.9; HRMS (ESI) calculated mass for $C_{10}H_{10}O_6Br$ (MH^+) 304.9661, found 304.9668.

2-Bromo-5-methoxyphenol (51)



A solution of 3-methoxyphenol (1.16 g, 9.36 mmol) in DCM (7.20 mL) under nitrogen atmosphere was cooled to 0°C in an ice bath. A solution of Br_2 (0.42 mL, 8.15 mmol) in DCM (2.40 mL) was then added to the reaction flask dropwise over 20 minutes. The reaction mixture was allowed to warm to 20°C after the addition of Br_2. After this time, the reaction was quenched by adding 10% aqueous $NaHCO_3$ aqueous solution dropwise immediately when it reached 20°C. The mixed solution was stirred at room temperature for 1 hour. After this time, the organic phase was separated, dried over anhydrous $MgSO_4$, filtered, and concentrated *in vacuo*. The crude material was purified by flash column chromatography using pentane:diethyl ether = 5:1 as the eluent to afford **51** (0.51 g, 27% yield). ^{1}H-NMR (400 MHz, Chloroform-d) δ 3.80 (d, J = 1.0 Hz, 3H), 5.54 (s, 1H), 6.45 (ddd, J = 9.0, 3.0, 1.0 Hz, 1H), 6.63 (dd, J = 3.0, 1.0 Hz, 1H), 7.34 (dd, J = 9.0, 1.0 Hz, 1H). ^{13}C-NMR (101 MHz, Chloroform-d) δ 55.6, 100.9, 101.6, 108.4, 132.0, 153.0, 160.6. These spectroscopic data correspond to previously reported data.[195]

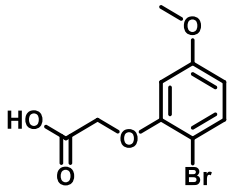
Ethyl 2-(2-bromo-5-methoxyphenoxy)acetate (52)



To a solution of **51** (0.48 g, 2.36 mmol) in DMF (10 mL) was added sodium hydride (60% dispersion in mineral oil, 0.24 g, 5.91 mmol). The solution was allowed to stir for 10 minutes followed by a dropwise addition of ethyl chloroacetate (0.28 mL, 2.60 mmol). The mixture was stirred at room temperature under nitrogen atmosphere overnight. After this time, the mixture was partitioned between water (10 mL) and EtOAc (20 mL). The layers were separated and the organic phase was washed with water (2 x 10 mL) and 5% LiCl aqueous solution (2 x 10 mL), dried over anhydrous $MgSO_4$, filtered, and concentrated *in vacuo* to afford **52** (0.46 g, 67% yield) which was used without further purification. ^{1}H-NMR (400 MHz, Chloroform-d) δ 1.32 (t, J = 7.0 Hz, 3H),

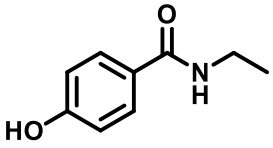
3.79 (s, 3H), 4.29 (q, J = 7.0 Hz, 2H), 4.69 (s, 2H), 6.42 (d, J = 2.5 Hz, 1H), 6.47 (dd, J = 8.5, 2.5 Hz, 1H), 7.45 (d, J = 8.5 Hz, 1H). ^{13}C-NMR (101 MHz, Chloroform-d) δ 14.2, 55.6, 61.5, 66.4, 101.6, 103.1, 107.3, 133.5, 155.1, 160.0, 168.2; HRMS (ESI) calculated mass for $C_{11}H_{14}O_4Br$ (MH^+) 289.0075, found 289.0067.

2-(2-Bromo-5-methoxyphenoxy)acetic acid (53)



To a solution of **52** (0.87 g, 3.00 mmol) in THF (10 mL) was added 1 M NaOH aqueous solution (6.00 mL, 6.00 mmol). The reaction mixture was allowed to stir at 40°C overnight. After this time, the aqueous layer was separated and the pH was adjusted to 3 by using 3 M HCl aqueous solution. The solution was then extracted with EtOAc (2 x 20 mL). The organic extracts were combined, washed with brine (15 mL), dried over anhydrous $MgSO_4$, filtered, and concentrated *in vacuo* to afford **53** (0.66 g, 84% yield) which was used without further purification. ^{1}H-NMR (400 MHz, Methanol-d4) δ 3.79 (s, 3H), 4.74 (s, 2H), 6.47 – 6.57 (m, 2H), 7.40 – 7.47 (m, 1H); ^{13}C-NMR (101 MHz, Methanol-d4) δ = 29.4, 65.4, 100.8, 102.2, 107.0, 133.1, 155.2, 160.3; HRMS (ESI) calculated mass for $C_9H_8O_4Br$ (MH^-) 258.9606, found 258.9612.

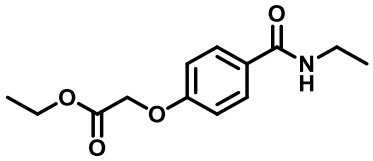
***N*-Ethyl-4-hydroxybenzamide (55)**



A solution of 4-hydroxybenzoic acid (4.97 g, 36.00 mmol) in anhydrous DMF (50 mL) was cooled to 0°C in an ice bath. HOBt (4.86 g, 36.00 mmol), triethylamine (6.00 mL, 43.00 mmol), ethylamine (2 M in THF, 18.00 mL, 36.00 mmol), and EDC·HCl (8.28 g, 43.00 mmol) were added under nitrogen atmosphere, respectively. The mixture was then allowed to warm up to room temperature and stirred overnight. After this time, the reaction mixture was diluted with water (100 mL) and the pH of the solution was adjusted to 4 using 3 M HCl aqueous solution. The solution was then extracted with EtOAc (5 x 50 mL). The organic phase was combined, washed with 5%

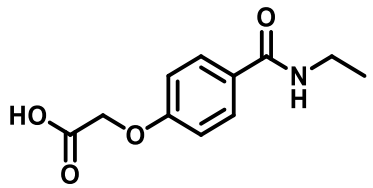
LiCl aqueous solution (5 x 30 mL), dried over anhydrous $MgSO_4$, filtered, and concentrated *in vacuo*. The crude material was purified by flash column chromatography using 100% EtOAc as the eluent to afford **55** (2.37 g, 40% yield). ^{1}H-NMR (400 MHz, Methanol-d4) δ 1.19 – 1.25 (m, 3H), 3.35 – 3.46 (m, 2H), 6.80 – 6.86 (m, 2H), 7.68 – 7.74 (m, 2H), 8.25 (s, 1H); ^{13}C-NMR (101 MHz, Methanol-d4) δ 13.6, 34.4, 114.6, 125.3, 128.7, 160.5, 168.6.

Ethyl 2-(4-(ethylcarbamoyl)phenoxy)acetate (56)



To a solution of **55** (0.74 g, 4.47 mmol) in DMF (15 mL) was added sodium hydride (60% dispersion in mineral oil, 0.45 g, 11.2 mmol). The solution was allowed to stir for 30 minutes followed a dropwise addition of ethyl chloroacetate (0.53 mL, 4.92 mmol). The reaction mixture was allowed to stir at room temperature under nitrogen atmosphere overnight. After this time, the mixture was diluted with water and extracted with EtOAc (4 x 25 mL). Then, the organic phase was washed with 5% LiCl aqueous solution (3 x 20 mL), dried over anhydrous $MgSO_4$, filtered, and concentrated *in vacuo* to afford **56** (0.18 g, 16% yield) which was used without further purification. ^{1}H-NMR (400 MHz, Methanol-d4) δ 1.23 (t, J = 7.0 Hz, 3H), 1.30 (t, J = 7.0 Hz, 3H), 3.41 (q, J = 7.0 Hz, 2H), 4.27 (q, J = 7.0 Hz, 2H), 4.79 (s, 2H), 6.95 – 7.08 (m, 2H), 7.76 – 7.86 (m, 2H); ^{13}C-NMR (101 MHz, Methanol-d4) δ 13.0, 13.6, 34.4, 61.0, 64.7, 114.0, 127.4, 128.6, 160.6, 168.0, 169.1.

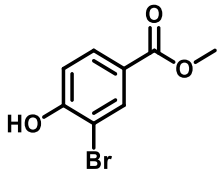
2-(4-(Ethylcarbamoyl)phenoxy)acetic acid (57)



To a solution of **56** (0.17 g, 0.70 mmol) in THF (10 mL) was added 1 M NaOH aqueous solution (1.40 mL, 1.40 mmol). The reaction mixture was allowed to stir at room temperature overnight. After this time, the mixture was diluted with water and washed with EtOAc (10 mL). The pH of aqueous phase was adjusted to be less than 3 using 1 M HCl aqueous solution and the mixture was

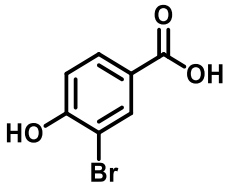
extracted with EtOAc (2 x 15 mL). The organic phase was combined and washed with brine (15 mL), dried over anhydrous $MgSO_4$, filtered, and concentrated *in vacuo* to give a white solid. The solid was washed with pentane and then dried to afford **57** (49 mg, 32% yield). ^{1}H-NMR (400 MHz, Methanol-d4) δ 1.23 (t, J = 7.0 Hz, 3H), 3.41 (q, J = 7.0 Hz, 2H), 4.75 (s, 2H), 6.96 – 6.96 (m, 2H), 7.75 – 7.87 (m, 2H).

Methyl 3-bromo-4-hydroxybenzoate (59)



The suspension of methyl 4-hydroxybenzoate (0.99 g, 6.50 mmol) in DCM (15 mL) was cooled to 0°C in an ice bath. Br_2 (0.17 mL, 6.50 mmol) was slowly added dropwise to a stirred suspension under nitrogen atmosphere. The suspension was allowed to warm up to room temperature and the reaction was stirred overnight. After this time, a solution of $Na_2S_2O_5$ (0.12 g, 0.65 mmol) in 4.0 mL of water was added to the mixture while keeping the temperature below 15°C. Then, MeOH (1.0 mL) was added to the mixture and stirred for further 1 hour at room temperature. The organic phase was then washed with water (2 x 20 mL) followed by brine (2 x 20 mL) and dried over anhydrous $MgSO_4$ and filtered. The organic phase was then concentrated *in vacuo* to afford **59** (1.50 g, quantitative yield) as a white solid. ^{1}H-NMR (400 MHz, Chloroform-d) δ 3.92 (s, 3H), 5.93 (s, 1H), 7.08 (d, J = 8.5 Hz, 1H), 7.95 (ddd, J = 8.5, 2.1, 0.5 Hz, 1H), 8.22 (d, J = 2.0 Hz, 1H). These spectroscopic data correspond to previously reported data.[196]

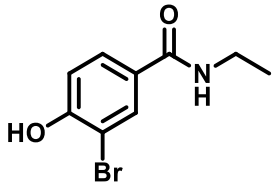
3-Bromo-4-hydroxybenzoic acid (60)[197]



To a solution of **59** (3.86 g, 16.70 mmol) in THF (25 mL) was added 1 M NaOH aqueous solution (33.40 mL, 33.40 mmol). The reaction mixture was allowed to stir at 50°C overnight. After this time, the solvent was evaporated *in vacuo* and the pH of the remaining aqueous phase was adjusted

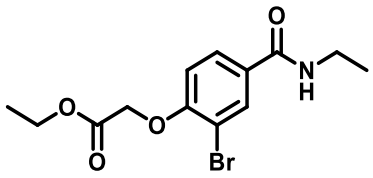
to 1 by using 3 M HCl aqueous solution. The resulting solid residues were collected and dissolved in water (30 mL). The solution was then extracted with EtOAc (3 x 30 mL). The organic extracts were combined and washed with brine (15 mL), dried over anhydrous $MgSO_4$, filtered, and evaporated *in vacuo* to afford **60** (3.44 g, 95% yield) which was used without further purification. ^{1}H-NMR (400 MHz, Methanol-d4) δ 6.95 (d, J = 8.5 Hz, 1H), 7.85 (dd, J = 8.5, 2.0 Hz, 1H), 8.13 (d, J = 2.0 Hz, 1H); ^{13}C-NMR (101 MHz, Methanol-d4) δ 109.1, 115.2, 122.9, 130.3, 134.7, 158.5, 167.2; HRMS (ESI) calculated mass for $C_7H_4O_3Br$ (MH^+) 214.9344, found 214.9350.

3-Bromo-*N*-ethyl-4-hydroxybenzamide (61)



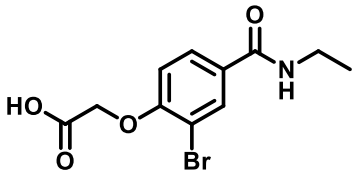
A solution of **60** (3.44 g, 15.80 mmol) in thionyl chloride (30 mL) was heated under a reflux condition (75°C) for 3 hours. After this time, the remaining solvent was removed *in vacuo*. The residue was azeotroped with benzene (2 x 5 mL) to insure the complete removal of thionyl chloride. The resulting crude acid chloride was dissolved in anhydrous DCM (30 mL). A solution of ethylamine (2 M in THF, 23.80 mL, 47.60 mmol) was added dropwise to the stirred solution at 0°C under nitrogen atmosphere. The reaction was allowed to warm up to room temperature and stirred overnight. After this time, the reaction mixture was diluted with DCM (20 mL), washed with 10% w/v aqueous $NaHCO_3$ (3 x 15 mL) and brine (3 x 15 mL). The organic phase was dried over anhydrous $MgSO_4$, filtered, and concentrated *in vacuo*. The crude material was purified by flash column chromatography using pentane: EtOAc = 2:1 as the eluent to afford **61** (2.43 g, 63% yield). R_f= 0.37 (pentane:EtOAc 1:1, v/v); ^{1}H-NMR (400 MHz, Acetone-d6) δ 1.19 (t, J = 7.0 Hz, 3H), 3.42 (qd, J = 7.0, 5.6 Hz, 2H), 7.07 (d, J = 8.5 Hz, 1H), 7.79 (dd, J = 8.5, 2.0 Hz, 1H), 8.08 (d, J = 2.0 Hz, 1H), 9.60 (s, 1H). ^{13}C-NMR (101 MHz, Acetone-d6) δ = 14.3, 34.4, 109.2, 115.8, 127.9, 128.0, 132.3, 156.6, 164.9; HRMS (ESI) calculated mass for $C_9H_{11}NO_2Br$ (MH^+) 243.9973, found 243.9975.

Ethyl 2-(2-bromo-4-(ethylcarbamoyl)phenoxy)acetate (62)



To a solution of **61** (2.10 g, 8.57 mmol) in DMF (15 mL) was added sodium hydride (60% dispersion in mineral oil, 0.85 g, 21.4 mmol). The solution was allowed to stir for 20 minutes followed by a dropwise addition of ethyl chloroacetate (1.00 mL, 9.43 mmol). The reaction mixture was allowed to stir at room temperature under nitrogen atmosphere overnight. After this time, the mixture was partitioned between water (25 mL) and EtOAc (50 mL). The layers were separated and the organic phase was washed with water (2 x 20 mL) and 5% LiCl aqueous solution (2 x 20 mL), dried over anhydrous $MgSO_4$, filtered, and concentrated *in vacuo* to afford **62** (1.0 g, 35% yield) which was used without further purification. R_f= 0.38 (pentane:EtOAc 1:1, v/v); ^{1}H-NMR (400 MHz, Acetone-d6) δ 1.19 (t, J = 7.0 Hz, 4H), 1.27 (t, J = 7.0 Hz, 4H), 3.40 (q, J = 7.0 Hz, 2H), 4.23 (q, J = 7.0 Hz, 2H), 4.93 (s, 2H), 7.08 (d, J = 8.5 Hz, 1H), 7.86 (dd, J = 8.5, 2.0 Hz, 1H), 8.12 (d, J = 2.0 Hz, 1H); ^{13}C-NMR (101 MHz, Acetone-d6) δ 13.5, 14.2, 29.5, 34.2, 60.8, 65.5, 110.9, 112.7, 127.8, 129.5, 132.2, 156.6, 164.2, 167.7; HRMS (ESI) calculated mass for $C_{13}H_{17}NO_4Br$ (MH^+) 330.0341, found 330.0343.

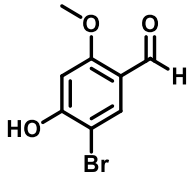
2-(2-Bromo-4-(ethylcarbamoyl)phenoxy)acetic acid (63)



To a solution of **62** (0.97 g, 2.94 mmol) in THF (10 mL) was added 1 M NaOH aqueous solution (5.88 mL, 5.88 mmol). The reaction mixture was allowed to stir at 40°C overnight. After this time, the aqueous layer was separated and the pH of the aqueous phase was adjusted to 3 by using 3 M HCl aqueous solution. The solution was then extracted with EtOAc (2 x 20 mL). The organic extracts were combined and washed with brine (15 mL), dried over anhydrous $MgSO_4$, filtered, and concentrated *in vacuo* to afford **63** (0.71 g, 80% yield) which was used without further purification. ^{1}H-NMR (400 MHz, Methanol-d4) δ 1.23 (t, J = 7.0 Hz, 4H), 3.40 (q, J = 7.0 Hz,

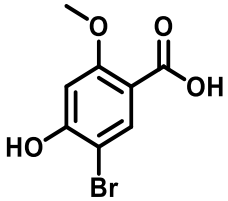
2H), 4.86 (s, 2H), 7.01 (d, J = 8.5 Hz, 1H), 7.80 (dd, J = 8.5, 2.0 Hz, 1H), 8.08 (d, J = 2.0 Hz, 1H); ^{13}C-NMR (101 MHz, Methanol-d4) δ 13.5, 34.5, 65.1, 111.2, 112.3, 127.6, 128.5, 132.2, 157.0, 166.6, 170.1; HRMS (ESI) calculated mass for $C_{11}H_{13}NO_4Br$ (MH^+) 302.0028, found 302.0038.

5-Bromo-4-hydroxy-2-methoxybenzaldehyde (65)



The suspension of methyl 4-hydroxy-2-methoxybenzaldehyde (0.11 g, 0.72 mmol) in DCM (2 mL) was cooled to 0°C in an ice bath. Br_2 (19 µL, 0.72 mmol) was slowly added dropwise to a stirred suspension under nitrogen atmosphere. The suspension was allowed to warm up to room temperature and the reaction was stirred overnight. After this time, a solution of $Na_2S_2O_5$ (14 mg, 72 µmol) in 0.44 mL of water was added to the mixture while keeping the temperature below 15°C. MeOH (0.15 mL) was then added to the mixture and the reaction was stirred for 1 hour at room temperature. The organic phase was then washed with water (2 x 20 mL) followed by brine (2 x 20 mL) and dried over anhydrous $MgSO_4$ and filtered. The organic phase was concentrated *in vacuo* followed by a purification by flash column chromatography using hexane:EtOAc = 7:3 as the eluent to afford **65** (46 mg, 28% yield). ^{1}H-NMR (400 MHz, Methanol-d4) δ 3.91 (s, 3H), 6.62 (s, 1H), 7.88 (s, 1H), 10.20 (s, 1H); ^{13}C-NMR (101 MHz, Chloroform-d) δ = 55.2, 99.6, 101.7, 119.3, 132.1, 160.5, 162.8, 184.8; HRMS (ESI) calculated mass for $C_8H_6O_3Br$ (MH^-) 228.9500, found 228.9509.

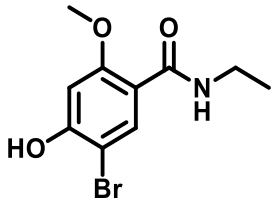
5-Bromo-4-hydroxy-2-methoxybenzoic acid (66)



To a stirred solution of **65** (46 mg, 0.20 mmol) in a mixture of DMSO (2 mL) and water (1 mL) at 0°C was added sodium dihydrogen phosphate(0.10 g, 0.80 mmol) and sodium chlorite (0.05 g, 0.70 mmol). The mixture was allowed to warm to room temperature and the reaction was stirred

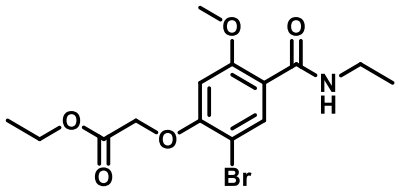
overnight. After this time, the mixture was diluted with water (10 mL) and the pH of the solution was adjusted to 8 by using solid $NaHCO_3$. The solution was washed with EtOAc (15 mL) and the pH of the aqueous layer was adjusted to 4 by the addition of 1 M HCl aqueous solution. The solution was again extracted with EtOAc (3 x 10 mL). The organic extracts were combined and washed with brine (15 mL), dried over anhydrous Na_2SO_4, filtered, and evaporated *in vacuo* to afford **66** (26 mg, 53% yield) which was used without further purification. ^{1}H-NMR (400 MHz, Acetone-d6) δ 3.98 (s, 3H), 6.83 (s, 1H), 8.07 (s, 1H); ^{13}C-NMR (101 MHz, Methanol-d4) δ 55.2, 99.7, 99.9, 111.4, 136.5, 159.4, 160.7, 166.4; HRMS (ESI) calculated mass for $C_8H_6BrO_4$ (MH^-) 244.9449, found 244.9453.

5-Bromo-*N*-ethyl-4-hydroxy-2-methoxybenzamide (67)



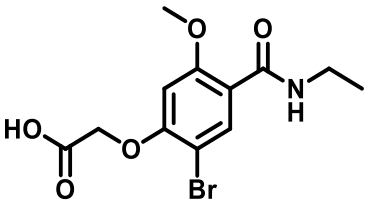
A solution of **66** (16 mg, 64 µmol) in thionyl chloride (3 mL) was heated under a reflux condition (75°C) for 2.5 hours. After this time, the remaining solvent was removed *in vacuo*. The residue was azeotroped with benzene (2 x 1 mL) to insure the complete removal of thionyl chloride. The resulting crude acid chloride was dissolved in anhydrous DCM (3.0 mL) under nitrogen atmosphere. A solution of ethylamine (2 M in THF, 4.87 mL, 9.74 mmol) was then added dropwise to the stirred solution and the reaction was allowed to stir overnight. After this time, the reaction mixture was diluted with DCM (5.0 mL) and washed with 10% w/v aqueous $NaHCO_3$ (3 x 5 mL) and brine (3 x 5 mL). The organic phase was then dried over anhydrous Na_2SO_4, filtered, and concentrated *in vacuo*. The crude material was purified by flash column chromatography using pentane:EtOAc = 1:2.5 as the eluent to afford **67** (5 mg, 26% yield). ^{1}H-NMR (400 MHz, Methanol-d4) δ1.22 (t, J = 7.0 Hz, 3H), 3.38 – 3.47 (m, 2H), 3.95 (s, 3H), 6.64 (s, 1H), 8.05 (s, 1H); ^{13}C-NMR (101 MHz, Methanol-d4) δ 13.6, 34.2, 55.2, 99.4, 100.7, 114.2, 135.2, 158.1, 158.5, 165.7; HRMS (ESI) m/z calculated for $C_{10}H_{13}BrNO_3$ (MH^+) 274.0079, found 274.0084.

Ethyl 2-(2-bromo-4-(ethylcarbamoyl)-5-methoxyphenoxy)acetate (68)



To a solution of **67** (0.31 g, 1.15 mmol) in DMF (10 mL) was added sodium hydride (60% dispersion in mineral oil, 0.12 g, 2.87 mmol). The solution was allowed to stir for 10 minutes followed by a dropwise addition of ethyl chloroacetate (14 µL, 1.26 mmol). The mixture was stirred at room temperature under nitrogen atmosphere overnight. After this time, the mixture was partitioned between water (10 mL) and EtOAc (20 mL). The layers were separated and the organic phase was washed with water (2 x 10 mL) and 5% LiCl aqueous solution (2 x 10 mL), dried over anhydrous $MgSO_4$, filtered, and concentrated *in vacuo* to afford **68** (0.35 g, 85% yield) which was used without further purification. R_f= 0.24 (pentane:EtOAc 1:1, v/v); ^{1}H-NMR (400 MHz, Chloroform-d) δ 1.25 (t, J = 7.0 Hz, 3H), 1.32 (t, J = 7.0 Hz, 3H), 3.49 (qd, J = 7.0, 5.5 Hz, 2H), 3.95 (s, 3H), 4.30 (q, J = 7.0 Hz, 2H), 4.76 (s, 2H), 6.46 (s, 1H), δ 8.43 (s, 1H); ^{13}C-NMR (101 MHz, Chloroform-d) δ =14.2, 14.9, 34.6, 56.3, 61.7, 66.8, 98.2, 104.2, 117.1, 136.9, 157.4, 157.7, 163.5, 168.0; HRMS (ESI) m/z calculated for $C_{14}H_{19}NO_5Br$ (MH^+) 360.0447, found 360.0447.

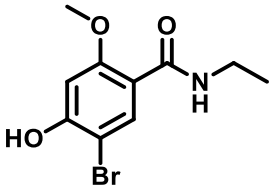
2-(2-Bromo-4-(ethylcarbamoyl)-5-methoxyphenoxy)acetic acid (69)



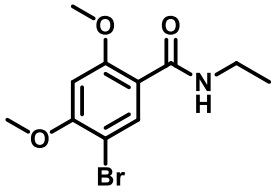
To a solution of **68** (0.35 g, 0.98 mmol) in THF (10 mL) was added 1 M NaOH aqueous solution (1.96 mL, 1.96 mmol). The reaction mixture was allowed to stir at 50°C for 3 hours. After this time, the aqueous layer was separated and the pH the aqueous layer was adjusted to 3 by using 3 M HCl aqueous solution. The solution was then extracted with EtOAc (2 x 15 mL). The organic extracts were combined and washed with brine (15 mL), dried over anhydrous $MgSO_4$, filtered, and evaporated *in vacuo* to afford **69** (0.27 g, 83% yield) which was used without further purification. ^{1}H-NMR (400 MHz, Acetone-d6) δ 1.17 (t, J = 7.0 Hz, 3H), 3.40 (qd, J = 7.0, 5.5 Hz,

2H), 4.03 (s, 3H), 4.97 (s, 2H), 6.86 (s, 1H), 8.26 (s, 1H); HRMS (ESI) calculated mass for $C_{12}H_{15}NO_5Br$ (MH+) 332.0134, found 332.0136.

5-Bromo-*N*-ethyl-4-hydroxy-2-methoxybenzamide (70) and 5-bromo-*N*-ethyl-2,4-dimethoxybenzamide (71)



70



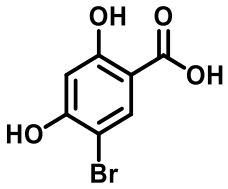
71

A solution of **69** (76 mg, 0.23 mmol) in Eaton's reagent (3 mL, excess) was heated to 80°C for 18 hours. After this time, the reaction mixture was cooled to room temperature. Water was added to the mixture and the mixture was stirred for 10 minutes. The mixture was extracted with EtOAc (3 x 10 mL) and washed with saturated $NaHCO_3$ aqueous solution (3 x 10 mL), water (2 x 10 mL), and brine (10 mL). The organic phase was dried over anhydrous $MgSO_4$, filtered, and evaporated *in vacuo*. The crude material was purified by flash column chromatography using EtOAc:DCM = 0.5:9.5 as the eluent to afford **70** (8 mg, 13% yield) and **71** (20 mg, 30% yield).

70: ^{1}H-NMR (400 MHz, Acetone-d6) δ 1.17 (t, J = 7.0 Hz, 3H) 3.39 (qd, J = 7.0, 5.5 Hz, 2H), 3.96 (s, 3H), 6.78 (s, 1H), 7.97 (s, 1H), 8.22 (s, 1H), 9.36 (s, 1H).

71: ^{1}H-NMR (400 MHz, Acetone-d6) δ 1.19 (t, J = 7.0 Hz, 3H), 3.43 (qd, J = 7.0, 5.5 Hz, 2H), 3.48 (s, 3H), 4.05 (s, 3H), 7.28 (s, 1H), 8.08 (s, 1H), 8.29 (s, 1H).

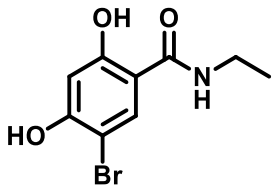
5-Bromo-2,4-dihydroxybenzoic acid (72)



To a stirred solution of 2,4-dihydroxybenzoic acid (1.03 g, 6.71 mmol) in acetic acid (7.20 mL) was added a prepared solution of bromine (0.38 mL, 7.38 mmol) in acetic acid (6.20 mL). The reaction was heated to 30°C and stirred for 2 hours. After this time, the reaction solution was

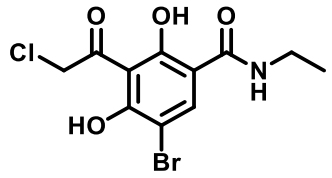
diluted with water and subsequently quenched with saturated $Na_2S_2O_3$ solution. The mixture was then extracted with EtOAc (4 x 25 mL). The organic phase was combined, dried over anhydrous $MgSO_4$, filtered, and the solvent was evaporated *in vacuo*. The crude material which was a yellow solid was recrystallised from a hot solution of acetonitrile:toluene = 1:1 to afford **72** (1.18 g, 76% yield). ^{1}H-NMR (400 MHz, Acetone-d6) δ 6.57 (s, 1H), 8.00 (s, 1H); HRMS (ESI) calculated mass for $C_7H_4O_4Br$ (MH^-) 230.9293, found 230.9302. The spectroscopic data corresponded to previously reported data.[198]

5-Bromo-*N*-ethyl-2,4-dihydroxybenzamide (73)



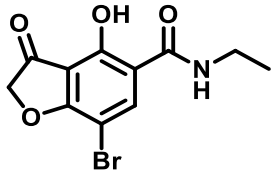
To a solution of **72** (1.88 g, 8.10 mmol) in DMF (30 mL) was added EDC·HCl (2.60 g, 13.5 mmol) and HOBt (1.82 g, 13.5 mmol) under nitrogen atmosphere. Triethylamine (1.90 mL, 13.5 mmol) was then added dropwise followed by ethylamine (2 M in THF, 3.40 mL, 6.80 mmol). The mixture was allowed to stir under nitrogen atmosphere at 50°C overnight. After this time, the mixture was diluted with water (50 mL) and the pH of the solution was adjusted to 4 with 3 M HCl aqueous solution. The solution was then extracted with EtOAc (5 x 30 mL) and washed with 5% LiCl aqueous solution (5 x 20 mL). The organic phase was combined, dried over anhydrous $MgSO_4$, filtered, and concentrated *in vacuo*. The crude material was purified by flash column chromatography using pentane:EtOAc = 4:1 as the eluent to afford **73** (1.2 g, 57% yield). ^{1}H-NMR (400 MHz, Methanol-d4) δ 1.22 (t, J = 7.0 Hz, 4H), 3.39 (q, J = 7.0 Hz, 2H), 6.43 (s, 1H), 7.91 (s, 1H); ^{13}C-NMR (101 MHz, Methanol-d4) δ = 13.5, 33.9, 99.4, 103.3, 108.9, 131.5, 158.4, 161.2, 168.6.

5-Bromo-3-(2-chloroacetyl)-*N*-ethyl-2,4-dihydroxybenzamide (74)



To a stirred solution of $AlCl_3$ (0.36 g, 2.70 mmol) in anhydrous DCM (2 mL) at 0°C under nitrogen atmosphere was added a solution of **73** (0.20 g, 0.77 mmol) in anhydrous DCM (3 mL). Chloroacetyl chloride (61 µL, 0.77 mmol) was then added carefully with the evolution of HCl gas. After stirring for 10 minutes at 0°C, the mixture was heated to reflux (40°C) for 3.5 hours. After this time, the reaction mixture was poured into ice-cold water and extracted with DCM (4 x 20 mL). The organic phase was combined and washed with brine (2 x 20 mL), dried over anhydrous $MgSO_4$, filtered, and concentrated *in vacuo*. The crude material was purified by flash column chromatography using 100% DCM as the eluent to afford **74** (55 mg, 21% yield). R_f= 0.4 (100% DCM); ^{1}H-NMR (400 MHz, Methanol-d4) δ 1.25 (t, J = 7.0 Hz, 4H), 3.44 (q, J = 7.0 Hz, 2H), 4.65 (s, 2H), 8.12 (s, 1H); ^{13}C-NMR (101 MHz, Methanol-d4) δ = 13.1, 34.4, 39.9, 104.4, 107.0, 115.0, 129.3, 149.2, 159.0, 163.9, 167.9; HRMS (ESI) calculated mass for $C_{11}H_{10}NO_4ClBr$ (MH^-) 333.9482, found 333.9498.

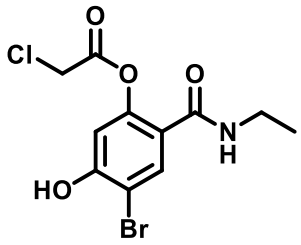
7-Bromo-*N*-ethyl-4-hydroxy-3-oxo-2,3-dihydrobenzofuran-5-carboxamide (75)



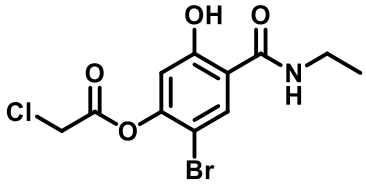
To a solution of **74** (0.27 g, 0.80 mmol) in acetonitrile (5 mL) was added K_2CO_3 (0.33 g, 2.40 mmol) under nitrogen atmosphere. The reaction mixture was heated to reflux (82°C) and the reaction was run under a reflux condition for 2 days. After this time, the mixture was cooled to room temperature. The solid residues were filtered off and washed with acetonitrile. The collected filtrate was concentrated *in vacuo*. The crude material was then purified by PTLC using pentane:EtOAc = 3:1 as the solvent to afford **75** (25 mg, 10% yield). ^{1}H-NMR (400 MHz, Methanol-d4) δ 1.23 (t, J = 7.0 Hz, 3H), 3.97 (qd, J = 7.0, 5.0 Hz, 2H), 4.86 (s, 2H), 8.28 (s, 1H);

^{13}C-NMR (101 MHz, Methanol-d4) δ 12.2, 39.3, 74.0, 102.1, 106.1, 115.4, 135.9, 156.8, 157.9, 163.3, 170.2; HRMS (ESI) calculated mass for $C_{11}H_9NO_4Br$ (MH^-) 297.9715, found 297.9717.

4-Bromo-2-(ethylcarbamoyl)-5-hydroxyphenyl 2-chloroacetate (76a) and 2-bromo-4-(ethylcarbamoyl)-5-hydroxyphenyl 2-chloroacetate (76b)



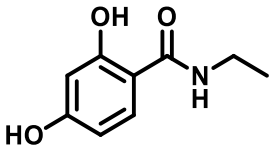
76a



76b

To a stirred solution of $AlCl_3$ (0.20 g, 1.50 mmol) in anhydrous DCM (2 mL) at 0°C under nitrogen atmosphere was added a solution of **73** (0.13 g, 0.50 mmol) in anhydrous DCM (2 mL). Chloroacetyl chloride (40 µL, 0.50 mmol) was then added carefully with the evolution of HCl gas. After stirring for 10 minutes at 0°C, the mixture was heated to reflux (40°C) for 2.5 hours. After this time, the reaction mixture was poured into ice-cold water and extracted with DCM (4 x 15 mL). The organic phase was combined and washed with brine (2 x 15 mL), dried over anhydrous $MgSO_4$, filtered, and concentrated *in vacuo*. The crude material was purified by flash column chromatography using 100% DCM as the eluent to afford **76a** and **76b** (76 mg, 45% yield). ^{1}H-NMR (400 MHz, Methanol-d4) δ 1.25 (t, J = 7.5 Hz, 3H), 3.43 (q, J = 7.5 Hz, 2H), 4.56 (s, 2H), 6.86 (s, 1H), 8.11 (s, 1H); HRMS (ESI) calculated mass for $C_{11}H_{12}NO_4ClBr$ (MH^-) 335.9638, found 335.9643.

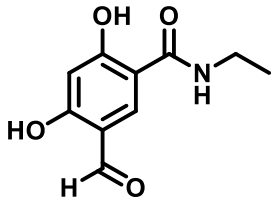
***N*-Ethyl-2,4-dihydroxybenzamide (77)**



To a solution of 2,4-dihydroxybenzoic acid (3.59 g, 23.30 mmol) in anhydrous DMF (40 mL) was added EDC·HCl (7.44 g, 38.80 mmol), HOBt (5.24 g, 38.80 mmol), triethylamine (5.41 mL, 38.80 mmol), and ethylamine (2 M in THF, 9.71 mL, 19.40 mmol). The mixture was allowed to stir

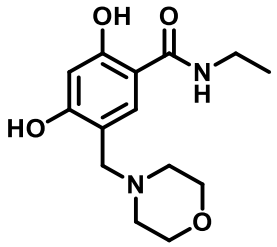
under nitrogen atmosphere at 50°C overnight. After this time, the mixture was diluted with water (50 mL) and the pH of the solution was adjusted to 4 with 3 M HCl aqueous solution. The solution was then extracted with EtOAc (5 x 30 mL) and washed with 5% LiCl aqueous solution (5 x 20 mL). The organic phase was combined, dried over anhydrous $MgSO_4$, filtered, and concentrated *in vacuo*. The crude material was purified by flash column chromatography using pentane:EtOAc = 2:1 as the eluent to afford **77** (3.40 g, 81% yield). ^{1}H-NMR (400 MHz, Methanol-d4) δ 1.23 (t, J = 7.0 Hz, 3H), 3.36 – 3.45 (m, 2H), 6.29 (d, J = 2.5 Hz, 1H), 6.33 (dd, J = 8.5, 2.5 Hz, 1H), 7.59 (d, J = 8.5 Hz, 1H); ^{13}C-NMR (101 MHz, Methanol-d4) δ = 13.6, 33.8, 102.5, 106.9, 107.2, 128.5, 162.2, 162.3, 169.8; HRMS (ESI) calculated mass for $C_9H_{12}NO_3$ (MH^+) 182.0817, found 182.0812.

_N_-Ethyl-5-formyl-2,4-dihydroxybenzamide (78)



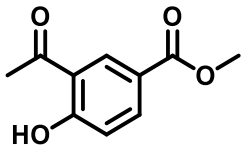
To a solution of **77** (2.22 g, 12.20 mmol) in trifluoroacetic acid (20 mL) was added hexamethylenetetramine (3.43 g, 24.50 mmol). The mixture was heated to reflux at 75°C for 4 hours. After this time, the mixture was cooled to room temperature followed by the addition of 3 M HCl aqueous solution (8.16 mL, 24.50 mmol). After stirring for 1 hour, the mixture was concentrated *in vacuo*. The resulting crude material was then purified by flash column chromatography using the gradient eluent from pentane:EtOAc 2:1 to 100% EtOAc to afford **78** (0.97 g, 38% yield). ^{1}H-NMR (400 MHz, Methanol-d4) δ 1.25 (t, J = 7.0 Hz, 3H), 3.61 (q, J = 7.0 Hz, 2H), 5.61 (s, 1H), 8.24 (s, 1H), 10.27 (s, 1H); ^{13}C-NMR (101 MHz, Methanol-d4) δ 12.3, 39.1, 78.5, 97.8, 109.5, 120.8, 127.8, 134.2, 161.5, 193.1; HRMS (ESI) calculated mass for $C_{10}H_{10}NO_4$ (MH^-) 208.0610, found 208.0620.

***N*-Ethyl-2,4-dihydroxy-5-(morpholinomethyl)benzamide (79)**



To a stirred solution of **78** (0.96 g, 4.59 mmol) in methanol (10 mL) was added morpholine (0.40 mL, 4.59 mmol) under nitrogen atmosphere. The solution was stirred for 10 minutes before adding 2-picoline borane complex (0.64 g, 6.00 mmol). The reaction mixture was allowed to stir overnight at room temperature. After this time, the mixture was concentrated *in vacuo* and purified by flash column chromatography using pentane:EtOAc = 1:5 as the eluent to afford **79** (0.32 g, 25% yield). ^{1}H-NMR (400 MHz, Methanol-d4) δ 1.23 (t, J = 7.0 Hz, 3H) 2.03 (s, 2H), 2.62 (s, 4H), 3.58 (q, J = 7.0 Hz, 2H), 3.76 (t, J = 4.5 Hz, 4H), 3.84 (s, 2H), 4.12 (q, J = 7.0 Hz, 2H), 5.59 (s, 1H), 7.92 (s, 1H); ^{13}C-NMR (101 MHz, Methanol-d4) δ 12.3, 38.9, 52.5, 66.3, 77.8, 107.1, 109.3, 119.7, 126.4, 157.1, 161.4, 162.9.

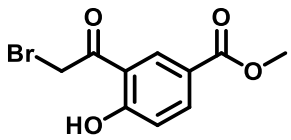
Methyl 3-acetyl-4-hydroxybenzoate (84)



To a degassed solution of **59** (5.60 g, 24.20 mmol) in ethanol (50 mL) was added triethylamine (8.44 mL, 60.60 mmol), 1,1'-bis(diphenylphosphino)ferrocene (0.54 g, 0.97 mmol), 1-(vinyloxy)butane (9.40 mL, 72.70 mmol), and palladium(II) acetate (0.14 g, 0.61 mmol) under nitrogen atmosphere. The mixture was degassed with nitrogen again then heated to 70°C. After an overnight stirring, the reaction was cooled to room temperature followed by a filtration to remove solid residues. The collected filtrate was concentrated *in vacuo*. The resulting residue was then re-dissolved in DCM (40 mL). 3 M HCl (24.00 mL, 72.70 mmol) was added to the solution and the reaction was allowed to stir at room temperature for 2 hours. After this time, the organic phase was separated, dried over anhydrous $MgSO_4$, and filtered. The solution was concentrated *in vacuo* followed by a purification by flash column chromatography using DCM:hexane = 1:1 as the eluent

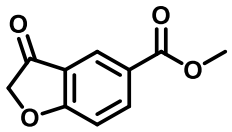
to afford **84** (2.86 g, 61% yield). ^{1}H-NMR (400 MHz, Chloroform-d) δ 2.73 (s, 3H), 3.95 (s, 3H), 7.04 (d, J = 8.5 Hz, 1H), 8.16 (dd, J = 8.5, 2.1 Hz, 1H), 8.51 (d, J = 2.0 Hz, 1H), 12.71 (s, 1H). The spectroscopic data corresponded to previously reported data.[199]

Methyl 3-(2-bromoacetyl)-4-hydroxybenzoate (85)



The suspension of $CuBr_2$ (0.16 g, 0.72 mmol) in EtOAc (0.50 mL) was heated to reflux (72°C) under nitrogen atmosphere. A solution of **84** (0.07 g, 0.36 mmol) in hot chloroform (1 mL) was added to the suspension. The resulting mixture was allowed to reflux (72°C) overnight. After this time, the mixture was cooled to room temperature, filtered to remove solid residues, and washed with DCM. The collected filtrate was concentrated *in vacuo* followed by a purification by flash column chromatography using hexane:diethyl ether = 9:1 as the eluent to afford **85** (38 mg, 39% yield). ^{1}H-NMR (400 MHz, Methanol-d4) δ 3.94 (s, 3H), 4.55 (s, 2H), 7.07 (d, J = 8.5 Hz, 1H), 8.18 (dd, J = 8.5, 2.0 Hz, 1H), 8.50 (d, J = 2.0 Hz, 1H); ^{13}C-NMR (101 MHz, Chloroform-d) δ 29.9, 52.3, 116.5, 119.1, 121.5, 132.8, 138.0, 165.6, 166.5, 197.1; HRMS (ESI) calculated mass for $C_{10}H_8O_4Br$ (MH^-) 270.9606, found 270.9609. The spectroscopic data corresponded to previously reported data.[200]

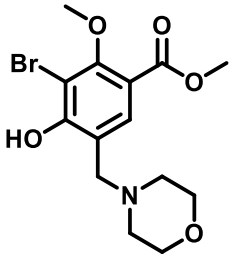
Methyl 3-oxo-2,3-dihydrobenzofuran-5-carboxylate (86)



To a solution of **85** (2.33 g, 8.53 mmol) in acetonitrile was added triethylamine (2.37 mL, 17.10 mmol). The reaction was allowed to stir at room temperature overnight under nitrogen atmosphere. After this time, the reaction was diluted with DCM (30 mL), washed with 1 M HCl aqueous solution (3 x 10 mL) and brine (2 x 10 mL), dried over anhydrous $MgSO_4$, and filtered. The organic phase was concentrated *in vacuo* and the resulting crude material was purified by flash column chromatography using hexane:DCM = 1:1 as the eluent to afford **86** (52 mg, 3% yield). ^{1}H-NMR (400 MHz, Methanol-d4) δ 3.95 (s, 1H), 4.75 (s, 2H), 7.22 (dd, J = 8.5, 1.0 Hz, 1H), 8.34 (dd, J =

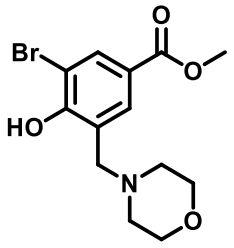
8.5, 2.0 Hz, 1H), 8.41 (dd, J = 2.0, 1.0 Hz, 1H); ^{13}C-NMR (101 MHz, Methanol-d4) δ = 52.4, 75.6, 113.7, 121.3, 124.6, 126.6, 139.1, 165.8, 176.4, 198.5; HRMS (ESI) calculated mass for $C_{10}H_8O_4$ (MH) 192.0423, found 192.0423.

Methyl 3-bromo-4-hydroxy-2-methoxy-5-(morpholinomethyl)benzoate (88)



To a solution of **22** (0.28 g, 0.98 mmol) in DCM (5 mL) was added Br_2 (55 µL, 1.08 mmol) dropwise at 0°C under nitrogen atmosphere. The solution was allowed to warm to room temperature and stirred overnight. Then, the solution of $Na_2S_2O_5$ (0.02 g, 0.10 mmol) in 0.64 mL of water was added to the mixture while keeping the temperature below 15°C. MeOH (0.2 mL) and the mixture was allowed to stir for further 1 hour at room temperature. The organic phase was washed with water (2 x 20 mL) and brine (2 x 20 mL), dried over anhydrous $MgSO_4$, and filtered. The solution was concentrated *in vacuo* followed by a purification by flash column chromatography using hexane:EtOAc = 7:3 as the eluent to afford **88** (26 mg, 8% yield). ^{1}H-NMR (400 MHz, Methanol-d4) δ 2.63 (s, 4H), 3.77 (s, 2H), 3.77 – 3.82 (m, 4H), 3.90 (s, 3H), 3.92 (s, 3H), 7.57 (s, 1H); ^{13}C-NMR (101 MHz, Chloroform-d) δ = 52.1, 52.7, 61.2, 61.9, 66.5, 107.5, 116.1, 116.8, 130.7, 158.9, 159.9, 165.4; HRMS (ESI) calculated mass for $C_{14}H_{19}NO_5Br$ (MH^-) 360.0447, found 360.0449.

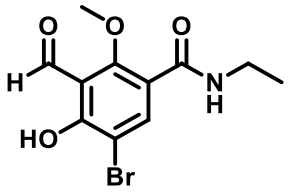
Methyl 3-bromo-4-hydroxy-5-(morpholinomethyl)benzoate (89)



To a solution of **38** (0.76 g, 3.00 mmol) in DCM (10 mL) was added Br_2 (0.17 mL, 3.30 mmol) dropwise at 0°C under nitrogen atmosphere. The solution was allowed to warm to room

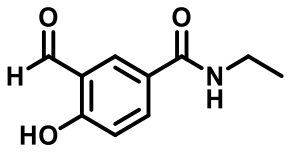
temperature and stirred overnight. Then, the solution of $Na_2S_2O_5$ (0.06 g, 0.30 mmol) in 1.8 mL of water was added to the mixture while keeping the temperature below 15°C. MeOH (0.6 mL) and the mixture was allowed to stir for further 1 hour at room temperature. The organic phase was washed with water (2 x 20 mL) and brine (2 x 20 mL), dried over anhydrous $MgSO_4$, and filtered. The solution was then concentrated *in vacuo* followed by a purification by flash column chromatography using hexane:DCM = 1:1 as the eluent to afford **89** (0.15 g, 15% yield). ^{1}H-NMR (400 MHz, Chloroform-d) δ 2.59 (s, 4H), 3.74 (s, 6H), 3.84 (s, 3H), 7.63 (d, J = 2.0 Hz, 1H), 8.10 (d, J = 2.0 Hz, 1H); ^{13}C-NMR (101 MHz, Chloroform-d) δ 52.1, 52.6, 61.4, 66.5, 110.0, 121.1, 122.0, 129.4, 134.1, 158.9, 165.7; HRMS (ESI) calculated mass for $C_{13}H_{17}NO_4Br$ (MH^+) 330.0341, found 330.0343.

5-Bromo-*N*-ethyl-3-formyl-4-hydroxy-2-methoxybenzamide (91)



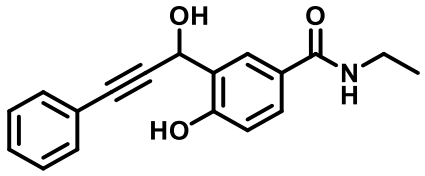
To a solution of **67** (0.76 g, 2.78 mmol) in trifluoroacetic acid (15 mL) was added hexamethylenetetramine (0.78 g, 5.56 mmol). The mixture was heated to reflux at 75°C for 6 hours. After this time, the reaction was cooled to room temperature and allowed to stir overnight. Then, 3 M HCl aqueous solution (1.85 mL, 5.56 mmol) was added and the reaction mixture was stirred for 1 hour. The mixture was then diluted with water (30 mL) and extracted with EtOAc (3 x 20 mL). The organic phase was combined and washed with saturated $NaHCO_3$ aqueous solution until pH of the washing was more than 7. The organic phase was then washed with brine (2 x 20 mL), dried over anhydrous $MgSO_4$, filtered, and concentrated *in vacuo*. The resulting crude material was purified by flash column chromatography using 100% diethyl ether as the eluent to afford **91** (0.12 g, 14% yield). ^{1}H-NMR (400 MHz, Methanol-d4) δ 1.24 (t, J = 7.0 Hz, 3H) , 3.41 – 3.48 (m, 2H), , 4.04 (s, 3H) , 6.67 (s, 1H) , 8.29 (s, 1H), 9.92 (s, 1H); HRMS (ESI) calculated mass for $C_{11}H_{13}NO_4Br$ (MH^+) 302.0028, found 302.0035.

***N*-Ethyl-3-formyl-4-hydroxybenzamide (93)**



To a solution of **55** (0.57 g, 3.45 mmol) in trifluoroacetic acid (10 mL) was added hexamethylenetetramine (0.97 g, 6.90 mmol). The mixture was heated to reflux at 75°C for 3 hours. After this time, the mixture was cooled to room temperature followed by the addition of 3 M HCl aqueous solution (2.30 mL, 6.90 mmol). After stirring for 1 hour, the mixture was diluted with water (30 mL) and extracted with EtOAc (3 x 20 mL). The organic phase was combined and washed with saturated $NaHCO_3$ aqueous solution until pH of the washing was more than 7. The organic phase was then washed with brine (2 x 20 mL), dried over anhydrous $MgSO_4$, filtered, and concentrated *in vacuo*. The resulting crude material was purified by flash column chromatography using pentane:EtOAc = 1:4 as the eluent to afford **93** (0.28 g, 42% yield). ^{1}H-NMR (400 MHz, Methanol-d4) δ 1.25 (t, J = 7.0 Hz, 3H), 3.43 (q, J = 7.0 Hz, 2H), 7.05 (d, J = 8.5 Hz, 1H), 8.03 (dd, J = 8.5, 2.5 Hz, 1H), 8.24 (d, J = 2.5 Hz, 1H), 10.14 (s, 1H); HRMS (ESI) calculated mass for $C_{10}H_{10}NO_4$ (MH^+) 194.0817, found 194.0820.

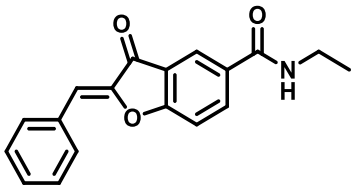
***N*-Ethyl-4-hydroxy-3-(1-hydroxy-3-phenylprop-2-yn-1-yl)benzamide (94)**



A solution of phenylacetylene (0.27 mL, 2.47 mmol) in anhydrous THF (10 mL) under nitrogen atmosphere was cooled to -78°C in a dewar using dry ice and acetone. BuLi (2.5 M in hexane, 1 mL, 2.47 mmol) was carefully and slowly added to the solution and the reaction mixture was allowed to stir at -78°C for 1 hour. Then, a prepared solution of **93** (0.22 g, 1.12 mmol) in anhydrous THF (4.5 mL) was added dropwise to the mixture and the mixture was allowed to stir at -78°C for 1 hour. After this time, the reaction mixture was slowly warmed up to 0°C by removing it from the dewar and placing it in an ice bath and stirred for 2 hours. Then, the reaction was allowed to warm up and stir at room temperature overnight. After this time, the reaction mixture was quenched with saturated NH_4Cl solution. The organic phase was separated and the aqueous

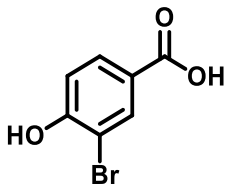
layer was extracted with EtOAc (2 x 20 mL). The organic phase was combined and washed with saturated $NaHCO_3$ aqueous solution (2 x 20 mL) and brine (20 mL), dried over anhydrous $MgSO_4$, filtered, and concentrated *in vacuo*. The resulting crude material was purified by flash column chromatography using the gradient eluent starting from pentane:EtOAc = 2:3 to 1:4 to afford **94** (0.18 g, 55% yield) as a yellow oil. R_f= 0.22 (EtOAc:pentane = 3:2, v/v); ^{1}H-NMR (400 MHz, Methanol-d4) δ 1.23 (t, J = 7.0 Hz, 3H), 3.41 (q, J = 7.0 Hz, 2H), 5.99 (s, 1H), 6.89 (d, J = 8.5 Hz, 1H), 7.32 – 7.37 (m, 3H), 7.45 – 7.50 (m, 2H), 7.68 (dd, J = 8.5, 2.5 Hz, 1H), 8.16 (d, J = 2.5 Hz, 1H); ^{13}C-NMR (101 MHz, Methanol-d4) δ 13.6, 34.4, 58.8, 84.6, 88.8, 114.7, 122.9, 125.5, 127.2, 127.6, 128.0, 128.0, 128.0, 131.2, 157.6, 168.5; HRMS (ESI) calculated mass for $C_{18}H_{16}NO_3$ (MH^-) 294.1130, found 294.1125.

(*Z*)-2-Benzylidene-*N*-ethyl-3-oxo-2,3-dihydrobenzofuran-5-carboxamide (95)



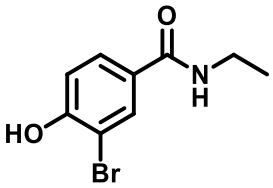
To a solution of **94** (0.17 g, 0.58 mmol) in anhydrous toluene (5 mL) was added K_2CO_3 (0.18 g, 1.27 mmol). The reaction mixture was heated to 50°C and stirred for 10 minutes. $AgNO_3$ (0.22 g, 1.27 mmol) was then added and the reaction mixture was heated to reflux (111°C) for 3 hours. After this time, the mixture was cooled to room temperature. The solid residues were filtered off with celite and washed with toluene. The collected filtrate was concentrated *in vacuo*. The resulting crude material was purified by flash column chromatography using DCM:EtOAc = 4:1 as the eluent. The product obtained from the first purification was subjected to the second purification by PTLC using pentane:EtOAc = 1:1 as the solvent to afford **95** (8 mg, 5% yield) as a yellow solid. R_f= 0.53 (EtOAc:pentane = 3:2, v/v); ^{1}H-NMR (400 MHz, Chloroform-d) δ 1.31 (t, J = 7.5 Hz, 3H) , 3.55 (qd, J = 7.5, 5.5 Hz, 2H), 6.29 (s, 1H), 6.96 (s, 1H), 7.43 (dd, J = 8.5, 0.5 Hz, 1H), 7.44 – 7.52 (m, 3H), 7.91 – 7.97 (m, 2H), 8.15 (dd, J = 2.0, 0.5 Hz, 1H), 8.27 (dd, J = 8.5, 2.0 Hz, 1H); ^{13}C-NMR (101 MHz, Chloroform-d) δ = 14.9, 35.2, 113.4, 114.4, 121.4, 122.5, 129.0, 130.4, 130.5, 131.7, 131.9, 136.9, 147.0, 165.8, 167.5, 184.1; HRMS (ESI) calculated mass for $C_{18}H_{16}NO_3$ (MH^+) 294.1130, found 294.1128.

3-Bromo-4-hydroxybenzoic acid (96)



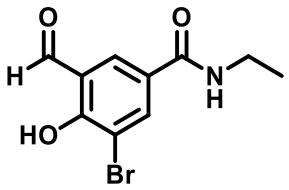
A dropping funnel was charged with a solution of bromine (2.03 mL, 39.60 mmol) in 1,4-dioxane (32 mL) and added dropwise to a stirred solution of 4-hydroxybenzoic acid (4.97 g, 36.00 mmol) in 1,4-dioxane (40 mL) over 15 minutes. The reaction mixture was allowed to stir at room temperature overnight. After this time, the reaction was quenched with saturated $Na_2S_2O_3$ solution. The reaction mixture was then extracted with EtOAc (5 x 25 mL). The organic phase was combined, dried over anhydrous $MgSO_4$, filtered, and concentrated *in vacuo*. The crude material was recrystallised from a solution of ethanol:water = 2:1 to afford **96** (2.94 g, 38% yield) as a white needle. ^{1}H-NMR (400 MHz, Methanol-d4) δ 6.95 (d, J = 8.5 Hz, 1H), 7.85 (dd, J = 8.5, 2.0 Hz, 1H), 8.13 (d, J = 2.0 Hz, 1H); ^{13}C-NMR (101 MHz, Methanol-d4) δ 109.1, 115.2, 123.0, 130.3, 134.7, 158.5, 167.2.

3-Bromo-*N*-ethyl-4-hydroxybenzamide (97)



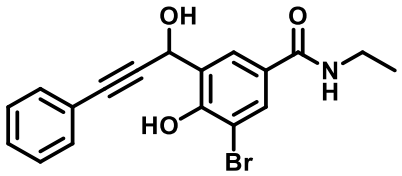
A solution of **96** (2.93 g, 13.50 mmol) in anhydrous DMF (30 mL) was cooled to 0°C in an ice bath. HOBt (2.19 g, 16.20 mmol), triethylamine (2.26 mL, 16.20 mmol), ethylamine (2 M in THF, 6.76 mL, 13.50 mmol), and EDC·HCl (3.11 g, 16.20 mmol) were added under nitrogen atmosphere, respectively. The mixture was heated to 50°C and stirred overnight. After this time, the mixture was diluted with water (50 mL) and extracted with EtOAc (5 x 30 mL). The organic phase was combined and washed with 5% LiCl aqueous solution (5 x 20 mL), dried over anhydrous $MgSO_4$, filtered, and concentrated *in vacuo* to afford **97** (2.10 g, 64% yield). ^{1}H-NMR (400 MHz, Methanol-d4) δ 1.23 (t, J = 7.0 Hz, 3H), 3.40 (q, J = 7.0 Hz, 2H), 6.95 (d, J = 8.5 Hz, 1H), 7.69 (dd, J = 8.5, 2.0 Hz, 1H), 8.01 (d, J = 2.0 Hz, 1H); HRMS (ESI) calculated mass for $C_9H_9NO_2Br$ (MH^-) 241.9817, found 241.9818.

3-Bromo-*N*-ethyl-5-formyl-4-hydroxybenzamide (98)



To a solution of **97** (0.84 g, 3.43 mmol) in trifluoroacetic acid (15 mL) was added hexamethylenetetramine (0.96 g, 6.87 mmol). The mixture was heated to reflux at 75°C for 64 hours. After this time, the mixture was cooled to room temperature followed by the addition of 3 M HCl aqueous solution (2.30 mL, 6.87 mmol). After stirring for 1 hour, the mixture was diluted with water (30 mL) and extracted with EtOAc (3 x 20 mL). The organic phase was combined and washed with saturated $NaHCO_3$ aqueous solution until pH of the washing was more than 7. The organic phase was then washed with brine (2 x 20 mL), dried over anhydrous $MgSO_4$, filtered, and concentrated *in vacuo*. The resulting crude material was purified by flash column chromatography using pentane:EtOAc = 2:3 as the eluent to afford **98** (0.59 g, 64% yield). ^{1}H-NMR (400 MHz, Methanol-d4) δ 1.25 (t, J = 3.5 Hz, 3H), 3.43 (dt, J = 14.5, 7.0 Hz, 2H), 8.26 (d, J = 2.0 Hz, 1H), 8.34 (d, J = 2.0 Hz, 1H), 10.02 (s, 1H); HRMS (ESI) calculated mass for $C_{10}H_9NO_3Br$ (MH^-) 269.9766, found 269.9771.

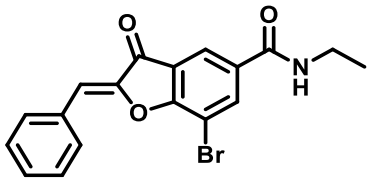
3-Bromo-*N*-ethyl-4-hydroxy-5-(1-hydroxy-3-phenylprop-2-yn-1-yl)benzamide (99)



A solution of phenylacetylene (0.69 mL, 6.24 mmol) in anhydrous THF (25 mL) under nitrogen atmosphere was cooled to -78°C in a dewar using dry ice and acetone. BuLi (2.5 M in hexane, 2.50 mL, 6.24 mmol) was carefully and slowly added to the solution and the reaction mixture was allowed to stir at -78°C for 1 hour. Then, a prepared solution of **98** (0.77 g, 2.84 mmol) in anhydrous THF (11 mL) was added dropwise to the mixture and the mixture was allowed to stir at -78°C for further 1 hour. After this time, the reaction mixture was slowly warm up to 0°C by removing it from the dewar and placing it in an ice bath and stirred for 2 hours. Then, the reaction was allowed to warm up and stir at room temperature overnight. After this time, the reaction

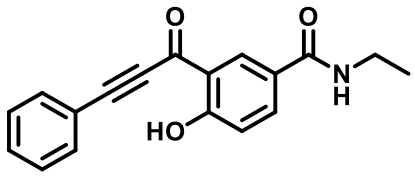
mixture was quenched with saturated NH_4Cl solution. The organic phase was separated and the aqueous layer was extracted with EtOAc (2 x 30 mL). The organic phase was combined and washed with saturated $NaHCO_3$ aqueous solution (2 x 20 mL) and brine (20 mL), dried over anhydrous $MgSO_4$, filtered, and concentrated *in vacuo*. The resulting crude material was purified by flash column chromatography using the gradient eluent starting from pentane:EtOAc = 2:3 to 1:4 to afford **99** (0.55 g, 52% yield) as an orange oil. R_f= 0.44 (EtOAc:pentane = 3:2, v/v); ^{1}H-NMR (400 MHz, Methanol-d4) δ 1.22 (t, J = 7.0 Hz, 3H), 3.36 – 3.45 (m, 2H), 6.01 (s, 1H), 7.31 – 7.37 (m, 3H), 7.47 (dd, J = 7.0, 3.0 Hz, 2H), 8.00 (d, J = 2.0 Hz, 1H), 8.11 (d, J = 2.0 Hz, 1H), 8.48 (t, J = 5.5 Hz, 1H); ^{13}C-NMR (101 MHz, Methanol-d4) δ = 13.6, 34.5, 60.1, 85.2, 88.0, 110.1, 122.6, 126.1, 127.1, 128.1, 128.2, 129.3, 131.3, 131.3, 154.2, 167.0; HRMS (ESI) calculated mass for $C_{18}H_{15}NO_3Br$ (MH^-) 372.0235, found 372.0230.

(*Z*)-2-Benzylidene-7-bromo-*N*-ethyl-3-oxo-2,3-dihydrobenzofuran-5-carboxamide (100)



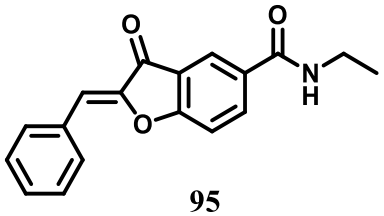
To a solution of **99** (0.11 g, 0.29 mmol) in anhydrous toluene (5 mL) was added K_2CO_3 (88 mg, 0.64 mmol). The reaction mixture was heated to 50°C and stirred for 10 minutes. $AgNO_3$ (0.11 g, 0.64 mmol) was added and the reaction mixture was heated to reflux (111°C) for 2 hours. After this time, the mixture was cooled to room temperature and filtered off through celite with a toluene wash to remove solid residues. The collected filtrate was concentrated *in vacuo*. The resulting crude material was purified by flash column chromatography using pentane:EtOAc = 4:1 as the eluent. The product obtained from the first purification was subjected to the second purification by flash column chromatography using pentane:EtOAc = 7:3 as the eluent to afford **100** (8 mg, 7% yield) as a white solid. ^{1}H-NMR (400 MHz, Chloroform-d) δ 1.31 (t, J = 7.0 Hz, 3H), 3.55 (qd, J = 7.0, 5.5 Hz, 2H), 6.20 (s, 1H), 7.03 (s, 1H), 7.46 – 7.56 (m, 3H), 7.97 – 8.02 (m, 2H), 8.07 (d, J = 1.5 Hz, 1H), 8.43 (d, J = 1.5 Hz, 1H); ^{13}C-NMR (101 MHz, Chloroform-d) δ 13.8, 35.3, 106.8, 115.8, 121.1, 122.8, 129.2, 130.8, 131.5, 131.7, 132.1, 139.2, 146.8, 164.5, 164.6, 183.3; HRMS (ESI) calculated mass for $C_{20}H_{18}N_2O_3Br$ (MH^+CH_3CN) 413.0501, found 413.0511.

***N*-Ethyl-4-hydroxy-3-(3-phenylpropioloyl)benzamide (101)**

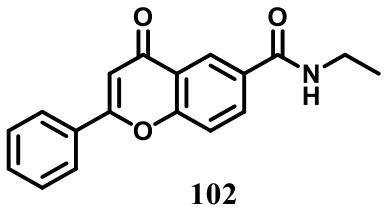


A solution of phenylacetylene (0.66 mL, 6.05 mmol) in anhydrous THF (24 mL) under nitrogen atmosphere was cooled to -78°C in a dewar using dry ice and acetone. BuLi (1.6 M in hexane, 3.78 mL, 6.05 mmol) was carefully and slowly added to the solution and the reaction mixture was allowed to stir at -78°C for 1 hour. Then, a prepared solution of **93** (0.53 g, 2.75 mmol) in anhydrous THF (2.75 mL) was added dropwise to the mixture and the mixture was allowed to stir at -78°C for further 1 hour. After this time, the reaction mixture was slowly warm up to 0°C by removing it from the dewar and placing it in an ice bath and stirred for 30 minutes. After this time, the reaction mixture was quenched with saturated NH_4Cl solution. The organic phase was separated and the aqueous layer was extracted with EtOAc (2 x 30 mL). The organic phase was combined and washed with saturated $NaHCO_3$ aqueous solution (2 x 20 mL) and brine (20 mL), dried over anhydrous $MgSO_4$, filtered, and concentrated *in vacuo*. The resulting crude material was dissolved in acetone (15 mL). MnO_2 was then added to the solution and the reaction was allowed to stir at room temperature for 24 hours. After this time, MnO_2 was filtered off with celite and washed with acetone. The filtrate was evaporated *in vacuo*. The resulting crude material was purified by flash column chromatography using DCM:EtOAc = 4:1 as the eluent to afford **101** (18 mg, 2% yield). ^{1}H-NMR (400 MHz, Methanol-d4) δ 1.27 (t, J = 7.0 Hz, 3H), 3.46 (q, J = 7.0 Hz, 2H), 7.09 (d, J = 8.5 Hz, 1H), 7.51 – 7.66 (m, 3H), 7.80 – 7.88 (m, 2H), 8.05 (dd, J = 8.5, 2.0 Hz, 1H), 8.76 (d, J = 2.0 Hz, 1H); HRMS (ESI) calculated mass for $C_{18}H_{16}NO_3$ (MH^+) 294.1130, found 294.1127.

(*Z*)-2-Benzylidene-*N*-ethyl-3-oxo-2,3-dihydrobenzofuran-5-carboxamide (95) and *N*-ethyl-4-oxo-2-phenyl-4*H*-chromene-6-carboxamide (102)



95



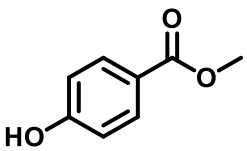
102

A solution of **101** (18 mg, 0.06 mmol) in anhydrous DMF (0.25 mL) under nitrogen atmosphere was cooled to 0°C in an ice bath followed by the addition of PPh_3 (2 mg, 6 µmol). The reaction solution was then warmed up to 30°C and stirred for 20 hours. After this time, the mixture was diluted with water and extracted with EtOAc (3 x 10 mL). The organic phase was combined and washed with 5% LiCl aqueous solution (2 x 10 mL) and brine (10 mL), dried over anhydrous $MgSO_4$, filtered, and concentrated *in vacuo*. The crude material was purified by flash column chromatography using DCM:EtOAc = 9:1 as the eluent to afford **95** (3 mg, 16% yield) and **102** (8 mg, 44% yield).

195: R_f= 0.29 (DCM:EtOAc = 4:1, v/v); ^{1}H-NMR (400 MHz, Methylene Chloride-d2) δ 1.25 (t, J = 7.0 Hz, 3H), 3.47 (qd, J = 7.0, 5.5 Hz, 2H), 6.23 (s, 1H), 6.92 (d, J = 0.5 Hz, 1H), 7.41 – 7.52 (m, 4H), 7.94 – 7.98 (m, 2H), 8.12 (dd, J = 2.0, 0.5 Hz, 1H), 8.19 (dd, J = 8.5, 2.0 Hz, 1H). HRMS (ESI) calculated mass for $C_{18}H_{16}NO_3$ (MH^+) 294.1130, found 294.1125.

102: R_f= 0.12 (DCM:EtOAc = 4:1, v/v); ^{1}H-NMR (400 MHz, DMSO-d6) δ 1.14 (t, *J* = 7.0 Hz, 3H), 3.28 – 3.32 (m, 2H), 7.11 (s, 1H), 7.50 – 7.65 (m, 3H), 7.88 (dd, *J* = 8.5, 0.5 Hz, 1H), 8.11 – 8.16 (m, 2H), 8.27 (dd, *J* = 8.5, 2.0 Hz, 1H), 8.57 (dd, *J* = 2.0, 0.5 Hz, 1H), 8.81 (t, *J* = 5.5 Hz, 1H). HRMS (ESI) calculated mass for $C_{18}H_{16}NO_3$ (MH^+) 294.1130, found 294.1127.

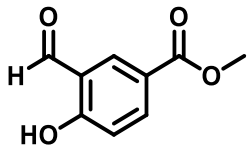
Methyl 4-hydroxybenzoate (**103**)



To a solution of 4-hydroxybenzoic acid (1.99 g, 14.40 mmol) in methanol (40 mL) was added 98% (w/v) sulfuric acid (2 mL). The reaction mixture was allowed to reflux at 65°C for 3 hours. After

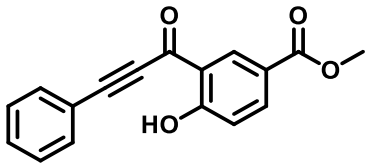
this time, the mixture was concentrated by evaporation of the solvent *in vacuo*. The crude solid was subsequently extracted with EtOAc (3 x 50 mL). The organic extracts were combined and washed with saturated $NaHCO_3$ aqueous solution (2 x 20 mL), dried over anhydrous $MgSO_4$, filtered, and evaporated *in vacuo*. This afforded **103** (2.09 g, 96% yield) which was used without further purification. ^{1}H-NMR (400 MHz, Chloroform-d) δ 3.92 (s, 3H), 6.59 (s, 1H), 6.88 – 6.93 (m, 2H), 7.94 – 7.99 (m, 2H). The spectroscopic data corresponded to previously reported data.[201]

Methyl 3-formyl-4-hydroxybenzoate (104)[194]



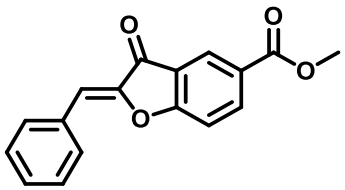
To a solution of methyl 4-hydroxybenzoate (**103**) (2.10 g, 13.70 mmol) in trifluoroacetic acid (20 mL) was added hexamethylenetetramine (3.85 g, 27.50 mmol). The mixture was heated to reflux at 75°C for 3 hours. After this time, the reaction mixture was cooled to room temperature and 3 M HCl aqueous solution (9.16 mL, 27.50 mmol) was then added. After stirring for 1 hour, the mixture was diluted with water (30 mL) and extracted with EtOAc (3 x 40 mL). The organic phase was combined and washed with saturated $NaHCO_3$ aqueous solution until pH of the washing was more than 7. The organic phase was washed with brine (2 x 30 mL), dried over anhydrous $MgSO_4$, filtered, and concentrated *in vacuo*. The resulting crude material was purified by flash column chromatography using pentane:DCM = 3:7 as the eluent to afford **104** (0.85 g, 34% yield). ^{1}H-NMR (400 MHz, Methanol-d4) δ 3.93 (s, 3H), 7.06 (d, J = 8.5 Hz, 1H), 8.17 (dd, J = 8.5, 2.0 Hz, 1H), 8.43 (d, J = 2.0 Hz, 1H), 10.15 (s, 1H); ^{13}C-NMR (101 MHz, Methanol-d4) δ = 51.2, 117.1, 121.1, 121.8, 134.0, 136.9, 164.6, 165.9, 194.6; HRMS (ESI) calculated mass for $C_9H_7O_4$ (MH^-) 179.0344, found 179.0350.

Methyl 4-hydroxy-3-(3-phenylpropioloyl)benzoate (105)

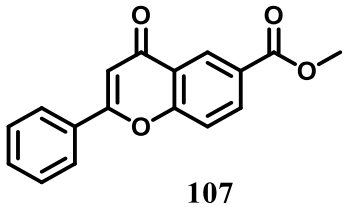


A solution of phenylacetylene (0.23 mL, 2.08 mmol) in anhydrous THF (8 mL) under nitrogen atmosphere was cooled to -78°C in a dewar using dry ice and acetone. BuLi (1.6 M in hexane, 1.30 mL, 2.08 mmol) was carefully and slowly added to the solution and the reaction mixture was allowed to stir at -78°C for 1hour. Then, a prepared solution of **104** (0.34 g, 1.89 mmol) in anhydrous THF (2 mL) was added dropwise and the reaction mixture was allowed to stir at -78°C for 2 hours. After this time, the reaction mixture was slowly warm up to 0°C by removing it from the dewar and placing it in an ice bath and stirred for 1 hours. Then, the reaction was allowed to warm up and stir at room temperature overnight. The mixture was then heated to reflux (66°C) for an additional 3 hours. After this time, the mixture was cooled to 0°C and quenched with saturated NH_4Cl solution. The organic phase was separated and the aqueous layer was extracted with EtOAc (2 x 20 mL). The organic phase was combined and washed with saturate $NaHCO_3$ aqueous solution (20 mL) and brine (20 mL), dried over anhydrous $MgSO_4$, filtered, and concentrated *in vacuo*. The obtained crude material was dissolved in anhydrous DCM (15 mL) under nitrogen atmosphere. DMP (0.96 g, 2.27 mmol) was added to the solution and the reaction was stirred at room temperature overnight before heating to reflux (40°C) for 3 hours. After cooling down to room temperature, the mixture was diluted with DCM (20 mL) and washed with water (20 mL), 1:1 solution of 10% $Na_2S_2O_3$:saturated $NaHCO_3$ (20 mL), and brine (20 mL). The organic phase was combined, dried over anhydrous $MgSO_4$, filtered, and concentrated *in vacuo*. The crude material was purified by flash column chromatography using pentane:diethyl ether = 7:3 as the eluent. The product obtained from the first purification was subjected to the second purification by flash column chromatography using pentane:DCM = 1:1 as the eluent to afford **105** (42 mg, 8% yield) as a yellow solid. ^{1}H-NMR (400 MHz, Chloroform-d) δ 3.98 (s, 3H), 7.07 (d, J = 8.5 Hz, 1H), 7.47 – 7.52 (m, 2H), 7.54 – 7.60 (m, 1H), 7.75 – 7.81 (m, 2H), 8.21 (ddd, J = 8.5, 2.0, 0.5 Hz, 1H), 8.91 (d, J = 2.0 Hz, 1H), 12.17 (s, 1H); HRMS (ESI) calculated mass for $C_{17}H_{11}O_4$ (MH^-) 279.0657, found 279.0663.

Methyl (*Z*)-2-benzylidene-3-oxo-2,3-dihydrobenzofuran-5-carboxylate (106) and Methyl 4-oxo-2-phenyl-4*H*-chromene-6-carboxylate (107)



106



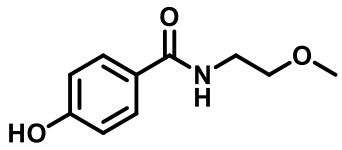
107

A solution of **105** (41 mg, 0.15 mmol) in anhydrous DMF (1 mL) under nitrogen atmosphere was cooled to 0°C in an ice bath followed by the addition of PPh_3 (4 mg, 0.02 mmol). The reaction solution was then warmed up to 30°C and stirred for 20 hours. After this time, the mixture was diluted with water and extracted with EtOAc (3 x 10 mL). The organic phase was combined and washed with 5% LiCl aqueous solution (2 x 10 mL) and brine (10 mL), dried over anhydrous $MgSO_4$, filtered, and concentrated *in vacuo*. The crude material was purified by flash column chromatography using pentane:EtOAc = 9:1 as the eluent to afford **106** (17 mg, 42% yield) and **107** (18 mg, 45% yield).

106: R_f= 0.66 (EtOAc:pentane = 3:7, v/v); ^{1}H-NMR (400 MHz, Chloroform-d) δ 3.97 (s, 3H), 6.98 (s, 1H), 7.43 (d, J = 8.5 Hz, 1H), 7.45 – 7.53 (m, 3H), 7.92 – 7.98 (m, 2H), 8.40 (dd, J = 8.5, 2.0 Hz, 1H), 8.55 (d, J = 1.5 Hz, 1H); ^{13}C-NMR (101 MHz, Chloroform-d) δ = 52.5, 113.0, 114.4, 121.8, 126.0, 126.9, 129.0, 130.4, 131.7, 131.8, 138.2, 147.0, 165.8, 168.4, 183.8; HRMS (ESI) calculated mass for $C_{17}H_{13}O_4$ (MH^+) 281.0814, found 281.0790.

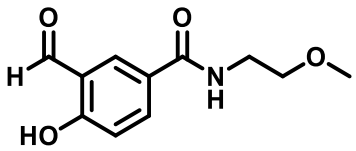
107: R_f= 0.41 (EtOAc:pentane = 3:7, v/v); ^{1}H-NMR (400 MHz, Chloroform-d) δ 3.98 (s, 3H), 6.86 (s, 1H), 7.52 – 7.61 (m, 3H), 7.64 (dt, J = 8.5, 1.5 Hz, 1H), 7.94 (ddd, J = 8.0, 2.5, 1.5 Hz, 2H), 8.37 (dq, J = 8.5, 1.5 Hz, 1H), 8.92 (s, 1H); ^{13}C-NMR (101 MHz, Chloroform-d) δ = 52.5, 107.9, 118.6, 123.6, 126.3, 127.3, 128.2, 129.2, 131.3, 132.0, 134.5, 158.7, 163.7, 165.8, 177.7; HRMS (ESI) calculated mass for $C_{17}H_{13}O_4$ (MH^+) 281.0814, found 281.0820.

4-Hydroxy-*N*-(2-methoxyethyl)benzamide (108)



A solution of 4-hydroxybenzoic acid (1.00 g, 7.23 mmol) in anhydrous DMF (20 mL) was cooled to 0°C in an ice bath. HOBt (1.46 g, 10.80 mmol), triethylamine (1.51 mL, 10.80 mmol), 2-methoxyethan-1-amine (0.65 mL, 7.23 mmol), and EDC·HCl (2.08 g, 10.80 mmol) were added under nitrogen atmosphere, respectively. The mixture was heated to 50°C and stirred overnight. After this time, the mixture was diluted with water (50 mL) and extracted with EtOAc (4 x 30 mL). The organic phase was combined and washed with 5% LiCl aqueous solution (3 x 20 mL), dried over anhydrous $MgSO_4$, filtered, and concentrated *in vacuo* to afford **108** (0.52 g, 37% yield) as a light brown solid which was used without further purification. R_f= 0.28 (EtOAc:pentane = 4:1, v/v); ^{1}H-NMR (400 MHz, Methanol-d4) δ 3.39 (s, 3H), 3.52 – 3.60 (m, 4H), 6.79 – 6.87 (m, 2H), 7.68 – 7.76 (m, 2H); ^{13}C-NMR (101 MHz, Methanol-d4) δ = 39.2, 57.5, 70.7, 114.6, 125.0, 128.8, 160.6, 168.8; HRMS (ESI) calculated mass for $C_{10}H_{14}NO_3$ (MH^+) 196.0974, found 196.0970.

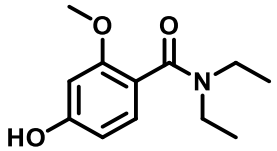
3-Formyl-4-hydroxy-*N*-(2-methoxyethyl)benzamide (109)



To a solution of **108** (0.52 g, 2.65 mmol) in trifluoroacetic acid (10 mL) was added hexamethylenetetramine (0.74 g, 5.30 mmol). The mixture was heated to reflux at 75°C for 3 hours. After this time, the reaction was cooled to room temperature followed by the addition of 3 M HCl aqueous solution (1.76 mL, 5.30 mmol). After stirring for 1 hour, the mixture was diluted with water (30 mL) and extracted with EtOAc (3 x 20 mL). The organic phase was combined and washed with saturated $NaHCO_3$ aqueous solution until pH of the washing was more than 7. The organic phase was washed with brine (2 x 20 mL), dried over anhydrous $MgSO_4$, filtered, and concentrated *in vacuo*. The resulting crude material was purified by flash column chromatography using DCM:EtOAc = 1:1 as the eluent to afford **109** (0.26 g, 44% yield) as a white solid. R_f= 0.24 (DCM:EtOAc = 1:1, v/v); ^{1}H-NMR (400 MHz, Methanol-d4) δ 3.40 (s, 3H), 3.58 (d, J = 1.0 Hz,

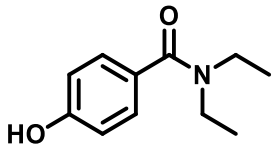
4H), 7.04 (d, J = 8.5 Hz, 1H), 8.03 (dd, J = 8.5, 2.5 Hz, 1H), 8.25 (d, J = 2.5 Hz, 1H), 10.14 (s, 1H); ^{13}C-NMR (101 MHz, Methanol-d4) δ 39.4, 57.5, 70.6, 117.0, 120.9, 125.9, 131.5, 135.0, 163.5, 167.3, 194.7; HRMS (ESI) calculated mass for $C_{11}H_{14}NO_4$ (MH^+) 224.0923, found 224.0925.

***N*,*N*-Diethyl-4-hydroxy-2-methoxybenzamide (111)**



A solution of **14** (0.84 g, 4.97 mmol) in anhydrous DMF (20 mL) was cooled to 0°C in an ice bath. HOBt (1.00 g, 7.45 mmol), triethylamine (1.04 mL, 7.45 mmol), diethylamine (0.52 mL, 4.97 mmol), and EDC·HCl (1.43 g, 7.45 mmol) were added under nitrogen atmosphere, respectively. The mixture was heated to 50°C and stirred overnight. After this time, the mixture was diluted with water (50 mL) and extracted with EtOAc (4 x 30 mL). The organic phase was combined and washed with 5% LiCl aqueous solution (3 x 20 mL), dried over anhydrous $MgSO_4$, filtered, and concentrated *in vacuo*. The resulting crude material was purified by flash column chromatography using pentane:EtOAc = 1:4 as the eluent to afford **111** (0.52 g, 47% yield) as an orange oil. R_f= 0.34 (EtOAc:pentane = 4:1, v/v); ^{1}H-NMR (400 MHz, Methanol-d4) δ 1.07 (t, J = 7.0 Hz, 3H), 1.24 (t, J = 7.0 Hz, 3H), 3.23 (q, J = 7.0 Hz, 2H), 3.43 – 3.68 (m, 2H), 3.80 (s, 3H), 6.44 (dd, J = 8.0, 2.0 Hz, 1H), 6.49 (d, J = 2.0 Hz, 1H), 6.99 (d, J = 8.0 Hz, 1H); ^{13}C-NMR (101 MHz, Methanol-d4) δ 11.7, 12.8, 39.2, 43.2, 54.5, 98.6, 106.9, 117.0, 127.9, 156.7, 159.8, 168.4; HRMS (ESI) calculated mass for $C_{12}H_{18}NO_3$ (MH^+) 224.1287, found 224.1284.

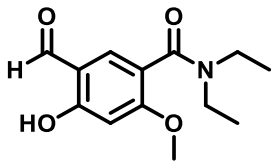
***N*,*N*-Diethyl-4-hydroxybenzamide (112)**[202]



A solution of 4-hydroxybenzoic acid (2.41 g, 17.50 mmol) in anhydrous DMF (30 mL) was cooled to 0°C in an ice bath. HOBt (3.54 g, 26.20 mmol), triethylamine (3.65 mL, 26.20 mmol), diethylamine (1.81 mL, 17.50 mmol), and EDC·HCl (5.02 g, 26.20 mmol) were added under nitrogen atmosphere, respectively. The mixture was heated to 50°C and stirred overnight. After

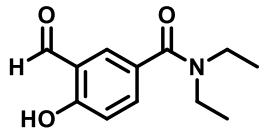
this time, the mixture was diluted with water (100 mL) and extracted with EtOAc (4 x 50 mL). The organic phase was combined and washed with 5% LiCl aqueous solution (4 x 30 mL), dried over anhydrous $MgSO_4$, filtered, and concentrated *in vacuo*. The resulting crude material was purified by flash column chromatography using DCM:EtOAc = 7:3 as the eluent to afford **112** (0.62 g, 18% yield) as a white solid. R_f= 0.22 (EtOAc:DCM = 3:7, v/v); ^{1}H-NMR (400 MHz, Methanol-d4) δ 1.21 (s, 6H), 3.36 (d, J = 20.5 Hz, 4H), 6.78 – 6.92 (m, 2H), 7.22 – 7.34 (m, 2H); ^{13}C-NMR (101 MHz, Methanol-d4) δ 11.7, 13.0, 39.6, 43.6, 114.8, 127.3, 127.8, 158.8, 172.6; HRMS (ESI) calculated mass for $C_{11}H_{16}NO_2$ (MH^+) 194.1181, found 194.1185.

***N*,*N*-Diethyl-5-formyl-4-hydroxy-2-methoxybenzamide (113)**



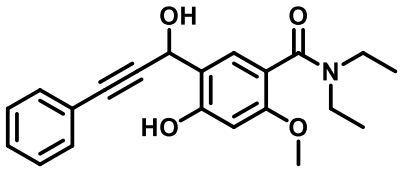
To a solution of **111** (0.52 g, 2.30 mmol) in trifluoroacetic acid (10 mL) was added hexamethylenetetramine (0.65 g, 4.60 mmol). The mixture was heated to reflux at 75°C for 3 hours. After this time, the reaction was cooled to room temperature followed by the addition of 3 M HCl aqueous solution (1.50 mL, 4.60 mmol). After stirring for 1 hour, the mixture was diluted with water (30 mL) and extracted with EtOAc (3 x 20 mL). The organic phase was combined and washed with saturated $NaHCO_3$ aqueous solution until pH of the washing was more than 7. The organic phase was then washed with brine (2 x 20 mL), dried over anhydrous $MgSO_4$, filtered, and concentrated *in vacuo*. The resulting crude material was purified by flash column chromatography using pentane:EtOAc = 1:4 as the eluent to afford **113** (0.22 g, 38% yield) as a yellow oil. R_f= 0.44 (EtOAc:pentane = 4:1, v/v); ^{1}H-NMR (400 MHz, Methanol-d4) δ 1.10 (t, J = 7.0 Hz, 3H), 1.26 (t, J = 7.0 Hz, 4H), 3.24 (d, J = 7.0 Hz, 2H), 3.57 (s, 2H), 3.92 (s, 3H), 6.63 (s, 1H), 7.56 (s, 1H), 9.87 (s, 1H); ^{13}C-NMR (101 MHz, Methanol-d4) δ 11.6, 12.8, 39.3, 43.3, 55.4, 98.9, 114.9, 119.2, 131.9, 162.4, 164.6, 168.4, 193.8; HRMS (ESI) calculated mass for $C_{13}H_{18}NO_4$ (MH^+) 252.1236, found 252.1235.

***N*,*N*-Diethyl-3-formyl-4-hydroxybenzamide (114)**



To a solution of **112** (0.62 g, 3.20 mmol) in trifluoroacetic acid (15 mL) was added hexamethylenetetramine (0.90 g, 6.40 mmol). The mixture was heated to reflux at 75°C for 3 hours. After this time, the reaction was cooled to room temperature followed by the addition of 3 M HCl aqueous solution (2.10 mL, 6.40 mmol). After stirring for 1 hour, the mixture was diluted with water (30 mL) and extracted with EtOAc (3 x 20 mL). The organic phase was combined and washed with saturated $NaHCO_3$ aqueous solution until pH of the washing was more than 7. The organic phase was then washed with brine (2 x 20 mL), dried over anhydrous $MgSO_4$, filtered, and concentrated *in vacuo*. The resulting crude material was purified by flash column chromatography using DCM:EtOAc = 3:2 as the eluent to afford **114** (0.27 g, 38% yield) as a light yellow oil. R_f= 0.53 (EtOAc:pentane = 4:1, v/v); ^{1}H-NMR (400 MHz, Methanol-d4) δ 1.22 (s, 6H), 3.47 (d, J = 68.0 Hz, 4H), 7.06 (d, J = 8.5 Hz, 1H), 7.60 (dd, J = 8.5, 2.0 Hz, 1H), 7.79 (d, J = 2.0 Hz, 1H), 10.13 (s, 1H); HRMS (ESI) calculated mass for $C_{12}H_{16}NO_3$ (MH^+) 222.1130, found 222.1124.

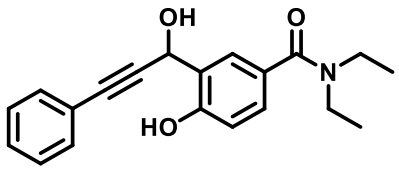
***N*,*N*-Diethyl-4-hydroxy-5-(1-hydroxy-3-phenylprop-2-yn-1-yl)-2-methoxybenzamide (115)**



A solution of phenylacetylene (0.17 mL, 1.58 mmol) in anhydrous THF (6.30 mL) under nitrogen atmosphere was cooled to -78°C in a dewar using dry ice and acetone. BuLi (2.5 M in hexane, 0.63 mL, 1.58 mmol) was carefully and slowly added to the solution and the reaction mixture was allowed to stir at -78°C for 1hour. Then, a prepared solution of **113** (0.18 g, 0.72 mmol) in anhydrous THF (3 mL) was added dropwise and the mixture was allowed to stir at -78°C for 2 hours. After this time, the reaction mixture was slowly warmed up to 0°C by removing it from the dewar and placing it in an ice bath and stirred for 1 hour. Then, the reaction mixture was allowed to warm up and stir at room temperature overnight. After this time, the mixture was cooled to 0°C and quenched with saturated NH_4Cl solution. The organic phase was separated and the aqueous

layer was extracted with EtOAc (2 x 20 mL). The organic phase was combined and washed with saturated $NaHCO_3$ aqueous solution (20 mL) and brine (20 mL), dried over anhydrous $MgSO_4$, filtered, and concentrated *in vacuo*. The crude material was purified by flash column chromatography using pentane:EtOAc = 3:7 as the eluent to afford **115** (92 mg, 36% yield) as an orange oil. R_f= 0.22 (EtOAc:pentane = 4:1, v/v); ^{1}H-NMR (400 MHz, Methanol-d4) δ 1.08 (t, J = 7.0 Hz, 3H), 1.24 (t, J = 7.0 Hz, 3H), 3.25 (q, J = 7.5 Hz, 2H), 3.54 (s, 2H), 3.81 (q, J = 2.5, 2.0 Hz, 3H), 5.93 (s, 1H), 6.54 (s, 1H), 7.30 – 7.47 (m, 6H); ^{13}C-NMR (101 MHz, Methanol-d4) δ 11.7, 12.9, 39.2, 43.3, 54.7, 58.2, 84.5, 89.1, 98.4, 117.0, 120.0, 122.9, 126.9, 128.1, 131.2, 131.3, 156.4, 156.6, 170.2; HRMS (ESI) calculated mass for $C_{21}H_{24}NO_4$ (MH^+) 354.1705, found 354.1694.

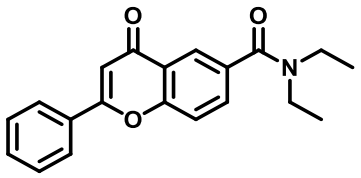
***N*,*N*-Diethyl-4-hydroxy-3-(1-hydroxy-3-phenylprop-2-yn-1-yl)benzamide (116)**



A solution of phenylacetylene (0.74 mL, 6.74 mmol) in anhydrous THF (26 mL) under nitrogen atmosphere was cooled to -78°C in a dewar using dry ice and acetone. BuLi (2.5 M in hexane, 2.70 mL, 6.74 mmol) was carefully and slowly added to the solution and the reaction mixture was allowed to stir at -78°C for 1hour. Then, a prepared solution of **114** (0.68 g, 3.06 mmol) in anhydrous THF (3 mL) was added dropwise and the mixture was allowed to stir at -78°C for 2 hours. After this time, the reaction mixture was slowly warmed up to 0°C by removing it from the dewar and placing it in an ice bath and stirred for 1 hour. Then, the reaction mixture was allowed to warm up and stir at room temperature overnight. After this time, the mixture was cooled to 0°C and quenched with saturated NH_4Cl solution. The organic phase was separated and the aqueous layer was extracted with EtOAc (2 x 30 mL). The organic phase was combined and washed with saturated $NaHCO_3$ aqueous solution (30 mL) and brine (30 mL), dried over anhydrous $MgSO_4$, filtered, and concentrated *in vacuo*. The crude material was purified by flash column chromatography using pentane:EtOAc = 1:1 as the eluent to afford **116** (0.50 g, 50% yield) as a yellow oil. R_f= 0.16 (EtOAc:pentane = 1:1, v/v); ^{1}H-NMR (400 MHz, Methanol-d4) δ 1.21 (s, 6H), 3.45 (d, J = 46.0 Hz, 4H), 6.00 (s, 1H), 6.91 (d, J = 8.5 Hz, 1H), 7.26 (dd, J = 8.5, 2.5 Hz,

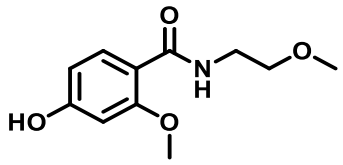
1H), 7.32 – 7.40 (m, 3H), 7.42 – 7.50 (m, 2H), 7.70 (d, *J* = 2.5 Hz, 1H); HRMS (ESI) calculated mass for $C_{20}H_{22}NO_3$ (MH^+) 324.1600, found 324.1611.

_N_,_N_-Diethyl-4-oxo-2-phenyl-4_H_-chromene-6-carboxamide (120)



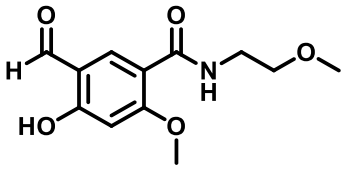
An oven-dried flask was charged with anhydrous DCM (3.91 mL) and cooled down to -78°C in a dewar using dry ice and acetone. Oxalyl chloride (0.17 mL, 2.04 mmol) was added to the reaction flask followed by DMSO (0.19 mL, 2.72 mmol). The reaction was stirred at -78°C for 15 minutes. After this time, a solution of **116** (0.22 g, 0.68 mmol) in anhydrous DCM (1.46 mL) was added slowly and the reaction was stirred at -78°C for 1 hour. Then, triethylamine (0.57 mL, 4.08 mmol) was added and the reaction was allowed to warm up to room temperature over 30 minutes. After this time, the reaction mixture was poured into cold 1 M HCl aqueous solution (20 mL) and extracted with EtOAc (3 x 20 mL). The organic phase was combined, dried over anhydrous $MgSO_4$, filtered, and concentrated *in vacuo*. The resulting crude material was purified by flash column chromatography using the gradient eluent starting from DCM:EtOAc = 9:1 to 100% EtOAc. The product obtained from the first purification was subjected to the second purification by PTLC using pentane:EtOAc = 6:4 as the solvent to afford **120** (12 mg, 6% yield) as a pale yellow solid. R_f= 0.12 (EtOAc:pentane = 1:1, v/v); ^{1}H-NMR (500 MHz, Methanol-d4) δ 1.14 – 1.22 (m, 3H), 1.26 – 1.33 (m, 3H), 3.34 (d, *J* = 7.5 Hz, 2H), 3.60 (d, *J* = 7.5 Hz, 2H), 6.97 (s, 1H), 7.56 – 7.62 (m, 3H), 7.83 – 7.85 (m, 2H), 8.05 – 8.05 (m, 2H), 8.14 (dd, *J* = 1.5, 1.0 Hz, 1H); ^{13}C-NMR (101 MHz, Methanol-d4) δ 13.0, 14.4, 41.1, 45.1, 108.0, 120.4, 124.2, 124.4, 127.7, 130.3, 132.5, 133.3, 133.7, 135.4, 158.0, 166.1, 171.8, 179.8; HRMS (ESI) calculated mass for $C_{20}H_{20}NO_3$ (MH^+) 322.1443, found 322.1443.

4-Hydroxy-2-methoxy-*N*-(2-methoxyethyl)benzamide (122)



A solution of **14** (0.76 g, 4.54 mmol) in anhydrous DMF (15 mL) was cooled to 0°C in an ice bath. HOBt (0.74 g, 5.45 mmol), triethylamine (0.76 mL, 5.45 mmol), 2-methoxyethan-1-amine (0.40 mL, 4.54 mmol), and EDC·HCl (1.04 g, 5.45 mmol) were added under nitrogen atmosphere, respectively. The mixture was heated to 50°C and stirred overnight. After this time, the mixture was diluted with water (100 mL) and extracted with EtOAc (4 x 30 mL). The organic phase was combined and washed with 5% LiCl aqueous solution (3 x 30 mL), dried over anhydrous $MgSO_4$, filtered, and concentrated *in vacuo* to afford **122** (0.57 g, 56% yield) as a brown oil which was used without further purification. R_f= 0.25 (EtOAc:pentane = 4:1, v/v); ^{1}H-NMR (400 MHz, Methanol-d4) δ 3.42 (s, 3H), 3.54 – 3.62 (m, 4H), 3.95 (s, 3H), 6.49 (dd, J = 8.5, 2.0 Hz, 1H), 6.54 (d, J = 2.0 Hz, 1H), 7.87 (d, J = 8.5 Hz, 1H); ^{13}C-NMR (101 MHz, Methanol-d4) δ 38.9, 55.0, 57.6, 70.7, 98.6, 107.6, 112.1, 132.7, 159.7, 162.3, 166.6; HRMS (ESI) calculated mass for $C_{11}H_{16}NO_4$ (MH^+) 226.1079, found 226.1087.

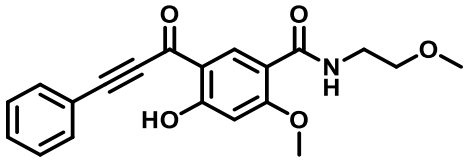
5-Formyl-4-hydroxy-2-methoxy-*N*-(2-methoxyethyl)benzamide (123)



To a solution of **122** (0.57 g, 2.53 mmol) in trifluoroacetic acid (10 mL) was added hexamethylenetetramine (0.71 g, 5.06 mmol). The mixture was heated to reflux at 75°C for 3 hours. After this time, the reaction mixture was cooled to room temperature followed by the addition of 3 M HCl aqueous solution (1.70 mL, 5.06 mmol). After stirring for 1 hour, the mixture was diluted with water (30 mL) and extracted with EtOAc (3 x 20 mL). The organic phase was combined and washed with saturated $NaHCO_3$ aqueous solution until pH of the washing was more than 7. The organic phase was then washed with brine (2 x 20 mL), dried over anhydrous $MgSO_4$, filtered, and concentrated *in vacuo*. The resulting crude material was purified by flash column

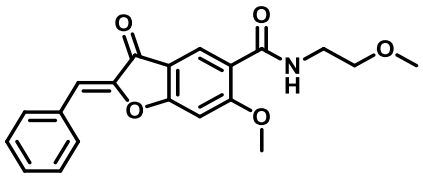
chromatography using 100% EtOAc as the eluent to afford **123** (0.21 g, 33% yield) as a pale yellow solid. R_f= 0.28 (100% EtOAc); ^{1}H-NMR (400 MHz, Methanol-d4) δ 3.42 (s, 3H), 3.54 – 3.66 (m, 4H), 4.05 (s, 3H), 6.68 (s, 1H), 8.35 (s, 1H), 9.93 (s, 1H); ^{13}C-NMR (101 MHz, Methanol-d4) δ 40.5, 57.3, 59.0, 72.0, 100.8, 116.1, 116.8, 138.6, 165.7, 166.6, 167.3, 195.6; HRMS (ESI) calculated mass for $C_{12}H_{16}NO_5$ (MH^+) 254.1028, found 254.1031.

4-Hydroxy-2-methoxy-*N*-(2-methoxyethyl)-5-(3-phenylpropioloyl)benzamide (124)



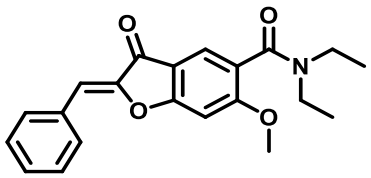
A solution of phenylacetylene (0.20 mL, 1.82 mmol) in anhydrous THF (7.30 mL) under nitrogen atmosphere was cooled to -78°C in a dewar using dry ice and acetone. BuLi (2.5 M in hexane, 0.73 mL, 1.82 mmol) was carefully and slowly added to the solution and the reaction mixture was allowed to stir at -78°C for 1 hour. Then, a prepared solution of **123** (0.21 g, 0.83 mmol) in anhydrous THF (3.30 mL) was added dropwise and the mixture was allowed to stir at -78°C for further 1 hour. After this time the reaction mixture was slowly warmed up to 0°C by removing it from the dewar and placing it in an ice bath and stirred for 2 hours. Then, the reaction mixture was allowed to warm up and stir at room temperature overnight. After this time, the reaction was heated to 50°C for 3 hours followed by a reflux (66°C) for further 3 hours. After this time, the reaction mixture was cooled to 0°C and quenched with saturated NH_4Cl solution. The organic phase was separated and the aqueous layer was extracted with EtOAc (2 x 20 mL). The organic phase was combined and washed with saturated $NaHCO_3$ aqueous solution (2 x 20 mL) and brine (20 mL), dried over anhydrous $MgSO_4$, filtered, and concentrated *in vacuo*. The resulting crude material was purified by flash column chromatography using DCM:EtOAc = 3:2 as the eluent to afford **124** (14 mg, 5% yield) as a pale yellow oil. ^{1}H-NMR (400 MHz, Chloroform-d) δ 3.44 (s, 3H) 3.57 – 3.64 (m, 2H), 3.66 – 3.73 (m, 2H), 4.05 (s, 3H), 6.53 (s, 1H), 7.42 – 7.47 (m, 2H), 7.49 – 7.54 (m, 1H), 7.75 – 7.81 (m, 2H), 9.11 (s, 1H), 12.40 (s, 1H); ^{13}C-NMR (101 MHz, Chloroform-d) δ 39.5, 56.7, 58.9, 71.2, 58.5, 97.1, 99.8, 114.6, 115.5, 119.6, 128.7, 131.2, 133.5, 139.1, 163.8, 164.1, 166.9, 181.0; HRMS (ESI) calculated mass for $C_{20}H_{20}NO_5$ (MH^+) 354.1336, found 354.1346.

(*Z*)-2-Benzylidene-6-methoxy-*N*-(2-methoxyethyl)-3-oxo-2,3-dihydrobenzofuran-5-carboxamide (125)



A solution of **124** (12 mg, 33 μmol) in anhydrous DMF (1 mL) under nitrogen atmosphere was cooled to 0°C in an ice bath. PPh_3 (2 mg, 6 μmol) was then added. The reaction mixture was warmed up to 50°C and stirred for 44 hours. After this time, the mixture was diluted with water (10 mL) and extracted with EtOAc (3 x 10 mL). The organic phase was combined and washed with 5% LiCl aqueous solution (2 x 10 mL) and brine (10 mL), dried over anhydrous $MgSO_4$, filtered, and concentrated *in vacuo*. The crude material was purified by PTLC using DCM:EtOAc = 1:4 as the solvent to afford **125** (8 mg, 67% yield) as pale yellow solid. R_f= 0.19 (EtOAc:DCM = 4:1, v/v); ^{1}H-NMR (400 MHz, Chloroform-d) δ 3.44 (s, 3H), 3.60 (dd, J = 5.5, 4.3 Hz, 2H), 3.67 – 3.73 (m, 2H), 4.12 (s, 3H), 6.89 (s, 1H), 6.90 (s, 1H), 7.41 – 7.51 (m, 3H), 7.86 (d, J = 5.5 Hz, 1H), 7.89 – 7.93 (m, 2H), 8.70 (s, 1H); ^{13}C-NMR (101 MHz, Chloroform-d) δ 39.7, 56.9, 58.8, 71.2, 95.4, 112.8, 115.1, 119.2, 124.8, 128.9, 129.9, 131.4, 132.1, 147.5, 163.9, 164.7, 169.1, 182.5; HRMS (ESI) calculated mass for $C_{20}H_{20}NO_5$ (MH^+) 354.1341, found 354.1350.

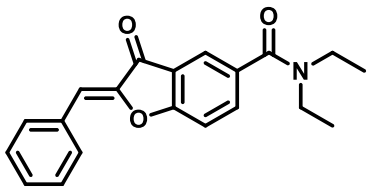
(*Z*)-2-Benzylidene-*N*,*N*-diethyl-6-methoxy-3-oxo-2,3-dihydrobenzofuran-5-carboxamide (126)



To a solution of **115** (0.32 g, 0.90 mmol) in anhydrous toluene (4 mL) was added K_2CO_3 (0.28 g, 1.99 mmol). The reaction mixture was heated to 50°C and stirred for 10 minutes. $AgNO_3$ (0.34 g, 1.99 mmol) was then added and the reaction mixture was heated to reflux (111°C) for 2 hours. After this time, the mixture was cooled to room temperature and filtered off through celite with a toluene wash to remove solid residues. The collected filtrate was concentrated *in vacuo*. The resulting crude material was purified by flash column chromatography using the gradient eluent

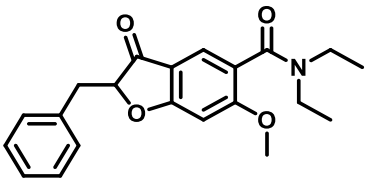
starting from pentane:EtOAc = 1:1 to 100% EtOAc to afford **126** (45 mg, 14% yield) as an orange solid. R_f= 0.59 (EtOAc:pentane = 4:1, v/v); ^{1}H-NMR (400 MHz, Chloroform-d) δ 1.07 (t, J = 7.0 Hz, 3H), 1.27 (t, J = 7.0 Hz, 3H), 3.12 – 3.23 (m, 2H), 3.59 (q, J = 7.0 Hz, 2H), 3.98 (s, 3H), 6.86 (s, 1H), 6.87 (s, 1H), 7.39 – 7.50 (m, 3H), 7.65 (s, 1H), 7.89 – 7.94 (m, 2H); ^{13}C-NMR (101 MHz, Chloroform-d) δ 12.8, 14.1, 39.1, 43.0, 56.5, 95.4, 112.6, 114.4, 123.5, 124.1, 128.9, 129.8, 131.4, 132.2, 147.6, 163.4, 166.9, 168.4, 182.6; HRMS (ESI) calculated mass for $C_{21}H_{22}NO_4$ (MH^+) 352.1549, found 352.1546.

(*Z*)-2-Benzylidene-*N*,*N*-diethyl-3-oxo-2,3-dihydrobenzofuran-5-carboxamide (127)



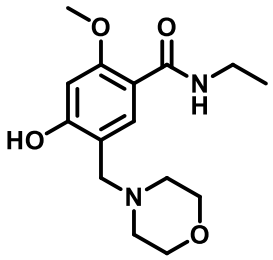
To a solution of **116** (0.12 g, 0.37 mmol) in anhydrous toluene (5 mL) was added K_2CO_3 (0.11 g, 0.81 mmol). The reaction mixture was heated to 50°C and stirred for 10 minutes. $AgNO_3$ (0.14 g, 0.81 mmol) was then added and the reaction mixture was heated to reflux (111°C) for 2 hours. After this time, the mixture was cooled to room temperature and filtered off with celite with a toluene wash to remove solid residues. The collected filtrate was concentrated *in vacuo*. The resulting crude material was purified by flash column chromatography using the gradient eluent starting from DCM:EtOAc = 4:1 to 7:3. The product obtained from the first purification was subjected to the second purification by PTLC using 100% DCM as the solvent. The obtained product was further purified by PTLC using DCM:MeOH = 9.98:0.02 as the solvent to afford **127** (8 mg, 7% yield) as a yellow solid. R_f= 0.34 (DCM:EtOAc = 4:1, v/v); ^{1}H-NMR (400 MHz, Chloroform-d) δ 1.23 (s, 6H), 3.46 (d, J = 82.0 Hz, 4H), 6.96 (s, 1H), 7.41 (dd, J = 8.5, 0.5 Hz, 1H), 7.43 – 7.53 (m, 3H), 7.77 (dd, J = 8.5, 2.0 Hz, 1H), 7.85 (dd, J = 2.0, 0.5 Hz, 1H), 7.91 – 7.99 (m, 2H); ^{13}C-NMR (101 MHz, Chloroform-d) δ 13.0, 14.2, 39.6, 43.6, 113.4, 114.0, 121.4, 122.6, 129.0, 130.2, 131.7, 132.0, 132.7, 135.8, 147.0, 166.2, 169.6, 184.1; HRMS (ESI) calculated mass for $C_{20}H_{20}NO_3$ (MH^+) 322.1443, found 322.1435.

2-Benzyl-*N*,*N*-diethyl-6-methoxy-3-oxo-2,3-dihydrobenzofuran-5-carboxamide (128)



An oven-dried flask containing **126** (26 mg, 73 μmol) in methanol (5 mL) was degassed with nitrogen for 10 minutes. $Pd(OH)_2$ on carbon (20% wt. loading, 10 mg, 14 μmol) was added to the solution. The reaction mixture was saturated with H_2 gas in a balloon and the mixture was stirred at room temperature under H_2 atmosphere overnight. The solid residues were filtered off with celite and washed with DCM. The filtrate was collected and concentrated *in vacuo*. The resulting crude material was purified by flash column chromatography using the gradient eluent starting from EtOAc:DCM = 1:19 to 1:4 to afford **128** (12 mg, 46% yield) as a colourless oil. R_f= 0.06 (EtOAc:DCM = 1:9, v/v); ^{1}H-NMR (400 MHz, Chloroform-d) δ 1.04 (t, J = 7.0 Hz, 3H), 1.24 (t, J = 7.0 Hz, 3H), 2.99 (dd, J = 14.5, 8.5 Hz, 1H), 3.15 (d, J = 18.0 Hz, 2H), 3.32 – 3.42 (m, 1H), 3.56 (dd, J = 7.5, 2.5 Hz, 2H), 3.89 (s, 3H), 4.83 (dd, J = 8.5, 3.5 Hz, 1H), 6.56 (s, 1H), 7.25 (q, J = 3.5 Hz, 1H), 7.29 – 7.34 (m, 4H), 7.46 (s, 1H); ^{13}C-NMR (101 MHz, Chloroform-d) δ 12.8, 14.0, 37.5, 39.1, 42.9, 56.3, 87.0, 95.2, 113.6, 123.0, 126.9, 127.0, 128.5, 129.3, 136.0, 164.4, 167.0, 174.9, 198.2; HRMS (ESI) calculated mass for $C_{21}H_{24}NO_4$ (MH^+) 354.1705, found 354.1707.

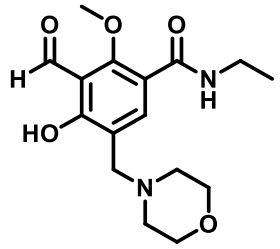
***N*-Ethyl-4-hydroxy-2-methoxy-5-(morpholinomethyl)benzamide (129)**



To a stirred solution of **113** (0.24 g, 1.09 mmol) in methanol (10 mL) was added morpholine (95 μL, 1.09 mmol) followed by 2-picoline borane complex (0.15 g, 1.43 mmol) under argon atmosphere. The reaction mixture was allowed to stir at room temperature overnight. After this time, the reaction mixture was concentrated *in vacuo* and purified by flash column chromatography using the gradient eluent of pentane:EtOAc = 1:1 to 1:4 to afford **129** (0.30 g, 94% yield) as a

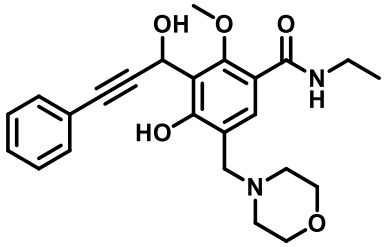
brown solid. R_f= 0.16 (EtOAc:pentane = 4:1, v/v); ^{1}H-NMR (400 MHz, Chloroform-d) δ 1.23 (t, J = 7.5 Hz, 3H) 2.58 (s, 4H), 3.47 (qd, J = 7.5, 5.5 Hz, 2H), 3.69 – 3.81 (m, 6H), 3.93 (s, 3H), 6.43 (s, 1H), 7.74 (t, J = 6.5 Hz, 1H), 7.90 (s, 1H); ^{13}C-NMR (101 MHz, Chloroform-d) δ 15.0, 34.5, 52.8, 56.0, 61.0, 66.8, 99.5, 112.9, 113.4, 132.8, 158.7, 161.7, 165.1; HRMS (ESI) calculated mass for $C_{15}H_{23}N_2O_4$ (MH^+) 295.1658, found 295.1653.

***N*-Ethyl-3-formyl-4-hydroxy-2-methoxy-5-(morpholinomethyl)benzamide (130)**



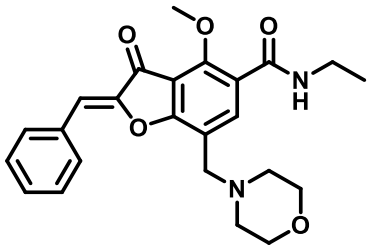
To a solution of **129** (0.30 g, 1.02 mmol) in trifluoroacetic acid (10 mL) was added hexamethylenetetramine (0.29 g, 2.04 mmol). The mixture was heated to reflux at 75°C for 48 hours. After this time, the reaction misture was cooled to room temperature followed by the addition of 3 M HCl aqueous solution (0.68 mL, 2.04 mmol). After stirring for 1 hour, the mixture was diluted with water (30 mL) and extracted with EtOAc (3 x 20 mL). The organic phase was combined and washed with saturated $NaHCO_3$ aqueous solution until pH of the washing was more than 7. The organic phase was then washed with brine (20 mL), dried over anhydrous $MgSO_4$, filtered, and concentrated *in vacuo*. The resulting crude material was purified by flash column chromatography using the gradient eluent from 100% EtOAc to acetone:EtOAc = 1:1 to afford **130** (84 mg, 25% yield) as a yellow oil. R_f= 0.03 (100% EtOAc); ^{1}H-NMR (400 MHz, Methanol-d4) δ 1.27 (t, J = 7.0 Hz, 3H), 2.57 (t, J = 4.5 Hz, 4H), 3.46 (q, J = 7.0 Hz, 2H), 3.63 (s, 2H), 3.72 (t, J = 4.5 Hz, 4H), 3.97 (s, 3H), 7.94 (s, 1H), 10.34 (s, 1H); ^{13}C-NMR (101 MHz, Methanol-d4) δ 13.1, 13.5, 53.0, 55.0, 63.5, 66.2, 113.8, 118.2, 120.6, 139.5, 161.4, 163.5, 166.1, 194.3; HRMS (ESI) calculated mass for $C_{16}H_{23}N_2O_5$ (MH^+) 323.1607, found 323.1601.

***N*-Ethyl-4-hydroxy-3-(1-hydroxy-3-phenylprop-2-yn-1-yl)-2-methoxy-5-(morpholinomethyl)benzamide (131)**



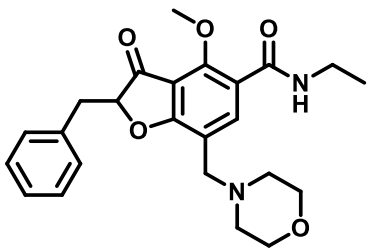
A solution of phenylacetylene (63 µL, 0.57 mmol) in anhydrous THF (2.30 mL) under nitrogen atmosphere was cooled to -78°C in a dewar using dry ice and acetone. BuLi (2.5 M in hexane, 0.23 mL, 0.57 mmol) was carefully and slowly added to the solution and the reaction mixture was allowed to stir at -78°C for 1 hour. Then, a prepared solution of **130** (84 mg, 0.26 mmol) in anhydrous THF (1.10 mL) was added dropwise and the mixture was allowed to stir at -78°C for further 1 hour. After this time, the reaction mixture was slowly warmed up to 0°C by removing it from the dewar and placing it in an ice bath and stirred for 2 hours. Then, the reaction mixture was allowed to warm up and stir at room temperature overnight. After this time, the reaction was heated to 50°C for 3 hours followed by a reflux (66°C) for further 3 hours. After this time, the reaction mixture was cooled to 0°C and quenched with saturated NH_4Cl solution. The organic phase was separated and the aqueous layer was extracted with EtOAc (2 x 20 mL). The organic phase was combined and washed with saturated $NaHCO_3$ aqueous solution (2 x 20 mL) and brine (20 mL), dried over anhydrous $MgSO_4$, filtered, and concentrated *in vacuo*. The resulting crude material was purified by flash column chromatography using 100% EtOAc as the eluent to afford **131** (30 mg, 28% yield) as a yellow oil. R_f= 0.25 (100% EtOAc); ^{1}H-NMR (400 MHz, Methanol-d4) δ 1.25 (t, J = 7.0 Hz, 3H), 2.62 (d, J = 4.5 Hz, 4H), 3.44 (q, J = 7.0 Hz, 2H), 3.76 (t, J = 4.5 Hz, 4H), 3.90 (s, 3H), 3.80 (s, 2H), 7.31 – 7.35 (m, 3H), 6.10 (s, 1H), 7.38 – 7.43 (m, 2H), 7.50 (s, 1H); ^{13}C-NMR (101 MHz, Methanol-d4) δ 13.5, 34.2, 52.4, 56.1, 59.9, 62.3, 66.3, 83.3, 89.3, 117.9, 118.3, 121.1, 123.0, 128.0, 128.0, 130.6, 131.1, 156.6, 159.4, 166.9; HRMS (ESI) calculated mass for $C_{24}H_{29}N_2O_5$ (MH^+) 425.2071, found 425.2078.

(*Z*)-2-Benzylidene-*N*-ethyl-4-methoxy-7-(morpholinomethyl)-3-oxo-2,3-dihydrobenzofuran-5-carboxamide (132)



To a solution of **131** (0.60 g, 1.42 mmol) in anhydrous toluene (4 mL) was added K_2CO_3 (0.43 g, 3.14 mmol). The reaction mixture was heated to 50°C and stirred for 10 minutes. $AgNO_3$ (0.53 g, 3.14 mmol) was then added and the reaction mixture was heated to reflux (111°C) for 20 hours. After this time, the mixture was cooled to room temperature and filtered off with celite and washed with EtOAc (2 x 15 mL) to remove solid residues. The collected filtrate was concentrated *in vacuo*. The resulting crude material was purified by flash column chromatography using 100% EtOAc as the eluent. The product obtained from the first purification was subjected to the second purification by alumina column chromatography using the gradient eluent starting from DCM:EtOAc = 3:2 to 100% EtOAc to afford **132** (87 mg, 14% yield) as a yellow solid. R_f= 0.09 (100% EtOAc); ^{1}H-NMR (400 MHz, Chloroform-d) δ 1.26 (t, J = 7.0 Hz, 3H), 2.54 – 2.61 (m, 4H), 3.51 (qd, J = 7.0, 5.5 Hz, 2H), 3.70 – 3.76 (m, 6H), 4.28 (s, 3H), 6.89 (s, 1H), 7.40 – 7.50 (m, 3H), 7.83 (t, J = 5.5 Hz, 1H), 7.88 – 7.94 (m, 2H), 8.52 (s, 1H); ^{13}C-NMR (101 MHz, Chloroform-d) δ 14.9, 34.7, 53.5, 55.6, 63.4, 67.0, 113.4, 113.7, 117.8, 120.0, 129.0, 130.2, 131.5, 132.1, 142.2, 146.9, 156.0, 164.0, 167.1, 181.5; HRMS (ESI) calculated mass for $C_{24}H_{27}N_2O_5$ (MH^+) 423.1920, found 423.1923.

2-Benzyl-*N*-ethyl-4-methoxy-7-(morpholinomethyl)-3-oxo-2,3-dihydrobenzofuran-5-carboxamide (12)

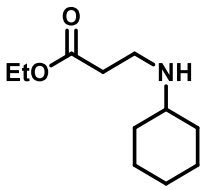


An oven-dried flask containing **132** (12 mg, 28 µmol) in methanol (5 mL) was degassed with nitrogen for 10 minutes. $Pd(OH)_2$ on carbon (20% wt. loading, 1 mg, 6 µmol) was added to the

solution. The reaction mixture was saturated with H_2 gas in a balloon and the mixture was stirred at room temperature under H_2 atmosphere overnight. The solid residues were filtered off with celite and washed with DCM. The filtrate was collected and concentrated *in vacuo*. The resulting crude material was purified by flash column chromatography using DCM:MeOH = 9.5:0.5 as the eluent. The product obtained from the first purification was subjected to the second purification by PTLC using chloroform:MeOH = 9.7:0.3 as the solvent to afford **12** (7 mg, 61% yield) as an off-white oily compound. R_f= 0.31 (chloroform:MeOH = 9.5:0.5, v/v); ^{1}H-NMR (400 MHz, Chloroform-d) δ 1.24 (t, J = 7.0 Hz, 3H), 2.48 (q, J = 4.0 Hz, 4H), 3.17 (dd, J = 14.5, 6.0 Hz, 1H), 3.40 (dd, J = 14.5, 4.0 Hz, 1H), 3.44 – 3.52 (m, 2H), 3.55 (d, J = 7.5 Hz, 2H), 3.73 (t, J = 4.5 Hz, 4H), 4.08 (s, 3H), 4.91 (dd, J = 6.5, 4.0 Hz, 1H), 7.16 – 7.28 (m, 6H), 7.73 (t, J = 5.0 Hz, 1H), 8.40 (s, 1H); ^{13}C-NMR (101 MHz, Chloroform-d) δ 14.8, 34.6, 37.4, 53.4, 55.0, 63.0, 66.9, 86.3, 113.0, 118.2, 118.2, 127.2, 128.3, 129.6, 134.8, 143.0, 155.4, 164.0, 174.2, 197.7; HRMS (ESI) calculated mass for $C_{24}H_{29}N_2O_5$ (MH^+) 425.2076, found 425.2084.

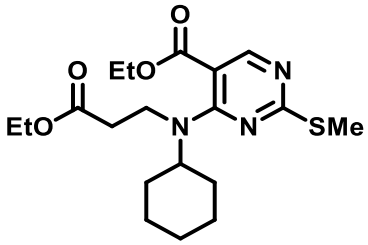
6.3 Synthetic procedures: Chapter 2

Ethyl 3-(cyclohexylamino)propanoate (153)[203]



To a solution of ethyl 3-chloropropanoate (1.18 mL, 8.70 mmol) and cyclohexylamine (1.00 mL, 8.70 mmol) in DMF (5 mL) was added K_2CO_3 (1.20 g, 8.70 mmol) and tetrabutylammonium iodide (TBAI) (5 mg, cat.). The reaction mixture was heated to 80°C and allowed to stir overnight. After this time, the mixture was diluted with water and extracted with DCM (3 x 30 mL). The organic phase was combined, dried over anhydrous $MgSO_4$, filtered, and concentrated *in vacuo*. The resulting crude material was purified by flash column chromatography using pentane:EtOAc = 1:1 as the eluent to afford **153** (0.78 g, 45% yield) as a clear colourless oil. ^{1}H-NMR (400 MHz, Chloroform-d) δ 1.01 – 1.13 (m, 2H), 1.13– 1.24 (m, 2H), 1.28 (t, J = 7.0 Hz, 3H), 1.44 (s, 1H), 1.59 – 1.67 (m, 1H), 1.70 – 1.79 (m, 2H), 1.85 – 1.94 (m, 2H), 2.44 (tt, J = 10.5, 3.0 Hz, 1H), 2.51 (t, J = 6.0 Hz, 2H), 2.91 (t, J = 6.0 Hz, 2H), 4.16 (q, J = 7.0 Hz, 2H); ^{13}C-NMR (101 MHz, Chloroform-d) δ 14.2, 25.0, 26.2, 33.6, 35.1, 42.1, 56.5, 60.4, 172.9; HRMS (ESI) calculated mass for $C_{11}H_{22}NO_2$ (MH^+) 200.1651, found 200.1664.

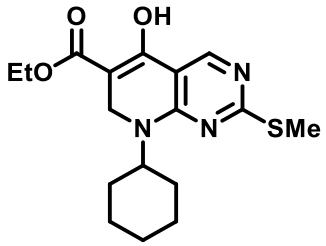
Ethyl 4-(cyclohexyl(3-ethoxy-3-oxopropyl)amino)-2-(methylthio)pyrimidine-5-carboxylate (154)



To a solution of **153** (0.78 g, 3.89 mmol) in DCM (15 mL) was added ethyl 4-chloro-2-methylthio-5-pyrimidinecarboxylate (0.90 g, 3.89 mmol) and DIPEA (0.67 mL, 3.89 mmol). The reaction mixture was stirred at room temperature overnight before quenching with the addition of water. The organic phase was washed with water (2 x 30 mL) and brine (20 mL), dried over anhydrous

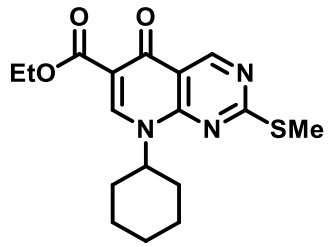
$MgSO_4$, filtered, and concentrated *in vacuo*. The resulting crude material was purified by flash column chromatography using the gradient eluent starting from pentane:DCM = 1:4 to 100% DCM to EtOAc:DCM = 1:1 to afford **154** (0.82 g, 54% yield) as a clear colourless oil. R_f= 0.43 (DCM:EtOAc = 4:1, v/v); ^{1}H-NMR (400 MHz, Chloroform-d) δ 1.10 – 1.25 (m, 3H), 1.28 (td, *J* = 7.0, 2.5 Hz, 3H), 1.38 (t, *J* = 7.0 Hz, 3H), 1.54 (td, *J* = 12.0, 3.4 Hz, 2H), 1.67 (d, *J* = 12.0 Hz, 1H), 1.85 (d, *J* = 12.0 Hz, 4H), 2.52 (s, 3H), 2.65 – 2.75 (m, 2H), 3.49 (t, *J* = 12.0 Hz, 1H), 3.77 – 3.86 (m, 2H), 4.16 (q, *J* = 7.0 Hz, 2H), 4.33 (q, *J* = 7.0 Hz, 2H), 8.42 (s, 1H); ^{13}C-NMR (101 MHz, Chloroform-d) δ 14.0, 14.2, 14.3, 25.4, 26.1, 30.7, 33.6, 39.6, 60.6, 61.3, 61.3, 106.5, 158.8, 159.3, 166.9, 171.9, 172.7; HRMS (ESI) calculated mass for $C_{19}H_{30}N_3O_4S$ (MH^+) 396.1957, found 396.1964.

Ethyl 8-cyclohexyl-5-hydroxy-2-(methylthio)-7,8-dihydropyrido[2,3-*d*]pyrimidine-6-carboxylate (155)



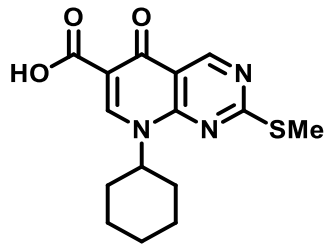
To a solution of **154** (0.32 g, 0.80 mmol) in toluene (5 mL) was slowly added a solution of KO^{t}Bu (0.13 g, 1.20 mmol) in THF (3 mL). After a complete addition, the reaction was quenched with water and the pH of the solution was adjusted to 7 using 1 M HCl aqueous solution. The solution was then extracted with DCM (3 x 20 mL), dried over anhydrous $MgSO_4$, filtered, and concentrated *in vacuo* to give the mixture of both **155** and its keto form in the ratio 2.5:1 (0.25 g, 89% yield) as a yellow solid. ^{1}H-NMR (400 MHz, Chloroform-d) δ 1.19 (qt, *J* = 12.5, 3.5 Hz, 1H), 1.36 (t, *J* = 7.0 Hz, 3H), 1.40 – 1.51 (m, 2H), 1.59 (td, *J* = 12.0, 3.5 Hz, 2H), 1.75 (d, *J* = 12.5 Hz, 3H), 1.90 (d, *J* = 12.5 Hz, 2H), 2.52 (s, 3H), 2.56 (s, 1H), 4.27 – 4.35 (m, 4H), 4.65 (tt, *J* = 12.0, 3.5 Hz, 1H), 8.21 (s, 1H), 12.04 (s, 1H); HRMS (ESI) calculated mass for $C_{17}H_{24}N_3O_3S$ (MH^+) 350.1538, found 350.1542.

Ethyl 8-cyclohexyl-2-(methylthio)-5-oxo-5,8-dihydropyrido[2,3-*d*]pyrimidine-6-carboxylate (156)



To a solution of **155** (4.08 g, 11.70 mmol) in DCM (120 mL) was added bromine (0.72 mL, 14.00 mmol). The reaction was stirred at room temperature for 30 minutes. After this time, the reaction solution was concentrated *in vacuo*. The crude mixture was re-dissolved in DCM (120 mL) and DIPEA (6.10 mL, 35.00 mmol) was added to the solution. The reaction was then heated to 30°C and stirred overnight. After this time, the reaction was partitioned with water (100 mL) and washed with brine (3 x 50 mL). The organic phase was dried over anhydrous $MgSO_4$, filtered, and concentrated *in vacuo*. The resulting crude material was purified by flash column chromatography using the gradient eluent starting from pentane:EtOAc = 4:1 to 100% EtOAc to afford **156** (3.28 g, 80% yield) as an off-white solid. R_f= 0.22 (pentane:EtOAc = 1:1, v/v); ^{1}H-NMR (400 MHz, Chloroform-d) δ 1.25 – 1.40 (m, 1H), 1.44 (t, J = 7.0 Hz, 3H), 1.56 (dtd, J = 13.0, 10.0, 3.5 Hz, 2H), 1.66 – 1.81 (m, 2H), 1.85 (d, J = 13.0 Hz, 1H), 2.05 (t, J = 15.0 Hz, 4H), 2.66 (s, 3H), 4.43 (q, J = 7.0 Hz, 2H), 5.24 (tt, J = 12.0, 3.5 Hz, 1H), 8.62 (s, 1H), 9.42 (s, 1H); ^{13}C-NMR (101 MHz, Chloroform-d) δ 14.4, 14.5, 25.2, 25.8, 32.3, 56.6, 61.4, 115.5, 116.0, 146.1, 153.9, 159.4, 165.0, 173.4, 175.8; HRMS (ESI) calculated mass for $C_{17}H_{22}N_3O_3S$ (MH^+) 348.1382, found 348.1390.

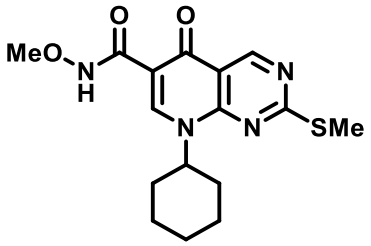
8-Cyclohexyl-2-(methylthio)-5-oxo-5,8-dihydropyrido[2,3-*d*]pyrimidine-6-carboxylic acid (157)



To a solution of **156** (0.16 g, 0.45 mmol) in 1,4-dioxane (3 mL) was added 1 M HCl aqueous solution (1.56 mL, 1.56 mmol). The reaction mixture was heated to reflux (101°C) for 4 hours

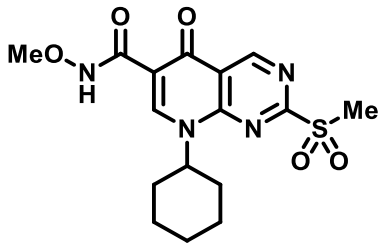
before cooling down to room temperature. The reaction flask was further cooled down to 0°C as the product started to crystallise. The mixture was filtered and washed with cold water to afford **157** (0.10 g, 72% yield) as an off-white solid. ^{1}H-NMR (400 MHz, Chloroform-d) δ 1.33 (qt, J = 13.0, 3.5 Hz, 1H), 1.57 (tdd, J = 13.0, 8.5, 3.5 Hz, 2H), 1.78 (qd, J = 12.5, 3.5 Hz, 2H), 1.87 (d, J = 13.5 Hz, 1H), 2.08 (t, J = 13.5 Hz, 4H), 2.70 (s, 3H), 5.36 (tt, J = 12.5, 3.5 Hz, 1H), 8.91 (s, 1H), 9.51 (s, 1H), 14.15 (s, 1H); ^{13}C-NMR (101 MHz, Chloroform-d) δ 14.6, 25.0, 25.8, 32.4, 57.6, 112.5, 113.9, 146.5, 153.7, 159.0, 165.5, 177.8, 177.8; HRMS (ESI) calculated mass for $C_{15}H_{18}N_3O_3S$ (MH^+) 320.1069, found 320.1080.

8-Cyclohexyl-*N*-methoxy-2-(methylthio)-5-oxo-5,8-dihydropyrido[2,3-*d*]pyrimidine-6-carboxamide (158)



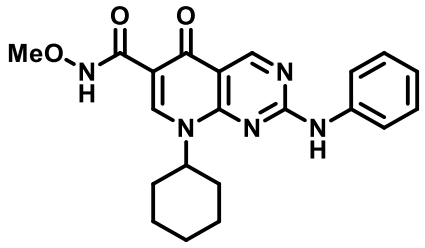
A solution of **157** (0.79 g, 2.50 mmol) in anhydrous DMF (25 mL) was cooled to 0°C in an ice bath. HOBt (0.51 g, 3.75 mmol), triethylamine (0.87 mL, 6.24 mmol), methoxyamine hydrochloride (0.21 g, 2.50 mmol), and EDC·HCl (0.72 g, 3.75 mmol) were added under nitrogen atmosphere. The mixture was heated to 50°C and stirred overnight. After this time, the mixture was diluted with water (50 mL) and extracted with EtOAc (5 x 30 mL). The organic phase was combined and washed with 5% LiCl aqueous solution (5 x 20 mL), dried over anhydrous $MgSO_4$, filtered, and concentrated *in vacuo* to afford **158** (0.87 g, 99% yield) as an off-white solid which was used without further purification. R_f= 0.34 (pentane:EtOAc = 3:7, v/v); ^{1}H-NMR (400 MHz, Chloroform-d) δ 1.26 – 1.42 (m, 1H), 1.49 – 1.63 (m, 2H), 1.81 (qd, J = 13.0, 12.5, 3.5 Hz, 3H), 2.05 (tt, J = 14.0, 3.5 Hz, 4H), 2.67 (s, 3H), 3.91 (s, 3H), 5.30 (ddd, J = 12.0, 8.5, 3.5 Hz, 1H), 8.90 (s, 1H), 9.44 (s, 1H), 11.89 (s, 1H); ^{13}C-NMR (101 MHz, Chloroform-d) δ 14.6, 25.0, 25.8, 32.3, 57.2, 64.6, 114.7, 115.2, 114.9, 153.4, 159.2, 161.9, 175.2, 176.5; HRMS (ESI) calculated mass for $C_{16}H_{21}N_4O_3S$ (MH^+) 349.1334, found 349.1342.

8-Cyclohexyl-*N*-methoxy-2-(methylsulfonyl)-5-oxo-5,8-dihydropyrido[2,3-*d*]pyrimidine-6-carboxamide (159)



To a solution of **158** (0.87 g, 2.49 mmol) in DCM (40 mL) at 0°C was added *m*CPBA (≤77% purity, 1.40 g, 6.22 mmol). The reaction mixture was allowed to stir at 0°C for 1 hour. After this time, the reaction was warmed up and stirred at room temperature overnight. After this time, the reaction was diluted with DCM (30 mL) and washed with saturated $NaHCO_3$ aqueous solution (4 x 25 mL) to remove the excess *m*CPBA. The organic phase was further washed with water (30 mL) and brine (30 mL), dried over anhydrous $MgSO_4$, filtered, and concentrated *in vacuo* to afford **159** (0.52 g, 55% yield) as an off-white solid which was used without further purification. R_f= 0.25 (DCM:EtOAc = 1:1, v/v); ^{1}H-NMR (400 MHz, Chloroform-d) δ 1.25 – 1.42 (m, 1H), 1.53 – 1.70 (m, 2H), 1.79 – 1.94 (m, 3H), 2.06 (t, J = 15.0 Hz, 4H), 3.48 (s, 3H), 3.93 (s, 3H), 5.38 (tt, J = 12.5, 3.5 Hz, 1H), 9.09 (s, 1H), 9.81 (s, 1H), 11.65 (s, 1H); ^{13}C-NMR (101 MHz, Chloroform-d) δ 24.9, 25.6, 32.3, 39.2, 58.4, 64.8, 117.0, 119.8, 146.4, 154.2, 160.9, 161.5, 166.7, 174.3; HRMS (ESI) calculated mass for $C_{16}H_{21}N_4O_5S$ (MH^+) 381.1233, found 381.1244.

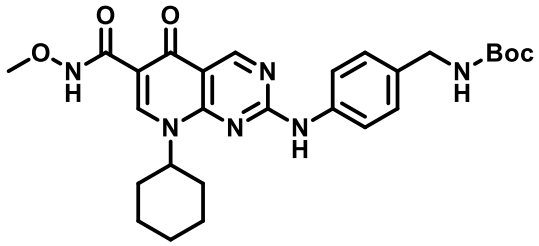
8-Cyclohexyl-*N*-methoxy-5-oxo-2-(phenylamino)-5,8-dihydropyrido[2,3-*d*]pyrimidine-6-carboxamide (10)



To a suspension of **159** (12 mg, 33 μmol) in isopropanol (2 mL) in a microwave vial was added aniline (9 μL, 98 μmol). The reaction mixture was put into a microwave reactor set at 90°C for 3 hours. After this time, the reaction was cooled to room temperature and the solvent was evaporated

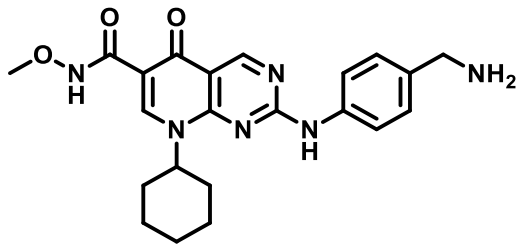
in vacuo. The resulting crude material was purified by flash column chromatography using the gradient eluent starting from DCM:EtOAc = 4:1 to 100% EtOAc to afford **10** (9 mg, 72% yield) as a white solid. R_f= 0.5 (100% EtOAc); ^{1}H-NMR (400 MHz, Chloroform-d) δ 1.30 – 1.39 (m, 1H), 1.48 – 1.62 (m, 2H), 1.72 – 1.91 (m, 3H), 2.00 – 2.14 (m, 4H), 3.91 (s, 3H), 5.12 – 5.26 (m, 1H), 7.18 – 7.24 (m, 1H), 7.40 – 7.48 (m, 2H), 7.65 – 7.72 (m, 2H), 7.87 (s, 1H), 8.83 (s, 1H), 9.40 (s, 1H), 12.03 (s, 1H); ^{13}C-NMR (101 MHz, Chloroform-d) δ 25.2, 26.1, 29.7, 32.3, 64.6, 112.2, 114.4, 120.2, 124.4, 129.1, 137.9, 144.4, 155.0, 159.9, 161.3, 162.3, 174.8; HRMS (ESI) calculated mass for $C_{21}H_{24}N_5O_3$ (MH^+) 394.1879, found 394.1884.

***Tert*-Butyl (4-((8-cyclohexyl-6-(methoxycarbamoyl)-5-oxo-5,8-dihydropyrido[2,3-*d*]pyrimidin-2-yl)amino)benzyl)carbamate (160)**



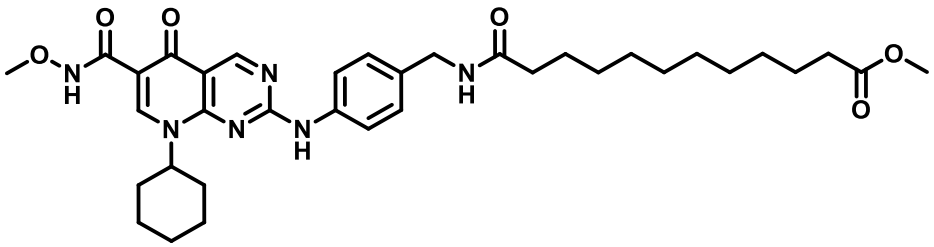
To a suspension of **159** (70 mg, 18 μmol) in isopropanol (3 mL) in a microwave vial was added 4-[(*N*-Boc)aminomethyl]aniline (45 mg, 20 μmol). The reaction mixture was put into a microwave reactor set at 90°C for 3 hours. After this time, the reaction was cooled to room temperature. The reaction mixture was then diluted with DCM (5 mL), washed with water (10 mL) and brine (10 mL), and concentrated *in vacuo*. The resulting crude material was purified by flash column chromatography using the gradient eluent starting from DCM:EtOAc = 7:3 to 1:1 to afford **160** (61 mg, 63% yield) as a pale yellow solid. R_f= 0.22 (DCM:EtOAc = 1:1, v/v); ^{1}H-NMR (400 MHz, Chloroform-d) δ 1.33 – 1.38 (m, 1H), 1.50 (s, 9H), 1.55 (d, J = 13.0 Hz, 2H), 1.73 – 1.92 (m, 3H), 2.01 – 2.14 (m, 4H), 3.91 (s, 3H), 4.36 (d, J = 6.0 Hz, 2H), 4.90 (s, 1H), 5.18 (t, J = 12.0 Hz, 1H), 7.35 (d, J = 8.5 Hz, 2H), 7.65 (d, J = 8.5 Hz, 2H), 8.84 (s, 1H), 9.39 (s, 1H), 12.02 (s, 1H); ^{13}C-NMR (101 MHz, Chloroform-d) δ 25.2, 26.1, 28.4, 29.7, 32.3, 44.2, 64.6, 79.7, 112.2, 114.4, 120.1, 128.2, 135.0, 137.1, 144.3, 155.0, 155.9, 161.3, 162.3, 174.8; HRMS (ESI) calculated mass for $C_{27}H_{35}N_6O_5$ (MH^+) 523.2669, found 523.2674.

2-((4-(Aminomethyl)phenyl)amino)-8-cyclohexyl-*N*-methoxy-5-oxo-5,8-dihydropyrido[2,3-*d*]pyrimidine-6-carboxamide (161)



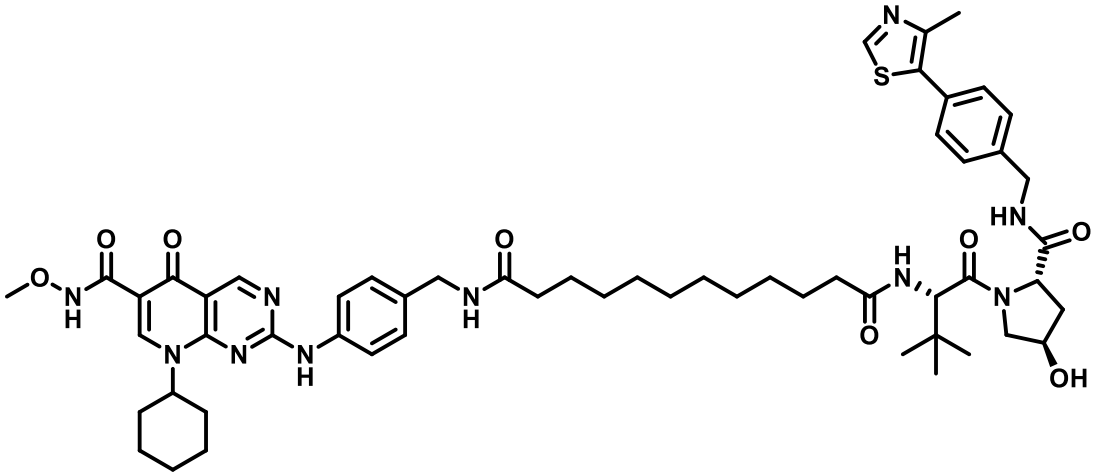
To a solution of **160** (59 mg, 0.11 mmol) in anhydrous THF (5 mL) was added tetrabutylammonium fluoride solution (1 M in THF, 1.12 mL, 1.12 mmol). The reaction mixture was heated to reflux (66°C) for 17 hours. After this time, the mixture was cooled to room temperature, diluted with EtOAc (10 mL), and washed with water (10 mL). The organic phase was separated and the pH of the aqueous phase was adjusted to 8 using saturated $NaHCO_3$ aqueous solution. The aqueous phase was extracted with DCM (2 x 15 mL). The organic phase was combined, dried over anhydrous $MgSO_4$, filtered, and concentrated *in vacuo*. The resulting crude material was purified by flash column chromatography using DCM:MeOH = 9:1 as the eluent to afford **161** (19 mg, 41% yield) as an off-white solid. R_f= 0.06 (DCM:MeOH = 9:1, v/v); ^{1}H-NMR (400 MHz, Chloroform-d) δ 0.81 – 0.97 (m, 1H), 1.27 – 1.44 (m, 1H), 1.46 – 1.93 (m, 4H), 2.08 (t, J = 14.5 Hz, 4H), 3.91 (s, 3H), 3.93 (s, 2H), 5.19 (t, J = 12.0 Hz, 1H), 7.39 (d, J = 8.0 Hz, 2H), 7.66 (d, J = 8.0 Hz, 2H), 7.91 (s, 1H), 8.83 (s, 1H), 9.39 (s, 1H), 12.03 (s, 1H); ^{13}C-NMR (101 MHz, Chloroform-d) δ 25.2, 26.1, 32.3, 46.0, 57.1, 64.6, 112.1, 114.4, 120.1, 127.8, 136.7, 139.3, 144.3, 155.1, 159.8, 161.2, 162.3, 174.8; HRMS (ESI) calculated mass for $C_{22}H_{27}N_6O_3$ (MH^+) 423.2145, found 423.2155.

Methyl 12-((4-((8-cyclohexyl-6-(methoxycarbamoyl)-5-oxo-5,8-dihydropyrido[2,3-*d*]pyrimidin-2-yl)amino)benzyl)amino)-12-oxododecanoate (162)



To a solution of **161** (13 mg, 31 µmol) and 12-methoxy-12-oxododecanoic acid (12 mg, 47 µmol) in anhydrous DMF (1.5 mL) was added trimethylamine (13 µL, 94 µmol). The reaction mixture was stirred at room temperature for 10 minutes followed by the addition of HATU (18 mg, 47 µmol). The reaction mixture was then stirred for additional 4 hours. After this time, the reaction mixture was diluted with EtOAc (10 mL), washed with 5% LiCl aqueous solution (2 x 10 mL) and water (2 x 10 mL), dried over anhydrous $MgSO_4$, filtered, and concentrated *in vacuo*. The resulting crude material was purified by flash column chromatography using DCM:EtOAc = 1:4 as the eluent to afford **162** (6 mg, 29% yield); ^{1}H-NMR (400 MHz, Chloroform-d) δ 0.87 – 0.94 (m, 1H), 1.23 – 1.39 (m, 12H), 1.53 (d, J = 3.5 Hz, 1H), 1.58 – 1.74 (m, 4H), 1.74 – 1.94 (m, 4H), 2.02 – 2.14 (m, 4H), 2.25 (t, J = 7.5 Hz, 2H), 2.32 (t, J = 7.5 Hz, 2H), 3.69 (s, 3H), 3.91 (s, 3H), 4.49 (d, J = 5.5 Hz, 2H), 5.16 (t, J = 12.5 Hz, 1H), 5.82 (td, J = 8.5, 7.5, 6.0 Hz, 1H), 7.35 (d, J = 9.5 Hz, 2H), 7.66 (d, J = 8.5 Hz, 2H), 8.83 (s, 1H), 9.39 (s, 1H), 11.97 (s, 1H); HRMS (ESI) calculated mass for $C_{35}H_{49}N_6O_6$ (MH^+) 649.3714, found 649.3715.

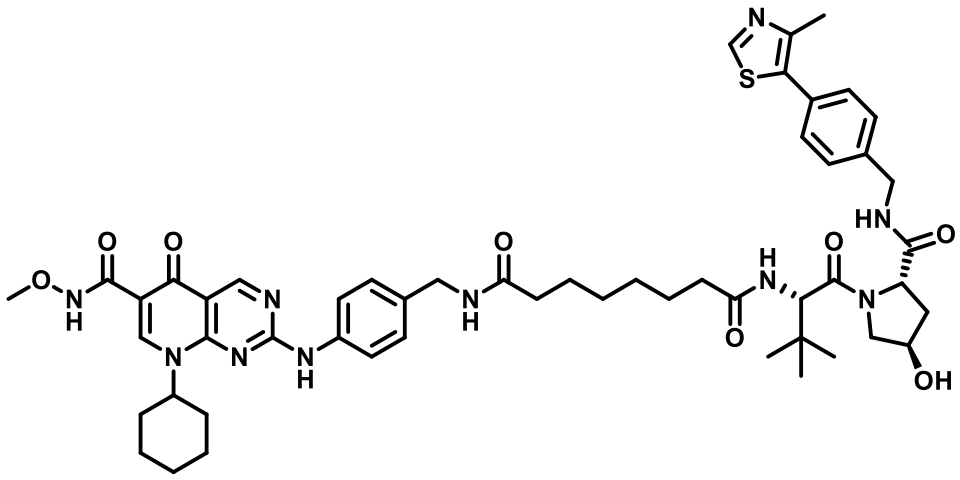
N^1-(4-((8-Cyclohexyl-6-(methoxycarbamoyl)-5-oxo-5,8-dihydropyrido[2,3-*d*]pyrimidin-2-yl)amino)benzyl)-N^{12}-((*S*)-1-((2*S*,4*R*)-4-hydroxy-2-((4-(4-methylthiazol-5-yl)benzyl)carbamoyl)pyrrolidin-1-yl)-3,3-dimethyl-1-oxobutan-2-yl)dodecanediamide (164)



To a solution of **161** (6 mg, 14 µmol) and **163** (13 mg, 21 µmol) in anhydrous DMF (1 mL) was added triethylamine (6 µL, 41 µmol). The reaction mixture was stirred at room temperature for 10 minutes followed by the addition of HATU (8 mg, 21 µmol). The reaction mixture was then stirred for additional 4 hours. After this time, the reaction mixture was diluted with EtOAc (10 mL), washed with 5% LiCl aqueous solution (2 x 10 mL) and water (2 x 10 mL), dried over anhydrous $MgSO_4$, filtered, and concentrated *in vacuo*. The resulting crude material was purified by flash column chromatography using EtOAc:MeOH = 5:0.1 as the eluent to afford **164** (4 mg, 26% yield) as a pale yellow solid. R_f= 0.03 (EtOAc:MeOH = 5:0.1, v/v); ^{1}H-NMR (400 MHz, Chloroform-d) δ 0.98 (s, 9H), 1.17 – 1.39 (m, 12H), 1.49 – 1.63 (m, 4H), 1.67 (t, J = 7.0 Hz, 2H), 1.73 – 1.93 (m, 3H), 2.00 – 2.15 (m, 5H), 2.15 – 2.30 (m, 5H), 2.49 – 2.55 (m, 1H), 2.57 (s, 3H), 3.64 (dd, J = 11.5, 3.5 Hz, 1H), 3.91 (s, 3H), 4.05 (p, J = 6.0 Hz, 1H), 4.16 (d, J = 11.5 Hz, 1H), 4.36 (dd, J = 15.0, 5.0 Hz, 1H), 4.47 (d, J = 5.5 Hz, 2H), 4.53 – 4.67 (m, 3H), 4.76 (t, J = 8.0 Hz, 1H), 5.16 (t, J = 12.5 Hz, 1H), 5.99 (t, J = 5.5 Hz, 1H), 6.43 (s, 1H), 7.33 (d, J = 8.0 Hz, 2H), 7.35 – 7.43 (m, 4H), 7.68 (d, J = 8.0 Hz, 2H), 8.54 (s, 1H), 8.83 (s, 1H), 8.92 (s, 1H), 9.38 (s, 1H), 12.00 (s, 1H); ^{13}C-NMR (101 MHz, Chloroform-d) δ 15.3, 25.1, 25.4, 25.5, 25.7, 26.1, 26.5, 29.0, 29.0, 29.1, 29.1, 29.2, 29.3, 29.7, 32.2, 34.8, 35.9, 36.4, 36.7, 43.0, 43.2, 56.8, 57.5, 58.6, 64.4, 64.6, 70.0, 112.1, 114.4, 120.3, 120.4, 128.3, 128.5, 129.4, 129.9, 134.6, 137.3, 138.8, 144.4, 150.8, 150.9,

155.1, 159.5, 160.9, 162.2, 170.8, 172.1, 173.1, 174.0, 174.8; HRMS (ESI) calculated mass for $C_{56}H_{75}N_{10}O_8S$ (MH^+) 1047.5490, found 1047.5493.

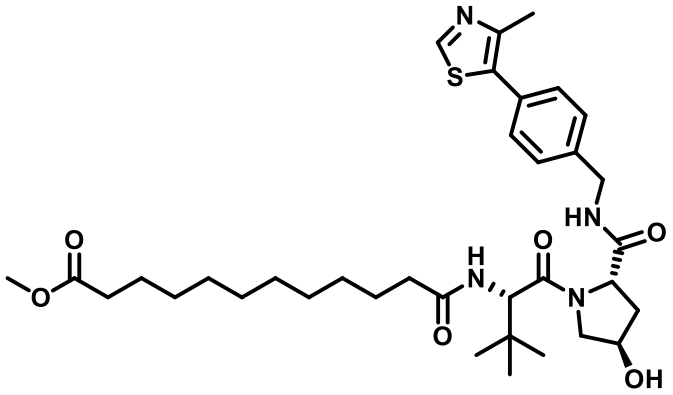
N^1-(4-((8-Cyclohexyl-6-(methoxycarbamoyl)-5-oxo-5,8-dihydropyrido[2,3-*d*]pyrimidin-2-yl)amino)benzyl)-N^8-((*S*)-1-((2*S*,4*R*)-4-hydroxy-2-((4-(4-methylthiazol-5-yl)benzyl)carbamoyl)pyrrolidin-1-yl)-3,3-dimethyl-1-oxobutan-2-yl)octanediamide (166)



To a solution of **161** (7 mg, 15 µmol) and **165** (9 mg, 15 µmol) in anhydrous DMF (1 mL) was added triethylamine (7 µL, 46 µmol). The reaction mixture was stirred at room temperature for 10 minutes followed by the addition of HATU (9 mg, 23 µmol). The reaction mixture was then stirred for additional 4 hours. After this time, the reaction mixture was diluted with EtOAc (10 mL), washed with 5% LiCl aqueous solution (2 x 10 mL) and water (2 x 10 mL), dried over anhydrous $MgSO_4$, filtered, and concentrated *in vacuo*. The resulting crude material was purified by flash column chromatography using DCM:MeOH = 9.5:0.5 as the eluent to afford **166** (8 mg, 52% yield) as a pale yellow solid. R_f= 0.47 (DCM:MeOH = 9:1, v/v); ^{1}H-NMR (500 MHz, Chloroform-d) δ 0.97 (s, 9H), 1.22 – 1.36 (m, 4H), 1.46 – 1.60 (m, 4H), 1.64 (t, J = 7.0 Hz, 2H), 1.69 – 1.81 (m, 2H), 1.84 (d, J = 13.5 Hz, 2H), 1.98 – 2.12 (m, 5H), 2.22 (t, J = 7.0 Hz, 4H), 2.47 (ddd, J = 13.0, 8.5, 4.5 Hz, 1H), 2.52 (s, 3H), 3.65 (dd, J = 11.5, 3.5 Hz, 1H), 3.88 (s, 3H), 4.10 – 4.16 (m, 1H), 4.27 – 4.33 (m, 1H), 4.42 (dd, J = 7.5, 5.5 Hz, 2H), 4.50 – 4.57 (m, 2H), 4.63 (dd, J = 15.0, 6.5 Hz, 1H), 4.75 (t, J = 8.0 Hz, 1H), 5.11 (t, J = 12.5 Hz, 1H), 6.16 (d, J = 8.5 Hz, 1H), 6.21 (s, 1H), 7.28 – 7.33 (m, 4H), 7.37 (d, J = 8.0 Hz, 2H), 7.53 (dd, J = 6.0, 3.0 Hz, 1H), 7.64 (d, J = 8.0 Hz, 2H), 8.62 (s, 1H), 8.79 (s, 1H), 8.93 (s, 1H), 9.29 (s, 1H), 11.94 (s, 1H); ^{13}C-NMR (101 MHz, Chloroform-d) δ 15.1, 25.1, 25.2, 26.1, 26.4, 28.1, 32.2, 32.2, 35.0, 36.0, 36.3, 36.3, 42.9, 43.2,

45.8, 56.9, 57.5, 58.7, 64.6, 70.1, 114.4, 120.4, 128.3, 128.5, 128.8, 129.3, 129.4, 130.9, 134.6, 137.4, 139.1, 144.4, 146.2, 150.9, 155.1, 160.7, 162.2, 162.2, 167.7, 171.1, 171.8, 173.2, 173.7, 174.7; HRMS (ESI) calculated mass for $C_{52}H_{67}N_{10}O_8S$ (MH^+) 991.4864, found 991.4859.

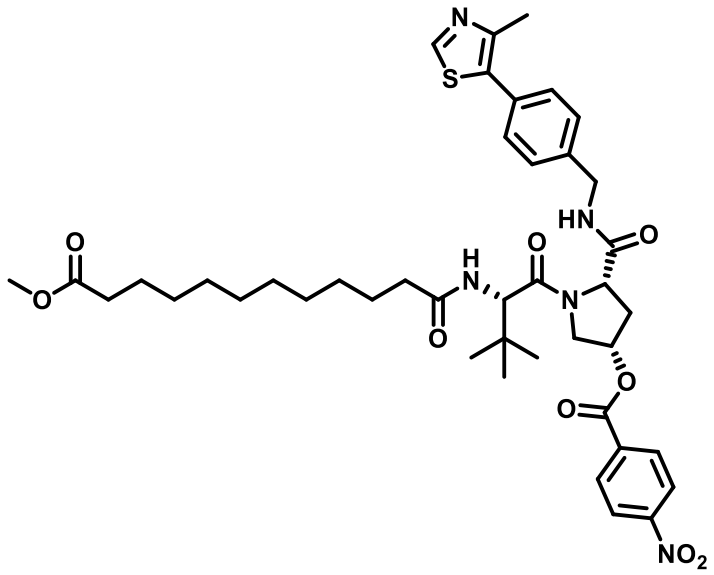
Methyl 12-(((*S*)-1-((2*S*,4*R*)-4-hydroxy-2-((4-(4-methylthiazol-5-yl)benzyl)carbamoyl)pyrrolidin-1-yl)-3,3-dimethyl-1-oxobutan-2-yl)amino)-12-oxododecanoate (167)



To a solution of (2*S*,4*R*)-1-((*S*)-2-Amino-3,3-dimethylbutanoyl)-4-hydroxy-*N*-(4-(4-methylthiazol-5-yl)benzyl)pyrrolidine-2-carboxamide hydrochloride (VHL ligand) (0.20 g, 0.40 mmol) and 12-methoxy-12-oxododecanoic acid (0.15 g, 0.60 mmol) in anhydrous DMF (15 mL) was added triethylamine (0.56 mL, 4.00 mmol). The reaction mixture was stirred at room temperature for 10 minutes followed by the addition of HATU (0.23 g, 0.60 mmol). The reaction mixture was then stirred for additional 4 hours. After this time, the solvent was removed *in vacuo* and the resulting residue was re-dissolved with EtOAc (25 mL). The organic phase was washed with water (2 x 20 mL) and brine (2 x 20 mL), dried over anhydrous $MgSO_4$, filtered, and concentrated *in vacuo*. The resulting crude material was purified by flash column chromatography using DCM:MeOH = 9.5:0.5 as the eluent to afford **167** (0.253 g, 96% yield) as a pale yellow oil. R_f= 0.22 (DCM:MeOH = 9.5:0.5, v/v); ^{1}H-NMR (400 MHz, Chloroform-d) δ 0.93 (s, 9H), 1.25 (d, J = 5.0 Hz, 12H), 1.59 (q, J = 7.0 Hz, 4H), 2.10 – 2.16 (m, 1H), 2.20 (d, J = 7.5 Hz, 2H), 2.29 (t, J = 7.5 Hz, 2H), 2.51 – 2.61 (m, 4H), 3.59 (dd, J = 11.5, 3.5 Hz, 1H), 3.66 (s, 3H), 4.14 (d, J = 11.5 Hz, 1H), 4.34 (dd, J = 15.0, 5.0 Hz, 1H), 4.50 (d, J = 8.5 Hz, 1H), 4.53 (s, 1H), 4.59 (dd, J = 15.0, 6.5 Hz, 1H), 4.72 (t, J = 7.5 Hz, 1H), 6.11 (d, J = 8.5 Hz, 1H), 7.28 – 7.34 (m, 1H), 7.37 (s,

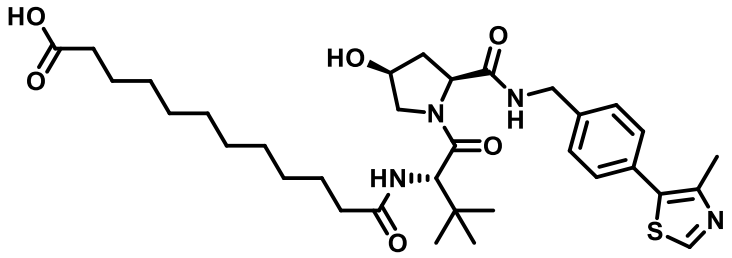
4H), 8.85 (s, 1H); HRMS (ESI) calculated mass for $C_{35}H_{53}N_4O_6S$ (MH^+) 657.3686, found 657.3690.

(3*S*,5*S*)-1-((*S*)-2-(12-Methoxy-12-oxododecanamido)-3,3-dimethylbutanoyl)-5-((4-(4-methylthiazol-5-yl)benzyl)carbamoyl)pyrrolidin-3-yl 4-nitrobenzoate (168)



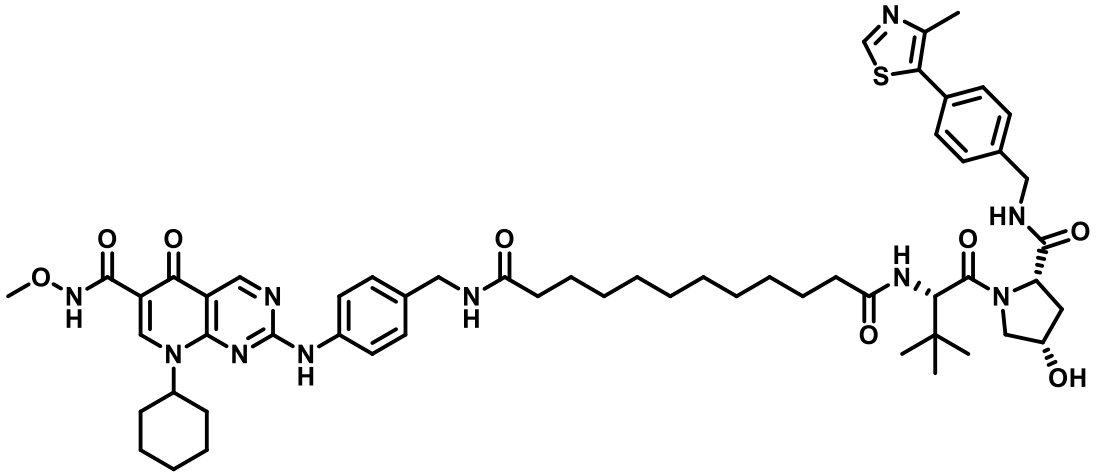
To a solution of **167** (0.13 g, 0.20 mmol), 4-nitrobenzoic acid (0.12 g, 0.70 mmol), and PPh_3 (0.18 g, 0.70 mmol) in anhydrous THF (1 mL) was added dropwise a solution of DMEAD (0.15 g, 0.62 mmol) in anhydrous THF (1 mL). The mixture was heated to reflux (66°C) for 48 hours. After this time, the mixture was cooled to room temperature and diluted with EtOAc (10 mL). The organic phase was washed with water (2 x 10 mL) and saturated $NaHCO_3$ aqueous solution (2 x 10 mL), dried over anhydrous $MgSO_4$, filtered, and concentrated *in vacuo*. The resulting crude material was purified by flash column chromatography using DCM:EtOAc = 1:1 as the eluent to afford **168** (76 mg, 47% yield). R_f= 0.59 (100% EtOAc). The product obtained from the purification still contained some impurities. However, it was used without further purification. ^{1}H-NMR (400 MHz, Chloroform-d) δ 0.93 (s, 9H), 1.18 – 1.34 (m, 12H), 1.48 – 1.67 (m, 4H), 2.20 (t, J = 7.5 Hz, 2H), 2.28 (t, J = 7.5 Hz, 3H), 2.36 (ddd, J = 14.5, 9.5, 5.0 Hz, 1H), 2.48 (s, 3H), 2.97 (dq, J = 14.5, 2.0 Hz, 1H), 3.64 (d, J = 1.5 Hz, 3H), 3.89 (dt, J = 11.5, 1.5 Hz, 1H), 4.30 – 4.42 (m, 2H), 4.46 – 4.61 (m, 2H), 4.83 (dd, J = 9.5, 2.0 Hz, 1H), 6.13 (d, J = 9.0 Hz, 1H), 7.21 – 7.35 (m, 4H), 7.44 (qd, J = 6.0, 2.0 Hz, 1H), 8.09 – 8.27 (m, 4H), 8.69 (d, J = 7.0 Hz, 1H); HRMS (ESI) calculated mass for $C_{42}H_{56}N_5O_9S$ (MH^+) 806.3799, found 806.3804.

12-(((*S*)-1-((2*S*,4*S*)-4-Hydroxy-2-((4-(4-methylthiazol-5-yl)benzyl)carbamoyl)pyrrolidin-1-yl)-3,3-dimethyl-1-oxobutan-2-yl)amino)-12-oxododecanoic acid (169)



To a solution of **168** (76 mg, 95 µmol) in ethanol (2 mL) was added a solution of 2 M NaOH (0.10 mL, 0.19 mmol). The mixture was stirred at room temperature overnight. After this time, the solvent was evaporated to dryness *in vacuo* and the residue was re-dissolved in a solution of 2 M NaOH (1 mL) and EtOAc (5 mL). The aqueous phase was separated and acidified with 5% acetic acid solution until the pH of the solution was 5. The aqueous phase was then extracted with EtOAc (2 x 10 mL). The organic phase was combined, dried over anhydrous $MgSO_4$, filtered, and concentrated *in vacuo*. The resulting crude material was purified by flash column chromatography using DCM:MeOH = 9.5:0.5 as the eluent to afford **169** (44 mg, 72% yield) as a colourless oil. R_f= 0.34 (DCM:MeOH = 9:1, v/v); ^{1}H-NMR (400 MHz, Chloroform-d) δ 0.92 (s, 9H), 1.16 – 1.43 (m, 12H), 1.58 (dtd, J = 13.5, 7.0, 6.5, 2.5 Hz, 4H), 2.17 – 2.23 (m, 2H), 2.23 – 2.27 (m, 1H), 2.27 – 2.35 (m, 3H), 2.51 (s, 3H), 3.87 (d, J = 11.0 Hz, 1H), 3.95 (dd, J = 11.0, 4.0 Hz, 1H), 4.27 (dd, J = 15.0, 4.5 Hz, 1H), 4.47 (t, J = 4.5 Hz, 1H), 4.58 (d, J = 9.0 Hz, 1H), 4.67 (dd, J = 14.5, 7.5 Hz, 2H), 6.65 (d, J = 9.0 Hz, 1H), 7.30 – 7.42 (m, 4H), 7.62 (dd, J = 7.5, 4.5 Hz, 1H), 8.74 (s, 1H); ^{13}C-NMR (101 MHz, Chloroform-d) δ 15.8, 24.5, 25.2, 26.4, 28.2, 28.4, 28.4, 28.6, 28.9, 33.8, 35.1, 35.5, 36.2, 43.5, 57.0, 58.7, 60.2, 71.0, 123.5, 128.1, 129.6, 130.9, 131.0, 137.5, 150.7, 172.5, 172.7, 173.7, 177.2; HRMS (ESI) calculated mass for $C_{34}H_{51}N_4O_6S$ (MH^+) 643.3529, found 643.3532.

N^1-(4-((8-Cyclohexyl-6-(methoxycarbamoyl)-5-oxo-5,8-dihydropyrido[2,3-*d*]pyrimidin-2-yl)amino)benzyl)-N^{12}-((*S*)-1-((2*S*,4*S*)-4-hydroxy-2-((4-(4-methylthiazol-5-yl)benzyl)carbamoyl)pyrrolidin-1-yl)-3,3-dimethyl-1-oxobutan-2-yl)dodecanediamide (170)



To a solution of **161** (27 mg, 65 µmol) and **169** (44 mg, 69 µmol) in anhydrous DMF (2 mL) was added triethylamine (29 µL, 0.21 mmol). The reaction mixture was stirred at room temperature for 10 minutes followed by the addition of HATU (39 mg, 0.10 mmol). The reaction mixture was then stirred for additional 3 hours. After this time, the reaction mixture was diluted with EtOAc (15 mL), washed with 5% LiCl aqueous solution (2 x 10 mL) and water (2 x 10 mL), dried over anhydrous $MgSO_4$, filtered, and concentrated *in vacuo*. The resulting crude material was purified by flash column chromatography using DCM:MeOH = 10:0.5 as the eluent. The product obtained from the first purification was subjected to the second purification with a column chromatography using the gradient eluent starting from EtOAc:MeOH = 10:0.2 to 9:1 to afford **170** (21 mg, 29% yield) as a pale yellow solid. R_f= 0.25 (EtOAc:MeOH = 9.5:0.5, v/v); ^{1}H-NMR (400 MHz, Chloroform-d) δ 0.93 (s, 9H), 1.23 (s, 12H), 1.45 – 1.71 (m, 6H), 1.72 – 1.81 (m, 2H), 1.85 (d, J = 13.0 Hz, 2H), 1.98 – 2.09 (m, 4H), 2.13 – 2.26 (m, 6H), 2.55 (d, J = 6.5 Hz, 3H), 3.83 (d, J = 11.0 Hz, 1H), 3.88 (s, 3H), 3.90 – 3.97 (m, 1H), 4.29 (dd, J = 15.0, 5.0 Hz, 1H), 4.41 – 4.50 (m, 3H), 4.56 (d, J = 9.0 Hz, 1H), 4.62 – 4.75 (m, 2H), 5.13 (t, J = 12.0 Hz, 1H), 5.87 (t, J = 5.5 Hz, 1H), 6.19 (d, J = 9.0 Hz, 1H), 7.30 (d, J = 8.5 Hz, 2H), 7.36 (d, J = 5.0 Hz, 4H), 7.64 (t, J = 9.0 Hz, 3H), 8.80 (s, 1H), 8.83 (s, 1H), 9.34 (s, 1H), 11.97 (s, 1H); ^{13}C-NMR (101 MHz, Chloroform-d) δ 15.4, 20.5, 25.1, 25.5, 25.7, 26.1, 26.4, 29.1, 29.1, 29.1, 29.2, 29.3, 32.2, 35.0, 35.3, 36.4, 36.7, 43.0, 43.4, 56.9, 58.6, 60.0, 64.6, 71.1, 112.0, 114.4, 128.3, 128.5, 128.6, 129.5, 130.2, 132.4,

134.5, 137.4, 138.0, 144.4, 147.0, 150.8, 155.1, 160.8, 162.2, 172.4, 172.6, 173.1, 173.2, 174.2, 174.7; HRMS (ESI) calculated mass for $C_{56}H_{75}N_{10}O_8S$ (MH^+) 1047.5490, found 1047.5509.

References

(1) Cancer https://www.who.int/news-room/fact-sheets/detail/cancer (accessed Dec 20, 2020).

(2) How cancers grow https://www.cancerresearchuk.org/about-cancer/what-is-cancer/how-cancers-grow (accessed Dec 20, 2020).

(3) National Cancer Institute. What Is Cancer? https://www.cancer.gov/about-cancer/understanding/what-is-cancer (accessed Dec 20, 2020).

(4) O'Connor, C.; Adams, J. U. *Essentials of Cell Biology*; NPG Education: Cambridge, MA, 2010.

(5) Vasir, J. K.; Labhasetwar, V. Targeted Drug Delivery in Cancer Therapy. *Technol. Cancer Res. Treat.* **2005**, *4* (4), 363–374.

(6) The American Cancer Society medical and editorial content team. How Targeted Therapies Are Used to Treat Cancer https://www.cancer.org/treatment/treatments-and-side-effects/treatment-types/targeted-therapy/what-is.html#:~:text=Traditional chemotherapy is cytotoxic to,and making new cancer cells (accessed Feb 4, 2021).

(7) Hoelder, S.; Clarke, P. A.; Workman, P. Discovery of Small Molecule Cancer Drugs: Successes, Challenges and Opportunities. *Mol. Oncol.* **2012**, *6* (2), 155–176.

(8) Gerber, D. E. Targeted Therapies: A New Generation of Cancer Treatments. *Am Fam Physician* **2008**, *77* (3), 311–319.

(9) Bhullar, K. S.; Lagarón, N. O.; McGowan, E. M.; Parmar, I.; Jha, A.; Hubbard, B. P.; Rupasinghe, H. P. V. Kinase-Targeted Cancer Therapies: Progress, Challenges and Future Directions. *Mol. Cancer* **2018**, *17* (1), 48.

(10) Cayman chemical. Kinase Inhibitors https://www.caymanchem.com/news/kinase-inhibitors (accessed Feb 4, 2020).

(11) Manning, G.; Whyte, D. B.; Martinez, R.; Hunter, T.; Sudarsanam, S. The Protein Kinase Complement of the Human Genome. *Science* **2002**, *298* (5600), 1912–1934.

(12) LaRonde-LeBlanc, N.; Wlodawer, A. The RIO Kinases: An Atypical Protein Kinase Family

Required for Ribosome Biogenesis and Cell Cycle Progression. *Biochim. Biophys. Acta - Proteins Proteomics* **2005**, *1754* (1), 14–24.

(13) Blume-Jensen, P.; Hunter, T. Oncogenic Kinase Signalling. *Nature* **2001**, *411* (6835), 355–365.

(14) Hunter, T. Signaling—2000 and Beyond. *Cell* **2000**, *100* (1), 113–127.

(15) Cohen, P. Protein Kinases — the Major Drug Targets of the Twenty-First Century? *Nat. Rev. Drug Discov.* **2002**, *1* (4), 309–315.

(16) Duong-Ly, K. C.; Peterson, J. R. The Human Kinome and Kinase Inhibition. *Curr. Protoc. Pharmacol.* **2013**, *Chapter 2*, Unit2.9.

(17) Ruetten, H.; Thiemermann, C. Effects of Tyrphostins and Genistein on the Circulatory Failure and Organ Dysfunction Caused by Endotoxin in the Rat: A Possible Role for Protein Tyrosine Kinase. *Br. J. Pharmacol.* **1997**, *122* (1), 59–70.

(18) Zwick, E.; Bange, J.; Ullrich, A. Receptor Tyrosine Kinases as Targets for Anticancer Drugs. *Trends Mol. Med.* **2002**, *8* (1), 17–23.

(19) Draw It to Know It. Receptor Tyrosine Kinases https://drawittoknowit.com/course/cell-biology/receptors/receptor-types/1124/receptor-tyrosine-kinases?curriculum=cell-biology&demo=true (accessed Feb 4, 2020).

(20) Robinson, D. R.; Wu, Y.-M.; Lin, S.-F. The Protein Tyrosine Kinase Family of the Human Genome. *Oncogene* **2000**, *19* (49), 5548–5557.

(21) Bethune, G.; Bethune, D.; Ridgway, N.; Xu, Z. Epidermal Growth Factor Receptor (EGFR) in Lung Cancer: An Overview and Update. *J. Thorac. Dis.* **2010**, *2* (1), 48–51.

(22) De Luca, A.; Esposito Abate, R.; Rachiglio, A. M.; Maiello, M. R.; Esposito, C.; Schettino, C.; Izzo, F.; Nasti, G.; Normanno, N. FGFR Fusions in Cancer: From Diagnostic Approaches to Therapeutic Intervention. *Int. J. Mol. Sci.* **2020**, *21* (18), 6856.

(23) Farooqi, A. A.; Siddik, Z. H. Platelet-Derived Growth Factor (PDGF) Signalling in Cancer: Rapidly Emerging Signalling Landscape. *Cell Biochem. Funct.* **2015**, *33* (5), 257–265.

(24) Shibuya, M. Vascular Endothelial Growth Factor (VEGF) and Its Receptor (VEGFR)

Signaling in Angiogenesis: A Crucial Target for Anti- and Pro-Angiogenic Therapies. *Genes Cancer* **2011**, *2* (12), 1097–1105.

(25) Rapisarda, A.; Melillo, G. Role of the VEGF/VEGFR Axis in Cancer Biology and Therapy. *Adv. Cancer Res.* **2012**, *114*, 237–267.

(26) Cannarile, M. A.; Weisser, M.; Jacob, W.; Jegg, A.-M.; Ries, C. H.; Rüttinger, D. Colony-Stimulating Factor 1 Receptor (CSF1R) Inhibitors in Cancer Therapy. *J. Immunother. Cancer* **2017**, *5* (1), 53.

(27) Swierczak, A.; Cook, A. D.; Lenzo, J. C.; Restall, C. M.; Doherty, J. P.; Anderson, R. L.; Hamilton, J. A. The Promotion of Breast Cancer Metastasis Caused by Inhibition of CSF-1R/CSF-1 Signaling Is Blocked by Targeting the G-CSF Receptor. *Cancer Immunol. Res.* **2014**, *2* (8), 765–776.

(28) Neet, K.; Hunter, T. Vertebrate Non-Receptor Protein–Tyrosine Kinase Families. *Genes to Cells* **1996**, *1* (2), 147–169.

(29) Greuber, E. K.; Smith-Pearson, P.; Wang, J.; Pendergast, A. M. Role of ABL Family Kinases in Cancer: From Leukaemia to Solid Tumours. *Nat. Rev. Cancer* **2013**, *13* (8), 559–571.

(30) Sen, B.; Johnson, F. M. Regulation of Src Family Kinases in Human Cancers. *J. Signal Transduct.* **2011**, *2011*, 865819.

(31) Pixley, F. J.; Stanley, E. R. CSF-1 Regulation of the Wandering Macrophage: Complexity in Action. *Trends Cell Biol.* **2004**, *14* (11), 628–638.

(32) Sacca, R.; Stanley, E. R.; Sherr, C. J.; Rettenmier, C. W. Specific Binding of the Mononuclear Phagocyte Colony-Stimulating Factor CSF-1 to the Product of the v-Fms Oncogene. *Proc. Natl. Acad. Sci. U. S. A.* **1986**, *83* (10), 3331–3335.

(33) Stanley, E. R.; Berg, K. L.; Einstein, D. B.; Lee, P. S. W.; Pixley, F. J.; Wang, Y.; Yeung, Y. G. Biology and Action of Colony-Stimulating Factor-1. *Mol. Reprod. Dev.* **1997**, *46* (1), 4–10.

(34) Sapi, E. The Role of CSF-1 in Normal Physiology of Mammary Gland and Breast Cancer:

An Update. *Exp. Biol. Med.* **2004**, *229* (1), 1–11.

(35) Walter, M.; Lucet, I. S.; Patel, O.; Broughton, S. E.; Bamert, R.; Williams, N. K.; Fantino, E.; Wilks, A. F.; Rossjohn, J. The 2.7 Å Crystal Structure of the Autoinhibited Human c-Fms Kinase Domain. *J. Mol. Biol.* **2007**, *367* (3), 839–847.

(36) Yeung, Y. G.; Stanley, E. R. Proteomic Approaches to the Analysis of Early Events in Colony-Stimulating Factor-1 Signal Transduction. *Mol. Cell. Proteomics* **2003**, *2* (11), 1143–1155.

(37) Rohrschneider, L. R.; Bourette, R. P.; Lioubin, M. N.; Algate, P. A.; Myles, G. M.; Carlberg, K. Growth and Differentiation Signals Regulated by the M-CSF Receptor. *Mol. Reprod. Dev.* **1997**, *46* (1), 96–103.

(38) Hamilton, J. A. CSF-1 Signal Transduction. *J. Leukoc. Biol.* **1997**, *62*, 145–155.

(39) Schubert, C.; Schalk-Hihi, C.; Struble, G. T.; Ma, H.-C.; Petrounia, I. P.; Brandt, B.; Deckman, I. C.; Patch, R. J.; Player, M. R.; Spurlino, J. C.; Springer, B. A. Crystal Structure of the Tyrosine Kinase Domain of Colony-Stimulating Factor-1 Receptor (CFMS) in Complex with Two Inhibitors. *J. Biol. Chem.* **2007**, *282* (6), 4094–4101.

(40) Griffith, J.; Black, J.; Faerman, C.; Swenson, L.; Wynn, M.; Lu, F.; Lippke, J.; Saxena, K. The Structural Basis for Autoinhibition of FLT3 by the Juxtamembrane Domain. *Mol. Cell* **2004**, *13* (2), 169–178.

(41) Mol, C. D.; Dougan, D. R.; Schneider, T. R.; Skene, R. J.; Kraus, M. L.; Scheibe, D. N.; Snell, G. P.; Zou, H.; Sang, B.-C.; Wilson, K. P. Structural Basis for the Autoinhibition and STI-571 Inhibition of c-Kit Tyrosine Kinase. *J. Biol. Chem.* **2004**, *279* (30), 31655–31663.

(42) Ullrich, A.; Schlessinger, J. Signal Transduction by Receptors with Tyrosine Kinase Activity. *Cell* **1990**, *61* (2), 203–212.

(43) Rosnet, O.; Birnbaum, D. Hematopoietic Receptors of Class III Receptor-Type Tyrosine Kinases. *Crit. Rev. Oncog.* **1993**, *4* (5), 595–613.

(44) Kumari, A.; Silakari, O.; Singh, R. K. Recent Advances in Colony Stimulating Factor-1 Receptor/c-FMS as an Emerging Target for Various Therapeutic Implications. *Biomed.*

Pharmacother. **2018**, *103*, 662–679.

(45) Mantovani, A.; Allavena, P. The Interaction of Anticancer Therapies with Tumor-Associated Macrophages. *J. Exp. Med.* **2015**, *212* (4), 435–445.

(46) Pollard, J. W. Trophic Macrophages in Development and Disease. *Nat. Rev. Immunol.* **2009**, *9* (4), 259–270.

(47) Mantovani, A.; Sozzani, S.; Locati, M.; Allavena, P.; Sica, A. Macrophage Polarization: Tumor-Associated Macrophages as a Paradigm for Polarized M2 Mononuclear Phagocytes. *Trends Immunol.* **2002**, *23* (11), 549–555.

(48) Biswas, S. K.; Sica, A.; Lewis, C. E. Plasticity of Macrophage Function during Tumor Progression: Regulation by Distinct Molecular Mechanisms. *J. Immunol.* **2008**, *180* (4), 2011–2017.

(49) Jones, C. V; Ricardo, S. D. Macrophages and CSF-1: Implications for Development and Beyond. *Organogenesis* **2013**, *9* (4), 249–260.

(50) Tan, H. Y.; Wang, N.; Li, S.; Hong, M.; Wang, X.; Feng, Y. The Reactive Oxygen Species in Macrophage Polarization: Reflecting Its Dual Role in Progression and Treatment of Human Diseases. *Oxid. Med. Cell. Longev.* **2016**, *2016*, 2795090.

(51) Pollard, J. W. Tumour-Educated Macrophages Promote Tumour Progression and Metastasis. *Nat Rev Cancer* **2004**, *4* (1), 71–78.

(52) Brownlow, N.; Mol, C.; Hayford, C.; Ghaem-Maghami, S.; Dibb, N. J. Dasatinib Is a Potent Inhibitor of Tumour-Associated Macrophages, Osteoclasts and the FMS Receptor. *Leukemia* **2008**, *23* (3), 590–594.

(53) Lin, Y.; Xu, J.; Lan, H. Tumor-Associated Macrophages in Tumor Metastasis: Biological Roles and Clinical Therapeutic Applications. *J. Hematol. Oncol.* **2019**, *12* (1), 76.

(54) Laoui, D.; Van Overmeire, E.; De Baetselier, P.; Van Ginderachter, J. A.; Raes, G. Functional Relationship between Tumor-Associated Macrophages and Macrophage Colony-Stimulating Factor as Contributors to Cancer Progression. *Front. Immunol.* **2014**, *5*, 489.

(55) Mantovani, A.; Marchesi, F.; Malesci, A.; Laghi, L.; Allavena, P. Tumour-Associated Macrophages as Treatment Targets in Oncology. *Nat. Rev. Clin. Oncol.* **2017**, *14* (7), 399–416.

(56) Chen, Y.; Song, Y.; Du, W.; Gong, L.; Chang, H.; Zou, Z. Tumor-Associated Macrophages: An Accomplice in Solid Tumor Progression. *J. Biomed. Sci.* **2019**, *26* (1), 78.

(57) Lewis, C. E.; Pollard, J. W. Distinct Role of Macrophages in Different Tumor Microenvironments. *Cancer Res.* **2006**, *66* (2), 605–612.

(58) Sica, A.; Rubino, L.; Mancino, A.; Larghi, P.; Porta, C.; Rimoldi, M.; Solinas, G.; Locati, M.; Allavena, P.; Mantovani, A. Targeting Tumour-Associated Macrophages. *Expert Opin. Ther. Targets* **2007**, *11*, 1219–1229.

(59) Qian, B.-Z.; Pollard, J. W. Macrophage Diversity Enhances Tumor Progression and Metastasis. *Cell* **2010**, *141* (1), 39–51.

(60) Condeelis, J.; Pollard, J. W. Macrophages: Obligate Partners for Tumor Cell Migration, Invasion, and Metastasis. *Cell* **2006**, *124* (2), 263–266.

(61) Svensson, J.; Jenmalm, M. C.; Matussek, A.; Geffers, R.; Berg, G.; Ernerudh, J. Macrophages at the Fetal–Maternal Interface Express Markers of Alternative Activation and Are Induced by M-CSF and IL-10. *J. Immunol.* **2011**, *187* (7), 3671–3682.

(62) Hamilton, J. A. Colony-Stimulating Factors in Inflammation and Autoimmunity. *Nat. Rev. Immunol.* **2008**, *8* (7), 533–544.

(63) El-Gamal, M. I.; Anbar, H. S.; Yoo, K. H.; Oh, C.-H. FMS Kinase Inhibitors: Current Status and Future Prospects. *Med. Res. Rev.* **2013**, *33* (3), 599–636.

(64) Lin, E. Y.; Nguyen, A. V; Russell, R. G.; Pollard, J. W. Colony-Stimulating Factor 1 Promotes Progression of Mammary Tumors to Malignancy. *J. Exp. Med.* **2001**, *193* (6), 727–740.

(65) Kacinski, B. M. CSF-1 and Its Receptor in Breast Carcinomas and Neoplasms of the Female Reproductive Tract. *Mol. Reprod. Dev.* **1997**, *46* (1), 71–74.

(66) Yee, L. D.; Liu, L. The Constitutive Production of Colony Stimulating Factor 1 by Invasive

Human Breast Cancer Cells. *Anticancer Res.* **2000**, *20* (6B), 4379–4383.

(67) Mancino, A. T.; Klimberg, V. S.; Yamamoto, M.; Manolagas, S. C.; Abe, E. Breast Cancer Increases Osteoclastogenesis by Secreting M-CSF and Upregulating RANKL in Stromal Cells. *J. Surg. Res.* **2001**, *100* (1), 18–24.

(68) Follows, G. A.; Tagoh, H.; Richards, S. J.; Melnik, S.; Dickinson, H.; De Wynter, E.; Lefevre, P.; Morgan, G. J.; Bonifer, C. C-FMS Chromatin Structure and Expression in Normal and Leukaemic Myelopoiesis. *Oncogene* **2005**, *24*, 3643–3651.

(69) Zhu, P.; Baek, S. H.; Bourk, E. M.; Ohgi, K. A.; Garcia-Bassets, I.; Sanjo, H.; Akira, S.; Kotol, P. F.; Glass, C. K.; Rosenfeld, M. G.; Rose, D. W. Macrophage/Cancer Cell Interactions Mediate Hormone Resistance by a Nuclear Receptor Derepression Pathway. *Cell* **2006**, *124* (3), 615–629.

(70) Lin, E. Y.; Li, J.-F.; Gnatovskiy, L.; Deng, Y.; Zhu, L.; Grzesik, D. A.; Qian, H.; Xue, X.-N.; Pollard, J. W. Macrophages Regulate the Angiogenic Switch in a Mouse Model of Breast Cancer. *Cancer Res* **2006**, *66* (23), 11238–11246.

(71) Wang, L.; Zheng, G.-G.; Ma, C.-H.; Lin, Y.-M.; Zhang, H.-Y.; Ma, Y.-Y.; Chong, J.-H.; Wu, K.-F. A Special Linker between Macrophage and Hematopoietic Malignant Cells: Membrane Form of Macrophage Colony-Stimulating Factor. *Cancer Res.* **2008**, *68* (14), 5639–5647.

(72) Mashkani, B.; Griffith, R.; Ashman, L. K. Colony Stimulating Factor-1 Receptor as a Target for Small Molecule Inhibitors. *Bioorg. Med. Chem.* **2010**, *18* (5), 1789–1797.

(73) Scott, D. A.; Aquila, B. M.; Bebernitz, G. A.; Cook, D. J.; Dakin, L. A.; Deegan, T. L.; Hattersley, M. M.; Ioannidis, S.; Lyne, P. D.; Omer, C. A.; Ye, M.; Zheng, X. Pyridyl and Thiazolyl Bisamide CSF-1R Inhibitors for the Treatment of Cancer. *Bioorg. Med. Chem. Lett.* **2008**, *18* (17), 4794–4797.

(74) Zhang, J.; Yang, P. L.; Gray, N. S. Targeting Cancer with Small Molecule Kinase Inhibitors. *Nat Rev Cancer* **2009**, *9* (1), 28–39.

(75) Cowan-Jacob, S. W.; Möbitz, H.; Fabbro, D. Structural Biology Contributions to Tyrosine Kinase Drug Discovery. *Curr. Opin. Cell Biol.* **2009**, *21* (2), 280–287.

(76) Liu, Y.; Gray, N. S. Rational Design of Inhibitors That Bind to Inactive Kinase Conformations. *Nat Chem Biol* **2006**, *2* (7), 358–364.

(77) Peng, Y.-H.; Shiao, H.-Y.; Tu, C.-H.; Liu, P.-M.; Hsu, J. T.-A.; Amancha, P. K.; Wu, J.-S.; Coumar, M. S.; Chen, C.-H.; Wang, S.-Y.; Lin, W.-H.; Sun, H.-Y.; Chao, Y.-S.; Lyu, P.-C.; Hsieh, H.-P.; Wu, S.-Y. Protein Kinase Inhibitor Design by Targeting the Asp-Phe-Gly (DFG) Motif: The Role of the DFG Motif in the Design of Epidermal Growth Factor Receptor Inhibitors. *J. Med. Chem.* **2013**, *56* (10), 3889–3903.

(78) Zuccotto, F.; Ardini, E.; Casale, E.; Angiolini, M. Through the "Gatekeeper Door": Exploiting the Active Kinase Conformation. *J. Med. Chem.* **2010**, *53* (7), 2681–2694.

(79) Wu, P.; Nielsen, T. E.; Clausen, M. H. FDA-Approved Small-Molecule Kinase Inhibitors. *Trends Pharmacol. Sci.* **2015**, *36* (7), 422–439.

(80) Jin, Y.; Xu, Z.; Yan, H.; He, Q.; Yang, X.; Luo, P. A Comprehensive Review of Clinical Cardiotoxicity Incidence of FDA-Approved Small-Molecule Kinase Inhibitors. *Frontiers in Pharmacology* **2020**, *11*, 891.

(81) O'Hare, T.; Walters, D. K.; Stoffregen, E. P.; Jia, T.; Manley, P. W.; Mestan, J.; Cowan-Jacob, S. W.; Lee, F. Y.; Heinrich, M. C.; Deininger, M. W. N.; Druker, B. J. In Vitro Activity of Bcr-Abl Inhibitors AMN107 and BMS-354825 against Clinically Relevant Imatinib-Resistant Abl Kinase Domain Mutants. *Cancer Res.* **2005**, *65* (11), 4500–4505.

(82) Dewar, A. L.; Zannettino, A. C. W.; Hughes, T. P.; Lyons, A. B. Inhibition of C-Fms by Imatinib: Expanding the Spectrum of Treatment. *Cell Cycle* **2005**, *4* (7), 851–853.

(83) Iqbal, N.; Iqbal, N. Imatinib: A Breakthrough of Targeted Therapy in Cancer. *Chemother. Res. Pract.* **2014**, *2014*, 357027.

(84) Rusnak, D. W.; Lackey, K.; Affleck, K.; Wood, E. R.; Alligood, K. J.; Rhodes, N.; Keith, B. R.; Murray, D. M.; Knight, W. B.; Mullin, R. J.; Gilmer, T. M. The Effects of the Novel, Reversible Epidermal Growth Factor Receptor/ErbB-2 Tyrosine Kinase Inhibitor, GW2016, on the Growth of Human Normal and Tumor-Derived Cell Lines *in Vitro* and *in Vivo*. *Mol. Cancer Ther.* **2001**, *1* (2), 85–94.

(85) Siegfried, J. M.; Gubish, C. T.; Rothstein, M. E.; Henry, C.; Stabile, L. P. Combining the

Multitargeted Tyrosine Kinase Inhibitor Vandetanib with the Antiestrogen Fulvestrant Enhances Its Antitumor Effect in Non-Small Cell Lung Cancer. *J. Thorac. Oncol.* **2012**, *7* (3), 485–495.

(86) Burns, C. J.; Wilks, A. F. C-FMS Inhibitors: A Patent Review. *Expert Opin. Ther. Pat.* **2011**, *21* (2), 147–165.

(87) Peyraud, F.; Cousin, S.; Italiano, A. CSF-1R Inhibitor Development: Current Clinical Status. *Curr. Oncol. Rep.* **2017**, *19* (11), 70.

(88) Lamb, Y. N. Pexidartinib: First Approval. *Drugs* **2019**, *79* (16), 1805–1812.

(89) Scott, D. A.; Aquila, B. M.; Bebernitz, G. A.; Cook, D. J.; Dakin, L. A.; Deegan, T. L.; Hattersley, M. M.; Ioannidis, S.; Lyne, P. D.; Omer, C. A.; Ye, M.; Zheng, X. Pyridyl and Thiazolyl Bisamide CSF-1R Inhibitors for the Treatment of Cancer. *Bioorg. Med. Chem. Lett.* **2008**, *18* (17), 4794–4797.

(90) Burns, C. J.; Harte, M. F.; Bu, X.; Fantino, E.; Giarrusso, M.; Joffe, M.; Kurek, M.; Legge, F. S.; Razzino, P.; Su, S.; Treutlein, H.; Wan, S. S.; Zeng, J.; Wilks, A. F. Discovery of 2-(α-Methylbenzylamino) Pyrazines as Potent Type II Inhibitors of FMS. *Bioorg. Med. Chem. Lett.* **2009**, *19* (4), 1206–1209.

(91) Ohno, H.; Kubo, K.; Murooka, H.; Kobayashi, Y.; Nishitoba, T.; Shibuya, M.; Yoneda, T.; Isoe, T. A C-Fms Tyrosine Kinase Inhibitor, Ki20227, Suppresses Osteoclast Differentiation and Osteolytic Bone Destruction in a Bone Metastasis Model. *Mol. Cancer Ther.* **2006**, *5* (11), 2634–2643.

(92) El-Gamal, M. I.; Jung, M.-H.; Oh, C.-H. Discovery of a New Potent Bisamide FMS Kinase Inhibitor. *Bioorg. Med. Chem. Lett.* **2010**, *20* (11), 3216–3218.

(93) Wall, M. J.; Chen, J.; Meegalla, S.; Ballentine, S. K.; Wilson, K. J.; DesJarlais, R. L.; Schubert, C.; Chaikin, M. A.; Crysler, C.; Petrounia, I. P.; Donatelli, R. R.; Yurkow, E. J.; Boczon, L.; Mazzulla, M.; Player, M. R.; Patch, R. J.; Manthey, C. L.; Molloy, C.; Tomczuk, B.; Illig, C. R. Synthesis and Evaluation of Novel 3,4,6-Substituted 2-Quinolones as FMS Kinase Inhibitors. *Bioorg. Med. Chem. Lett.* **2008**, *18*, 2097–2102.

(94) Wiesmann, M.; Daniel, D. L.; Pryer, N.; Sutton, J.; Sung, V.; Wang, T.; Jeffry, U.; Oei, Y.;

Kaufman, S.; Lenahan, W.; Lee, I.; Huh, K.; Sim, J. BLZ945, a Selective c-Fms (CSF-1R) Kinase Inhibitor for the Suppression of Tumor-Induced Osteolytic Lesions in Bone. *Cancer Res.* **2010**, *70* , 3629–3629.

(95) Davidson, R. W. M. Design and Synthesis of Novel Compounds to Inhibit CSF-1R & Evaluation of Novel Substrates and Reactivities in NHC Catalysis, Doctoral dissertation, Imperial College London, London, 2014.

(96) Meyers, M. J.; Pelc, M.; Kamtekar, S.; Day, J.; Poda, G. I.; Hall, M. K.; Michener, M. L.; Reitz, B. A.; Mathis, K. J.; Pierce, B. S.; Parikh, M. D.; Mischke, D. A.; Long, S. A.; Parlow, J. J.; Anderson, D. R.; Thorarensen, A. Structure-Based Drug Design Enables Conversion of a DFG-in Binding CSF-1R Kinase Inhibitor to a DFG-out Binding Mode. *Bioorg. Med. Chem. Lett.* **2010**, *20* (5), 1543–1547.

(97) Huang, H.; Hutta, D. A.; Rinker, J. M.; Hu, H.; Parsons, W. H.; Schubert, C.; DesJarlais, R. L.; Crysler, C. S.; Chaikin, M. A.; Donatelli, R. R.; Chen, Y.; Cheng, D.; Zhou, Z.; Yurkow, E.; Manthey, C. L.; Player, M. R. Pyrido[2,3-d]Pyrimidin-5-Ones: A Novel Class of Antiinflammatory Macrophage Colony-Stimulating Factor-1 Receptor Inhibitors. *J. Med. Chem.* **2009**, *52* (4), 1081–1099.

(98) Boumendjel, A. Aurones: A Subclass of Flavones with Promising Biological Potential. *Curr. Med. Chem.* **2003**, *10*, 2621–2630.

(99) Zwergel, C.; Gaascht, F.; Valente, S.; Diederich, M.; Bagrel, D.; Kirsch, G. Aurones: Interesting Natural and Synthetic Compounds with Emerging Biological Potential. *Nat. Prod. Commun.* **2012**, *7*, 389–394.

(100) Haudecoeur R, B. A. Recent Advances in the Medicinal Chemistry of Aurones. *Curr Med Chem* **2012**, *19*, 2861–2875.

(101) Schoepfer, J.; Fretz, H.; Chaudhuri, B.; Muller, L.; Seeber, E.; Meijer, L.; Lozach, O.; Vangrevelinghe, E.; Furet, P. Structure-Based Design and Synthesis of 2-Benzylidene-Benzofuran-3-Ones as Flavopiridol Mimics. *J. Med. Chem.* **2002**, *45* (9), 1741–1747.

(102) French, K. J.; Schrecengost, R. S.; Lee, B. D.; Zhuang, Y.; Smith, S. N.; Eberly, J. L.; Yun, J. K.; Smith, C. D. Discovery and Evaluation of Inhibitors of Human Sphingosine Kinase.

Cancer Res. **2003**, *63* (18), 5962–5969.

(103) Huang, W.; Liu, M. Z.; Li, Y.; Tan, Y.; Yang, G. F. Design, Syntheses, and Antitumor Activity of Novel Chromone and Aurone Derivatives. *Bioorg. Med. Chem.* **2007**, *15* (15), 5191–5197.

(104) Wallez, V.; Durieux-Poissonnier, S.; Chavatte, P.; Boutin, J. A.; Audinot, V.; Nicolas, J. P.; Bennejean, C.; Delagrange, P.; Renard, P.; Lesieur, D. Synthesis and Structure−Affinity−Activity Relationships of Novel Benzofuran Derivatives as MT2 Melatonin Receptor Selective Ligands. *J. Med. Chem.* **2002**, *45* (13), 2788–2800.

(105) Sim, H. M.; Loh, K. Y.; Yeo, W. K.; Lee, C. Y.; Go, M. L. Aurones as Modulators of ABCG2 and ABCB1: Synthesis and Structure-Activity Relationships. *ChemMedChem* **2011**, *6* (4), 713–724.

(106) Sato, S.; Sakamoto, T.; Miyazawa, E.; Kikugawa, Y. One-Pot Reductive Amination of Aldehydes and Ketones with α-Picoline-Borane in Methanol, in Water, and in Neat Conditions. *Tetrahedron* **2004**, *60* (36), 7899–7906.

(107) Agarwal, A. K.; Johnson, A. P.; Fishwick, C. W. G. Synthesis of de Novo Designed Small-Molecule Inhibitors of Bacterial RNA Polymerase. *Tetrahedron* **2008**, *64* (43), 10049–10054.

(108) Annette, R.; Oliver, R. Sodium Chlorite-Hydrogen Peroxide — A Mild and Selective Reagent for the Oxidation of Aldehydes to Carboxylic Acids. *J. für Prakt. Chemie* **2000**, *342* (6), 605–608.

(109) Brimble, M. A.; Flowers, C. L.; Hutchinson, J. K.; Robinson, J. E.; Sidford, M. Synthesis of the Phthalide-Containing Anti-Helicobacter Pylori Agents CJ-13,015, CJ-13,102, CJ-13,103, CJ-13,104 and CJ-13,108. *Tetrahedron* **2005**, *61* (42), 10036–10047.

(110) Lawrence, N. J.; Rennison, D.; McGown, A. T.; Hadfield, J. A. The Total Synthesis of an Aurone Isolated from Uvaria Hamiltonii: Aurones and Flavones as Anticancer Agents. *Bioorg. Med. Chem. Lett.* **2003**, *13* (21), 2097–2102.

(111) Ramos-Tomillero, I.; Paradís-Bas, M.; De Pinho Ribeiro Moreira, I.; Bofill, J. M.; Nicolás, E.; Albericio, F. Formylation of Electron-Rich Aromatic Rings Mediated by

Dichloromethyl Methyl Ether and $TiCl_4$: Scope and Limitations. *Molecules* **2015**, *20* (4), 5409–5422.

(112) Akselsen, Ø. W.; Skattebøl, L.; Hansen, T. V. Ortho-Formylation of Oxygenated Phenols. Tetrahedron Lett. **2009**, *50* (46), 6339–6341.

(113) Pan, W.; Dong, D.; Wang, K.; Zhang, J.; Wu, R.; Xiang, D.; Liu, Q. Efficient One-Pot Synthesis of Highly Substituted Pyridin-2(1*H*)-Ones via the Vilsmeier−Haack Reaction of 1-Acetyl,1-Carbamoyl Cyclopropanes. *Org. Lett.* **2007**, *9*, 2421–2423.

(114) Fu, X.; Pu, W.; Zhang, G.; Wang, C. Synthesis of Salicylaldehydes from Phenols via Copper-Mediated Duff Reaction. *Res. Chem. Intermed.* **2015**, *41* (11), 8147–8158.

(115) Wang, Z. Duff Reaction. *Comprehensive Organic Name Reactions and Reagents*; John Wiley & Sons, Inc.: 2010.

(116) Morimoto, H.; Fujiwara, R.; Shimizu, Y.; Morisaki, K.; Ohshima, T. Lanthanum(III) Triflate Catalyzed Direct Amidation of Esters. *Org. Lett.* **2014**, *16*, 2018–2021.

(117) Sabot, C.; Kumar, K. A.; Meunier, S.; Mioskowski, C. A Convenient Aminolysis of Esters Catalyzed by 1,5,7-Triazabicyclo[4.4.0]Dec-5-Ene (TBD) under Solvent-Free Conditions. *Tetrahedron Lett.* **2007**, *48* (22), 3863–3866.

(118) Wang, J.; Liu, J.; Lan, H.; Chu, W.; Sun, Z. Selective Friedel–Crafts Acylation Reactions of 2-Arylphenoxyacetic Acids: A Simple and Efficient Methodology to Synthesize Dibenzoxepine and Arylcoumaranone Derivatives. *Synthesis (Stuttg).* **2015**, *47* (19), 3049–3060.

(119) Wang, S.; Xu, L.; Lu, Y.-T.; Liu, Y.-F.; Han, B.; Liu, T.; Tang, J.; Li, J.; Wu, J.; Li, J.-Y.; Yu, L.-F.; Yang, F. Discovery of Benzofuran-3(2*H*)-One Derivatives as Novel DRAK2 Inhibitors That Protect Islet β-Cells from Apoptosis. *Eur. J. Med. Chem.* **2017**, *130*, 195–208.

(120) Gall, E. L.; Alexandre, D.; Thierry, M.; Michel, T. An Expedient Three-Component Synthesis of Tertiary Benzylamines. *Synthesis (Stuttg).* **2010**, 2, 249–254.

(121) Pu, Y. J.; Vaid, R. K.; Boini, S. K.; Towsley, R. W.; Doecke, C. W.; Mitchell, D. A Practical

Method for Functionalized Peptide or Amide Bond Formation in Aqueous−Ethanol Media with EDC as Activator. *Org. Process Res. Dev.* **2009**, *13* (2), 310–314.

(122) Eaton, P. E.; Carlson, G. R.; Lee, J. T. Phosphorus Pentoxide-Methanesulfonic Acid. Convenient Alternative to Polyphosphoric Acid. *J. Org. Chem.* **1973**, *38* (23), 4071–4073.

(123) Toyoda, T.; Sasakura, K.; Sugasawa, T. Exclusive Ortho *α*-Chloroacetylation of Phenols. *J. Org. Chem.* **1981**, *46* (1), 189–191.

(124) Tsujihara, K.; Hongu, M.; Saito, K.; Kawanishi, H.; Kuriyama, K.; Matsumoto, M.; Oku, A.; Ueta, K.; Tsuda, M.; Saito, A. Na^+-Glucose Cotransporter (SGLT) Inhibitors as Antidiabetic Agents. 4. Synthesis and Pharmacological Properties of 4′-Dehydroxyphlorizin Derivatives Substituted on the B Ring. *J. Med. Chem.* **1999**, *42* (26), 5311–5324.

(125) Donnelly, J. A.; Maloney, D. E. *α*-Halogenoketones—XIV: Studies in the Chemistry of 2′-Hydroxyacrylophenones. *Tetrahedron* **1979**, *35* (24), 2883–2888.

(126) Bringmann, G.; Menche, D.; Kraus, J.; Mühlbacher, J.; Peters, K.; Peters, E. M.; Brun, R.; Bezabih, M.; Abegaz, B. M. Atropo-Enantioselective Total Synthesis of Knipholone and Related Antiplasmodial Phenylanthraquinones. *J. Org. Chem.* **2002**, *67* (16), 5595–5610.

(127) Ollevier, T.; Desyroy, V.; Asim, M.; Brochu, M. C. Bismuth Triflate-Catalyzed Fries Rearrangement of Aryl Acetates. *Synlett* **2004**, 15, 2794–2796.

(128) Barlaam, B.; Cosulich, S.; Degorce, S.; Fitzek, M.; Green, S.; Hancox, U.; Lambert-van der Brempt, C.; Lohmann, J.-J.; Maudet, M.; Morgentin, R.; Pasquet, M.-J.; Péru, A.; Plé, P.; Saleh, T.; Vautier, M.; Walker, M.; Ward, L.; Warin, N. Discovery of (R)-8-(1-(3,5-Difluorophenylamino)Ethyl)-*N*,*N*-Dimethyl-2-Morpholino-4-Oxo-4*H*-Chromene-6-Carboxamide (AZD8186): A Potent and Selective Inhibitor of PI3K*β* and PI3K*δ* for the Treatment of PTEN-Deficient Cancers. *J. Med. Chem.* **2015**, *58* (2), 943–962.

(129) Li, S.; Jin, F.; Viji, M.; Jo, H.; Sim, J.; Kim, H. S.; Lee, H.; Jung, J. K. A Novel Cyclization/Oxidation Strategy for a Two-Step Synthesis of (*Z*)-Aurone. *Tetrahedron Lett.* **2017**, *58* (14), 1417–1420.

(130) Yoshida, M.; Fujino, Y.; Saito, K.; Doi, T. Regioselective Synthesis of Flavone Derivatives

via DMAP-Catalyzed Cyclization of o-Alkynoylphenols. *Tetrahedron* **2011**, *67* (51), 9993–9997.

(131) Brownlow, N.; Mol, C.; Hayford, C.; Ghaem-Maghami, S.; Dibb, N. J. Dasatinib Is a Potent Inhibitor of Tumour-Associated Macrophages, Osteoclasts and the FMS Receptor. *Leukemia* **2009**, *23* (3), 590–594.

(132) Cooper, G. M. Protein Degradation. *In The Cell: A Molecular Approach. 2nd Edition*; Sinauer Associates: 2000.

(133) Amm, I.; Sommer, T.; Wolf, D. H. Protein Quality Control and Elimination of Protein Waste: The Role of the Ubiquitin–Proteasome System. *Biochim. Biophys. Acta - Mol. Cell Res.* **2014**, *1843* (1), 182–196.

(134) Kleiger, G.; Mayor, T. Perilous Journey: A Tour of the Ubiquitin–Proteasome System. *Trends Cell Biol.* **2014**, *24* (6), 352–359.

(135) Grice, G. L.; Nathan, J. A. The Recognition of Ubiquitinated Proteins by the Proteasome. *Cell. Mol. Life Sci.* **2016**, *73* (18), 3497–3506.

(136) Burslem, G. M.; Crews, C. M. Proteolysis-Targeting Chimeras as Therapeutics and Tools for Biological Discovery. *Cell* **2020**, *181* (1), 102–114.

(137) Wolf, D. H.; Hilt, W. The Proteasome: A Proteolytic Nanomachine of Cell Regulation and Waste Disposal. *Biochim. Biophys. Acta - Mol. Cell Res.* **2004**, *1695* (1), 19–31.

(138) Buckley, D. L.; Crews, C. M. Small-Molecule Control of Intracellular Protein Levels through Modulation of the Ubiquitin Proteasome System. *Angew. Chem. Int. Ed. Engl.* **2014**, *53* (9), 2312–2330.

(139) Sakamoto, K. M.; Kim, K. B.; Kumagai, A.; Mercurio, F.; Crews, C. M.; Deshaies, R. J. Protacs: Chimeric Molecules That Target Proteins to the Skp1–Cullin–F Box Complex for Ubiquitination and Degradation. *Proc. Natl. Acad. Sci.* **2001**, *98* (15), 8554–8559.

(140) Konstantinidou, M.; Li, J.; Zhang, B.; Wang, Z.; Shaabani, S.; Ter Brake, F.; Essa, K.; Dömling, A. PROTACs– a Game-Changing Technology. *Expert Opin. Drug Discov.* **2019**, *14* (12), 1255–1268.

(141) Pettersson, M.; Crews, C. M. PROteolysis TArgeting Chimeras (PROTACs) — Past, Present and Future. *Drug Discov. Today Technol.* **2019**, *31*, 15–27.

(142) Li, X.; Song, Y. Proteolysis-Targeting Chimera (PROTAC) for Targeted Protein Degradation and Cancer Therapy. *J. Hematol. Oncol.* **2020**, *13* (1), 50.

(143) Lai, A. C.; Crews, C. M. Induced Protein Degradation: An Emerging Drug Discovery Paradigm. *Nat. Rev. Drug Discov.* **2017**, *16* (2), 101–114.

(144) Wang, Y.; Jiang, X.; Feng, F.; Liu, W.; Sun, H. Degradation of Proteins by PROTACs and Other Strategies. *Acta Pharm. Sin. B* **2020**, *10* (2), 207–238.

(145) Winter, G. E.; Buckley, D. L.; Paulk, J.; Roberts, J. M.; Souza, A.; Dhe-Paganon, S.; Bradner, J. E. Phthalimide Conjugation as a Strategy for *in Vivo* Target Protein Degradation. *Science* **2015**, *348* (6241), 1376–1381.

(146) Bai, L.; Zhou, B.; Yang, C.-Y.; Ji, J.; McEachern, D.; Przybranowski, S.; Jiang, H.; Hu, J.; Xu, F.; Zhao, Y.; Liu, L.; Fernandez-Salas, E.; Xu, J.; Dou, Y.; Wen, B.; Sun, D.; Meagher, J.; Stuckey, J.; Hayes, D. F.; Li, S.; Ellis, M. J.; Wang, S. Targeted Degradation of BET Proteins in Triple-Negative Breast Cancer. *Cancer Res.* **2017**, *77* (9), 2476–2487.

(147) Testa, A.; Hughes, S. J.; Lucas, X.; Wright, J. E.; Ciulli, A. Structure-Based Design of a Macrocyclic PROTAC. *Angew. Chemie Int. Ed.* **2020**, *59* (4), 1727–1734.

(148) Sakamoto, K. M.; Kim, K. B.; Verma, R.; Ransick, A.; Stein, B.; Crews, C. M.; Deshaies, R. J. Development of Protacs to Target Cancer-Promoting Proteins for Ubiquitination and Degradation. *Mol. Cell. Proteomics* **2003**, *2* (12), 1350–1358.

(149) Huang, H.-T.; Dobrovolsky, D.; Paulk, J.; Yang, G.; Weisberg, E. L.; Doctor, Z. M.; Buckley, D. L.; Cho, J.-H.; Ko, E.; Jang, J.; Shi, K.; Choi, H. G.; Griffin, J. D.; Li, Y.; Treon, S. P.; Fischer, E. S.; Bradner, J. E.; Tan, L.; Gray, N. S. A Chemoproteomic Approach to Query the Degradable Kinome Using a Multi-Kinase Degrader. *Cell Chem. Biol.* **2018**, *25* (1), 88–99.

(150) Lai, A. C.; Toure, M.; Hellerschmied, D.; Salami, J.; Jaime-Figueroa, S.; Ko, E.; Hines, J.; Crews, C. M. Modular PROTAC Design for the Degradation of Oncogenic BCR-ABL. *Angew. Chem. Int. Ed. Engl.* **2016**, *55* (2), 807–810.

(151) Deshaies, R. J. Prime Time for PROTACs. *Nat. Chem. Biol.* **2015**, *11* (9), 634–635.

(152) Gu, S.; Cui, D.; Chen, X.; Xiong, X.; Zhao, Y. PROTACs: An Emerging Targeting Technique for Protein Degradation in Drug Discovery. *BioEssays* **2018**, *40* (4), 1700247.

(153) Zou, Y.; Ma, D.; Wang, Y. The PROTAC Technology in Drug Development. *Cell Biochem. Funct.* **2019**, *37* (1), 21–30.

(154) Cohen, P.; Tcherpakov, M. Will the Ubiquitin System Furnish as Many Drug Targets as Protein Kinases? *Cell* **2010**, *143* (5), 686–693.

(155) Clague, M. J.; Heride, C.; Urbé, S. The Demographics of the Ubiquitin System. *Trends Cell Biol.* **2015**, *25* (7), 417–426.

(156) Schneekloth, J. S.; Fonseca, F. N.; Koldobskiy, M.; Mandal, A.; Deshaies, R.; Sakamoto, K.; Crews, C. M. Chemical Genetic Control of Protein Levels: Selective *in Vivo* Targeted Degradation. *J. Am. Chem. Soc.* **2004**, *126* (12), 3748–3754.

(157) Schneekloth, A. R.; Pucheault, M.; Tae, H. S.; Crews, C. M. Targeted Intracellular Protein Degradation Induced by a Small Molecule: En Route to Chemical Proteomics. *Bioorg. Med. Chem. Lett.* **2008**, *18* (22), 5904–5908.

(158) Montrose, K.; Krissansen, G. W. Design of a PROTAC That Antagonizes and Destroys the Cancer-Forming X-Protein of the Hepatitis B Virus. *Biochem. Biophys. Res. Commun.* **2014**, *453* (4), 735–740.

(159) Tinworth, C. P.; Lithgow, H.; Ian, C. Small Molecule-Mediated Protein Knockdown as a New Approach to Drug Discovery. *Med. Chem. Commun.* **2016**, *7*, 2206–2216.

(160) Bondeson, D. P.; Mares, A.; Smith, I. E. D.; Ko, E.; Campos, S.; Miah, A. H.; Mulholland, K. E.; Routly, N.; Buckley, D. L.; Gustafson, J. L.; Zinn, N.; Grandi, P.; Shimamura, S.; Bergamini, G.; Faelth-Savitski, M.; Bantscheff, M.; Cox, C.; Gordon, D. A.; Willard, R. R.; Flanagan, J. J.; Casillas, L. N.; Votta, B. J.; den Besten, W.; Famm, K.; Kruidenier, L.; Carter, P. S.; Harling, J. D.; Churcher, I.; Crews, C. M. Catalytic *in Vivo* Protein Knockdown by Small-Molecule PROTACs. *Nat. Chem. Biol.* **2015**, *11* (8), 611–617.

(161) An, S.; Fu, L. Small-Molecule PROTACs: An Emerging and Promising Approach for the

Development of Targeted Therapy Drugs. *EBioMedicine* **2018**, *36*, 553–562.

(162) Neklesa, T. K.; Winkler, J. D.; Crews, C. M. Targeted Protein Degradation by PROTACs. *Pharmacol. Ther.* **2017**, *174*, 138–144.

(163) Gadd, M. S.; Testa, A.; Lucas, X.; Chan, K.-H.; Chen, W.; Lamont, D. J.; Zengerle, M.; Ciulli, A. Structural Basis of PROTAC Cooperative Recognition for Selective Protein Degradation. *Nat. Chem. Biol.* **2017**, *13* (5), 514–521.

(164) Ohoka, N.; Okuhira, K.; Ito, M.; Nagai, K.; Shibata, N.; Hattori, T.; Ujikawa, O.; Shimokawa, K.; Sano, O.; Koyama, R.; Fujita, H.; Teratani, M.; Matsumoto, H.; Imaeda, Y.; Nara, H.; Cho, N.; Naito, M. *In Vivo* Knockdown of Pathogenic Proteins via Specific and Nongenetic Inhibitor of Apoptosis Protein (IAP)-Dependent Protein Erasers (SNIPERs). *J. Biol. Chem.* **2017**, *292* (11), 4556–4570.

(165) Nowak, R. P.; DeAngelo, S. L.; Buckley, D.; He, Z.; Donovan, K. A.; An, J.; Safaee, N.; Jedrychowski, M. P.; Ponthier, C. M.; Ishoey, M.; Zhang, T.; Mancias, J. D.; Gray, N. S.; Bradner, J. E.; Fischer, E. S. Plasticity in Binding Confers Selectivity in Ligand-Induced Protein Degradation. *Nat. Chem. Biol.* **2018**, *14* (7), 706–714.

(166) Smith, B. E.; Wang, S. L.; Jaime-Figueroa, S.; Harbin, A.; Wang, J.; Hamman, B. D.; Crews, C. M. Differential PROTAC Substrate Specificity Dictated by Orientation of Recruited E3 Ligase. *Nat. Commun.* **2019**, *10* (1), 131.

(167) Lu, J.; Qian, Y.; Altieri, M.; Dong, H.; Wang, J.; Raina, K.; Hines, J.; Winkler, J. D.; Crew, A. P.; Coleman, K.; Crews, C. M. Hijacking the E3 Ubiquitin Ligase Cereblon to Efficiently Target BRD4. *Chem. Biol.* **2015**, *22* (6), 755–763.

(168) Zengerle, M.; Chan, K.-H.; Ciulli, A. Selective Small Molecule Induced Degradation of the BET Bromodomain Protein BRD4. *ACS Chem. Biol.* **2015**, *10* (8), 1770–1777.

(169) Jiang, X.; Yu, J.; Zhou, Z.; Kongsted, J.; Song, Y.; Pannecouque, C.; De Clercq, E.; Kang, D.; Poongavanam, V.; Liu, X.; Zhan, P. Molecular Design Opportunities Presented by Solvent-Exposed Regions of Target Proteins. *Med. Res. Rev.* **2019**, *39* (6), 2194–2238.

(170) Farnaby, W.; Koegl, M.; Roy, M. J.; Whitworth, C.; Diers, E.; Trainor, N.; Zollman, D.; Steurer, S.; Karolyi-Oezguer, J.; Riedmueller, C.; Gmaschitz, T.; Wachter, J.; Dank, C.;

Galant, M.; Sharps, B.; Rumpel, K.; Traxler, E.; Gerstberger, T.; Schnitzer, R.; Petermann, O.; Greb, P.; Weinstabl, H.; Bader, G.; Zoephel, A.; Weiss-Puxbaum, A.; Ehrenhöfer-Wölfer, K.; Wöhrle, S.; Boehmelt, G.; Rinnenthal, J.; Arnhof, H.; Wiechens, N.; Wu, M.-Y.; Owen-Hughes, T.; Ettmayer, P.; Pearson, M.; McConnell, D. B.; Ciulli, A. BAF Complex Vulnerabilities in Cancer Demonstrated via Structure-Based PROTAC Design. *Nat. Chem. Biol.* **2019**, *15* (7), 672–680.

(171) Bondeson, D. P.; Smith, B. E.; Burslem, G. M.; Buhimschi, A. D.; Hines, J.; Jaime-Figueroa, S.; Wang, J.; Hamman, B. D.; Ishchenko, A.; Crews, C. M. Lessons in PROTAC Design from Selective Degradation with a Promiscuous Warhead. *Cell Chem. Biol.* **2018**, *25* (1), 78–87.

(172) Nabet, B.; Roberts, J. M.; Buckley, D. L.; Paulk, J.; Dastjerdi, S.; Yang, A.; Leggett, A. L.; Erb, M. A.; Lawlor, M. A.; Souza, A.; Scott, T. G.; Vittori, S.; Perry, J. A.; Qi, J.; Winter, G. E.; Wong, K.-K.; Gray, N. S.; Bradner, J. E. The DTAG System for Immediate and Target-Specific Protein Degradation. *Nat. Chem. Biol.* **2018**, *14* (5), 431–441.

(173) Wurz, R. P.; Dellamaggiore, K.; Dou, H.; Javier, N.; Lo, M.-C.; McCarter, J. D.; Mohl, D.; Sastri, C.; Lipford, J. R.; Cee, V. J. A "Click Chemistry Platform" for the Rapid Synthesis of Bispecific Molecules for Inducing Protein Degradation. *J. Med. Chem.* **2018**, *61* (2), 453–461.

(174) Delport, A.; Hewer, R. Inducing the Degradation of Disease-Related Proteins Using Heterobifunctional Molecules. *Molecules* **2019**, *24* (18), 3272.

(175) Burslem, G. M.; Smith, B. E.; Lai, A. C.; Jaime-Figueroa, S.; McQuaid, D. C.; Bondeson, D. P.; Toure, M.; Dong, H.; Qian, Y.; Wang, J.; Crew, A. P.; Hines, J.; Crews, C. M. The Advantages of Targeted Protein Degradation Over Inhibition: An RTK Case Study. *Cell Chem. Biol.* **2018**, *25* (1), 67–77

(176) Hines, J.; Lartigue, S.; Dong, H.; Qian, Y.; Crews, C. M. MDM2-Recruiting PROTAC Offers Superior, Synergistic Antiproliferative Activity via Simultaneous Degradation of BRD4 and Stabilization of P53. *Cancer Res.* **2019**, *79* (1), 251–262.

(177) Wan, Y.; Yan, C.; Gao, H.; Liu, T. Small-Molecule PROTACs: Novel Agents for Cancer

Therapy. *Future Med. Chem.* **2020**, *12* (10), 915–938.

(178) Sekine, K.; Takubo, K.; Kikuchi, R.; Nishimoto, M.; Kitagawa, M.; Abe, F.; Nishikawa, K.; Tsuruo, T.; Naito, M. Small Molecules Destabilize CIAP1 by Activating Auto-Ubiquitylation. *J. Biol. Chem.* **2008**, *283*, 8961–8968.

(179) Itoh, Y.; Ishikawa, M.; Naito, M.; Hashimoto, Y. Protein Knockdown Using Methyl Bestatin−Ligand Hybrid Molecules: Design and Synthesis of Inducers of Ubiquitination-Mediated Degradation of Cellular Retinoic Acid-Binding Proteins. *J. Am. Chem. Soc.* **2010**, *132* (16), 5820–5826.

(180) Okuhira, K.; Demizu, Y.; Hattori, T.; Ohoka, N.; Shibata, N.; Nishimaki-Mogami, T.; Okuda, H.; Kurihara, M.; Naito, M. Development of Hybrid Small Molecules That Induce Degradation of Estrogen Receptor-Alpha and Necrotic Cell Death in Breast Cancer Cells. *Cancer Sci.* **2013**, *104* (11), 1492–1498.

(181) Toure, M.; Crews, C. M. Small-Molecule PROTACS: New Approaches to Protein Degradation. *Angew. Chem. Int. Ed. Engl.* **2016**, *55*, 1966–1973.

(182) Zoppi, V.; Hughes, S. J.; Maniaci, C.; Testa, A.; Gmaschitz, T.; Wieshofer, C.; Koegl, M.; Riching, K. M.; Daniels, D. L.; Spallarossa, A.; Ciulli, A. Iterative Design and Optimization of Initially Inactive Proteolysis Targeting Chimeras (PROTACs) Identify VZ185 as a Potent, Fast, and Selective von Hippel–Lindau (VHL) Based Dual Degrader Probe of BRD9 and BRD7. *J. Med. Chem.* **2019**, *62* (2), 699–726.

(183) Shi, Q.; Chen, L. Cereblon: A Protein Crucial to the Multiple Functions of Immunomodulatory Drugs as Well as Cell Metabolism and Disease Generation. *J. Immunol. Res.* **2017**, *2017*, 9130608.

(184) Lu, G.; Middleton, R. E.; Sun, H.; Naniong, M.; Ott, C. J.; Mitsiades, C. S.; Wong, K. K.; Bradner, J. E.; Kaelin, W. G. The Myeloma Drug Lenalidomide Promotes the Cereblon-Dependent Destruction of Ikaros Proteins. *Science* **2014**, *343* (6168), 305–309.

(185) Krönke, J.; Udeshi, N. D.; Narla, A.; Grauman, P.; Hurst, S. N.; McConkey, M.; Svinkina, T.; Heckl, D.; Comer, E.; Li, X.; Ciarlo, C.; Hartman, E.; Munshi, N.; Schenone, M.; Schreiber, S. L.; Carr, S. A.; Ebert, B. L. Lenalidomide Causes Selective Degradation of

IKZF1 and IKZF3 in Multiple Myeloma Cells. *Science* **2014**, *343* (6168), 301–305.

(186) Sun, Y.; Zhao, X.; Ding, N.; Gao, H.; Wu, Y.; Yang, Y.; Zhao, M.; Hwang, J.; Song, Y.; Liu, W.; Rao, Y. PROTAC-Induced BTK Degradation as a Novel Therapy for Mutated BTK C481S Induced Ibrutinib-Resistant B-Cell Malignancies. *Cell Res.* **2018**, *28* (7), 779–781.

(187) Powell, C. E.; Gao, Y.; Tan, L.; Donovan, K. A.; Nowak, R. P.; Loehr, A.; Bahcall, M.; Fischer, E. S.; Jänne, P. A.; George, R. E.; Gray, N. S. Chemically Induced Degradation of Anaplastic Lymphoma Kinase (ALK). *J. Med. Chem.* **2018**, *61* (9), 4249–4255.

(188) Schiedel, M.; Herp, D.; Hammelmann, S.; Swyter, S.; Lehotzky, A.; Robaa, D.; Oláh, J.; Ovádi, J.; Sippl, W.; Jung, M. Chemically Induced Degradation of Sirtuin 2 (Sirt2) by a Proteolysis Targeting Chimera (PROTAC) Based on Sirtuin Rearranging Ligands (SirReals). *J. Med. Chem.* **2018**, *61* (2), 482–491.

(189) Buhimschi, A. D.; Armstrong, H. A.; Toure, M.; Jaime-Figueroa, S.; Chen, T. L.; Lehman, A. M.; Woyach, J. A.; Johnson, A. J.; Byrd, J. C.; Crews, C. M. Targeting the C481S Ibrutinib-Resistance Mutation in Bruton's Tyrosine Kinase Using PROTAC-Mediated Degradation. *Biochemistry* **2018**, *57* (26), 3564–3575.

(190) Zhang, C.; Han, X. R.; Yang, X.; Jiang, B.; Liu, J.; Xiong, Y.; Jin, J. Proteolysis Targeting Chimeras (PROTACs) of Anaplastic Lymphoma Kinase (ALK). *Eur. J. Med. Chem.* **2018**, *151*, 304–314.

(191) Pei, H.; Peng, Y.; Zhao, Q.; Chen, Y. Small Molecule PROTACs: An Emerging Technology for Targeted Therapy in Drug Discovery. *RSC Adv.* **2019**, *9* (30), 16967–16976.

(192) Boyle, R. G.; Walker, D. W.; Boyce, R. J.; Scott, P.; Francine, F.; Vo, C. H. Pharmaceutical Compounds. WO 2015/120390 A1, 2015.

(193) Meisel, J. W.; Hu, C. T.; Hamilton, A. D. Heterofunctionalized Cavitands by Macrocyclization of Sequence-Defined Foldamers. *Org. Lett.* **2019**, *21* (19), 7763–7767.

(194) Akanksha; Maiti, D. Microwave-Assisted Palladium Mediated Decarbonylation Reaction: Synthesis of Eulatachromene. *Green Chem.* **2012**, *14* (8), 2314–2320.

(195) Zhao, Y.; Li, Z.; Yang, C.; Lin, R.; Xia, W. Visible-Light Photoredox Catalysis Enabled Bromination of Phenols and Alkenes. *J. Org. Chem.* **2014**, *10*, 622–627.

(196) Talukdar, R. Single-Step Dual Functionalization: One-Pot Bromination-Cross-Dehydrogenative Esterification of Hydroxy Benzaldehydes with CCl_3Br – A Comparison with Selectfluor. *Synlett* **2019**, *30* (14), 1713–1718.

(197) Maksimenko, S. I.; Novikova, N. S.; Kondrat'eva, R. V; Kuz'min, V. E.; Ognichenko, L. N.; Yarkova, M. Y. Synthesis and Mesomorphic Properties of Esters Derived from Alkanediols. *Russ. J. Org. Chem.* **2007**, *43* (12), 1773–1780.

(198) Tisdale, E. J.; Vong, B. G.; Li, H.; Kim, S. H.; Chowdhury, C.; Theodorakis, E. A. Total Synthesis of Seco-Lateriflorone. *Tetrahedron* **2003**, *59* (35), 6873–6887.

(199) Chakor, J. N.; Merlini, L.; Dallavalle, S. Enantioselective Total Synthesis and Absolute Configuration of the Alleged Structure of Crassinervic Acid. *Tetrahedron* **2011**, *67* (34), 6300–6307.

(200) Ettaoussi, M.; Péres, B.; Klupsch, F.; Delagrange, P.; Boutin, J.-A.; Renard, P.; Caignard, D.-H.; Chavatte, P.; Berthelot, P.; Lesieur, D.; Yous, S. Design and Synthesis of Benzofuranic Derivatives as New Ligands at the Melatonin-Binding Site MT3. *Bioorg. Med. Chem.* **2008**, *16* (9), 4954–4962.

(201) Li, P.; Zhao, J.; Lang, R.; Xia, C.; Li, F. Copper-Catalyzed Methyl Esterification of Aromatic Aldehydes and Benzoic Alcohols by TBHP as Both Oxidant and Methyl Source. *Tetrahedron Lett.* **2014**, *55* (2), 390–393.

(202) Cheung, C. W.; Buchwald, S. L. Palladium-Catalyzed Hydroxylation of Aryl and Heteroaryl Halides Enabled by the Use of a Palladacycle Precatalyst. *J. Org. Chem.* **2014**, *79* (11), 5351–5358.

(203) Player, M. R.; Parsons, W. H.; Huang, H.; Hutta, D. A.; Hu, H.; Rinker, J. 5-oxo-5,8-dihydro-pyrido-pyrimidines as Inhibitors of C-FMS Kinase. US2008/114007, 2008, A1